Melanie Wolf, BSc MSc

Synthesis and Characterization of Germanium and Antimony Organometallics

DOCTORAL THESIS

to achieve the university degree of
Doktorin der technischen Wissenschaften
submitted to

Graz University of Technology

Supervisor
Univ.-Prof. Dipl.-Chem. Dr.rer.nat. Frank Uhlig

Institute of Inorganic Chemistry

Faculty of Technical Chemistry, Chemical and Process Engineering, Biotechnology

Graz 2017

AFFIDAVIT

I declare that I have authored this thesis independently, that I have not used other than the declared sources/resources, and that I have explicitly indicated all material which has been quoted either literally or by content from the sources used. The text document uploaded to TUGRAZonline is identical to the present doctoral thesis.

4.1. 2017

Date

Signature

Abstract

While organosilicon and organotin compounds have already found widespread use, less is known on the preparation and properties of germanium derivatives, due to challenging and cost intensive preparation. Notwithstanding, organogermanium compounds are considered to be promising starting materials for commercial products and industrial applications, polymerization materials or the generation of nanoparticles, the latter finding usage in energy storage systems. The worldwide increasing energy consumption is without dispute of great importance, thus new and superior materials need to be developed in order to improve the performance of current battery systems.

This work aimed to provide an overview over organogermanium chemistry with respect to not only the successful preparation of organogermanium species but also their difficult characterization, and to help comprehend the difficulties deriving from the nature of the element. For these reasons, a series of organometallic compounds, including tetraarylgermanes, organogermanium halides, hydrides and hydrochlorides have been synthesized and fully characterized. In this work, preparation methods were investigated in detail and enhanced towards selectivity, yields and complexity. Alternative pathways showing promising results are presented, reducing the problems of formation of mixtures. The extended solid state structures were investigated towards the presence of non-covalent secondary interactions arising from the aryl substituents through X-ray crystallography, which have a reputation for helping to stabilize the compounds and strongly depend on the nature and steric bulk of the aryl ligand and its environment. These results bring us one step closer to solving the problem of how to better understand the preparation of arylgermanium compounds, whose approach has had people wondering for years.

Kurzfassung

Während organische Verbindungen des Siliciums und Zinns weitreichende Anwendungen gefunden haben, sieht die Realität bei Germanium aufgrund anspruchsvoller und kostenaufwändiger Darstellung anders aus: weder über geeignete Darstellungsmethoden, noch über Eigenschaften dieser Verbindungen ist viel bekannt. Verbindungen des Germaniums werden immer häufiger im Zusammenhang zukünftiger industrieller Prozesse und kommerziellen Materialen erwähnt und die Herstellung von Polymeren oder Nanopartikeln stellen Einsatzmöglichkeiten dar. Der weltweit steigende Energiebedarf und die damit einhergehende stetige Nachfrage nach neuen, außergewöhnlichen Materialien zur Verbesserung der Leistungsfähigkeit von beispielsweise Energiespeichern, stellt eine interessante, zudem profitable Motivation dar.

Der Herausforderung eine Reihe neuer Verbindungen, darunter Organogermanium halide, -hydride und -hydrochloride, ob dem Mangel an möglichen Darstellungsmethoden und fehlenden Informationen zu synthetisieren und zu charakterisieren, wurde sich im Zuge dieser Arbeit gestellt, um nicht nur einen Überblick über den derzeitigen Stand von Organogermaniumverbindungen zu schaffen, sondern auch aufzuzeigen, weshalb dieses Forschungsthema so herausfordern ist. Bereits bekannte Darstellungsmethoden wurden untersucht und hinsichtlich Selektivität, Ausbeute und Komplexität verbessert. Alternative Methoden zeigen vielversprechende Ergebnisse und beseitigen Schwierigkeiten hinsichtlich der Bildung von Nebenprodukten und Gemischen. Festkörperstrukturen wurden hinsichtlich sekundärer Wechselwirkungen, welche dafür bekannt sind zur Stabilität im Festkörper beizutragen und von der Art und sterischem Anspruch des Liganden abhängen, untersucht.

Diese Resultate tragen dazu bei, die Darstellung dieser Verbindungen und deren Zugang besser zu verstehen, ein Problem, an dem schon viele gescheitert sind.

Danksagung

Großer Dank gilt in erster Line meinem Betreuer Prof. Frank Uhlig. Du hast sowohl zu meiner wissenschaftlichen, als auch meiner persönlichen Weiterentwicklung beigetragen. Ich danke dir für deine Ideen und deinen Rat, dein Vertrauen in mich, die nötigen Freiheiten und vor allem deine Menschlichkeit. Ich hoffe, dass sich unsere Wege auch in Zukunft des Öfteren kreuzen werden.

Prof. Roland Fischer und Dr. Ana Torvisco danke ich für die Unterstützung mit Röntgenstrukturanalysen, aber auch ihre Hilfe außerhalb ihrer Expertise. Danke, dass eure Bürotür jederzeit für mich offen stand. Mein Dank geht auch an Michaela Flock für die theoretischen Berechnungen und Simulationen, Monika Filzwieser für die Elementaranalysen, Prof. Klaus Reichmann für die Durchführung der TGA- Analysen, Prof. Erich Leitner und Karin Bartl für die Messung verschiedenster GCMS Proben.

Liebe Kollegen: Danke! Für die tatkräftige Unterstützung, die humorvollen Momente, die Kuriositäten, die wissenschaftlichen Diskussionen und dass ihr immer noch über meine Geschichten lachen könnt. Aus vielen Arbeitskollegen wurden Freunde, die mich auch nach diesem Lebensabschnitt noch begleiten werden. Ein großes Dankeschön an die Salatgang, insbesondere Angela, Elisabeth, Johanna und Stefan. Ein besonderes Dankeschön an Astrid für die Unterstützung in und außerhalb des Labors. Ohne dich hätte ich des Öfteren den Wald vor lauter Bäumen nicht mehr gesehen- oder das Germanium vor lauter Naphthalin. Judith danke ich für die Durchführung der Thermolyse Experimente. Ich möchte diese Chance auch nützen, um mich bei meinen zahlreichen Studenten zu bedanken, im Besonderen jedoch bei meinen Bachelorstudenten: Beate Steller, Michael Traxler und Michael Hafner, euch danke ich insbesondere für die Zeit und Motivation, die ihr in dieses Projekt investiert habt.

Mein Dank gilt auch der Marshall Plan Foundation, die mir den Aufenthalt an der Oklahoma State University ermöglicht hat und in diesem Sinne natürlich Prof. Weinert und seiner Arbeitsgruppe für die herzliche Aufnahme. Dies gilt insbesondere für Sangeetha: ohne dich wäre ich vermutlich professionelle Tornadojägerin geworden.

Besonderer Dank geht an meine Familie, ohne die dies alles nicht möglich gewesen wäre. Mit dem Gefühl aufzuwachsen, dass man alles erreichen könne, wenn man es nur will, hat mich zu dem Menschen gemacht, der ich heute bin. Danke Mama! Dafür, dass du mich in meinen Entscheidungen stärkst und mir öfters einen Schubs in die richtige Richtung gibst. Vor allem aber auch, dass du mir auch nach über einem Vierteljahrhundert immer noch mein Lieblingsessen kochst und mich daran erinnerst regelmäßig zum Arzt zu gehen. Lieber Papa, danke für deinen Humor und deine Wissensbegierde. Du hast meine Neugierde und Leidenschaft zu den Naturwissenschaften geweckt. Danke, dass du bedingungslos hinter mir stehst, jede noch so absurde Idee unterstützt und mir immer wieder die wesentlichen Dinge im Leben zeigst.

Danke auch an Julia, Judith, Elisabeth und Svenja. Dafür, dass ihr stets zur Stelle seid, wenn Not an der Frau ist, mich auf den Boden der Tatsachen zurückholt, die Dinge immer wieder in einem anderen Licht erscheinen lässt und es möglich macht sämtliche Sorgen für einige Zeit zu vergessen.

Und natürlich möchte ich zuallerletzt meiner besseren Hälfte Bernhard danken. Du schaffst es immer wieder, mich in den unmöglichsten Situationen zum Lachen zu bringen und bist für mich da, wann immer ich dich brauche. Danke, dass du mir immer noch beim Suchen meiner verlegten Sachen hilfst, trotz Höhenangst mit mir Achterbahn fährst, immer in deinem Koffer Platz für mein Übergepäck einplanst und meine Leidenschaften mit mir teilst. Mögen viele weitere Abenteuer folgen.

Content

List of abbreviations

ATR-IR	attenuated total reflection - infrared spectroscopy
BuLi	butyllithium
CCl_4	carbon tetrachloride
DBP	dibenzoyl peroxide
DCM	dichloromethane
DFT	density functional theory
DI	direct insertion
DIBAL-H	diisobutylaluminiumhydrid
DME	dimethoxymethane
DSC	differential scanning calorimetry
EDX	energy dispersive X-ray analysis
EI	electron impact ionization
Et_2O	diethylether
EtOH	ethanol
GC	gas chromatography
$GeCl_4$	germanium tetrachloride
GeO_2	germanium dioxide
GLC	gas liquid chromatography
H_2SO_4	sulfuric acid
HCl	hydrochloric acid
HOMO	highest occupied molecular orbital
i	iso
$LiAlH_4$	ithium aluminum hydride
LiCl	lithium chloride
LUMO	lowest unoccupied molecular orbital

m	*meta*
MS	mass spectroscopy
Na_2SO_4	sodium sulfate
NCS	*N*-chlorosuccinimide
NMR	nuclear magnetic resonance
o	*ortho*
OTf	trifluoromethanesulfonate
p	*para*
ppm	parts per million
$SbCl_3$	antimony trichloride
SEM	scanning electron microscope
t	*tert*
HOTf	trifluoromethanesulfonic acid
TGA	thermogravimetric analysis
THF	tetrahydrofurane
TMEDA	Tetramethylethylendiamin
UV	ultraviolett
Vis	visible
X	halide
ΔH	enthalpy

Chapter 1

Literature

1.1. Organogermanium compounds

Elemental germanium, first discovered in 1886 by Clemens Winkler, is mostly available in the form of sulfides in rare minerals such as Argyrodite (Ag_8GeS_6) and Germanite ($Cu_6FeGe_2S_8$). In compounds, germanium occurs in oxidation state II and IV. Germanium compounds in oxidation state II are rather unstable and can be easily oxidized to the more stable germanium(IV) derivatives, which is why we only find germanium(IV) compounds in nature. Elemental germanium is available from sphalerite zinc ores, where the sulfides are transformed into the oxides by roasting (Figure 1). The mixture of ZnO and GeO_2 is then extracted with sulfuric acid. After treatment with HCl or chlorine gas and therefore transformation into $GeCl_4$, the volatile $GeCl_4$ is distilled. It can then be hydrolyzed to GeO_2. Further treatment with hydrogen yields elemental germanium, which can be purified in zone melting processes.[1]

$$GeS_2 + 3\,O_2 \longrightarrow GeO_2 + 2\,SO_2$$

$$GeO_2 + 4\,HCl \longrightarrow GeCl_4 + 2\,H_2O$$

$$GeO_2 + 2\,Cl_2 \longrightarrow GeCl_4 + O_2$$

$$GeO_2 + 2\,H_2 \longrightarrow GeH_2 + 2\,H_2O$$

Figure 1. Preparation and isolation of germanium dioxide, germanium tetrachloride and germanium dihydride.

Organogermanes are compounds containing a germanium-carbon bond and have been thoroughly investigated, however are not yet widely used as intermediates or reagents in organic synthesis. Over the years the interest in organometallic chemistry of germanium originated again, nonetheless the chemistry of Group 14 elements is still dominated by silicon. Up to the middle of the 20th century, organogermanium compounds were the least understood among all of the group 14 elements. The first organogermanium compound reported, Et_4Ge, was synthesized in 1887 by Winkler *via* reaction of germanium tetrachloride and diethylzinc. For almost half a century, no new organogermanium compounds were reported due to high prices and scarcity.[2] Fortunately, the chemistry of organogermanium compounds started to revise in the second quarter of the 20th century, when new sources of germanium were found and finally flourished in the 1960s, with new chemists joining the field. Organogermanium compounds are considered as potential candidates for electronics, energy storage and medical applications, due to their medical and biological usage.[3-7] Certain germanium compounds have low mammalian toxicity, but marked activity against bacteria, so their usage as antibacterial agents has been considered. Furthermore organo-, oligo- and polygermanes have gained interest due to their special characteristics, including electroluminescence, conductivity, absorption in the UV-region, as well as thermochroism. Therefore, it is highly probable that germanium will play a crucial role in the world's future. There is no doubt that progress will be driven by the demand for new materials and enhanced performance of applications, thus making the quest for new materials increasingly important.

Because compounds of germanium are closer in their properties to the isostructural silicon compounds as compared to tin and lead, germanium is often regarded to being quite similar to its lighter homologue silicon, although the band gap, electron and hole mobility and conductivity are higher in bulk elemental germanium. This is also the reason why bulk germanium metal is of interest for electrochemical applications and why germanium-silicon alloys have found use as semiconductor materials for electronics. Differences in the chemical properties of organic compounds of group 14 elements are ascribed by the in-

crease in the covalent atomic radius, bond distances and polarities, and the decrease of bond dissociation energy going downward from silicon to lead. Since the thermal and chemical stability of C–M bonds decreases in the order Si > Ge > Sn > Pb, the Ge–C bond is weaker than in comparable silicon derivatives. The electronegativity of the group 14 elements changes non-monotonically. The electronegativity of Ge, C and H are all very similar (Figure 2), thus the polarities of the Ge–C, and also the Ge–H bond respectively, are strongly dependent on the substituents used (Figure 3).[8]

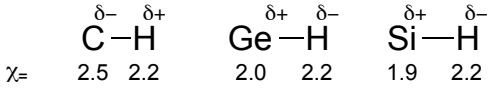

Figure 2. Polarities and electronegativities of hydrogen, carbon, silicon and germanium.

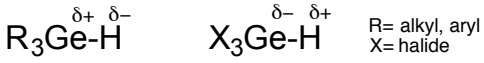

Figure 3. Polarity of germanium hydrides in dependence of substituents employed.

Additionally, due to Ge and H (Ge 2.0, H 2.2) showing similar electronegativities, the polarity of the Ge–H bond in organogermanium hydrides compared to the Si–H bond is rather small, thus explaining the differences in reactivity of organogermanium hydrides compared to organosilicon hydrides (Figure 4).

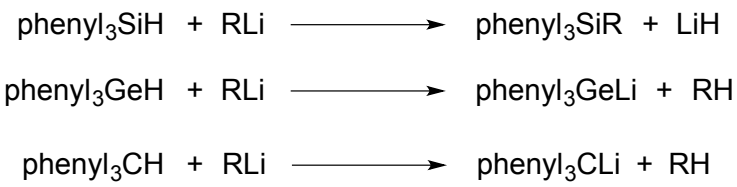

Figure 4. Reactivity of group 14 organo hydrides.

The reactivity of organometallic hydrides of group 14 elements increases with the atomic number and the quantity of hydrogens, while the thermal stability decreases. Although the Si–H bond hydrolyzes easily, this is not the case for germanium, tin and lead compounds.

1.1.1. Tetraarylgermanes

Although tetraarylgermanes rarely find straightforward usage in industrial applications, they represent important starting materials for the preparation of other organogermanium compounds. The application of organolithium (Figure 5) or Grignard reagents (Figure 6) with germanium halides is the most common route for the introduction of aromatic ligands around germanium.[9-12]

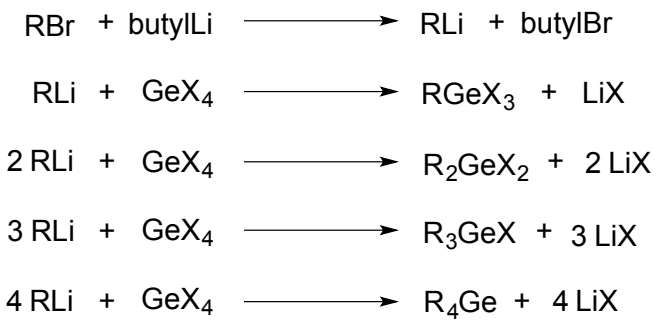

Figure 5. Employment of organolithium reagents, in this case butyllithium, for the preparation of organogermanes.

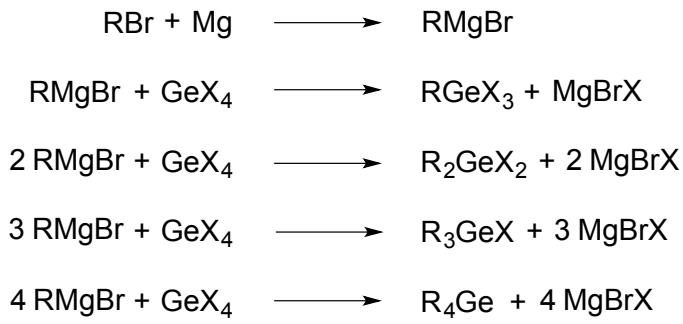

Figure 6. Formation of the Grignard reagent and subsequent reaction with germanium tetrahalide to prepare organogermanes.

Another possibility for the preparation of tetra- but also triorganogermanes is a two-step reaction starting from GeO_2 by preparing a hexacoordinated germanium complex and further reaction with Grignard reagents. Cerveau *et al*. reported the hypervalent germanium complex in 1988 and also investigated the reactions of the same with organometallic derivatives (Figure 7). This pathway provides an alternative route for organometallic compounds, which are normally synthesized by employment of $GeCl_4$.[13,14]

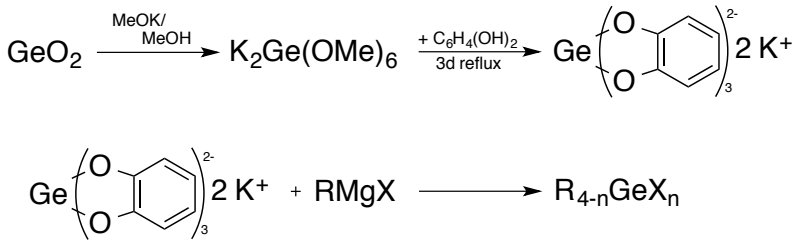

Figure 7. Preparation of tetragermanes and trisubstituted germanium halides starting from germanium dioxide using the hexacoordinated anionic complex $K_2[(C_6H_4O_2)_3Ge]$ (28) as an intermediate.

1.1.2. Organogermanium halides

Organogermanium halides have been of interest for quite some time, since they are powerful starting materials for the preparation of other germanium compounds. They are normally stable at room temperature, but the Ge–X bond can be easily hydrolyzed by water, resulting in the formation of hydroxides, oligomeric or polymeric metalloxanes, for what reason exclusion of water is very important.

Various different pathways have been reported for the preparation of organogermanium halides, starting from germanium metal, other halides, arylgermanium compounds or hydrides. As already mentioned, Grignard and organolithium reagents are readily used compounds for the introduction of aryl groups onto a germanium halide, however such reactions usually result in a mixture of products, with mono-, di- or triarylgermanium halides present, regardless of the stoichiometry.[15-19] Even with an excess of Grignard or organolithium reagent, high yields are rare. A further complication is the occurrence of halogen-metal exchange when using educts with different halogens.[9] Lithium or magnesium reagents are recommended for introducing alkyl groups in the synthesis of very sterically hindered molecules.[20] $phenyl_3GeBr$ was first prepared by Morgan and Drew using the Grignard route.[10]

As already mentioned in Chapter 1.1.1 for the preparation of tetrasubstituted organogermanes, Cerveau *et al.* were also able to successfully gain trisubstituted

germanium halides by preparing the hexaanionic germanium complex starting from GeO_2 and further reaction with Grignard reagents.[14]

Comproportionation reactions of group 14 elements are widely known in literature and have been used a lot for silicon and tin derivatives (Figure 8).

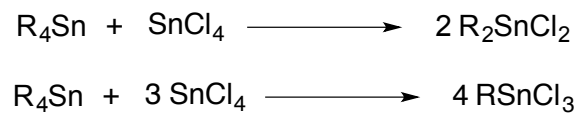

Figure 8. Kocheshkov redistribution reaction of tetraalkyl- or tetraaryl tin compounds with tin tetrachloride.[21,22]

However, when it comes to germanium, equilibria are often set up, resulting in a mixture of products from which it is very difficult to separate the desired compounds. High temperatures are of importance, although can be lowered using catalysts, nevertheless the heterogeneity of the mixtures adjusting the experimental conditions are challenging. Redistribution reactions have been carried out between arylgermanes and germanium halides in the presence of catalytic amounts of $AlCl_3$, in some cases with the help of microwave irradiation (Figure 9 and Figure 10).[23-26]

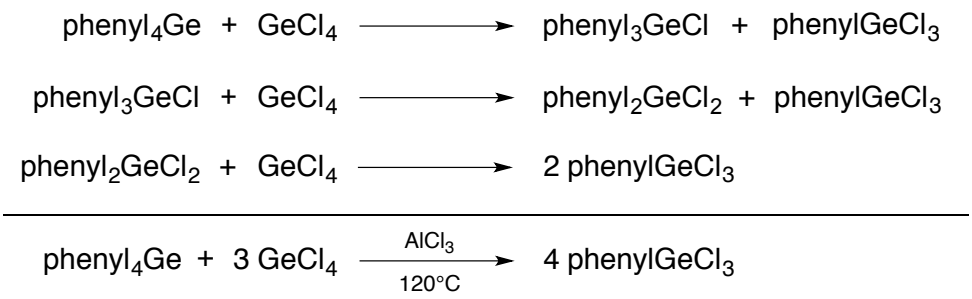

Figure 9. Preparation of $phenylGeCl_3$ over redistribution reactions.

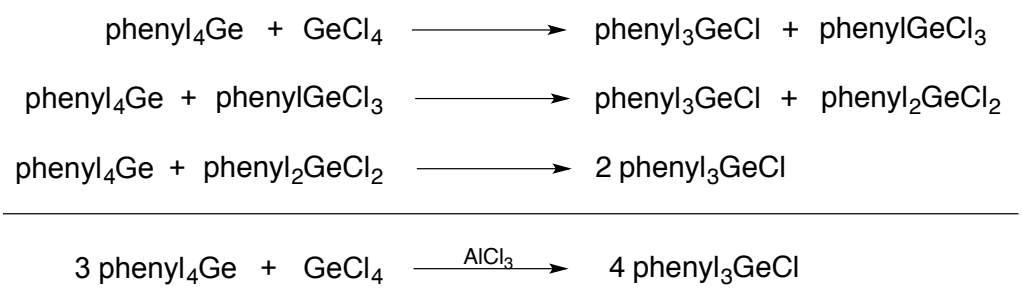

Figure 10. Preparation of phenyl$_3$GeCl over redistribution reactions.

Transmetalation reactions with organomercury compounds are known, however have never experienced widespread use due to the high toxicity of organomercury compounds and low yields.[27-29] phenyl$_2$Hg has been employed for the preparation of phenylGeCl$_3$, however, arylmercury compounds are not widely used due to their difficult handling.[28]

The reaction of arylsilicium chlorides with germanium tetrachloride in the presence of aluminum trichloride (Figure 11) was investigated closely. Reactions of diphenylsilicium dichloride and germanium tetrachloride afforded diphenylgermanium dichloride.[30] Later, it was shown, that diphenylgermanium dichloride was formed not only in the case of diphenylsilicium dichloride used as a reactant, but also with triphenylsilicium chloride and tetraphenylsilane. An increase of catalyst concentration lead to the formation of phenylgermanium trichloride, while at lower concentrations the di- and triphenylgermanium chlorides were favored. The reaction of phenylsilicium trichloride with germanium tetrachloride gave phenylgermanium trichloride in good yields, with no influence of the catalyst concentration.[31]

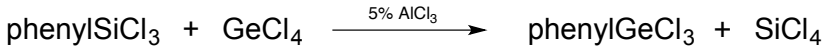

Figure 11. Transfer of a phenyl moiety from a silicon to a germanium central atom with AlCl$_3$ as a catalyst.

Kultyshev *et al.* expanded the previously used method for the transmetalation from tin to germanium in order to prepare arylgermanium trichlorides, *via* reaction of an aryltributylstannane with GeCl$_4$.[32,33]

Halogenation of organogermanes is yet another possibility for the preparation of arylgermanium halides. While bromides and iodides can be prepared using elemental halides, chlorides are normally prepared by employment of a halocarbon solvent.[34] Kraus and Foster were able to prepare phenyl$_3$GeBr by the bromination of phenyl$_4$Ge in CCl_4.[11] Simons *et al.* prepared tri-*m*-tolylgermanium bromide and tri-*o*-tolylgermanium bromide by refluxing the tetrasubstituted compounds in CCl_4 in the presence of bromine (Figure 12).[9] Other useful halogenating compounds include hydrogen halides or haloalkanes. However, the reactions are difficult to control and intermediate stages of the types $RGeX_3$, R_2GeX_2 and R_3GeX are very challenging to separate.

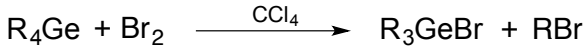

Figure 12. Cleavage of tetraorganogermanes by bromine, with *e.g.* R= phenyl, *o*-tolyl, *m*-tolyl.

If the organogermanium hydride is available, the halogenation using haloalkanes, inorganic chloride or even elemental halides is an useful route, with good yields, since the Ge-H bond can be substituted more easily than the Ge-C bond. In recent years, this route has shown to be a successful way to isolate the desired halogen without the formation of product mixtures. It was shown several times that carbon tetrachloride with DBP (dibenzoyl peroxide) and *N*-chlorosuccinimide or *N*-bromosuccinimide are useful reagents for the replacement of hydrogen (Figure 13).[15,16,35,36]

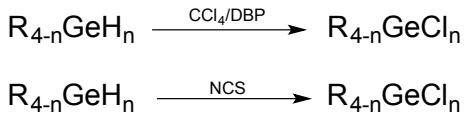

Figure 13. Chlorination of organogermanium hydrides using CCl_4/DBP or NCS, with R= phenyl, 2,6-^{i}propyl$_2$phenyl, 2,4,6-mesityl, 2,4,6-^{i}propyl$_3$phenyl.

Ohshita *et al.* were able to replace the hydrogen atom in organogermanium hydrides one at the time by usage of $CuCl_2$ in ether or toluene, yielding the organogermanium hydrochlorides.[37] Treatment of phenyl$_2$GeH$_2$ with $CuCl_2$/CuI lead

to the formation of phenyl$_2$GeCl$_2$, however, in the absence of the catalytic CuI only monohalogenation occurs (Figure 14).

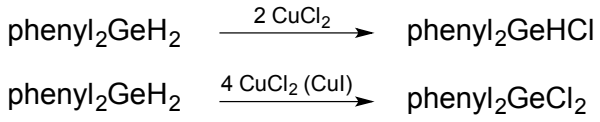

Figure 14. Mono- or double chlorination of phenyl$_2$GeH$_2$, dependent on the employment of CuCl$_2$ or CuCl$_2$ (CuI).

The same reaction was performed for the chlorination of (*o*-^{t}butylphenyl)GeH.[17] Organogermanium hydrochlorides are of interest because of their use in dehydrohalogenative coupling reactions in order to prepare digermanes and preparation methods involve the redistribution between organogermanes and germanium tetrachloride, monohalogenation with reactants such as chloromethoxymethane, *N*-bromosuccinimide, *N*-iodosuccinimide, HgCl$_2$ or HgBr$_2$, or partial hydrogenation.[16,38,39]

Reaction of an arylbromide with GeCl$_2$·dioxane in the presence of catalytic amounts of AlCl$_3$ lead to the insertion of the germanium moiety into the C-Br bond, resulting in a mixture of germanium trichlorides and tribromides. Through this route phenyl-, *p*-tolyl- and 2,4,6-mesitylgermanium halides could be obtained.[40] Two other possibilities are the usage of germylenes or the addition of germanium hydrides to unsaturated compounds.[41-43] The first case demonstrates that the reaction of elemental germanium with germanium tetrachloride leads to the formation of dichlorogermylene, which can then react further to the desired arylgermanium halide, although side products were formed due to disproportionation reactions (Figure 15).[44]

Figure 15. Preparation of phenylGeCl$_3$ *via* reaction of germanium metal and germanium tetrachloride and subsequent reaction of the dichlorogermylene with phenylchloride. [44]

1.1.3. Organogermanium hydrides

Arylgermanium hydrides R_3GeH, R_2GeH_2 and $RGeH_3$ are of high demand because they exhibit important features that might possibly lead to a range of new applications and are powerful precursors for the synthesis of oligo- and polygermanes. Furthermore, volatile germanium compounds can also be used for the preparation of thin films, epitaxial growth or germanium alloys in microelectronics. However, germanium hydrides, especially the aryl derivatives, have been neglected because of a limited range of preparation methods. In 1902, Voegelen *et al.* were able to synthesize the first hydrogen compound of germanium upon reaction of zinc with germanium in the presence of sulfuric acid leading to the generation of GeH_4.[45,46] Since then, various other germanium hydrides were synthesized. In 1955, Gilman could show that tetraphenylgermane reacts with lithium metal to form the germyllithium phenyl$_3$GeLi, a very useful intermediate itself, which can be further transformed into the corresponding hydride (Figure 16).[47]

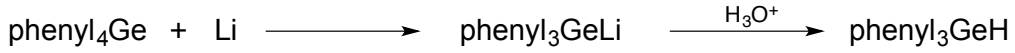

Figure 16. Formation of triphenylgermyllithium and transformation into phenyl$_3$GeH.

The cleavage of aryldigermanes by alkali metals in ether based solvents such as 1,2-dimethoxyethane is yet another alternative route for the preparation of germanium hydrides (Figure 17).[48]

Figure 17. Cleavage of hexaphenyldigermane using lithium metal and transformation into phenyl$_3$GeH.

The reduction of triarylgermanium halides using either lithium or metal hydrides in anhydrous organic solvents has been reported, *e.g.* treatment of phenyl$_3$GeCl with lithium metal in THF gave the germyllithium intermediate, which

can be reacted further to give phenyl$_3$GeH, as was shown in the previous case (Figure 18).[49]

Figure 18. Reactions between phenyl substituted germanium compounds and lithium metal.

Triorganogermanium hydrides can, contrary to the silicon or tin counterparts, in which cases reactions of R_3EH (E = Si, Sn) with organometals lead to alkylation, be prepared upon reduction of R_3GeX, *e.g*. with zinc amalgam in hydrochloric acid.

The usage of metal hydrides, such as lithium aluminum hydride ($LiAlH_4$) or sodium borohydride ($NaBH_4$), is the most direct and effective route to organogermanium hydrides and has been reported numerous times.[15-17,19,40,50] For example, the reaction of phenyl$_3$GeBr with $LiAlH_4$ in diethyl ether yields the desired hydride compound (Figure 19).

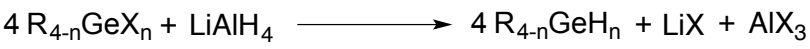

Figure 19. Hydrogenation of organogermanium halides using lithium aluminum hydride ($LiAlH_4$) with *e.g.* R = phenyl, *p*-tolyl, *o*-^{t}butylphenyl, 2,4,6-mesityl.

Diarylgermanium dihydrides are very useful starting materials, as was demonstrated 1990 by Castel *et al.*, when successfully preparing diarylgermyl lithium compounds using a modified hydrogermolysis reaction. Organogermyl alkalimetal compounds can be used for the preparation of asymmetric hydropolygermanes, germylation of organic halides, carbonyl compounds and metal halides.[51]

1.1.4. Applications: Oligo- and Polygermanes and Nanoparticles

The concept of molecular wires, in this case compounds of group 14 elements with element-element bonds (Figure 20), has attracted a lot of interest in the last years, due to their possible applications in industrial application, such as molecular electronics and nanotechnologies. However, studies into their potential applications have been limited due to the lack of preparative approaches to synthetic building blocks and cost intensive preparation.[52] Nevertheless, the constant request towards improvement makes the development of alternative materials a profitable challenge.

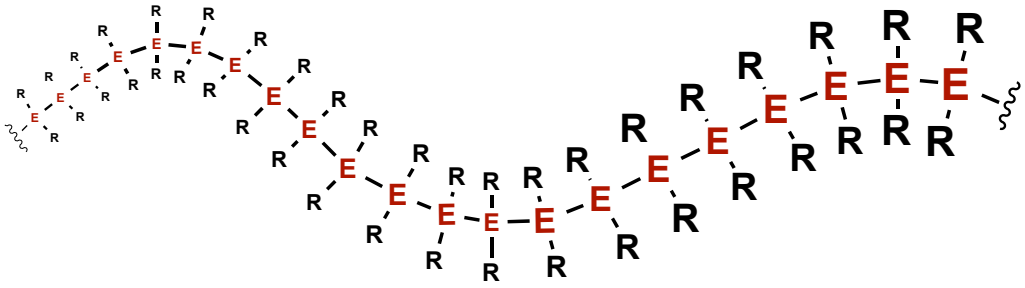

Figure 20. Scheme of an aryl substituted group 14 molecular wire (E = Si, Ge, Sn).

Nowadays, the most common molecular conductors are carbon based, although oligomeric and polymeric silanes and stannanes have been explored as well.[53-60] Compared to the modest interest in the organometallic chemistry of germanium, the field of oligo- and polygermanes has not been studied as extensively, although the first oligomer was already prepared in 1925 by Morgan and Drew.[10] Nevertheless, the promise of new optical and electronic properties of these compounds prompted persistent efforts in their preparation and characterization, since well-defined oligogermanes could not only be used for industrial applications, but compounds in the nanometer scale could give more insight into the properties of germanium nanostructures. The key to enhancing performance of today's applications lie without doubt in the materials used and thus, even though new materials have to meet a lot of requirements as possible replacement candidate, organogermanes might meet these requirements.

The Ge-Ge single bond is considered to be stable, but weaker than the C–C or Si–Si bond. Functional groups or halogens tend to stabilize the Ge-Ge bond. Most known oligogermanes are bearing electron donor groups, since oligogermanes bearing electron-withdrawing ligands are unstable and tend to decompose.[61]

The most interesting feature of heavier group 14 analogues is their so-called σ-conjugation, which has been already described for oligosilanes.[62-65] Nevertheless, differences are expected due to different conformational behavior attributed to the differences in bond length. The effective overlap of hybridized atomic orbitals of the elements next to each other leads to the distribution of electron density along the chain. In detail, the pair of electrons in the HOMO is delocalized across the germanium-germanium backbone making $\sigma \rightarrow \sigma^*$ electronic transitions possible. This attribute results in broad but distinct absorbance peaks in UV/VIS spectra and shifts of λ_{max} to lower energy.[62,66-68] The energy of the HOMO-LUMO gap in these compounds decreases with an increase in the number of catenated germanium atoms. Additionally, σ-delocalization leads to properties known for unsaturated hydrocarbons, such as absorption in the UV region, luminescence, conductivity, thermochroism as well as optical and electrochemical properties. Those properties highly depend on the nature and steric demand of the substituents and the chain length.[69] This was shown for the characteristic electronic absorption bands of polygermanes, which are normally around 300-350 nm, and for the decreasing ionization potential of oligogermanes in reliance to the number of germanium atoms.[70-72]

Oligogermanes are also electrochemically active. Cyclic voltammetry and differential pulse voltammetry have shown to be useful methods for investigating this behavior. Germanium polymers show non-linear optical properties, fluorescence and semiconductive behavior as well. These properties are even more prominent than in comparable silicon derivatives due to the smaller band gap and higher electron and hole mobility in germanium.

Ge–Ge bonds have been achieved by various methods, amongst them are Wurtz-type condensation reactions, the employment of Grignard or organolithium reagents, usage of samarium(II)iodide or germylene insertion into haloger-

manes, therefore making the aforementioned precursors all the more important (Figure 21). The first digermane hexaphenyldigermane was synthesized by reacting phenyl$_3$GeBr with sodium metal *via* a Wurtz-type coupling.[10] After that, Wurtz-type reactions between germanium halides and an alkali metal (Kipping method) were used various times, even though the preparation conditions were very difficult and the reactions were normally accompanied by low yields, and formation of side products.[73-76] Similar problems have been described when employing Grignard or organolithium reagents, depending on the conditions and stoichiometry used.[77-87] *p*-tolyl$_3$GeGe(methyl)$_2$ was prepared from *p*-tolyl$_3$GeH *via* lithiation with ^{n}BuLi and further treatment with methylGeBr.[88]

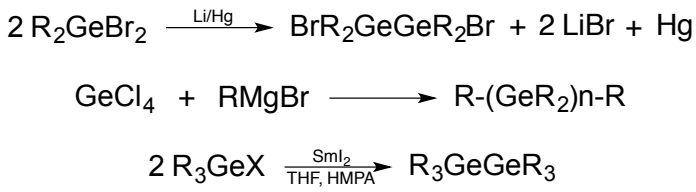

Figure 21. Various methods to generate Ge-Ge bonds, R = alkyl or aryl.

It is assumed that discrete linear oligogermanes with sufficing Ge atoms show similar properties and behavior as polygermanes, including *e.g*. fluorescence near the UV- region. The, up to this point, longest linear oligogermane ^{i}propyl$_3$Ge(Ge(phenyl)$_2$)$_4$Ge^{i}propyl$_3$ was obtained starting from the cyclic compound Ge$_4$phenyl$_{12}$, which was cleaved using bromide in benzene, followed by conversion into the hydride and hydrogermolysis reaction with ^{i}propyl$_3$GeN(methyl)$_2$.[89]

The hydrogermolysis reaction, the reaction of a reactive α-germyl nitrile intermediate with a labile Ge–C bond that reacts with a Ge-H bond (Figure 22), has found widespread use. According to various working groups it is the key step in forming Ge-Ge bonds, since germanium atoms can be added to the chain stepwise, allowing the control over the number of germanium atoms and their substituents (Figure 22).[18,19,88,90-92]

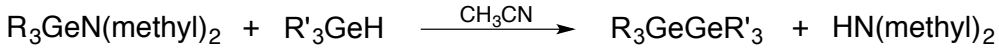

Figure 22. Formation of Ge-Ge bonds by employment of the hydrogermolysis reaction, *e.g.* R = ethyl, ^{i}propyl, ^{n}butyl, ^{i}butyl, phenyl, *p*-tolyl.

A first attempt to transform substituted organogermanes into polygermanes was made in the 1980s by Trefonas *et al.*, when ^{n}butylgermanium dichloride was reacted with sodium to eliminate sodium chloride, a route that has been used prior for the preparation of polysilanes (Figure 23).[93]

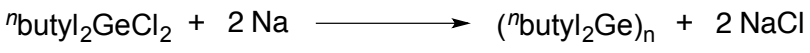

Figure 23. Preparation of (^{n}butyl$_2$Ge)$_n$.

In 1994, it was shown that temperature, as well as the choice of solvent, have an impact not only on the yield, but also on the molecular weight distribution. With the employed Wurtz-type coupling reactions molecular weight distribution is normally larger, but also depends on the nature of the precursor used.[72] This suggests that the mechanism of these kinds of reactions is more complex than it appears. Other possibilities for the preparation of polygermanes are the electrochemical synthesis of polygermanes and the reaction of organolithium reagents with GeCl$_2$·dioxane (Figure 24).[94-96]

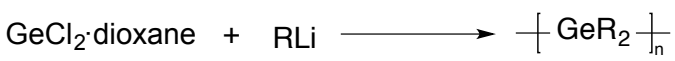

Figure 24. Reaction of GeCl$_2$·dioxane with organolithium reagents to yield polygermanes, with R = methyl, ^{n}butyl and phenyl.

Polygermanes are quite light sensitive and tend to degrade photochemically as well as at higher temperatures, thus limiting their use.[72,97] Encapsulation and immobilization in an inert inorganic matrix helps with these problems without degrading Ge–Ge σ-conjugation.[98] Fa and Zeng investigated the effects of substituents on the bandgap of polygermanes *via* compulsory methods, showing that the bandgap can be reduced when using sterically more demanding ligands.

For instance, in the case of polydiphenylgermane, the tensile strain results in a significant bandgap reduction.[99]

Since the preparation of oligo- and polygermanes is not only difficult, but also very cost intensive, several attempts were made to replace a number of germanium atoms with silicon or tin and investigations regarding the consequences were conducted. Very recently, Zaitsev *et al.* investigated the effect of introducing silicon and tin atoms in germanium compounds. It was demonstrated that incorporation of tin atoms leads to a bathochromic shift in the UV absorption and an increase of the oxidation potential.[88] Brook *et al.* were able to introduce the $(methyl_3Si)_3Ge$ moiety and the working group of Marschner was later able to prepare $(methyl_3Si)_3GeK$, which shows potential to be used as single-source precursors in the synthesis of germanium nanowires containing a crystalline germanium core with a silicon oxide shell.[100-102] Investigation towards the influence of replacing silicon with germanium atoms were made by the same group, showing that no mayor differences could be seen.[62]

In consequence of semiconductor nanoparticles showing unique size- and shape dependent electronic and optical properties, they have gained some interest in the past. Moreover, the discovery of visible photoluminescence from silicon and germanium nanostructures opened up a new field of possible applications. Germanium nanoparticles are expected to function as direct band gap materials.[103-108]

However, the lack of simple synthetic approaches for the preparation of Ge nanoparticles, which are mainly based on thin film- or physical methods, for example chemical vapor deposition, etching and plasma techniques, limited their use thus far. Moreover, the difficulty regarding size control made using germanium nanoparticles in a larger scale very challenging. Other successful routes to germanium nanomaterials include metal hydride reduction of nonpolar solutions of tetravalent germanium compounds, germanium ion implantation by molecular beams, RF sputtering, as well as the employment of supercritical solvents.[52,109-118] Often high temperatures or strong reducing agents are required, entailing problems with either contamination and difficult work-up or high energy up-

take.[119,120] Matioszek *et al.* could show that the conditions required for the generation of nanoparticles are highly dependent on the nature of the ligand used, giving more insight into the chemistry of main group metal nanoparticles and possibly leading to future low temperature thermolysis pathways.[121] Schrick *et al*. were able to prepare germanium nanoparticles starting from linear and branched oligogermanes and could show that the nanoparticle size highly depends on the number of catenated germanium atoms. Interestingly, their nanoparticles showed fluorescence.[122] Prabakar *et al.* synthesized germanium nanocrystals *via* hydride reduction, using lithium aluminum hydride, lithium triethyl borohydride, lithium borohydride or sodium borohydride, of germanium tetrachloride in inverse micelles.[123] Crystalline germanium nanocrystals were synthesized in supercritical hexane and octanol starting from diphenylgermanium dihydride.[113] Oxide-embedded germanium nanocrystals showing luminescence were prepared by the reductive thermal processing of polymers from phenylgermanium trichloride.[108] Heath *et al.* were able to prepare nanostructures in three different sizes from germanium chlorides and organogermanium chlorides by ultrasonic mediated reduction.[124] Some nanocrystals showed strong blue luminescence. This makes the compounds interesting for application as optical probes, since germanium quantum dots are becoming popular as replacements for fluorescent dyes. Other toxic quantum dots, based in biological fluorescence imaging, due to their resistance to photobleaching, could also be replaced.[125,126]

Due to the increasing energy consumption the demand of today's world for novel energy storage systems and the quest for materials, which might enhance their performance, have become an extensive task.[127-132] In the past germanium has been considered as Li-allyoing electrode material for next generation lithium ion batteries, possibly improving the capacity compared to standard graphite anodes.[127,133-136] Graphite itself has a relatively low theroretical capacity of 372 mAh/g. Incorporating Ge as a Li alloying anode leads to an increase of theoretical capacity about 4 times higher than that of the commercial graphite anode (to 1623 mAh/g). Although the theoretical capacity of the Li-Ge system is by far lower compared to the theoretical capacity of Li-Si, Ge has the big advantage

that the diffusion rate of Li^+ in Ge is significantly higher and furthermore shows a higher electrical conductivity (10^4 times higher than silicon).[135]

However, the biggest obstacles to face are the poor cycling stability and the rapid capacity loss.[137] Nanomaterials with bigger surfaces provide more active reaction sites for Li^+, which might be an effective approach for improvement. The agglomeration of nanoparticles displays yet another problem, which normally leads to limitation of the lithium ion diffusion pathway. Therefore Jin *et al.* prepared Ge nanoparticles under the aid of *in-situ* grown graphene, creating hybrid nanostructures to prevent this problem. Promising results towards improving cyclability, but also eliminating particle agglomeration and pulverization were reported.[138]

1.2. Organoantimony compounds

Antimony is an inherent part of nature, and is abundant in the form of sulfide minerals, such as stibnite, which is the predominant ore mineral of antimony, tetraedrit or pyrostilpnit. It also occurs as the degradation product Sb_2O_3 in form of valentinite. Various methods for the isolation of antimony are known, most starting with Sb_2S_3 (Figure 25).[1]

$$Sb_2S_3 + 5\ O_2 \longrightarrow Sb_2O_4 + 3\ SO_2$$

$$Sb_2O_4 + 4\ C \longrightarrow 2\ Sb + 4\ CO$$

Figure 25. Preparation and isolation of antimony.

The extraction depends on the composition and quality of the ore. Sulfide ores with an antimony content higher than 40% are melted in the presence of iron to yield elemental antimony and iron sulfide. Industrial synthesis for sulfides with lower antimony concentration involves the roasting of antimony ores at 550-

600°C to convert the sulfide into the oxide Sb_2O_4 or Sb_2O_3, respectively. The process depends on the amount of air used during roasting followed by reduction with carbon. Antimony isolated this way contains minor impurities, *e.g.* sulfur, arsenic or lead. These can be removed upon melting in presence of sodium nitrate and sodium carbonate and can be separated in form of oxidation products. Metallic antimony is used in alloys with tin and lead for energy storage systems, bullets, microelectronics and plain bearings.

The field of organoantimony chemistry has afforded early interest with the first organoantimony compound synthesized around 1850 by Löwig and Schweizer.[139] While the development of other group 15 elements such as phosphorus progressed steadily, organoantimony compounds were neglected for several years and a lot of examples found in literature can be considered only to be convenient extensions of work with phosphorus. The advantages of Sb ligand systems compared to P and As compounds clearly lie in their higher flexibility and reactivity. In general, there is a progressive variation in physical properties going from nitrogen to bismuth, with some properties, including electronegativity or bond energies not following a pattern and nitrogen differing considerably. The metallic and electropositive character increases from nitrogen to bismuth, while their ionization potentials decrease.

One reason why organoantimony compounds have been neglected might be that the Sb–C or Sb–Sb bond is not as stable as related congeners and therefore working at low temperatures and inert gas atmosphere is a necessity. Compounds of antimony have been used as therapeutic and pharmaceutical agents for quite some time, but were replaced with organoarsenicals after the discovery of arsanilic acid. With the discovery of Penicillin in the 1940's the demand for organoarsenicals decreased rapidly, although some are still used as pesticides. The interest in organoantimony compounds gained momentum again in the 1980's due to their potential employment as useful precursors in material science, organic synthesis or industrial applications.

1.2.1. Triorganostibanes

Triorganometal compounds of antimony are amongst the organometallic compounds with the longest history, due to them being used in organic synthesis such as Wittig-type coupling reactions, as reducing agents or as aryl donors. Their employment in palladium-catalyzed processes as aryl group donors has been described various times.[140-143] However, tervalent stibanes have been investigated to a lesser extent than the pentavalent organic compounds of antimony.[144,145]

The most common methods to prepare tervalent antimony compounds include employment of Grignard or organometallic reagents, in the latter case *e.g.* organolithium, organomercury or organocadmium (Figure 26).[146-149]

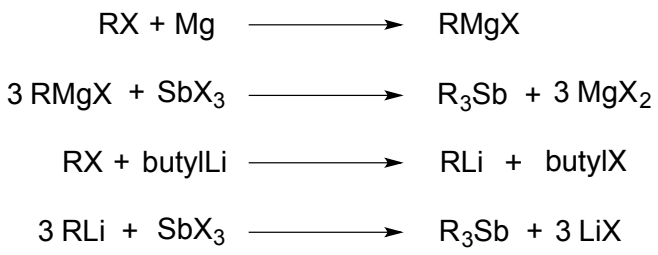

Figure 26. Reaction of antimony halide with organometallic reagents, *e.g.* Grignard or organolithium reagents.

These preparations are often accompanied with difficulties in controlling the reactions, work-up and low yields, as described for 2,4,6-mesityl derivatives.[150] Other routes involve the formation of alkali metal antimonides, which can then react with a wide variety of electrophiles, or the usage of metal oxides as starting materials.[151-153] Lee *et al.* were able to prepare (phenanthrenyl)$_3$Sb by reacting 9-phenanthrenyllithium with $SbCl_3$.[154]

Triorganstibanes can be considered as Lewis bases or donors, for which reason several transition metal complexes have been reported. Their reactivity highly depends on the nature of the substituent and their structure. While alkyl compounds are air-sensitive and strong reducing agents, aryl analogues, which are

often crystalline, seem to be more stable. Larger ligands, such as 2,6-dimesitylphenyl are known for helping to stabilize the compounds.[155]

In 2005, Yasuike *et al.* were able to show that trivalent triarylstibane, amongst them triphenylstibane itself, is an effective catalyst for the oxidation of diaryl-α-ketoalcohols into the corresponding α-diketones under aerobic conditions.[156] Interestingly, the same catalytic reaction carried out with other group 15 analogues did not give any adequate results. While pentavalent organoantimony compounds are known as efficient reagents in palladium-catalyzed C-C bond formation, tervalent compounds are limited due to the necessity of additional oxidants being present. In 2003, it was shown however, that triarylstibanes can act as mildly efficient arylating agents when peroxide and Li_2PdCl_4 in catalytic amounts are present.[157]

Tri-*o*-tolylstibane undergoes oxidative addition reactions when reacted with oximes in the presence of ^{t}butyl hydroperoxide, as has been reported by Sharutin *et al.*[158,159] Moreover, it was shown that tri-*m*-tolylstibane reacts with benzoic acid in the presence of ^{t}butylhydroperoxide in order to form tri-*m*-tolylantimony dibenzoate.[160] Tri-*p*-tolylstibane reacts with trifluoroacetic, trichloroacetic and iodoacetic acids in the absence of oxygen in order to form tri-*p*-tolylantimony dicarboxylates. Reaction of tri-*p*-tolylstibane with toluenesulfonic acid and 2,4,6-trinitrophenol leads to the formation of tri-*p*-tolylantimony bis(toluenesulfonate) and bis(2,4,5-trinitrophenoxide).[161]

1.2.2. Organoantimony halides and hydrides

A well-established pathway for the preparation of organoantimony halides is the thermolysis of the corresponding pentacoordinated species R_3SbX_2 with loss of an alkyl or aryl halide. The process is time consuming and yields vary greatly. It has been observed that compounds bearing ligands with higher steric demand tend to have lower decomposition temperatures. Moreover thermal stability

decreases from chloride to iodide compounds.[162] Other pathways include the partial alkylation of SbX_3 with Grignard or organolithium reagents, which works in the case of sterically less demanding substituents, arylation using group 14 element compounds or comproportionation reactions between R_3Sb with SbX_3.[150,163-165] Exchange reactions (Figure 27) have been reported to result in product mixtures making purification and work-up difficult. The preparation of $phenyl_2SbX$ and $phenylSbX_2$ (X = Cl, Br) has been achieved by reaction of $phenyl_3Sb$ and SbX_3 in the theoretical molar ratios. No solvents or heat are required.[166,167]

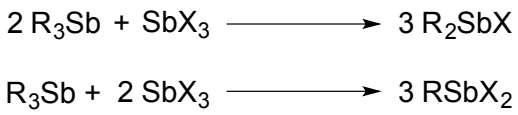

Figure 27. Comproportionation reactions of trisubstituted antimony compounds.

Nunn *et al.* reported that while $phenyl_nSbX_{3-n}$ (with X = Cl and Br and n = 1 and 2) can be handled under air, the corresponding alkyl substituted compounds must be protected against oxidation.[166] This praises the benefits of using aryl substituted organoantimony compounds on the one hand, on the other hand preparation turns out to be rather difficult, nor do the reactions proceed with high yields.[168,169] Millington and Sowerby successfully prepared *p*-tolylantimony dichloride and bromide starting from *p*-bromotoluene, lithium metal and antimony trichloride and reacting it with freshly sublimed antimony trichloride.[170] Transmetalation reactions are yet another possible pathway, however this method is hardly used due to difficulties in terms of controlling the reaction, ligand exchange processes, disproportionation reactions or the cleavage of distibanes.[166,171-174]

The reaction of 2,6-dimesitylphenylMgBr with $SbCl_3$ yields 2,6-dimesitylphenyl$SbBr_2$ by halide exchange. Copolovici *et al.* were able to obtain chiral organostibanes, with three different substituents attached to the antimony center, which have been of interest because of the potential usage as chiral sources for the inductive generation of optical activity.[175]

Secondary bonding plays an important factor in solid state structures of tervalent antimony halides.[170] The interactions of the Lewis acidic centers at the metal and Lewis basic centers at the halogen atoms lead to the formation of extended structures. Intermolecular metal-halogen interactions between pyramidal molecules have already been described for *p*-tolylantimony(II)dichloride and dibromide. Exchanging a halogen with an organic ligand reduces the Lewis acidity and weakens intermolecular interactions. Becker *et al.* were able to show that some of those compounds not only form halogen bridges but also interact like Menshutkin complexes over non classical Sb···arene or Sb···π contacts, which determine the structure significantly.[176]

Antimony hydrides have been used as reducing agents or as precursors for electronic materials, however preparation and application is rather difficult, due to their low thermal stability. Many organoantimony hydrides are known to already decompose at room temperatures to form elemental antimony, or compounds with Sb-Sb bonds, as seen for phenylSbH_2.[1] However stability can be improved by using ligands with increased steric bulk, as could be shown for ^{i}butyl$_2$SbH, ^{t}butylCH_2SBH_2 *p*-tolylSbH_2, 2,4,6-mesityl$_2$SbH and 2,6-[2,4,6-^{i}propyl$_3$phenyl]$_2C_6H_3SbH_2$.[177-183] Antimony hydrides can be readily prepared from their halide analogues and normally show higher reactivity, thus have been used in organic synthesis for the reduction of carbonyl compounds such as aldehydes and ketones to the corresponding alcohols or benzotrichloride to benzylidenechloride.[177,184,185] Other reactions include the hydration of styrole and phenylacetylene or the addition to acetylene.[186,187] In 1998, Breunig and Probst investigated the reaction between *p*-tolylSbH_2 and phenyl$_2$SbH with organic compounds such as styrene, styrole or phenylacetylene, aldehydes and ketones or organohalides in great detail.[182]

1.2.3. Higher antimony derivatives and applications

To this date aryl substituted antimony compounds have shown various usable features in organic synthesis, coordination chemistry or as precursors for other organometallic compounds. Synthetic applications of organoantimony compounds are rapidly increasing, with a wide variety of possible reactions known, including self-coupling reactions, photoreactions, cross-coupling reactions etc.[140,144,167,188-195] Organometallic compounds possibly showing luminescence are becoming of great interest due to their potential employment in photochemical and electroluminescent devices. While phosphors have been investigated to a great extent, the heavier analogues might be interesting as well, due to their strong spin-orbital coupling. Moreover, they do not interfere with the electronic transitions of the ligand and allow valence expansion, first shown by the Wang group.[196] It was shown that heavier main group elements enhance the phosphorescent emission of the ligands.

Additionally, group 15 compounds incorporating chalcogenides have received growing interest as single-source precursors, enabling the synthesis of binary materials of the general type Sb_2E_3 (E = S, Se, Te), for their use in solar cells, battery materials or nanoparticles.[197] While several hybrid donor polydentates containing one antimony center in combination with other group 15 or 16 elements are known, compounds containing two antimony donor atoms are difficult to prepare and their coordination chemistry has been neglected. Levason *et al.* were able to prepare 2,3-, 2,4-, and 2,5-xylyldistibanes as well as the 2,4- and 2,5-phenylene distibane starting from $(methyl)_2SbCl$ and the respective di-Grignard and examine their coordination modes by employing them in reactions with nickel, iron and tungsten carbonyls.[198]

Group 15 compounds bearing an element-element bond have been mostly of interest due to their unusual color phenomena and possible application as ligands, however the number of known compounds decreases dramatically if Sb-Sb units are considered, for though compounds like these were already prepared early on, distibanes were not synthesized efficiently until the 1980s.[143,147,199,200] Comparison with other group 15 compounds shows that the strength of the

bond decreases from arsenic to bismuth with arsenic compounds dominating the field. It was first reported in 1934 by Paneth *et al.* that $[methyl_2Sb]_2$, prepared by using methyl radicals and elemental antimony, shows "thermochromic" behavior, meaning the distibane is bright red in solid state, but melts at 17°C to a yellow liquid.[201] This behavior was also observed for several other distibanes, such as $[methyl_3Si)_2Sb]_2$, $[methyl_3Ge)_2Sb]_2$, $[ethyl_2Sb]_2$ and 3,3',4,4'-tetramethylbistibole.[202-205] The reason for this phenomena are weak intermolecular metal-metal interactions, which are formed in the solid state, when bearing sterically less demanding organic substituents, leading to extended chain- like structures (Figure 28).

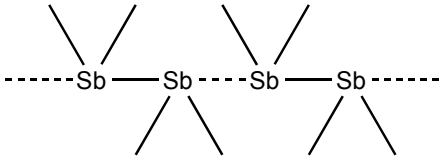

Figure 28. Intermolecular interactions between antimony metal centers shown as dotted lines on the example $[methyl_2Sb]_2$.

The strength of these interactions depends on the bulkiness of the organic substituents and their electronic properties; however Sb–Sb contacts are normally smaller than the sum of van der Waals radii and therefore make electronic interactions possible. These interactions are normally broken upon melting, leading to a bathochromic shift between fluid and solid phases, causing the change in color.[206,207] In contrast, tetra^{n}propyl-, tetraphenyl- and tetramesityldistibane are yellow and do not show this behavior upon melting.[208] This behaviour, and also the investigations towards thermostability make apparent that the organic residues used mainly determine the properties. $[phenyl_2Sb]_2$ was reported to be a promising reagent for substitution chemistry, making it an excellent radical trap.[209] In 2014, the distibylation of unsaturated carbon-carbon bonds with distibane was reported by Ohshita *et al.*, with $[phenyl_2Sb]_2$ reacting with acetylenes in order to form *anti*-adducts, one of them showing phosphorescence.[210]

Another interesting field of organoantimony chemistry is without doubt the abundance of ring structures containing Sb–Sb bonds. Dehaloganation of alkylan-

timony dibromides with magnesium in THF at room temperature normally results in formation of cyclostibanes. In solution, pentameric rings dominate over tetrameric ones. Trimeric species can be observed as a side product.[211] Tri- and tetramembered ring systems are preferably formed at higher temperatures. Evaporation of solvents leads to the formation of black polymers or large rings, although this is a reversible process. The polymers normally show less reactivity than the corresponding rings, as observed with oxidation reactions. The reactivity of the rings is highly dependent on the nature of the substituent, with sterically less demanding groups reacting faster and allowing an equilibria between ring and chain like structures.[212] Interestingly, reduction of phenylantimony dibromide did not show the same results. The reduction results in a polymer, clearly distinguishable by its black color. However, addition of cyclic solvents, *e.g.* 1,4-dioxane, toluene or benzene, made the isolation of the six-membered ring possible. Moreover, it is important that no side products, including $SbBr_3$, and/or oxygen are present.[213,214] Breunig *et al.* state that the rings are only stable in air as crystals but react in solution with traces of air to give white solids, namely $(RSbO)_x$. Comparison of various tolyl derivatives showed that intermolecular interactions are not essential for the stabilization of antimony six-membered rings in the crystal.[211]

Chapter 2

Results and Discussion

2.1. Germanium compounds

2.1.1. Synthesis

Various organogermanium compounds were synthesized and characterized using NMR, IR, single crystal X-ray and GCMS methods. In all cases the germanium atom is bonded to at least one aromatic ligand. The ligands were chosen carefully concerning their steric bulk, bearing either one or two methyl groups in different positions towards the germanium atom, or include even larger polyaromatic systems. All ligands used are presented in Figure 29.

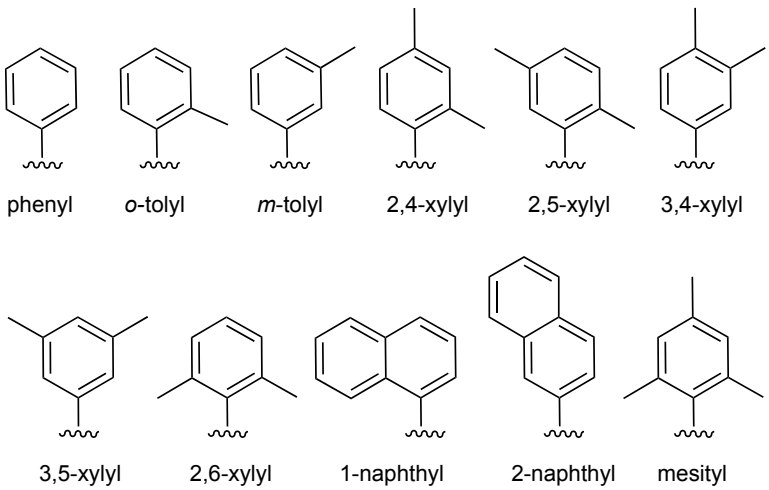

Figure 29. Aromatic ligands employed for the preparation of organogermanium compounds.

2.1.1.1. Tetraarylgermanes and triarylgermanium halides

Although tetraarylgermanes have no significant direct application, they make useful precursors for the preparation of other organogermanium species. Since the synthesis of organogermanium compounds does not follow the usual pattern known for the silicon and tin derivatives, numerous different pathways have been studied thus far. Due to this fact, there are a multiplicity of different methods known, but unfortunately until now, no versatile pathway could be found for the preparation of these compounds, a problem which has been discussed repeatedly in literature.[69,78,215] Most methods are unsatisfactory in terms of yields and formation of side products and include various steps and/or difficult work-up procedures. In this work, a number of different procedures were employed for the preparation of tetraarylgermanes, which turned out to be successful in a greater or lesser extent.

As mentioned in Chapter 1.1.1, one of the most often used methods is the employment of Grignard or organolithium reagents although entailing various disadvantages. These drawbacks include the formation of mixtures, from which the desired product is very difficult or in some cases impossible to separate, long and challenging work-up procedures and low yields, and as a consequence cost intensive preparation over a number of steps.[12] However, despite initial problems, known pathways were adjusted over the course of this work, enabling control of the reaction and therefore the formation of side products and yields in a reasonable way.

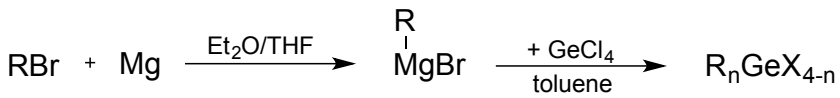

Figure 30. Grignard route for the preparation of R_4Ge and R_3GeX for R = *o*-tolyl (5), *m*-tolyl (1), 2,4-xylyl (6), 2,5-xylyl (7), 2,6-xylyl (8), 3,4-xylyl (2), 3,5-xylyl (3), 1-naphthyl (9) and 2-naphthyl (4).

In the case of the Grignard route (Figure 30), the synthesis of tetraarylgermanes and triarylgermanium halides follows the generally known Grignard route with varying stoichiometry of the Grignard reagent towards $GeCl_4$. By fol-

lowing this pathway only one product, either the tetraarylgermane or the triarylgermanium halide, is formed under the same reaction conditions (Figure 31).

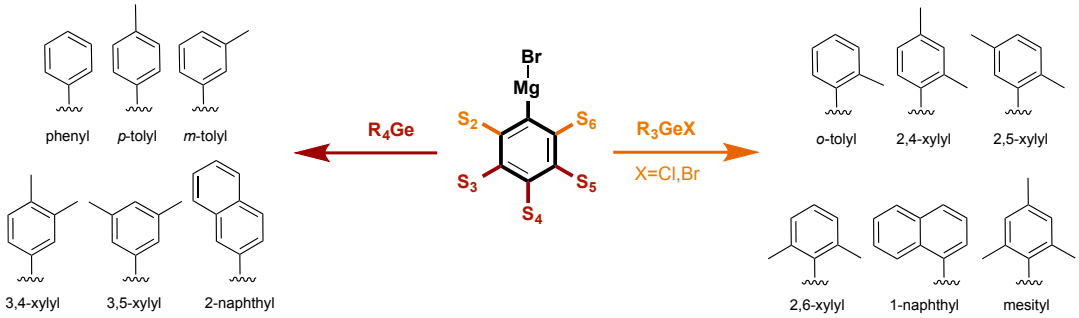

Figure 31. Influence of the steric bulk of the aryl substituents on product formation using the Grignard route.

It can be observed schematically in Figure 31, that while substituents in the 3-, 4- or 5-position do not have an impact on the nature of the product formed and thus lead to the tetraarylgermane, introduction of a carbon substituent in the *ortho* position exclusively leads to the formation of a triarylgermanium halide. Consequently, the steric demand seems to be too elevated in order for the reaction to conclude to the tetrasubstituted product. Despite this being described before, it can now be confirmed for a variety of aryl substituents showing different substitution patterns.[9,75,216,217]

Dumler *et al.* observed similar results for the preparation of 2,5-xylyl$_3$GeBr, once more proving the concept. 2,5-xylyl$_4$Ge can be prepared using a different pathway by reacting 2,5-xylylLi and 2,5-xylyl$_3$GeBr (Figure 32), although yields decreased notably compared to the introduction of ligands with less steric bulk.[218]

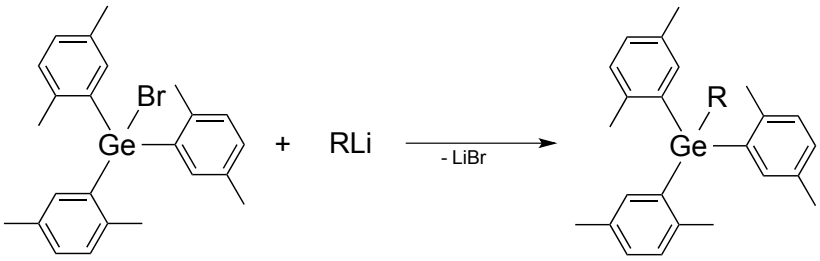

Figure 32. Reaction between 2,5-xylyl$_3$GeBr and RLi to generate 2,5-xylyl$_3$RGe with R = phenyl, *o*-tolyl, *m*-tolyl, *p*-tolyl, 2,5-xylyl and 3,4- xylyl.

Our observations were once more supported by results of Simons *et al.* concerning the preparation of *o*-tolyl$_4$Ge.[7] As opposed to this, Takeuchi *et al.* claim to prepare *o*-tolyl$_4$Ge using the Grignard route, however this could not be reproduced within the course of this work.[9,219] However, it is possible to prepare *o*-tolyl$_4$Ge over other preparation pathways, *e.g.* by reacting the Grignard reagent with zinc chloride, forming the arylzinc, which can be further reacted with $GeCl_4$, although the formation of mixtures is observed (Figure 33).[9]

Figure 33. Preparation of *o*-tolyl$_4$Ge using an arylzinc intermediate.[9]

Interestingly, this is not only observed in the case of methyl groups, but also when comparing the sterically more crowded moieties 1-naphthyl and 2-naphthyl. In 1952, West reported that all attempts to synthesize 1-naphthyl$_4$Ge over organolithium or Grignard reagents were unsuccessful, agreeing with the results of this work. Interestingly, reaction of 1-naphthylLi with 1-naphthyl$_3$GeBr gave small amounts of 1-naphthyl$_4$Ge (Figure 34).[217]

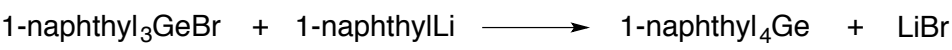

Figure 34. Preparation of 1-naphthyl$_4$Ge.[217]

Compulsory approximations, namely DFT calculations, were conducted and compared to the results by direct means conforming indeed, that the outcome of the reaction depends on the steric bulk of the ligands used. The reaction mechanism was investigated and the reaction enthalpies ΔH were calculated (ΔH= H(R_4Ge) + H($MgBr_2$) – H(R_3GeBr) – H(RMgBr)) (Figure 35, Table 1). The Gaussian09 program package[220] was used for all calculations at the mPW1PW91 hybrid functional[221] level together with 6-311+G(d) basis sets. All structures were optimized and verified to be minima by vibrational frequency calculations.

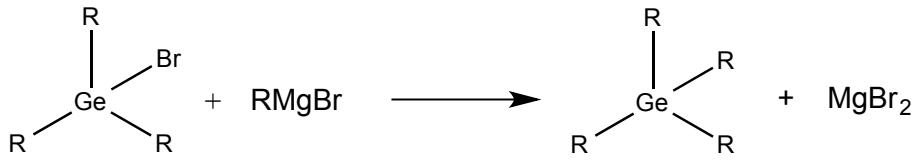

Figure 35. Base reaction for the calculation of the enthalpies ΔH, in dependence of the aryl residue used.

Table 1. DFT calculated reaction enthalpy ΔH values in kJ/mol for the preparation of R_4Ge in dependence of the aryl residue.

R	ΔH (kJ/mol)
2-naphthyl	-103.5
phenyl	-102.9
***m*-tolyl**	-102.4
3,5-xylyl	-102.3
3,4-xylyl	-101.4
2,5-xylyl	-90.5
1-naphthyl	-85.5
***o*-tolyl**	-68.0
2,4-xylyl	-54.1
2,4,6-mesityl	-41.5
2,6-xylyl	-36.0

It can be observed in Table 1 that the reaction enthalpy varies in value depending on the functional group introduced. It was possible to isolate and even recrystallize all systems showing a reaction enthalpy higher than -100 kJ/mol over the Grignard route. In contrast, all reactions showing lower values (ΔH< -100 kJ/mol) seemed to stop at the trisubstituted stage and the triarylgermanium halide was formed. Therefore, DFT calculations support the observation that formation of tetraarylgermanes is highly dependent on the steric bulk of the ligand used, since with increasing steric demand the reaction enthalpy decreases noticeably, showing the lowest value for the crowded 2,6-xylyl$_4$Ge.

In all cases it is crucial to use an excess of Grignard reagent compared to $GeCl_4$, in order to avoid side products. As already mentioned before, the reaction between the Grignard reagent and the germanium halide might be limited by steric

factors, thus forming product mixtures if not enough Grignard reagent is deployed.[16] The stoichiometry is adjusted for every ligand used, also depending on the performance of the Grignard reaction. In this case, it must be noted that a higher excess of Grignard reagent towards $GeCl_4$ is necessary for the preparation of tetraarylgermanes compared to the triarylgermanium halides, for the desired product to be formed and not stop at the trisubstituted intermediate. In the case of 2-naphthyl$_4$Ge (4), only a ratio of 1:5 was employed because of cost reasons.

Since a slight excess of magnesium is used for the Grignard reaction it is important for any magnesium residues to be removed before further reaction with $GeCl_4$ in order to avoid the formation of digermanes as described by Glockling *et al.* (Figure 36).[84]

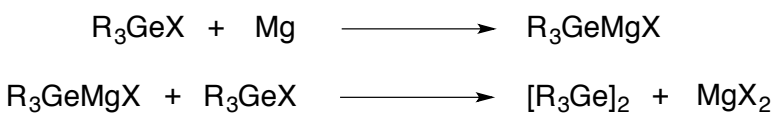

Figure 36. Side reaction leading to the formation of digermanes in the presence of magnesium, R = benzyl, phenyl, *o*-tolyl, *m*-tolyl, *p*-tolyl.[84]

For this reason, the Grignard solution was usually filtered *via* cannula. $GeCl_4$ in toluene was then added dropwise to the ethereal Grignard solution at 0°C and allowed to warm to room temperature. More toluene was added and the ethereal solvents were removed under *vacuo*. In some cases, the reaction mixture was refluxed for at least one hour, or stirred overnight at room temperature. After the reaction was complete, the mixture was quenched using diluted HCl (3-10%). The organic layer was separated *via* cannula and the water layer was washed twice with toluene. The organic layers were dried over Na_2SO_4 and the solution was filtered hot. Na_2SO_4 was washed several times with hot toluene and the filtrates were combined. It is important that the solution is filtered off hot from Na_2SO_4, due to product crystallizing at room temperature, and thus reducing yields. Toluene was removed under *vacuo* to receive the desired product, which was purified by washing with solvents or crystallized from toluene either at lower temperatures or *via* evaporation techniques.

It was observed for all ligands that the synthesis under inert gas atmosphere, even after quenching, afforded higher yields compared to work-up procedures under air. However, tetraarylgermanes seem to be stable in air for a reasonable time before decomposition, noticeable due to change of color.

Halide exchange (Figure 37) overcomplicates purification procedures, due to the fact that R_3GeCl and R_3GeBr species show very similar physical properties, making separation using standard techniques including extraction, crystallization or chromatographic methods difficult, if not impossible in certain cases. This problem was reported for other group 14 elements as well.[9,222,223]

Figure 37. Halide exchange upon reaction of R_3GeCl with $MgBr_2$.

Since R_3GeX can be transformed into the hydride derivatives without additional purification steps, further separation of the chlorides and bromides was not necessary, nonetheless stoichiometry cannot be applied correctly, which in some cases caused inconvenience. $GeBr_4$ was employed in rare cases upon investigating whether the desired product would be easier to separate from other germanium species *e.g.* diarylgermanium dibromides or arylgermanium tribromides. Halide exchange could be avoided, but unfortunately no further improvements could be observed. Since $GeCl_4$ is more cost-effective and is readily commercially available, $GeCl_4$ was used for all further experiments. Conversely, the replacement of arylbromides with arylchlorides was investigated. Problems occurred when trying to initiate the Grignard reaction, since no commonly established reaction starting aids, *e.g.* heat, iodine or dibromoethane, helped in the case of 1-naphthylchloride. Although the Grignard reaction did initiate in the case of phenylchloride as a comparison, yields were generally lower and thus substitution of RBr did not justify the effort.

In rare cases, the formation of hydrolysis side products was noticed, however this could be prevented when working under inert gas and quenching with diluted acids instead of degassed water. The nature, amount, and concentration of

the acid applied were investigated, showing that 10% HCl worked best when added in small portions until no further reaction was visible. Excess of 10% HCl however did not have an impact on the reaction itself, however, it is important to use degassed water in all cases. If not enough diluted acid is added, residual Grignard reagent interferes during work-up procedures, normally preventing the product from solidifying.

All attempts to crystallize 2,4-xylyl$_3$GeX (6) were unsuccessful. Recrystallization in solvents such as toluene, benzene, THF, Et_2O, DCM and DME at 0°C, -30°C and -80°C, or by evaporation of the same were not successful. For this reason, the oils obtained were used without further purification for further hydrogenation.

Although lithiation might work in most cases, it was only tried for selected ligands, namely 2,6-xylyl, 1-naphthyl and 9-anthracenyl (Figure 38).

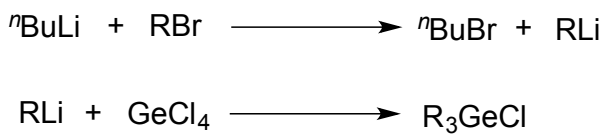

Figure 38. Lithiation of RBr and further reaction with $GeCl_4$ for R =2,6-xylyl, 1-naphthyl, 9-anthracenyl.

The Grignard route seemed to provide better yields and easier handling, although being more time consuming. Another well-known approach to tetraarylgermanes and triarylgermanium halides is the preparation route of Corriu *et al.*, which although claiming to be quite easy, never found widespread use. Reaction of a hexacoordinated germanium complex with an excess of Grignard reagents is supposed to give tetraorganogermanes in good yields, with no side products.[13,14]

Starting from GeO_2 upon reaction with 2,3-butanediol in the presence of potassium methoxide and degassed methanol as the solvent, $K_2[(C_4H_6O_2)_3Ge]$ (28) is formed.

This mixture was stirred for at least 1.5 hours, before removal of solvent. The purified product was then reacted with catechol and refluxed for 2 hours. Due to difficult characterization, it was difficult to establish whether the complex $K_2[(C_6H_4O_2)_3Ge]$ (29) was even formed. Normally, the powder showed a slightly pink color, which indicated that the desired intermediate was obtained. However, when reacting the hexaanionic complex with an excess of several tolyl, xylyl or naphthyl Grignard reagents, it was not possible to reproduce the reaction and to prepare any of the desired products. Often, the reaction resulted in a blue (Figure 39), cloudy solution, which turned dark green upon work-up, indicating some kind of decomposition. After purification, no products could be detected *via* NMR or GCMS methods.

Figure 39. Reaction of 1-naphthylMgBr with $K_2[(C_6H_4O_2)_3Ge]$ (29).

Another possible approach for the preparation of triarylgermanium halides includes distribution reactions, which are widely known in the case of silicon or tin compounds. Even though Zhun *et al.* were able to synthesize phenyl$_3$GeCl, they never isolated the product, but only verified its presence by chromatographic methods.[30,31] Zaitsev *et al.* were able to obtain phenyl$_3$GeCl in good yield (81%) by reacting phenyl$_4$Ge with $GeCl_4$ in a 3.3:1 ratio in the presence of $AlCl_3$.[224] Nevertheless, it was not possible to control those reactions on a lab scale for sterically more demanding ligands, such as 1-naphthyl or 2,6-xylyl (see Chapter 2.1.1.3).

Compounds 3,5-xylyl$_3$GeCl (11) and 2-naphthyl$_3$GeCl (12) were prepared from the respective tetraarylgermane by addition of trifluoromethanesulfonic acid (HOTf) in freshly distilled DCM, thus only yielding the chlorine derivative (Figure 40).

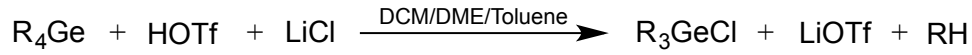

Figure 40. Reaction of R_4Ge with trifluoromethanesulfonic acid (HOTf) and further reaction with LiCl to yield R_3GeCl.

After stirring at room temperature for at least 24 hours the reaction progress was monitored using ^{19}F NMR. In case the reaction is not complete, further stirring at room temperature is advised. In the case of 2-naphthyl$_3$GeCl (12), LiCl was suspended in DME, added at 0°C and stirred for 24 hours. Toluene was added and DCM and DME were removed under reduced pressure. After filtration *via* cannula, the product was dried in *vacuo*, yielding a colorless solid. In contrast, for the 3,5-xylyl reaction, DCM was removed under *vacuo* and the solid was dissolved in DME again before adding LiCl as a solid in small portions at 0°C. The mixture was stirred for 24 hours, during which time yellow solids, probably sulfur side products, precipitated. All solvents were removed and the solid was dissolved in toluene again, filtered *via* cannula and the colorless solution was reduced under *vacuo*. Yields were low, presumably due to the fact, that not enough information was gathered regarding handling of the reactions at the time the experiments were conducted. It was shown in later experiments concerning the action of trifluoromethanesulfonic acid (HOTf) on triarylgermanium halides that cooling down the reaction in its entirety improved yields and prevented the formation of side products to some extent. Nevertheless, clean products of 3,5-xylyl$_3$GeCl (11) and 2-naphthyl$_3$GeCl (12) were obtained.

Since preparation methods including Grignard reagents always yielded a mixture of chloride and bromide derivative, another pathway was employed in order to obtain pure R_3GeCl compounds. Preparation from the hydride derivatives is well-known and was achieved according to literature procedures for 2,5-xylyl$_3$GeH (15) by stirring the educt in freshly distilled CCl_4 in the presence of

catalytic amounts of Pd for several days (Figure 41). After filtration *via* cannula the product was removed under *vacuo* yielding the desired 2,5-xylyl$_3$GeCl (13) in 80% yield.

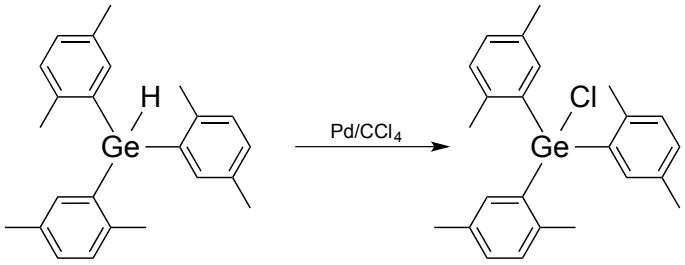

Figure 41. Chlorination of 2,5-xylyl$_3$GeH (15) to prepare 2,5-xylyl$_3$GeCl (13).

Another alternative would be the reaction of 2,5-xylyl$_3$GeH (15) in CCl_4 in the presence of DBP and reflux for 6 hours, noticeably reducing the reaction time and probably enhancing yields. Because of focus onto hydride species, these first attempts were not extended to other compounds.

2.1.1.1.1. 1-naphthyl$_3$GeX- a "special case"

Although the preparation of 1-naphthyl$_3$GeX (9) was described in literature, either reproduction was not possible by the preparation methods published or a mixture of products was obtained.[14,217] Therefore, 1-naphthyl$_3$GeX (9) was synthesized *via* the Grignard route (Figure 42) as well, even though accompanied by various obstacles.

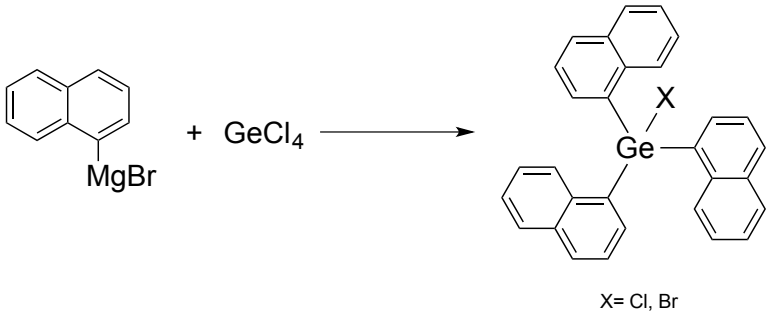

Figure 42. Preparation of 1-naphthyl$_3$GeX (9).

For easier handling, higher amounts of solvents had to be used due to the fact that the Grignard reagent solidifies when cooling down. This even occurred in some cases when higher amounts of solvents where used, wherefore the Grignard reagent was generally cannulated hot or filtered of using a Schlenk-frit charged with Celite®, the latter one being the favored method. In the case of 1-naphthyl$_3$GeX (9), problems occurred not only because of the solidified Grignard reagent or the formation of mixtures, but also because of the formation of naphthalene. In order to improve the preparation of 1-naphthyl$_3$GeX (9) parameters possibly having an influence on the reaction were studied including *i)* time, *ii)* stoichiometry, *iii)* temperature, *iv)* educts, *v)* solvents, and *vi)* work-up procedures.

i) It could be shown that extension of reaction times did not result in higher yields or fewer side products. Best performance was observed when the reaction was kept at reflux for at least one hour before stirring at room temperature for at least two hours before quenching.

ii) As mentioned before, an excess of Grignard reagents is necessary for the desired product to be formed exclusively. However, even if no diarylgermanium halides or triarylgermanium halides could be detected, the formation of free naphthalene was still observed.

iii) The reactions were carried out at 0°C, room temperature and at about 110°C (boiling toluene), with only few differences. The reaction seems to perform best when adding $GeCl_4$ at 0°C, letting the mixture warm to room temperature before exchanging all ethereal solvents with toluene and subsequent refluxing for 1 hour.

iv) In order to avoid halide exchange and product mixtures, $GeBr_4$ was employed, although no improvement was observed. The employment of the corresponding arylchloride instead of the arylbromide leads to difficulty initiating the reaction and was dismissed further on.

v) A very crucial step in the synthesis of 1-naphthyl$_3$GeX seemed to be the solvent exchange after the addition of $GeCl_4$. This concludes, that the higher boiling

temperature of toluene is necessary for the reaction to conclude. Furthermore, it was observed that the Grignard reaction performs better in THF instead of Et_2O, the latter occasionally forming two phases with red and brown color.

vi) Work-up procedures included the extraction and filtration of the product using different solvents, sublimation, Soxhlet extraction, condensation and fractional crystallization of the product. Initial thoughts concerning the sublimation of free naphthalene in order to purify the products were soon dismissed, due to the fact that the product seemed to be labile at room temperature, leading to the decomposition of 1-naphthyl$_3$GeX (9) and formation of more naphthalene. Washing the mixture several times with cold toluene/pentane (1:10) seemed to be the most successful way to obtain pure 1-naphthyl$_3$GeX (9), although decreasing the yield for about 5-10%, due to the partial solubility of 1-naphthyl$_3$GeX (9) in the solvent mixture.

2.1.1.2. Triarylgermanium hydrides

As already mentioned several times, the aim of this work was to synthesize not only arylgermanium halides, but also their hydrogenated derivatives, the latter ones being important precursors for not only organometallic chemistry, but also industrial applications. After successfully being able to reproduce triarylgermanium halides in good yields, attempts were made for the preparation of the hydride derivatives. In this case, the triarylgermanium halide was reduced with a remote excess of $LiAlH_4$ in ethereal solvents (Figure 43).

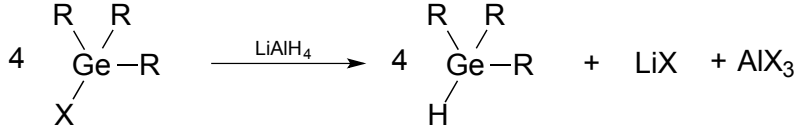

Figure 43. Hydrogenation of R_3GeX with R = 2,4-xylyl (6), 2,5-xylyl (7), 2,6-xylyl (8), 3,5-xylyl (11), 1-naphthyl (9).

It is important for the $LiAlH_4$ to be new, wherefore pellets are used and ground before addition. Usually, the germanium starting material was dissolved, cooled to 0°C and $LiAlH_4$ was added as a solid in small portions. In some cases, the order was reversed but nevertheless leading to the same results. THF was preferably used instead of Et_2O, because solids normally precipitated in Et_2O. This precipitation reduced yields and made work-up procedures more complicated, since all solids had to be redissolved for purification. For the preparation of 2,5-xylyl$_3$GeH (15) it is advisable to use more solvent for easier handling due to solubility reasons. In all cases, immediate reaction could be observed, indicated by gas formation. After the reaction was complete, the mixture was quenched with 3% H_2SO_4 and cannulated onto a saturated tartrate solution. The organic layer was transferred *via* cannula onto Na_2SO_4. After filtration *via* cannula, and washing of Na_2SO_4 several times, the combined filtrates are dried under *vacuo*. In all cases colorless powder were obtained which were further purified by extraction with solvents and/or crystallization. Crystallization was achieved from toluene at low temperatures or *via* evaporation methods.

2.1.1.3. Diarylgermanium hydrochlorides and diarylgermanium dihydrides

For successful further reactions including polymerization and functionalization of arylgermanium compounds, presence of at least two accessible substituents, such as Cl or H, is necessary. For this reason, attempts were made to prepare several diarylgermanium halides and hydrides. However, as already mentioned in Chapter 2.1.1.1 it was not possible to allocate the preparation methods for silicon and tin, which have been studied intensively by our working group, onto germanium. Application of Grignard reagents towards $GeCl_4$ with a ratio of 2:1 to form R_2GeX_2 directly, lead to a mixture of products again, as has been described for the preparation of *p*-tolyl$_2$GeBr$_2$.[18] Amadoruge *et al.* treated this mixture directly with $LiAlH_4$ in order to prepare the hydride derivatives, which could then

be separated *via* vacuum distillation. In general, while separation of halides is difficult because of the similarity of their physical properties, the properties for hydrides differ enough for easier separation.[85,225] Yields are generally low when using this preparation method, as for example for *p*-tolyl$_2$GeH$_2$ (8%), which is why after some initial attempts this route was not pursued any further.[18]

Zhun *et al.* were able to prepare phenylGeCl$_3$, phenyl$_2$GeCl$_2$ and phenyl$_3$GeCl over a variety of different reaction routes.[30,31] These included aryl group transfer from various Ph$_n$SiCl$_{4-n}$ compounds in the presence of metal halides such as AlCl$_3$ or SbCl$_3$. The best yield (88%) without any other germanium side products was achieved when reacting phenyl$_3$SiCl with GeCl$_4$ in a 3:1 ratio under the presence of 10 wt% AlCl$_3$. Similar reactions were carried out several times using antimony, silicon or tin 1-naphthyl or 2,6-xylyl substituted compounds (Figure 44). However, all efforts to prepare diarylgermanium compounds over the same routes resulted in a mixture of products, incomplete conversion or showed no reaction at all, no matter the stoichiometry, central element of the educt or ligand used. If the desired compound was detected *via* GCMS methods, yields were too low and purification too complicated for the desired product to be isolated. For this reason, it must be noted that all compounds reported by Zhun *et al.* were only characterized by GLC chromatography, but never actually isolated.[30,31]

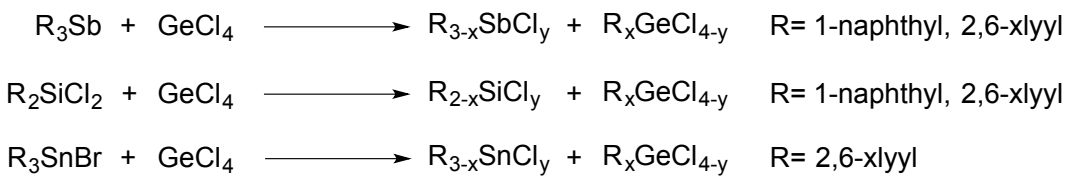

Figure 44. Redistribution reactions carried out for the preparation of R$_3$GeX, R$_2$GeX and R$_3$GeX.

Due to the fact that the polarity of the Ge-C bond is higher than compared to the silicon derivatives, organogermanium compounds are expected to cleave off aromatic groups under acidic conditions even more easily than their silicon analogues.[217] Moreover, the β-effect of germanium, a special type of hyperconjugation, promotes electrophilic substitution, since the electron rich Ge-C bond stabilizes a cation in β-position to germanium.[226-228] Eaborn *et al.* were able to show

that the relative magnitude of the β- effect for group 14 elements follows Sn > Ge > Si when reacting phenylMe_3E (E = Si, Ge, Sn) with aqueous-ethanolic perchloric acid.[229] R-Ge cleavage can be achieved also by employment of halogens, interhalogenes, such as iodine monochlorides and iodine monobromides, or hydrogen halides.[34,230] Uhlig described the employment of trifluoromethanesulfonic acid (HOTf) onto germanium, leading to the electrophilic substitution of an aryl group (Figure 45). This route has been emphasized to be very useful in the case of silicon and tin derivatives.[231-239]

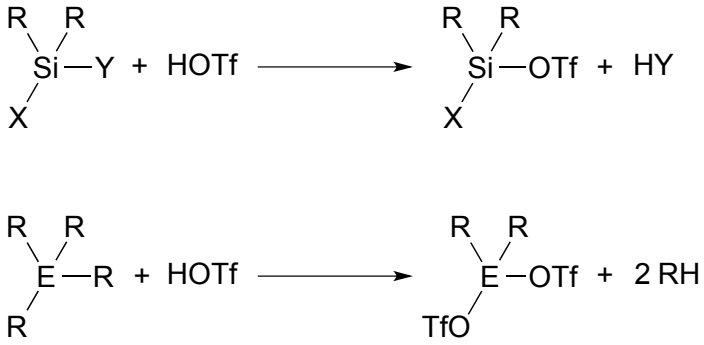

Figure 45. Reaction between tetraorgano group 14 compounds and trifluoromethane sulfonic acid (HOTf) X,Y= 1-naphthyl, phenyl, Cl, H; R = methyl, ethyl, ^{t}butyl E = Si, Ge, Sn, Pb.[234]

It was shown that the reaction rate slows down aryl > Cl > H > alkyl, with phenyl groups being cleaved off more readily than alkyl groups. Uhlig *et al.* stated that the thermal stability is highly dependent on the ligands used and observed a lower stability for germanium triflates, leading to the formation of polymers.[234] Zaitsev *et al.* stated that the triflate compounds seem to be unstable and tend to decompose under the formation of germylenes.[240] Sterically more demanding groups might hinder decomposition to some extent, showing once more the importance of understanding different ligand systems introduced onto the central atom.

Because of these promising investigations reactions were carried out in analogy to described pathways. Different variations of the reaction were performed, however a general procedure is described here (Figure 46).

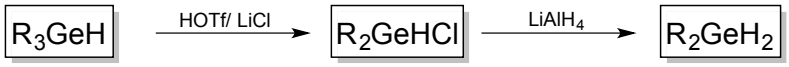

Figure 46. Reaction of R_3GeH with trifluoromethanesulfonic acid (HOTf) and further reactions to R_2GeHCl and R_2GeH_2.

A Schlenk was charged with triarylgermanium hydride in DCM and cooled down to at least 0°C using a ethanol bath cooled down by a metal coil attached to a cryostat. HOTf was added dropwise in small portions *via* syringe. The reaction usually became slightly yellow and cloudy. Stirring for at least 24 hours is of importance, but the reaction progress can be easily monitored by ^{19}F NMR spectroscopy. Since the OTf group is an excellent leaving group it can be easily exchanged by nucleophiles such as chlorides. Zaitsev *et al.* did use an excess of NH_4Cl, but in this work LiCl was used.[224] It is vital to use anhydrous LiCl for the reaction to perform, since LiCl is very hygroscopic. LiCl was added in dry DME, causing the reaction to warm slightly and become clear. After an additional 24 hours, the reaction was normally cloudy, but colors varied widely from colorless to yellow depending on temperature, purification of the educts, amount of HOTf used and time. If yellow precipitation is visible, it is recommended to filter the solution *via* cannula. Further steps vary depending on the desired product.

If the intermediate products R_2GeHCl were desired, the solvents were removed and the obtained solid was dissolved in toluene. After filtration *via* cannula and removal of toluene under *vacuo* the desired product was obtained in form of colorless solids. Crystallization was achieved from toluene at low temperatures or *via* evaporation methods.

If the diarylgermanium dihydride (R_2GeH_2) was the desired product, dry toluene was added at 0°C and all other solvents were removed under *vacuo* before addition of $LiAlH_4$ as a powder in small portions. After allowing to warm temperature and a total stirring time of about three hours the reaction was quenched with 3% H_2SO_4, cannulated onto a saturated tartrate solution and the organic layer was then dried over Na_2SO_4. After filtration *via* cannula and washing Na_2SO_4 at least twice, the combined filtrates were dried under *vacuo*, yielding

colorless solids. Crystallization was achieved from toluene at low temperatures or *via* evaporation methods.

In case educts remained after work-up, washing with pentane was generally helpful, because the triarylgermanium hydride is not soluble in pentane, but the diarylgermanium dihydride is to a certain extent. While diarylgermanium dihydrides are soluble in pentane at room temperature, they crystallize again at 0°C. All dihydrides were recrystallized from toluene at either low temperatures or *via* evaporation methods.

It is important to exclude oxygen and water throughout the reaction, otherwise exposure leads to the formation of bridged derivatives, as was seen during a reaction of 2,6-xylyl$_3$GeH (16), when [2,6-xylyl$_2$Ge]$_2$O (27) (Figure 47) was obtained after the reaction was shortly exposed to air.

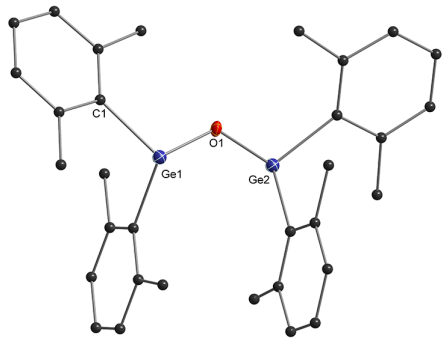

Figure 47. Crystal structure of [2,6-xylyl$_2$Ge]$_2$O (27). All non-carbon atoms shown as 30% shaded ellipsoids. Hydrogen atoms removed for clarity.

In all cases the scale up seemed to be somewhat difficult, as was tried several times for 2,5-xylyl$_3$GeH (15), 2,6-xylyl$_3$GeH (16) and 1-naphthyl$_3$GeH (18). Whenever more than 15 mmol R$_3$GeH were used, yields were degrading and many side products were detected.

As was already mentioned, different variations of this reaction were employed, in which *i)* solvents *ii)* germanium starting materials *iii)* hydrogenation agents *iv)* temperatures *v)* stoichiometry *vi)* time and *vii)* adapted varieties of preparation methods were investigated.

i) The reaction was performed in different solvents, *e.g*. DCM, DME and toluene and a combination thereof. According to literature, DCM was the solvent of choice for the addition of HOTf. Toluene can be used instead, although yields were generally better when using DCM. DME was chosen for the addition of LiCl, since it enhances the solubility of LiCl in DCM in comparison to neat addition. In the last step, toluene is added in order to eliminate salts, which are formed during the reaction. In cases where the hydride is the desired product, hydrogenation was performed in toluene instead of ethereal solvents having no impact on the yields and composition of products compared to the normal procedure. After initial experiments, it was observed that removal of solvent in the initial part of the reaction leads to the precipitation of side and sulfur degradation products, thus lowering the yields and affecting the further reactions. For this reason, all further used solvents, in this case toluene, must be added before removal of the previously used one.

ii) Due to time and cost reasons, only selected ligand systems were investigated regarding R-Ge cleavage. In the case of R_4Ge, 3,5-xylyl$_4$Ge (3) and 2-naphthyl$_4$Ge (4) were chosen as representatives, while 2,5-xylyl$_3$GeH (15), 2,6-xylyl$_3$GeH (16) and 1-naphthyl$_3$GeH (18) were chosen to represent R_3GeH. Triarylgermanium hydrides are favored over the tetraarylgermanes because fewer reaction steps are required for the preparation of R_2GeH_2 and stoichiometry can be adjusted more accurately. It can be stated that the reaction starting from 2,5-xylyl$_3$GeH (15) usually performs the smoothest, even at higher temperatures. 1-naphthyl$_2$GeH$_2$ (24) again seems to decompose at higher temperatures, however can be isolated and purified at lower temperatures. While xylene is easily removed from the product mixture, the only way to remove naphthalene without consequences on the product in terms of yield and product quality is by washing various times with pentane/toluene mixtures.

iii) Although employment of DIBAL-H (Figure 48) seems to be a good alternative for the hydrogenation of the diarylgermanium hydrochloride intermediate, various unidentified side products where generated, lowering yields and compli-

cating the purification process. For this reason, $LiAlH_4$ seems to be the better choice.

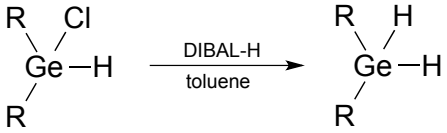

Figure 48. Hydrogenation with DIBAL-H with R = 2,5-xylyl (19), 2,6-xylyl (20).

iv) As already mentioned before, germanium triflates seem to be temperature unstable, therefore temperatures are a very important factor. It is important for the reaction temperature to be constantly below 0°C in order to control the formation of sulfur byproducts, normally detectable by color and smell. In the case of the 1-naphthyl moiety, it was shown that even lower temperatures (-30°C) were necessary for the desired product 1-naphthyl$_2$GeH$_2$ (24) to be formed, while the intermediate 1-naphthyl$_2$GeHCl (20) could be isolated at 0°C already. However, all products obtained were stable at room temperature after purification.

v) Stoichiometry of HOTf towards the arylgermanium hydride was investigated regarding possibly cleaving off two aryl groups at the same time. Using two equivalents of HOTf as compared to the germanium starting material did not result in a controlled substitution of additional aryl groups, but rather lead to a mixture of products, formation of sulfur side products and decomposition of the starting material, independent of temperatures used. Already Orndorff *et al.* observed that upon addition of bromine onto phenyl$_4$Ge, the removal of two phenyl groups at once is accompanied by the formation of side products.[27] Zaitsev *et al.* postulate that only one aryl group can be cleaved off at a time using trifluoromethanesulfonic acid (HOTf) due to the electron acceptor ability of OTf, which makes further electrophilic substitution difficult.[224] This however, is contrary to results made from Uhlig and also within in our working group, where it was shown that in the case of the phenyl moiety, which is not included in this work, introduction of two triflate groups (OTf) in one step was possible.[234] Nevertheless, when this was attempted for 2,5-xylyl$_3$GeH (15), 2,6-xylyl$_3$GeH (16) and

1-naphthyl$_3$GeH (18), only R_2GeH_2 and other unidentified side products were obtained. In rare cases, even when only applying a slight excess of HOTf, trace amounts of monoarylgermanium trihydrides were detected, possibly because of impure educts, even though all educts were normally screened *via* GCMS methods. This, however, stresses the importance of accurate stoichiometry and diminishes the possibility to use R_3GeX as candidates in terms of precursors, since stoichiometry can not be appointed correctly due to different composition accounted for by halide exchange. A reason for this might be, that the dihydrides are more stable than the trihydrides, for which reason the reactions stops at this stage. This would therefore explain why it would be possible to obtain phenyl$_2$GeH$_2$ straight from phenyl$_4$Ge. In the case of 3,5-xylyl$_4$Ge (3), small amounts of 3,5-xylyl$_2$GeH$_2$ were detected *via* GCMS as well, however, could not be isolated.

vi) Time is yet another important factor to be taken into consideration. Because of consistent screening of the reaction progress of the first reaction using ^{19}F NMR, it was observed that the reaction must be stirred for at least 24 hours for complete consumption of HOTf. It is advisable to let the reaction stir longer in some cases in order to prevent the formation of mixtures due to triarylgermanium hydrides and diarylgermanium dihydrides present.

vii) Attempts were made to simplify the preparative complexity by altering not only reactions time and stoichiometry, but also modify the reaction itself. For this reason, addition of LiCl was forgone and the germanium triflate intermediates were subjected to the hydrogenating agent. This was attempted for $LiAlH_4$, as well as DIBAL-H, resulting in a mixture of products, some of them unidentified, independent of the hydrogenation agent employed. All efforts made in order to utilize the triarylgermanium halide mixtures as starting materials were unsuccessful thus far. At this point the advantages regarding shorter reaction times and less reactions steps are outweighed by the fact, that it is not possible to adjust the correct amount of HOTf, because of the variation in composition of R_3GeX. It was shown that fewer side products were obtained when using triarylgermanium hydride as the starting material. Less yellow precipitate, possibly

sulfur degradation products, was obtained, making further work-up procedures easier. However, application of either pure triarylgermanium chloride or bromide without the other halide present were not conducted due to the fact that $GeBr_4$ would have to be used for the preparation of R_3GeBr, thus increasing the preparation costs immensely. The preparation of R_3GeCl was discussed in Chapter 2.1.1.1. However, since this method would not lower the preparative effort, no further investigations were conducted.

2.1.1.4. Arylgermanium trihydrides

Little is known about the preparation, isolation and behavior of arylgermanium trihydrides, and only few aryl substituted germanium trihydrides are published since preparation methods are even more challenging and cost intensive compared to higher arylated germanium compounds.[16,40,241-244] It can be assumed, that $RGeH_3$ are the most reactive arylgermanium hydrides, therefore making the preparation all the more interesting.

In this work, arylgermanium trihydrides were prepared over the same route as the diarylgermanium dihydrides but with R_2GeH_2 as the starting materials (Figure 49).

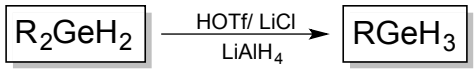

Figure 49. Reaction of R_2GeH_2 with trifluoromethanesulfonic acid (HOTf) to prepare $RGeH_3$.

Unfortunately, reactions were more problematic and yields were generally lower. Low yields and small amounts of product can be explained not only because of difficult and time-consuming preparation of educts and therefore smaller set ups, but also because of the instability and reactivity of the products. Work-up procedures are more difficult due to the fact that the arylgermanium trihydrides are very volatile, thus already evaporating under reduced pressure at room temperature, which makes it challenging to remove solvents without low-

ering the yields. For all these reasons, the isolation of the $RGeH_2Cl$ intermediate was forgone up to this point.

In the case of 2,6-xylylGeH_3 (26), a colorless, sometimes slightly yellow liquid was obtained, which was purified from side products *via* condensation methods. 2,5-xylylGeH_3 was characterized by standard techniques, however isolation of larger amounts of product for further experiments was unsuccessful until now. In all cases, the products seem to be very reactive, as is visible in the case of NMR measurements, when mixtures of $CDCl_3$ and $RGeH_3$ turn rapidly yellow if no precautionary arrangements against air are taken.

Alternatively, arylgermanium hydrides can be prepared over the Grignard route by preparation of the arylgermanium trihalides and subsequent hydrogenation. If the stoichiometry is adjusted accordingly (1:1 Grignard reagent towards $GeCl_4$), less side products are obtained compared to the preparation of R_2GeX_2. Halide exchange is observed, but does not play an important role upon reaction with an excess of $LiAlH_4$. Yields are generally low, due to the trihydrides being very volatile, but also because of difficult work-up procedures. For this reason, the reaction pathway involving trifluoromethanesulfonic acid (HOTf) is favored.

2.1.1.5. Initial investigations towards potential applications

TGA/DSC and thermolysis studies

Thermolysis of group 14 elements has been studied intensively in the case of silicon compounds, thus leading to a number of possible applications, *e.g.* composite materials, electronic and photovoltaic devices, coatings or as silicon source in vapor deposition methods.[245-247] Since thermolysis reactions carried out for silicon and tin derivatives have shown very promising results, it was nearly inevitable to not extend this research to germanium. The formation of pure germanium and germanium oxides from organogermanes *via* thermolysis under

constant argon flow was examined. Because of the instability of 1-naphthylgermanium compounds and thus making promising candidates for such applications, the compounds 1-naphthyl$_3$GeX (9) and 1-naphthyl$_3$GeH (18) were chosen for further investigation by either TGA or thermolysis/SEM experiments. SEM measurements were performed before and after thermolysis. Since it was not possible to conduct any further experiments, all data obtained can only be considered as preliminary results, which have to be verified by future experiments.

1-naphthyl$_3$GeX (9) was analyzed *via* thermogravimetric analysis in combination with differential scanning calorimetry and mass spectrometry. Upon heating the organogermanium halide to 1000°C with a heating rate of 5K/min, melting and decomposition occurs, thus giving important information for subsequent thermolysis experiments.

As seen in Figure 50, a total mass loss of 91.07% is observed. The bigger loss step located between 315°C and 450°C with a mass loss of 86.51% probably corresponds to a loss of all substituents from the central atom during the heating process, when taking into account that a mixture of 1-naphthyl$_3$GeBr and 1-naphthyl$_3$GeCl was used. Two endothermic peaks are observed at 245.3°C and at 623.7°C. The peak at 245.3°C might be a first order phase transition related to the melting of the sample, being more or less in accordance with the value reported under air (239°C) and those found in literature.[14] The peak at 623.7°C might be attributed to complete decomposition.

In conclusion, the TGA/DSC analysis of 1-naphthyl$_3$GeX (9) might indicate the cleavage of naphthyl groups. However, further experiments have to be carried out.

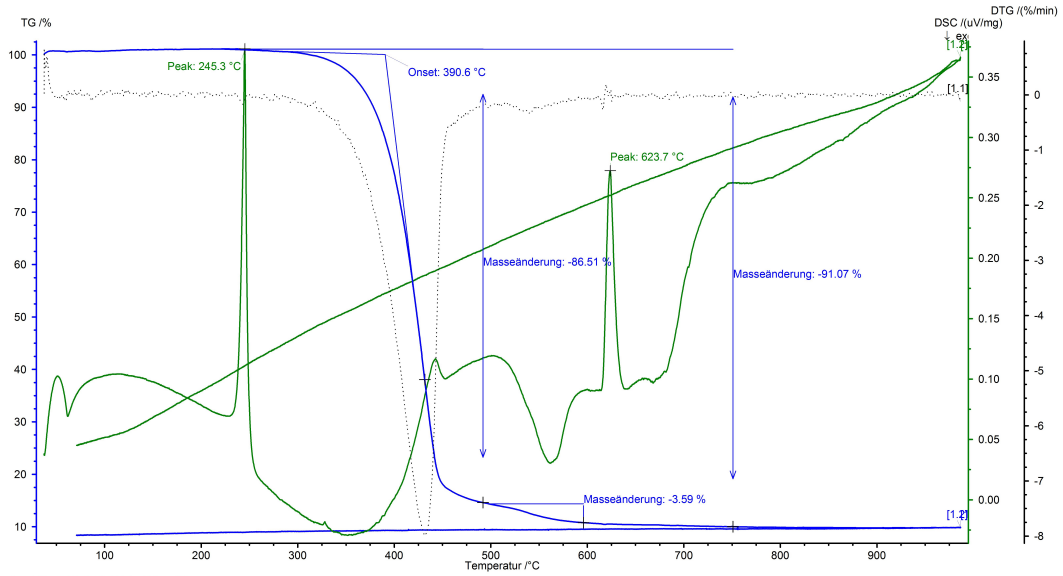

Figure 50. TGA/DSC of 1-naphthyl$_3$GeX (9).

1-naphthyl$_3$GeH (18) was chosen as a good candidate for thermolysis and was heated using a Carbolite single zone horizontal tube furnace GHA12/600 (Figure 51).

Figure 51. GHA 12/600 furnace.

The colorless powder was put into a ceramic sample holder under inert gas (N_2) and put into the oven. A one step heating process with 10°C/min up to 650°C was conducted with a continuous argon flow of 2l/min. The white powder turned into black solid upon thermolysis. A total mass loss of about 75-80% was observed *via* EDX measurements. After cooling down, pure naphthalene crystals were visible at the outlet of the furnace, indicating the loss of naphthyl groups once more. SEM analysis (Figure 52) before and after thermolysis shows the loss of crystallinity.

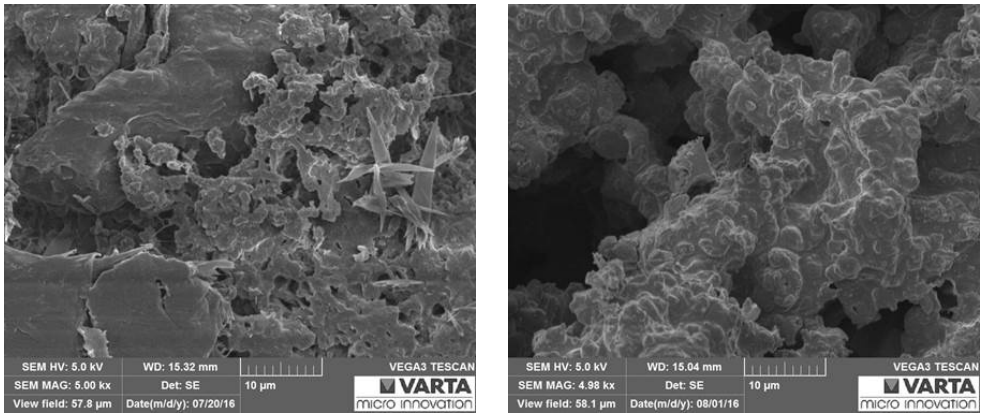

Figure 52. SEM pictures of 1-naphthyl$_3$GeH (18) before and after thermolysis.

No further TGA measurements were conducted, due to incompatibility of the samples with the experiment requirements. Since TGA gives useful and required information for further thermolysis experiments, further experiments have to be renounced but will be resumed in the future. Therefore, all results obtained are preliminary and have to be repeated to be confirmed. Triarylgermanium hydride and the disubstituted derivatives might give even more promising results.

Dehydrogenative coupling reactions by employment of TMEDA

It is known that group 14 hydrides make useful precursors for the dehydrogenative coupling reaction in order to form element-element bonds in the presence of amine bases as catalysts.[248-250] TMEDA (N, N, N', N'- tetramethylethylenediamine) makes a useful catalyst for polymerization reactions (Figure 53),

leading to mostly insoluble polymers, however solubility can be increased for aryl substituents such as *p*-butylphenyl, as was reported in 2011.[54] In the case of *o*-tolylSnH$_3$ aryl decorated tin nanoparticles were formed (Figure 54).[251]

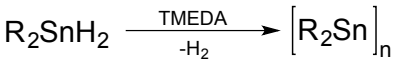

Figure 53. Preparation of polystannanes using TMEDA.

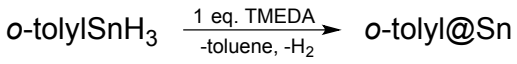

Figure 54. Formation of *o*-tolyl decorated Sn nanoparticles by reaction of *o*-tolylSnH$_3$ with TMEDA.

The fact that little is known about dehydrogenative coupling reactions of aryl-germanium di- and trihydrides, more specifically their behavior towards polymerization and formation of aryl decorated nanoparticles provided the encouragement to perform similar experiments.

1 drop of 2,6-xylylGeH$_3$ (26) was suspended in 2 ml dry Et$_2$O, 3 drops of freshly distilled TMEDA were added slowly at room temperature. Although in the case of tin hydrides the reaction starts immediately, turning yellow and dark brown within minutes, this could not be observed in the case of germanium. The reaction solution turned slightly cloudy and a white solid precipitated on the sides of the vessel. After stirring for 4 days, all solvents and residual TMEDA were removed under *vacuo*. Since not enough product was obtained for GCMS analysis, the product was only analyzed *via* elemental analysis. A loss of carbon content was observed, but further investigations need to be implemented for confirmation.

For the reaction between 2,5-xylyl$_2$GeH$_2$ (22) and TMEDA (Figure 55), 0.11 g 2,5-xylyl$_2$GeH$_2$ were dissolved in 1.5 ml dry Et$_2$O, and 0.06 ml TMEDA were added dropwise. No reaction was observed upon stirring at room temperature for 52 hours. Dry toluene was added and after removal of Et$_2$O the reaction was heated to 90°C and stirred for an additional 2 days. After removal of solvents and

TMEDA a colorless solid was obtained, which was further analyzed *via* elemental analysis, showing no noticeable change of carbon content. This might indicate, that the dihydride species is either not reactive enough or more forceful conditions need to be applied.

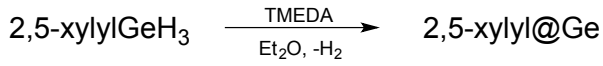

Figure 55. Reaction of 2,5-xylylGeH$_3$ with TMEDA to prepare 2,5-xylyl decorated nanoparticles.

Preparation of cyclic and linear and oligogermanes

Other oligo- and polymerization reactions were performed, including the hydrogermolysis reaction of ^{i}propyl$_3$GeN(methyl)$_2$ (31) with phenyl$_3$GeH to prepare the digermane (^{i}propyl$_3$Ge)$_2$. Acetonitrile is used not only as a solvent, but also as a key synthetic reagent, because it converts the germanium amide educt R$_3$GeN(methyl)$_2$ into the more reactive species α-germyl nitrile R$_3$GeCH$_2$CN.

For the preparation of (phenyl$_2$Ge)$_4$ (35), phenyl$_2$GeCl$_2$ was dissolved in toluene and added slowly to a boiling suspension of sodium in toluene. It is very important that the dropping rate is adjusted correctly for the phenyl$_2$GeCl$_2$ to be added over about 30-35 minutes after starting a timer for 1 hour. A dark purple solution is obtained, which is refluxed only for the remaining hour to avoid the formation of side products, namely the favored five-membered ring (phenyl$_2$Ge)$_5$ before filtered hot over Celite®. The desired product recrystallizes upon cooling to room temperature in form of colorless needles in a yellow solution. The crystals were recrystallized from toluene at low temperatures. Cleavage of this ring can be easily achieved by dissolving (phenyl$_2$Ge)$_4$ (35) in benzene and addition of enough Br$_2$ for the orange color to remain constant. A colorless solid precipitates, yielding (phenyl$_2$Ge)$_4$Br$_2$ (36) after filtration. The halide oligomer can be easily reduced by standard hydrogenation using LiAlH$_4$ in Et$_2$O at room temperature. After 12 hours of stirring, the solvent was removed, again yielding a colorless solid, namely (phenyl$_2$Ge)$_4$H$_2$ (37). Due to time constraints, no further experiments were conducted with the tetramer.

2.1.2. Characterization

2.1.2.1. X-ray crystallography

On the way towards these crucial starting materials, a large variety of aromatic germanium compounds were synthesized and their solid state structure elucidated *via* single crystal X-ray crystallography. While not previously mentioned in literature, the common feature of all aryl substituted germanium hydrides and halogenides is the presence of intermolecular secondary non-covalent interactions: electrostatic interactions in the form of π-stacking stemming from the aromatic substituents and van der Waals contacts from the halogenide substituent and adjacent hydrogens, C–H···X (X = Cl, Br). While individually these are weak interactions, combined they offer an overall stabilizing effect to these molecules in the solid state and aid in their crystallization.

The role of aromatic non-covalent interactions in the stabilization of compounds in solid state and their importance in chemical and biological processes have been well documented.[252-255] However, their presence and ultimately their effect on arylgermanium species has been rarely discussed or simply overlooked. In an effort to expand the existing library of compounds and study the underlying factors leading to solid state structures, we present a series of novel arylgermanium compounds with aryl substituents ranging in steric demand from phenyl to polyaromatic substituents such as 1-naphthyl. The types of non-covalent interactions present in these systems will be highlighted and compared to previously reported compounds. In addition, the nature of the aromatic substituent and its direct effects on the type of electrostatic interaction that arises in these structures will be discussed.

Crystallographic Studies

Electrostatic interactions in the form of π-stacking stemming from the aromatic substituents of aryl substituted germanium halides and hydrides are depicted in Figure 56 with acceptable ranges found in biological and organic systems.[252-255] All novel aryl substituted germanium compounds presented display

non-covalent interactions in the solid state through their corresponding aromatic substituents. These stabilizing interactions are described and compared to those present in previously reported Group 14 species.[256-259] In the case of the aryl substituted germanium chlorides and bromides, contacts arising due to van der Waals forces from the halogenide substituent and adjacent hydrogens, C–H···X (X = Cl, Br), are also presented and fall within expected values.[260] The crystallographic data and details for all compounds presented can be found in the appendix.

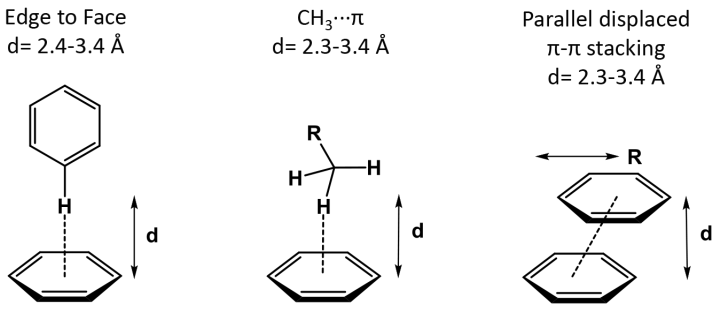

Figure 56. Types of secondary non-covalent electrostatic interactions.

2.1.2.1.1. Tetraarylgermanes- R_4Ge

Compounds *m*-tolyl$_4$Ge (1), 3,4-xylyl$_4$Ge (2), 3,5-xylyl$_4$Ge (3) and 2-naphthyl$_4$Ge (4) (Figure 57) are comparable to previously reported tetraarylgermanes (Table 2).

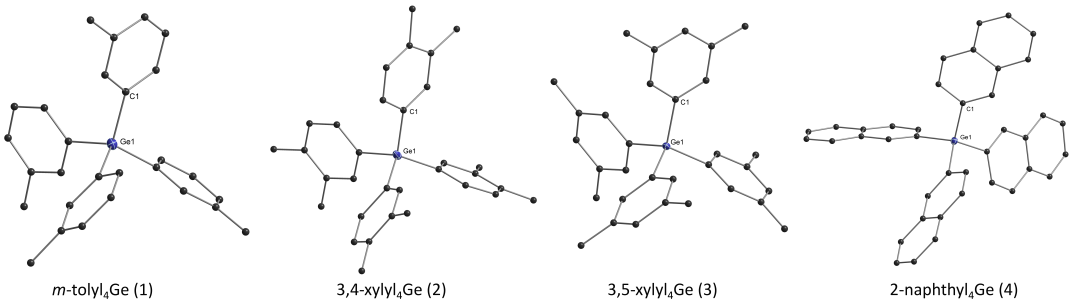

Figure 57. Crystal structures of presented solid state tetraarylgermanes. All non-carbon atoms shown as 30% shaded ellipsoids. Hydrogen atoms removed for clarity.

Each molecule is in a near tetrahedral environment with average C–Ge–C angles of 109°. With respect to averaged Ge–C bond lengths, these fall within a narrow range of 1.94–1.96 Å and are not affected by the degree of bulkiness afforded by the organic substituent onto the germanium atom.

Table 2. List of selected bond lengths and angles and non-covalent interactions for selected tetraaryl substituted germanes.

	Space Group	Ge–C (Å) (avg.)	C–Ge–C (°) (avg.)	Edge to Face (Å)	$CH_3\cdots\pi$ (Å)
phenyl$_4$Ge[261-263]	*P*-42$_1$*c*	1.960(2)	109.5(2)	3.29	—
***o*-tolyl$_4$Ge**[9,264]	*P*-1	1.954(4)	109.5(2)	2.77 – 3.10	—
***m*-tolyl$_4$Ge (1)**[9]	*I*4$_1$/*a*	1.946(3)	109.47(13)	3.18	2.69
***p*-tolyl$_4$Ge**[265]	*Pc*	1.949(5)	109.5(2)	*	*
3,4-xylyl$_4$Ge (2)	*P*2$_1$/*c*	1.943(7)	109.45(9)	3.18	2.93 – 3.16
3,5-xylyl$_4$Ge (3)	*P*2/*c*	1.953(2)	109.48(9)	2.72	2.69 – 3.11
2-naphthyl$_4$Ge (4)	*P*2$_1$/*n*	1.953(2)	109.47(6)	2.54 – 3.04	—

*No hydrogen atoms reported

In most cases, tetraaryl substituted germanes display highly ordered packing motifs in the solid state creating 3D networks through the presence of non-covalent electrostatic interactions.

Table 2 summarizes the non-covalent interactions in presented tetraaryl substituted germanes. All compounds display edge to face interactions in the extended solid state. While not reported in literature, phenyl$_4$Ge[261-263] (3.29 Å) displays a slightly longer edge to face interaction. Despite the *o*-tolyl residue having a methyl group capable of displaying $CH_3\cdots\pi$ interactions, *o*-tolyl$_4$Ge[9,264] only displays edge to face interactions (2.77–3.10 Å) and crystallizes in the lowest symmetry space group (Table 2). It is possible that the methyl in the *ortho* position is simply too far away from the aryl residues of neighboring molecules and no such interaction is observed. $CH_3\cdots\pi$ interactions are, however, observed in all other instances when methyl groups are present, *m*-tolyl$_4$Ge (1)[9] (2.69 Å), 3,4-xylyl$_4$Ge (2) (2.93–3.16 Å) and 3,5-xylyl$_4$Ge (3) (2.69–3.11 Å) (Figure 58).

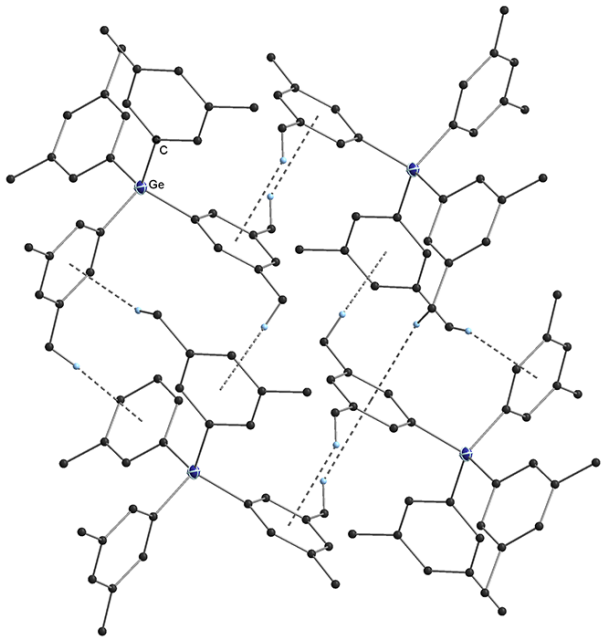

Figure 58. Crystal packing diagram for 3,5-xylyl$_4$Ge (3). $CH_3\cdots\pi$ interactions highlighted by dashed bonds. All non-carbon atoms shown as 30% shaded ellipsoids. Edge to face interactions and hydrogen atoms not involved in intermolecular interactions removed for clarity.

Lastly, in 2-naphthyl$_4$Ge (4), the bulkiness of all four naphthyl residues around the central germanium atom does not allow for any π–π stacking interactions to be observed, however, the closest edge to face interactions (2.54–3.04 Å) are observed for this species (Figure 59).

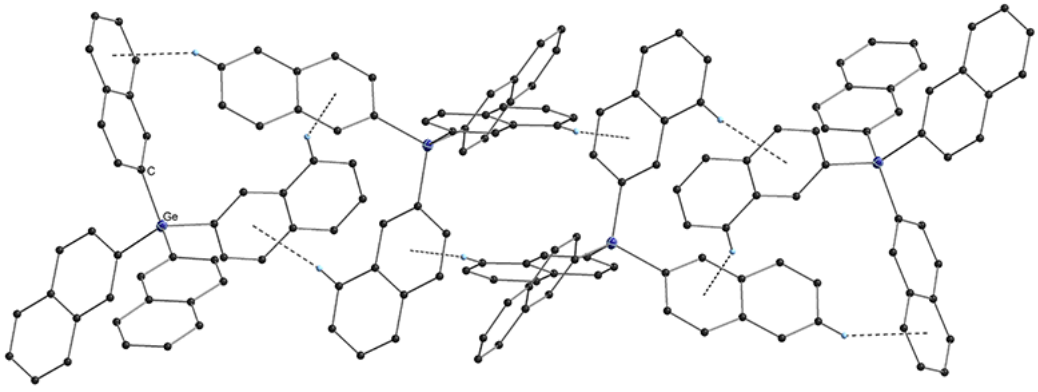

Figure 59. Crystal packing diagram for 2-naphthyl$_4$Ge (4). Edge to face interactions highlighted by dashed bonds. All non-carbon atoms shown as 30% shaded ellipsoids. Hydrogen atoms not involved in intermolecular interactions removed for clarity.

2.1.2.1.2. Triarylgermanium halides

Triarylgermanium chlorides - R_3GeCl

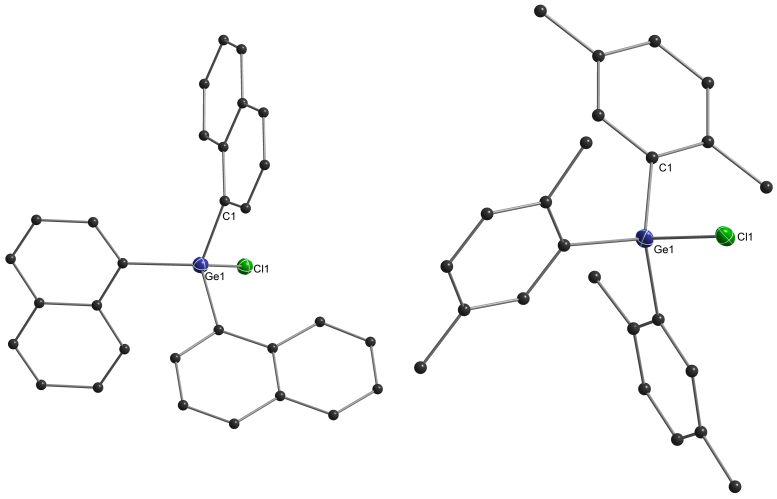

1-naphthyl$_3$GeCl (9) 2,5-xylyl$_3$GeCl (13)

Figure 60. Crystal structures of presented solid state triarylgermanium chlorides. All non-carbon atoms shown as 30% shaded ellipsoids. Hydrogen atoms removed for clarity.

In contrast to the tetraarylgermanes, the degree of bulkiness of the residue around the central germanium atom does seem to have an effect on averaged Ge–C bond lengths (Table 3) in the triarylgermanium chloride species. In phenyl$_3$GeCl[264,266] an averaged Ge–C bond length of 1.933(5) Å is observed, with 2,5-xylyl$_3$GeCl (13) and 1-naphthyl$_3$GeCl · thf (9a) displaying similar lengths, 1.947(3) Å and 1.944(6) Å respectively. However, addition of a ^{t}butyl group at the *ortho* position, as observed in 2-^{t}butylphenyl$_3$GeCl,[17] results in a slight elongation to 1.989(4) Å and a subsequent C–Ge–Cl widening to 109.1(1)° as compared to 106.0(1)° for phenyl$_3$GeCl. Counterintuitively, the narrowest C–Ge–C of 109.8(2) Å is also observed for 2-^{t}butylphenyl$_3$GeCl, highlighting the crowded environment of the central germanium atom and a direct consequence of the wider C–Ge–Cl angle. Despite the crowded environment in 2-^{t}butylphenyl$_3$GeCl, the longest Ge–Cl bond length is observed for 1-naphthyl$_3$GeCl · thf (9a) (2.239(4) Å), which is a pronounced elongation as compared to phenyl$_3$GeCl (2.191(2) Å).

Table 3. List of selected bond lengths and angles for selected triaryl substituted germanium chlorides.

	Space Group	Ge–C (Å) (avg.)	Ge–Cl (Å)	C–Ge–C (°) (avg.)	C–Ge–Cl (°) (avg.)
phenyl$_3$GeCl[264,266]	$P2_1/c$	1.933(5)	2.191(2)	112.7(2)	106.0(1)
2,5-xylyl$_3$GeCl (13)	*P*-1	1.947(3)	2.205(3)	113.06(5)	105.59(3)
2-^{t}butylphenyl$_3$GeCl[17]	*P*-1	1.989(4)	2.198(1)	109.8(2)	109.1(1)
1-naphthyl$_3$GeCl · thf (9a)	*P*-1	1.944(6)	2.239(4)	111.21(3)	107.69(2)

Table 4. List of non-covalent interactions for selected triaryl substituted germanium chlorides.

	Edge to Face (Å)	$CH_3\cdots\pi$ (Å)	C–H···Cl (Å)
phenyl$_3$GeCl[264,266]	2.66 – 3.33	—	2.93 – 3.52
2,5-xylyl$_3$GeCl (13)	—	3.07 – 3.24	2.69 – 3.15
2-^{t}butylphenyl$_3$GeCl[17]	2.69 – 3.01	3.21	3.07 – 3.26
1-naphthyl$_3$GeCl · thf (9a)	2.75 – 3.32	—	2.89 – 3.27

As observed for the tetraarylgermanes, all triaryl chloride derivatives display edge to face interactions in the extended solid state (Table 4) leading to 3D networks. As expected, the addition of methyl substituents on the aryl residues of 2,5-xylyl$_3$GeCl (13) and 2-^{t}butylphenyl$_3$GeCl[17] results in $CH_3\cdots\pi$ interactions, 3.07–3.24 Å and 3.21 Å respectively, between the methyl groups and aryl residues from neighboring molecules. Despite the capacity for 1-naphthyl$_3$GeCl · thf (9a) to potentially display π–π stacking interactions, the bulkiness of three naphthyl residues around the central germanium and the solvent of crystallization of THF hinders the naphthyl residues from neighboring molecules from approaching each other in a planar fashion to allow this type of interaction. This results in quite perpendicular edge to face interactions between the naphthyl residues (2.75–3.32 Å) (Figure 61). The THF molecules are also found to display edge to face interactions with the naphthyl residues (2.85–3.12 Å). In addition to the electrostatic interactions described above, all of the triarylgermanium chloride derivatives display van der Waals interactions from the chloride substituent and hydrogens (C–H···Cl) from neighboring molecules.

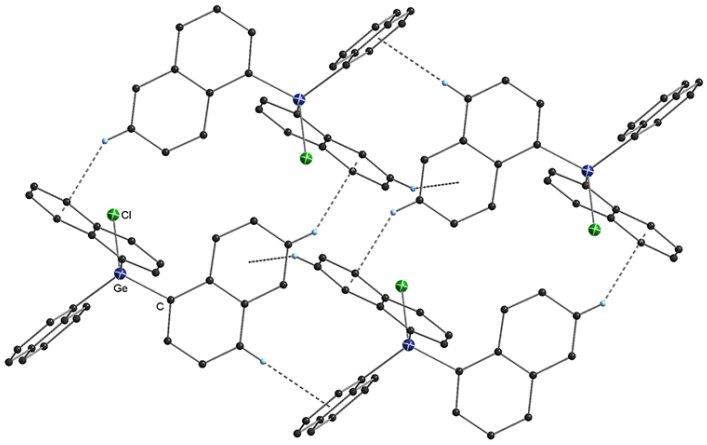

Figure 61. Crystal packing diagram for 1-naphthyl$_3$GeCl · thf (9a). Edge to face interactions highlighted by dashed bonds. All non-carbon atoms shown as 30% shaded ellipsoids. C–H···Cl contacts, solvent of crystallization (THF) and hydrogen atoms not involved in intermolecular interactions removed for clarity.

Triarylgermanium bromides - R_3GeBr

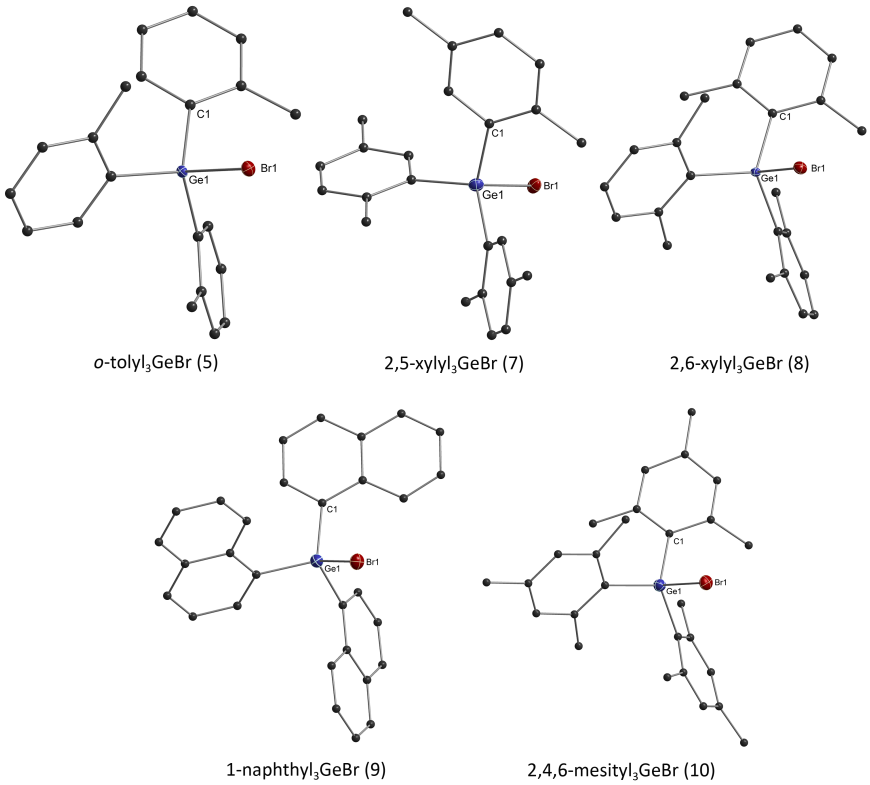

Figure 62. Crystal structures of presented solid state triarylgermanium bromides. All non-carbon atoms shown as 30% shaded ellipsoids. Hydrogen atoms removed for clarity.

As observed in the triarylgermanium chloride species, the presence of substituents on the *ortho* position of the aryl residue in the triarylgermanium bromide results in Ge–C bond elongation (Table 5). As compared to phenyl$_3$GeBr[267] (1.934(1) Å), a slight increase in the average Ge–C bond lengths is seen for *o*-tolyl$_3$GeBr (5) (1.947(2) Å) and 2,5-xylyl$_3$GeBr (7) (1.948(2) Å). However, with the increase of steric bulk around the germanium center due to methyl groups at both the 2- and 6 positions of the aryl residue, this bond elongation becomes more pronounced, with averaged Ge–C distances of 1.977(3) Å in 2,6-xylyl$_3$GeBr (8) and 1.971(6) Å in 2,4,6-mesityl$_3$GeBr (10). Finally, as expected, the larger ^{t}butyl substituent on the ortho position of the aryl residue in 2-tbutylphenylGe3Br17 causes the longest Ge–C bond length of 1.997(2) Å.

Consequently, 2-tbutylphenyl3GeBr17 displays a wider C–Ge–Br angle of 110.66(6)° and narrower C–Ge–C angle of 108.26(6)°, whereas all other molecules display wider C–Ge–C angles than C–Ge–Br angles, highlighting the steric strain from the ^{t}butyl substituent of the aryl residue on the central germanium atom environment. This increased steric bulk around the germanium center is also manifested by an increased Ge–Br bond in 2-^{t}butylphenyl$_3$GeBr[17] (2.362(1) Å) and 2,4,6-mesityl$_3$GeBr (10) (2.364(4) Å) as compared to phenyl$_3$GeBr[267] (2.318(7) Å).

Curiously, all four trinaphthylgermanium halide derivatives and the novel germanium hydride crystallize in the presence of either a solvent of crystallization as seen for 1-naphthyl$_3$GeH · toluene (18), 1-naphthyl$_3$GeCl · thf (9a), 1-naphthyl$_3$GeBr · toluene (9b), 1-naphthyl$_3$GeBr · $CHCl_3$ (9c), or with a naphthyl molecule as seen in 1-naphthyl$_3$GeBr · naphthalene (9d). This highlights the inherent difficulties with isolating naphthyl derivatives of germanium.

Both Ge–C and Ge–Br bond lengths do not seem to be affected by the solvent of crystallization or cocrystallized naphthyl molecule, and compare well to other triarylgermanium bromides with aryl residues substituted at the *ortho* position.

Table 5. List of selected bond lengths and angles for selected triaryl substituted germanium bromides.

	Space Group	Ge–C (Å) (avg.)	Ge–Br (Å)	C–Ge–C (°) (avg.)	C–Ge–Br (°) (avg.)
phenyl$_3$GeBr[267]	$P2_1/c$	1.934(1)	2.318(7)	112.4(4)	106.3(4)
***o*-tolyl$_3$GeBr (5)**	$P2_1/c$	1.947(2)	2.339(3)	111.79(8)	107.05(5)
2,5-xylyl$_3$GeBr (7)	$P2_1/c$	1.948(2)	2.357(4)	113.11(10)	105.50(7)
2,6-xylyl$_3$GeBr (8)	*P*-1	1.977(3)	2.345(5)	115.01(14)	103.12(10)
1-naphthyl$_3$GeBr · toluene (9b)	*R*-3	1.946(5)	2.346(4)	110.84(7)	108.07(7)
1-naphthyl$_3$GeBr · CHCl$_3$ (9c)	*P*-1	1.945(6)	2.346(8)	111.67(19)	107.18(17)
1-naphthyl$_3$GeBr · naphthalene (9d)	*R*-3	1.946(3)	2.357(5)	111.03(13)	107.86(9)
2,4,6-mesityl$_3$GeBr (10)	*P*-1	1.971(6)	2.364(4)	115.28(2)	102.77(4)
2-^{t}butylphenylGe$_3$Br[17]	*R*-3	1.997(2)	2.362(1)	108.26(6)	110.66(6)

Table 6. List of non-covalent interactions for selected triaryl substituted germanium bromides.

	Edge to Face (Å)	CH$_3$···π (Å)	C–H···Br (Å)
phenyl$_3$GeBr[267]	2.59 – 3.09	—	3.03
***o*-tolyl$_3$GeBr (5)**	2.68 – 3.28	2.82 – 3.39	2.99 – 3.21
2,5-xylyl$_3$GeBr (7)	—	3.04 – 3.44	3.24 – 3.38
2,6-xylyl$_3$GeBr (8)	3.01	3.15	3.10 – 3.20
1-naphthyl$_3$GeBr · toluene (9b)	3.13 – 3.31	—	3.15 – 3.36
1-naphthyl$_3$GeBr · CHCl$_3$ (9c)	3.11 – 3.13	—	3.13 – 3.24
1-naphthyl$_3$GeBr · naphthalene (9d)	2.57 – 3.02	—	2.91 – 3.47
2,4,6-mesityl$_3$GeBr (10)	—	2.91 – 3.03	3.21 – 3.44
2-^{t}butylphenylGe$_3$Br[17]	2.86	—	3.32 – 3.43

With respect to the type of secondary non-covalent interactions in the extended solid state of triarylgermanium bromides, clear trends begin to arise related to the substitution pattern of the aryl residue (Table 6). Unsurprisingly, phenyl$_3$GeBr[267] only displays edge to face interactions (2.59–3.09 Å) due to the obvious lack of a methyl substituent or a polyaromatic residue. In *o*-tolyl$_3$GeBr (5), edge to face interactions (2.68–3.28 Å) are observed and as expected, the addition of a methyl substituent at the *ortho* position results in the presence of

$CH_3\cdots\pi$ interactions (2.82–3.39 Å). However, in the case of 2-^{t}butylphenylGe_3Br,[17] only edge to face interactions are observed in contrast to 2-^{t}butylphenylGe_3Cl[17] which displays both edge to face and $CH_3\cdots\pi$ interactions.

As observed for 2,5-xylyl$_3$GeBr (7) and 2,6-xylyl$_3$GeBr (8), the addition of a second methyl group alone does not dictate the type of interaction that will be present. More importantly, the positions of the methyl groups with respect to each other on the aryl residue have a greater impact on the type of interactions present in the extended solid state. In 2,6-xylyl$_3$GeBr (8) (Figure 63), methyl substitution on the 2- and 6 positions of the aryl residue result in $CH_3\cdots\pi$ (3.15 Å) interactions. Edge to face (3.01 Å) interactions are then observed from the hydrogens on either the 4- or 5 positions.

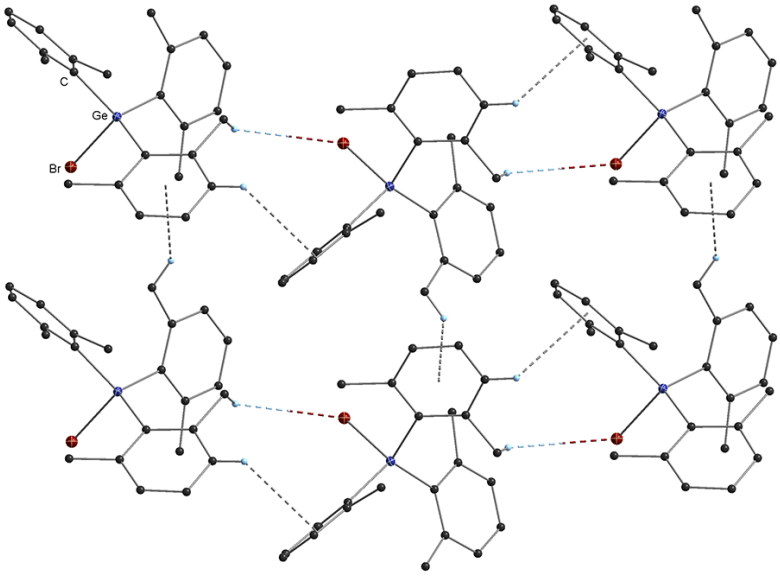

Figure 63. Crystal packing diagram for 2,6-xylyl$_3$GeBr (8). Edge to face, $CH_3\cdots\pi$ interactions and C–H···Br contacts highlighted by dashed bonds. All non-carbon atoms shown as 30% shaded ellipsoids. Hydrogen atoms not involved in intermolecular interactions removed for clarity.

However, by moving these methyl substituents to the 2- and 5 positions, as observed in 2,5-xylyl$_3$GeBr (7), the remaining hydrogens are no longer capable of reaching the aryl residues from neighboring molecules. At the expense of edge to face interactions, the molecules of 2,5-xylyl$_3$GeBr (7) arrange themselves in the extended solid state in order to maximize $CH_3\cdots\pi$ interactions and are therefore

preferred. Further proof of the effect of the methyl substituents' position on the type of electrostatic non-covalent interactions is the fact that all presented 2,5-xylylgermanium derivatives (chloride (13), bromide (7), hydride (15) or hydride/chloride (19)) only display $CH_3\cdots\pi$ interactions. Expectedly, addition of a third methyl group, as seen in 2,4,6-mesityl$_3$GeBr (10), results in the presence of only $CH_3\cdots\pi$ interactions (2.91–3.03 Å). In contrast to all other triarylgermanium bromides, which crystallize as closely packed 3D networks, the lack of edge to face interactions due to the methyl substitution on the mesityl residue of 2,4,6-mesityl$_3$GeBr (10) results in 1D columns of molecules that do not interact with neighboring molecules.

As was observed in the case of 1-naphthyl$_3$GeCl · thf (9a), the bulkiness of three naphthyl residues around the central germanium atom and the cocrystallized solvents in 1-naphthyl$_3$GeBr · toluene (9b) and 1-naphthyl$_3$GeBr · $CHCl_3$ (9c) or naphthalene molecule as seen in 1-naphthyl$_3$GeBr · naphthalene (9d) (Figure 64) circumvent the possibility for π–π stacking interactions.

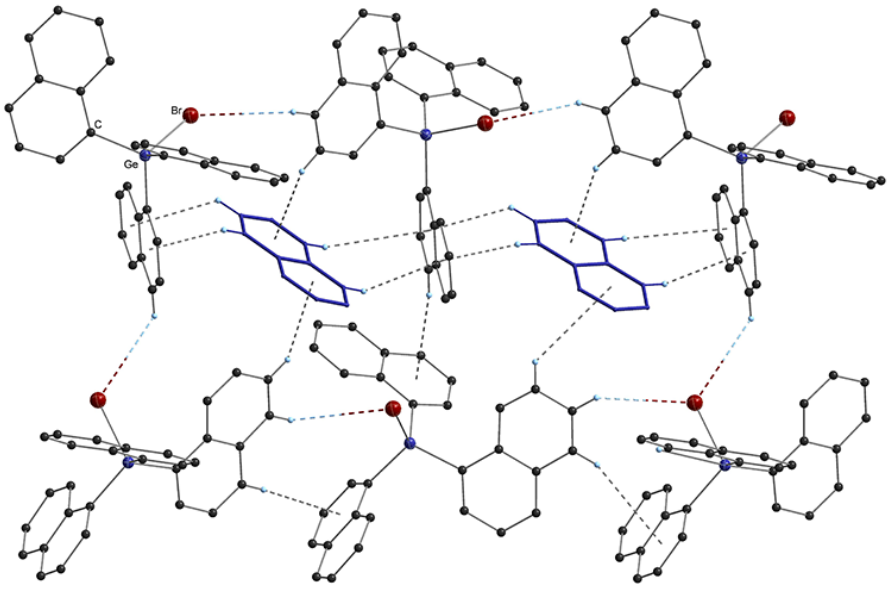

Figure 64. Crystal packing diagram for 1-naphthyl$_3$GeBr · naphthalene (9d). Edge to face interactions and C–H···Br contacts highlighted by dashed bonds. All non-carbon atoms shown as 30% shaded ellipsoids. Hydrogen atoms not involved in intermolecular interactions removed for clarity.

In addition to the naphthyl residues of compounds (9b-d) displaying edge to face interactions with neighboring molecules, these also display interactions with the cocrystallized molecule. While 1-naphthyl$_3$GeBr · toluene (9b) and 1-naphthyl$_3$GeBr · naphthalene (9d) exhibit the expected edge to face interactions between the naphthyl residue and the cocrystallized molecule, 1-naphthyl$_3$GeBr · $CHCl_3$ (9c) displays both CH_3···π interactions from the chloroform molecule to the naphthyl residues and additional C–H···Cl contacts (2.85 Å). Predictably, all of the triarylgermanium bromide derivatives display van der Waals interactions from the bromide substituent and hydrogens (C–H···Br) from neighboring molecules (Table 6).

2.1.2.1.3. Triarylgermanium hydrides - R_3GeH

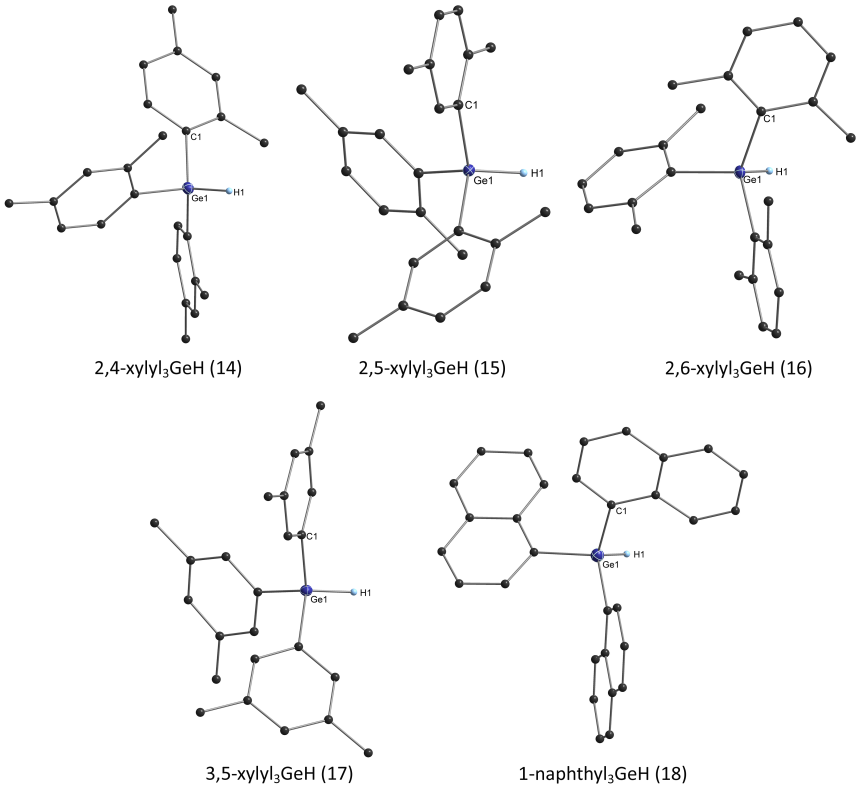

2,4-xylyl$_3$GeH (14) 2,5-xylyl$_3$GeH (15) 2,6-xylyl$_3$GeH (16)

3,5-xylyl$_3$GeH (17) 1-naphthyl$_3$GeH (18)

Figure 65. Crystal structures of presented solid state triarylgermanium. All non-carbon atoms shown as 30% shaded ellipsoids. All hydrogen atoms except those bonded to germanium removed for clarity.

Consistent with increase in steric demand around the central germanium atom, the longest Ge–C bond lengths are observed for aryl residues substituted at both the 2- and 6 positions, including 2,6-xylyl$_3$GeH (16) (1.973(2) Å) and 2-^{t}butylphenylGe$_3$H[17] (1.984(2) Å) as compared to phenyl$_3$GeH (1.944(4) Å) (Table 7).[268] It should be noted that compounds *o*-tolyl$_3$GeH[269] and 2,4,6-mesityl$_3$GeH[270] are highly disordered and therefore excluded from any further crystallographic discussions. This elongation is less pronounced for compounds that have methyl substitution at only one *ortho* position of the aryl residue 2,4-xylyl$_3$GeH (14) (1.957(2) Å), 2,5-xylyl$_3$GeH (15) (1.958(2) Å), and 1-naphthyl$_3$GeH · toluene (18) (1.954(5) Å). In the case of 3,5-xylyl$_3$GeH (17) (1.949(2) Å), substituting the aryl residue at the 3- and 5 positions has no effect on the Ge–C bond length and compares well with phenyl$_3$GeH.[268]

With respect to Ge–H bond lengths, these range from 1.37–1.71 Å. While aryl residue substitution patterns seem to have an effect on the Ge–C bond, unfortunately the same cannot be concluded for the Ge–H bond lengths. This is due to the inherent difficulties in locating light atoms (hydrogen) next to heavy atoms because of their poor scattering abilities and therefore discussions regarding these distances become flawed.

Table 7. List of selected bond lengths and angles for selected triaryl substituted germanium hydrides.

	Space Group	Ge–C (Å) (avg.)	Ge–H (Å)	C–Ge–C (°) (avg.)	C–Ge–H (°) (avg.)
phenyl$_3$GeH[268]	*P*-1	1.944(5)	1.50(5)	109.27(2)	109.67(2)
	*P*2$_1$/*c*	1.944(4)	1.45(3)	110.77(1)	108.33(2)
***o*-tolyl$_3$GeH**[269]	*C*2/*c*	1.961(2)	1.71(2)	106.57(2)	112.69(2)
3,5-xylyl$_3$GeH (17)	*P*2$_1$/*c*	1.949(2)	1.50(2)	109.73(6)	109.2(8)
2,4-xylyl$_3$GeH (14)	*P*2$_1$/*n*	1.957(2)	1.47(2)	108.56(8)	110.37(8)
2,5-xylyl$_3$GeH (15)	*P*2$_1$/*c*	1.958(2)	1.48(2)	109.60(8)	109.31(8)
2,6-xylyl$_3$GeH (16)	*P*2$_1$/*n*	1.973(2)	1.46(2)	110.77(6)	103.8(9)
1-naphthyl$_3$GeH · toluene (18)	*R*-3	1.954(5)	1.55(2)	108.91(13)	110.54(12)
2,4,6-mesityl$_3$GeH[270]	*C*2/*c*	2.045(3)	*	109.2(3)	*
2-^{t}butylphenylGe$_3$H[17]	*P*-1	1.984(2)	1.37(2)	108.10(9)	111(1)

*Hydrogen atom not found on difference map

Table 8. List of selected non-covalent interactions for selected triaryl substituted germanium hydrides.

	Edge to Face (Å)	**$CH_3\cdots\pi$ (Å)**
phenyl$_3$GeH[268]	2.97 – 3.02	—
	—	—
***o*-tolyl$_3$GeH**[269]	—	—
3,5-xylyl$_3$GeH (17)	2.92 – 3.24	2.99 – 3.35
2,4-xylyl$_3$GeH (14)	—	2.79 – 2.88
2,5-xylyl$_3$GeH (15)	—	2.75 – 2.96
2,6-xylyl$_3$GeH (16)	2.64	—
1-naphthyl$_3$GeH · toluene (18)	2.60 – 3.12	—
2,4,6-mesityl$_3$GeH[270]	—	—
2-^{t}butylphenylGe$_3$H[17]	3.08	3.31

In agreement with the triarylgermanium chloride and bromide derivatives, the types of interactions displayed in the triarylgermanium hydrides are dependent on the position of the substituent on the aryl residue. As is the case for all triphenyl halide derivatives, phenyl$_3$GeH[268] only displays edge to face interactions (2.97–3.02 Å). As expected for 2,4-xylyl$_3$GeH (14) and 2,5-xylyl$_3$GeH (15) (Figure 66), only $CH_3\cdots\pi$ interactions are observed, 2.79–2.88 Å and 2.75–2.96 Å respectively.

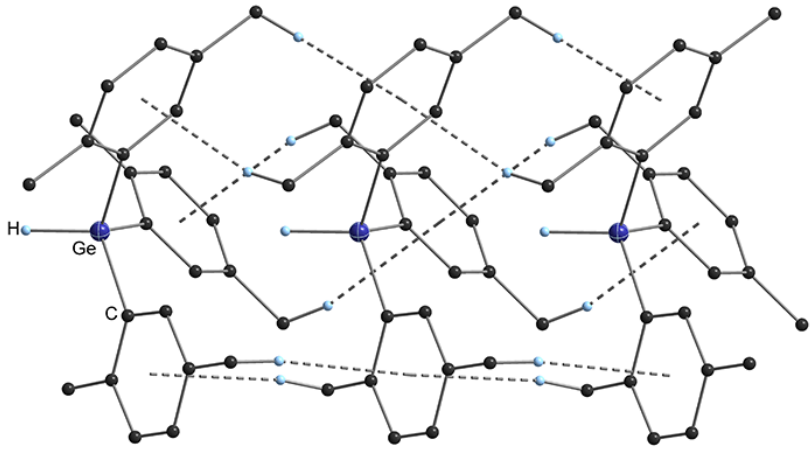

Figure 66. Crystal packing diagram for 2,5-xylyl$_3$GeH (15). $CH_3\cdots\pi$ interactions highlighted by dashed bonds. All non-carbon atoms shown as 3% shaded ellipsoids. Hydrogen atoms not involved in intermolecular interactions removed for clarity.

In contrast to the halide derivatives, 2,5-xylyl$_3$GeCl (13) and 2,5-xylyl$_3$GeBr (7), 2,4-xylyl$_3$GeH (14) and 2,5-xylyl$_3$GeH (15) crystallize in linear 1D infinite chains of molecules propagated by only $CH_3\cdots\pi$ interactions. As a consequence of allowing all the methyl substituents from all the aryl residues to maximize their interaction with neighboring molecules through $CH_3\cdots\pi$ interactions, the Ge–H bonds of all molecules all face in the same linear direction. This results in the hydride substituents attached to the germanium central atoms to approach the exposed sides of the germanium central atom of the neighboring molecule with a Ge–H···Ge distance of 3.74 Å in 2,4-xylyl$_3$GeH (14) with an angle of 175.91° and 3.69 Å in 2,5-xylyl$_3$GeH (15) with an angle of 179.20°. These distances fall within range of previously reported Ge–H···Ge contacts.[271,272] By changing the positions of the methyl substituent in 2,6-xylyl$_3$GeH (16), as has been discussed, a higher propensity for edge to face interactions should be observed and indeed it is the case, with only edge to face interactions present in the extended solid state resulting in a close packed 3D network. Confirming the strength of $CH_3\cdots\pi$ interactions on their capitalizing effect on the orientation of molecules, no close Ge–H···Ge contacts are observed due to loss of linear molecule chains. This is also perhaps due to the steric effects that are afforded by the methyl substituents at both *ortho* positions hindering the hydride substituent from approaching the germanium metal center of neighboring molecules. A similar preference for close packed 3D network is observed for 3,5-xylyl$_3$GeH (17) (Figure 67), where methyl substitution at the 3- and 5 position of the aryl residue allows for both edge to face (2.92–3.24 Å) and $CH_3\cdots\pi$ interactions (2.99–3.35 Å).

In the case of 2-^{t}butylphenylGe$_3$H,[17] both edge to face (3.08 Å) and $CH_3\cdots\pi$ interactions (3.31 Å) are observed as is seen in 2-^{t}butylphenyl$_3$GeCl.[17] As is the case for all four trinaphthylgermanium halide derivatives, 1-naphthyl$_3$GeC · thf (9a), 1-naphthyl$_3$GeBr · toluene (9b), 1-naphthyl$_3$GeBr · $CHCl_3$ (9c), and 1-naphthyl$_3$GeBr · naphthalene (9d), the bulkiness of three naphthyl residues around the central germanium atom and the cocrystallized solvent of toluene in 1-naphthyl$_3$GeH · toluene (18) (Figure 68) does not allow for π–π stacking inter-

actions in the solid state and a 3D network propagated by edge to face interactions (2.60–3.12 Å) is observed.

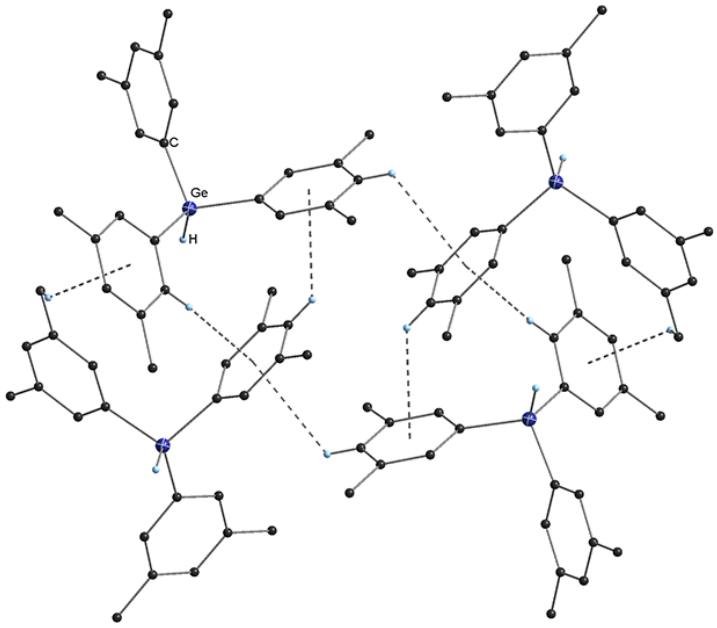

Figure 67. Crystal packing diagram for 3,5-xylyl$_3$GeH (17). Edge to face interactions and $CH_3\cdots\pi$ interactions highlighted by dashed bonds. All non-carbon atoms shown as 30% shaded ellipsoids. Hydrogen atoms not involved in intermolecular interactions removed for clarity.

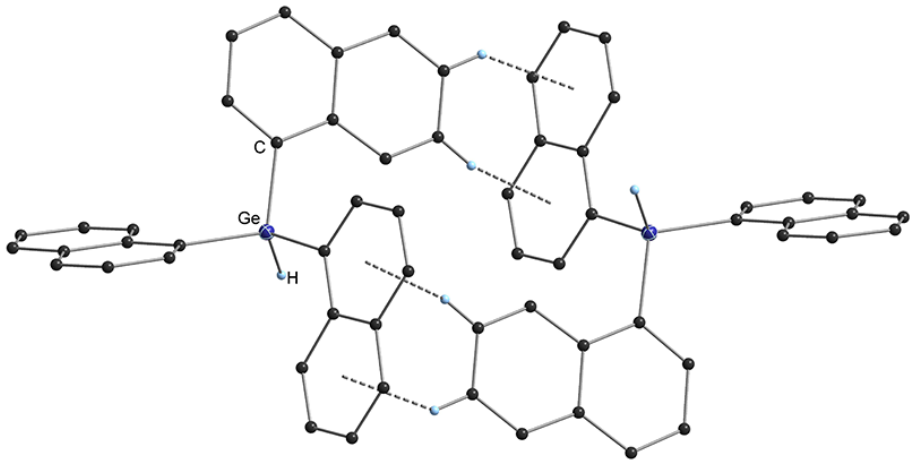

Figure 68. Crystal packing diagram for 1-naphthyl$_3$GeH (18). Edge to face interactions highlighted by dashed bonds. All non-carbon atoms shown as 30% shaded ellipsoids. Hydrogen atoms not involved in intermolecular interactions removed for clarity.

2.1.2.1.4. Diarylgermanium hydrochlorides -R_2GeHCl

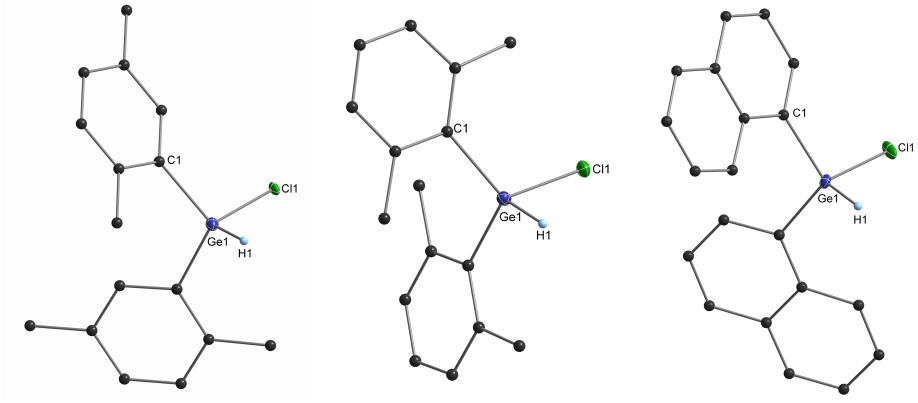

2,5-xylyl$_2$GeHCl (19) 2,6-xylyl$_2$GeHCl (20) 1-naphthyl$_2$GeHCl (21)

Figure 69. Crystal structures of presented solid state diarylgermanium hydrochlorides. All non-carbon atoms shown as 30% shaded ellipsoids. All hydrogen atoms except those bonded to germanium removed for clarity.

In the novel series of diarylgermanium hydrochlorides, averaged Ge–C bond lengths fall within a narrow range of 1.94–1.95 Å and do not seem to be affected by the degree of bulkiness afforded by the organic substituent onto the germanium atom. As was described above, there are inherent difficulties in locating hydrogen atoms next to heavy atoms, therefore the Ge–H bonds, falling in a range of 1.43–1.48 Å are mentioned, but any bulk substituent effects on the Ge–H bond cannot be considered. These bond lengths are also comparable to a series of novel diarylgermanium hydrides (1.41–1.47 Å) described below. The most marked substituent effect on the germanium metal center environment is in regards to the Cl—Ge—H angle of 84.19(7)° in 2,6-xylyl$_2$GeHCl (20) as compared to the much wider angles of 109(2)° in 2,5-xylyl$_2$GeHCl (19) and 103.3(7)°. This suggests that the narrower angle in 2,6-xylyl$_2$GeHCl (20) is a consequence of increased steric bulk afforded by methyl substitution at both *ortho* positions.

Table 9. List of selected bond lengths for diarylgermanium hydrochlorides.

	Space Group	Ge–C (Å) (avg.)	Ge—Cl (Å)	Ge—H (Å)
2,5-xylyl$_2$GeHCl (19)	$P2_1$	1.945(3)	2.134(4)	1.43(4)
2,6-xylyl$_2$GeHCl (20)	$P2_1/n$	1.954(3)	2.194(3)	1.48(3)
1-naphthyl$_2$GeHCl (21)	$P2_1/c$	1.935(3)	2.186(5)	1.41(2)

Table 10. List of selected angles for diarylgermanium hydrochlorides.

	C—Ge—C (°) (avg.)	C—Ge—Cl (°) (avg.)	C—Ge—H (°) (avg.)	Cl—Ge—H (°)
2,5-xylyl$_2$GeHCl (19)	114.42(14)	105.91(10)	110.10(15)	109(2)
2,6-xylyl$_2$GeHCl (20)	115.74(2)	108.79(2)	113.31(2)	84.19(7)
1-naphthyl$_2$GeHCl (21)	113.61(7)	109.82(5)	113.4(7)	103.3(7)

Table 11. List of non-covalent interactions for diarylgermanium hydrochlorides.

	π–π Stacking (Å)		Edge to Face (Å)	$CH_3\cdots\pi$ (Å)	C–H···Cl (Å)
	d	R			
2,5-xylyl$_2$GeHCl (19)	—	—	—	2.62 – 2.87	3.03 – 3.41
2,6-xylyl$_2$GeHCl (20)	—	—	3.39	—	2.93 – 3.22
1-naphthyl$_2$GeHCl (21)	3.52	1.76	2.93 – 2.95	—	2.73 – 3.33

In the extended solid state, compound 2,5-xylyl$_2$GeHCl (19) crystallizes in infinite 1D chains of molecules (Figure 70) propagated by only $CH_3\cdots\pi$ interactions (2.62–2.87 Å) (Table 11) in conjunction with the positions of the methyl substituents in the 2,5-xylyl residue as described in previous sections and similar to 2,4-xylyl$_3$GeH (14) and 2,5-xylyl$_3$GeH (15).

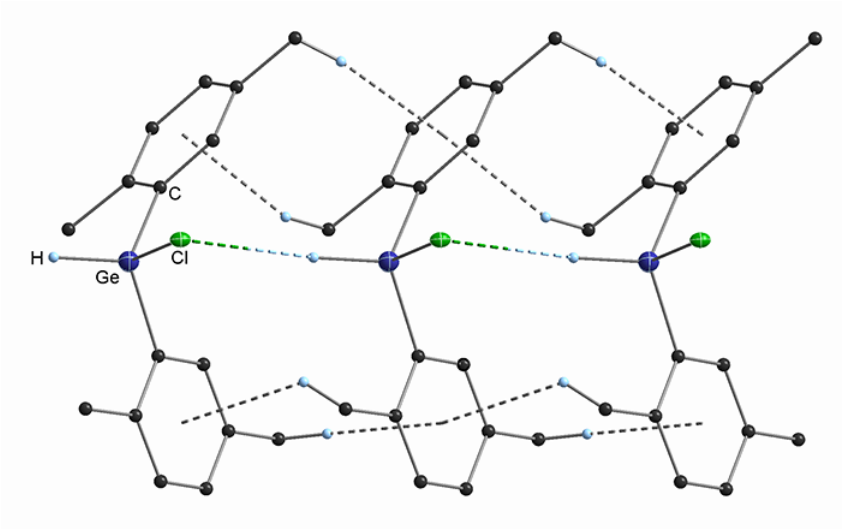

Figure 70. Crystal packing diagram for 2,5-xylyl$_3$GeHCl (19). $CH_3\cdots\pi$ interactions and C–H···Cl contacts highlighted by dashed bonds. All non-carbon atoms shown as 30% shaded ellipsoids. Hydrogen atoms not involved in intermolecular interactions removed for clarity.

In addition, these rows of molecules also arrange themselves to allow the Ge–H bond of all molecules to all face in the same linear direction. This results in the hydride substituents attached to the germanium central atoms to approach the exposed sides of the germanium central atom of the neighboring molecule with a Ge–H···Ge distance of 3.52 Å with an angle of 173.39°. In addition, to the Ge–H···Ge contacts between neighboring molecules in the chain, the chloride substituent interacts with the hydride substituent of the adjacent molecule to allow a C–H···Cl contact (3.38 Å). In contrast to 2,4-xylyl$_3$GeH (14) and 2,5-xylyl$_3$GeH (15), the rows are interacting through further C–H···Cl (3.03 – 3.41 Å) contacts with neighboring rows creating a 3D network, whereas for the monohydrides, contacts between rows was not observed. The change in methyl substituent position on the aryl residue of 2,6-xylyl$_2$GeHCl (20) does not allow rows of Ge–H···Ge facing molecules as was observed for 2,6-xylyl$_3$GeH (16). The unsubstituted *meta* position in 2,6-xylyl$_2$GeHCl (20) interacts with neighboring molecules thorough edge to face interactions (3.39 Å). In addition to C–H···Cl contacts (2.93 – 3.22 Å), 2,6-xylyl$_2$GeHCl (20) displays close Cl···Cl contacts of 3.83 Å creating a 3D network.[273,274] Finally, in contrast to all previously discussed naphthyl germanium derivatives, 1-naphthyl$_2$GeHCl (21) displays close π–π stacking interactions between each naphthyl residue and a neighboring molecule (Figure 71) with a distance of 3.52 Å and a displacement of 1.76 Å between the naphthyl residues.

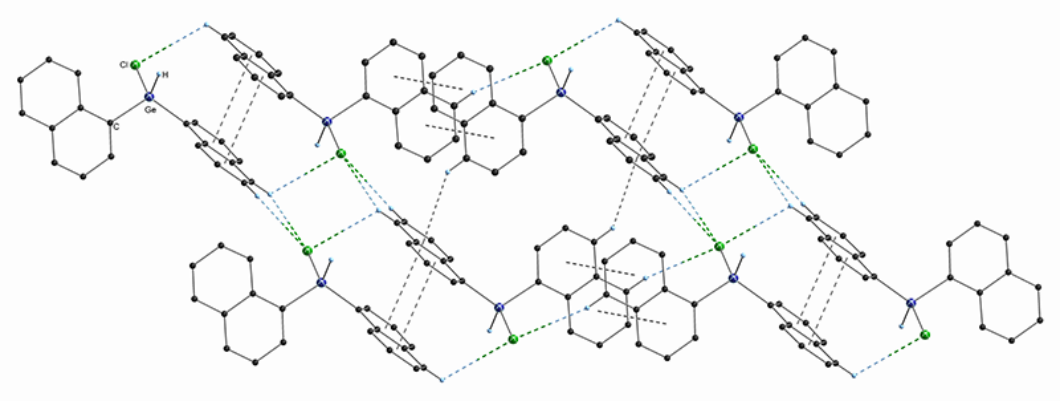

Figure 71. Crystal packing diagram for 1-naphthyl$_3$GeHCl (21). π–π stacking, edge to face interactions and C–H···Cl contacts highlighted by dashed bonds. All non-carbon atoms shown as 30% shaded ellipsoids. Hydrogen atoms not involved in intermolecular interactions removed for clarity.

The molecules in 1-naphthyl$_2$GeHCl (21) orient themselves in order to maximize these interactions and no Ge–H···Ge or Cl···Cl contacts are observed. Not surprisingly, perpendicular edge to face interactions (2.93–2.95 Å) between naphthyl residues of neighboring molecules and C–H···Cl contacts (2.73–3.33 Å) are still present and a 3D network is observed.

2.1.2.1.5. Diarylgermanium dihydrides -R_2GeH_2

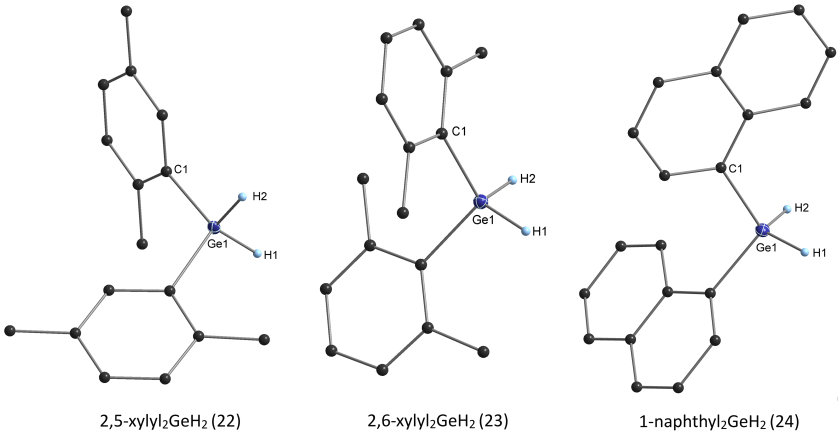

2,5-xylyl$_2$GeH$_2$ (22) 2,6-xylyl$_2$GeH$_2$ (23) 1-naphthyl$_2$GeH$_2$ (24)

Figure 72. Crystal structures of presented solid state diarylgermanium dihydrides. All non-carbon atoms shown as 30% shaded ellipsoids. All hydrogen atoms except those bonded to germanium removed for clarity.

In the novel series of diarylgermanium dihydrides, averaged Ge–C bond lengths fall within a narrow range of 1.94–1.95 Å (Table 12) and are quite comparable to Ge–C bond lengths of all other presented novel and literature known arylgermanium species (1.93–1.99 Å). For the dihydride series, as was observed for the diarylgermanium hydrochlorides derivatives, the Ge–C bond length does not seem to be affected by the degree of bulkiness afforded by the organic substituent onto the germanium atom. In addition, Ge–H bond lengths also fall in a comparable range of 1.41–1.47 Å. With respect to C–Ge–C angles, all compounds with methyl substituted aryl residues display similar angles of 113.70(4)° in 2,5-xylyl$_2$GeH$_2$ (22), 112.87(5)° in 2,6-xylyl$_2$GeH$_2$ (23), and 113.2(1)° in 2,4,6-mesityl$_2$GeH$_2$.[17] In accordance with the steric bulk afforded by the methyl

substituent on the *ortho* position, these molecules subsequently display narrower H–Ge–H angles of 108.23(8)° in 2,5-xylyl$_2$GeH$_2$ (22), 106.9(12)° in 2,6-xylyl$_2$GeH$_2$ (23), and 107.35(3)° in 2,4,6-mesityl$_2$GeH$_2$[17] as compared to their C—Ge—C angles. However, the less encumbering naphthyl residues in 1-naphthyl$_2$GeH$_2$ (24) lead to a reversed effect on the germanium metal environment. In 1-naphthyl$_2$GeH$_2$ (24), the widest H–Ge–H angle is observed, 113.3(15)°, and concurrently displays the widest C–Ge–C angle of 108.98(10)°. Further demonstrating the effect of the nature of the residue on the germanium metal center, all C–Ge–H angles fall in a narrow range of 108.23(8)–109.18(9)°.

Table 12. List of selected bond lengths and angles for diarylgermanium hydrochlorides.

	Space Group	Ge–C (Å) (avg.)	Ge–H (Å) (avg.)	C–Ge–C (°)	H–Ge–H (°)	C–Ge–H (°) (avg.)
2,5-xylyl$_2$GeH$_2$ (22)	*P*-1	1.949(4)	1.45(2)	113.70(4)	110.2(11)	108.23(8)
2,6-xylyl$_2$GeH$_2$ (23)	$P2_1/c$	1.962(2)	1.41(2)	112.87(5)	106.9(12)	109.18(9)
2,4,6-mesityl$_2$GeH$_2$ [17]	*C*2/*c*	1.965(2)	1.43(3)	113.2(1)	107.35(3)	109.06(3)
1-naphthyl$_2$GeH$_2$ (24)	*Pbca*	1.952(2)	1.47(2)	108.98(10)	113.3(15)	108.63(12)

Table 13. List of non-covalent interactions for diarylgermanium hydrochlorides.

	π–π Stacking (Å)		Edge to Face (Å)	$CH_3\cdots\pi$ (Å)
	d	R		
2,5-xylyl$_2$GeH$_2$ (22)	—	—	—	2.69 – 2.82
2,6-xylyl$_2$GeH$_2$ (23)	—	—	2.94	2.78
2,4,6-mesityl$_2$GeH$_2$ [17]	—	—	—	2.71
1-naphthyl$_2$GeH$_2$ (24)	3.53	1.49	2.79 – 2.80	—

In the extended solid state, compound 2,5-xylyl$_2$GeH$_2$ (22) crystallizes in infinite chains of molecules (Figure 73) propagated by only $CH_3\cdots\pi$ interactions (2.69–2.82 Å) (Table 13) in conjunction with the positions of the methyl substituents in the 2,5-xylyl residue as described in previous sections and similar to 2,4-xylyl$_3$GeH (14), 2,5-xylyl$_3$GeH (15) and 2,5-xylyl$_3$GeHCl (19).

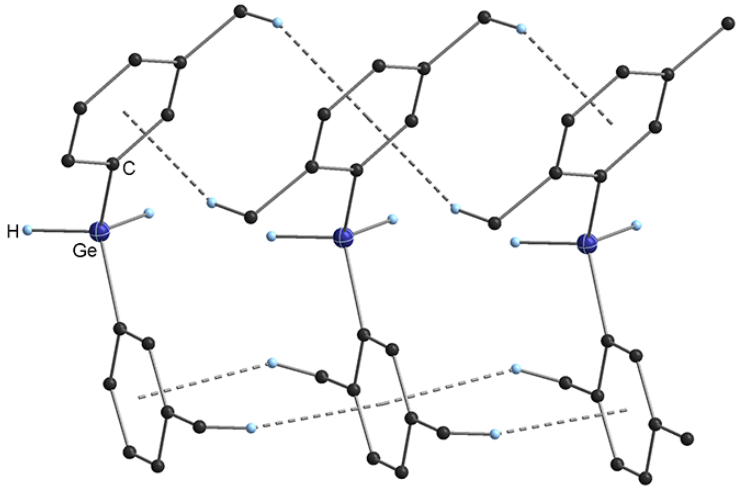

Figure 73. Crystal packing diagram for 2,5-xylyl$_2$GeH$_2$ (22). CH$_3$···π interactions highlighted by dashed bonds. All non-carbon atoms shown as 30% shaded ellipsoids. Hydrogen atoms not involved in intermolecular interactions removed for clarity.

No other interactions are observed between these rows, leading to 1D chains, in contrast to 2,5-xylyl$_3$GeHCl (19) where the chloride substituent interacts through C–H···Cl contacts with neighboring rows creating a 3D network. As a consequence of allowing all the methyl substituents from all both aryl residues to maximize their interaction with neighboring molecules through CH$_3$···π interactions, the Ge–H bonds of all molecules in 2,5-xylyl$_2$GeH$_2$ (22) all face in the same linear direction. This results in the hydride substituents attached to the germanium central atoms to approach the exposed sides of the germanium central atom of the neighboring molecule with the closest Ge–H···Ge distance of 3.47 Å and most linear angle of 179.53° as compared to 3.52 Å and 173.39° in 2,5-xylyl$_2$GeHCl (19), 3.69 Å and 179.20° in 2,5-xylyl$_3$GeH (15), and 3.74 Å and 175.91° in 2,4-xylyl$_3$GeH (14). This is a consequence of the smaller hydride substituents as compared to a chloride or a third aryl residue on the germanium metal center. As concluded in previous sections, the change in methyl substituent position in 2,6-xylyl$_2$GeH$_2$ (23) (Figure 74) results in the capability of the aryl residue to engage in both edge to face and CH$_3$···π creating a 3D network. Unsurprisingly, addition of a third methyl group, as seen in 2,4,6-mesityl$_2$GeH$_2$,[17] results in the presence of only CH$_3$···π interactions (2.71 Å).

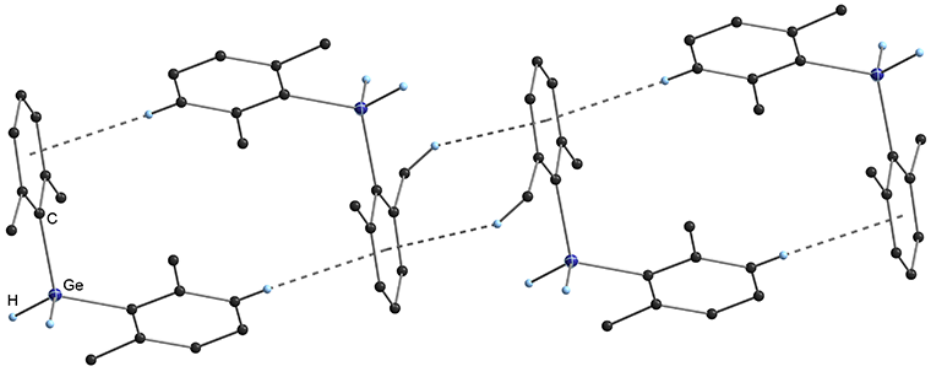

Figure 74. Crystal packing diagram for 2,6-xylyl$_2$GeH$_2$ (23). Edge to face and CH$_3$···π interactions highlighted by dashed bonds. All non-carbon atoms shown as 30% shaded ellipsoids. Hydrogen atoms not involved in intermolecular interactions removed for clarity.

Finally, as was observed for 1-naphthyl$_2$GeHCl (21) and in contrast to all previously discussed naphthyl germane derivatives, 1-naphthyl$_2$GeH$_2$ (24) displays close π–π stacking interactions between one of its naphthyl residues and a neighboring molecule (Figure 75) with a distance of 3.53 Å and a displacement of 1.49 Å between the naphthyl residues. The presence of these close π–π stacking interactions circumvents the need for cocrystallization molecules necessary for the stabilization of the aforementioned trinaphthyl derivatives. The remaining naphthyl residues display edge to face (2.79–2.80 Å) interactions with neighboring molecules to create a closely packed 3D network.

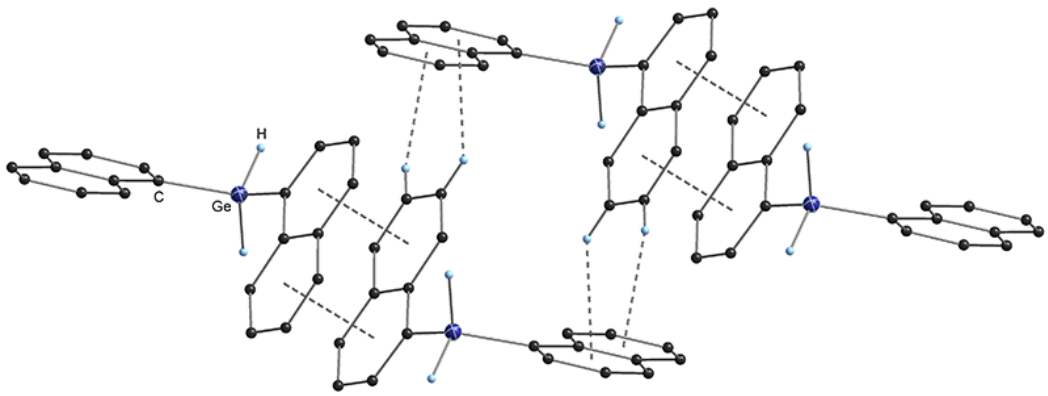

Figure 75. Crystal packing diagram for 1-naphthyl$_2$GeH$_2$ (24). π–π stacking and edge to face interactions highlighted by dashed bonds. All non-carbon atoms shown as 30% shaded ellipsoids. Hydrogen atoms not involved in intermolecular interactions removed for clarity.

2.1.2.1.6. Conclusions

A series of aryl substituted germanium halides and hydrides have been fully characterized with X-ray crystallography, which has been proven to be the most important characterization technique available to gain information regarding structural elucidation. The effects of aryl residue bulk, methyl substitution pattern and substituent on the germanium metal environment has been discussed for a variety of tetra-, tri- and diaryl species. Consistent with increased in steric demand around the central germanium atom, the longest Ge–C bond lengths are observed for aryl residues substituted at both the 2- and 6 positions. With respect to Ge–H bond lengths from triaryl and diaryl substituted germanium hydrides, these range from 1.37–1.71 Å. While aryl residue substitution patterns seem to have an effect on the Ge–C bond, unfortunately the same cannot be concluded for the Ge–H bond lengths. This is due to the inherent difficulties in locating light atoms (hydrogen) next to heavy atoms because of their poor scattering abilities.

All trinaphthylgermanium halide and hydride derivatives crystallize in the presence of either a solvent of crystallization as seen for 1-naphthyl$_3$GeH · toluene (18), 1-naphthyl$_3$GeCl · thf (9a), 1-naphthyl$_3$GeBr · toluene (9b), 1-naphthyl$_3$GeBr · $CHCl_3$ (9c), or with a naphthyl molecule as seen in 1-naphthyl$_3$GeBr · naphthalene (9d). This highlights the inherent difficulties with isolating naphthyl derivatives of germanium. In contrast, the diarylgermanium hydrides 1-naphthyl$_2$GeHCl (21) and 1-naphthyl$_2$GeH$_2$ (24) crystallize in the absence of solvent molecules. This is a direct consequence of the ability of the diaryl hydride derivatives to exhibit strong electrostatic non-covalent interactions in the extended solid state.

While not previously mentioned in literature, electrostatic interactions in the form of π-stacking stemming from the aromatic substituents (π–π stacking, edge to face and $CH_3\cdots\pi$ interactions) and van der Waals contacts from the halogenide substituent and adjacent hydrogens, C–H···X (X = Cl, Br) offer an overall stabilizing effect to these molecules in the solid state and aid in their crystallization. The types of non-covalent interactions present in these systems are directly depend-

ent on the nature of the aryl substituent. The most prominent type of non-covalent interaction is edge to face interactions and was found in compounds regardless of their bulk or methyl substitution pattern. However, the presence of $CH_3\cdots\pi$ interactions was more dependent on not just the addition of methyl substituents to the aryl residue but to their relative position on the aromatic ring. In the case of germanium derivatives with the 2,6-xylyl residue, both edge to face and $CH_3\cdots\pi$ interactions were present creating extended 3D networks. On the other hand, in the case of germanium derivatives with the 2,4- or 2,5-xylyl residue, $CH_3\cdots\pi$ interactions were solely observed. This also had a direct effect on the extended solid state, whereas 2,6-xylyl germanium derivatives exhibited 3D networks, 2,4- or 2,5-xylyl germanium derivatives in most cases crystallized as 1D chains.

Despite the capacity for the naphthyl residue in naphthylgermanium derivatives (4, 9, 11, 17) to potentially display π–π stacking interactions, the bulkiness of four or three naphthyl residues around the central germanium and the solvent of crystallization hindered the naphthyl residues from neighboring molecules from approaching each other in a planar fashion to allow this type of interaction. However, π–π stacking interactions were finally observed for both 1-naphthyl$_2$GeHCl (21) and 1-naphthyl$_2$GeH$_2$ (24). These compounds both crystallize as 3D networks through additional edge to face interactions and C–H···Cl contacts for the 1-naphthyl$_2$GeHCl (21). C–H···X contacts (X = Cl, Br) were present in all arylgermanium halides and helped to obtain 3D networks in the extended solid state.

2.1.2.2. NMR spectroscopy

While NMR spectroscopy is a very useful technique for the characterization and control of the reaction progress for group 14 elements, germanium is yet another exception. In the case of ^{29}Si or ^{117}Sn/^{119}Sn NMR spectroscopy, much

information regarding the group 14 central atom and its bonding environment is provided. However, this cannot be said for ^{73}Ge spectroscopy, the only NMR-active nucleus of germanium. While ^{29}Si and ^{119}Sn, like ^{1}H or ^{13}C, are spin $^{1}/_{2}$ nuclei, ^{73}Ge has a spin of $^{9}/_{2}$ with a large quadrupole moment, often leading to broad lines, though which can be improved in a symmetric environment. With a natural abundance of 7.7%, ^{73}Ge is additionally lacking sensitivity compared to the other group 14 elements.[275] This, and the fact that only few working groups are capable of performing ^{73}Ge NMR measurements, makes the preparation, isolation and characterization of organogermanium compounds much harder.

To further complicate matters, ^{13}C NMR spectroscopy gives little indication whether the organometallic compound has been formed or not, making its use impractical. Moreover so when trying to monitor the reaction progress and not only clean products.

For comparison purposes, phenyl and mesityl substituted compounds are also included in the study. However, being measured in different environments and despite the synthesis of arylgermanium compounds being studied for quite some time, either no detailed data or no data at all are available. Spectral parameters including shifts are dependent on the solvents used. Therefore, all compounds prepared within the course of this work were measured in $CDCl_3$ for easier comparison, however, references included within this compilation might have measured in other solvents, thus only approximate comparison is possible. All ^{13}C and ^{1}H shifts can be examined in detail in Chapter 3.6.1 for each compound prepared within the course of this work.

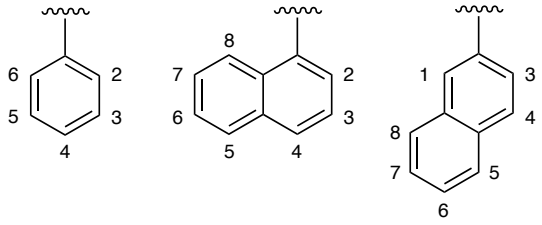

Figure 76. The numbering of carbon positions of 1-phenyl, 1-naphthyl and 2-naphthyl substituted germanium compounds.

Not much can be said about the NMR shifts of R_4Ge since comparable data are not measured in $CDCl_3$, however all shifts are within expected ranges. Similar patterns can be observed when looking at R_3GeX.

It is noticeable, however, that 1-naphthyl$_3$GeX (9) and 2-naphthyl$_3$GeCl are clearly distinguishable from tolyl and xylyl compounds, with the aromatic protons shifting downfield.

m-tolyl$_4$Ge (1) shows a multiplet at 7.13 ppm in the aromatic region and a singlet at 2.21 ppm corresponding to the methyl group in the ^{1}H NMR spectrum. All ^{13}C NMR signals correspond to the respective carbon atoms. The ^{1}H NMR spectrum for 3,4-xylyl$_4$Ge (2) contains a doublet at 7.25 ppm for the 5,6-H, a doublet at 7.11 ppm for the 2-H and two single peaks at 2.25 and 2.20 ppm, corresponding to the methyl groups. The ^{13}C NMR spectrum shows 8 signals, corresponding to the respective carbon atoms. 3,5-xylyl$_4$Ge (3) shows a singlet at 7.12 ppm for the 2,6-H, another singlet at 7.01 ppm for the 4-H and a singlet at 2.27 ppm for the methyl groups. The ^{13}C NMR spectrum contains 5 signals, as would be expected. The ^{1}H NMR spectrum for 2-naphthyl$_4$Ge (4) contains a singlet at 8.12 ppm for the 1-H, a doublet at 7.87 for 3-H, a doublet at 7.85 for 4-H, a triplet at 7.74 for 5,8-H and a multiplet at 7.48 for 6,7-H. In the ^{13}C NMR spectrum, the signals corresponding to all the carbon atoms are present as singlets, containing 10 in total.

Similar pattern can be observed in the case of R_3GeX. The ^{1}H NMR spectrum of *o*-tolyl$_3$GeX (5) contains a doublet at 7.46 ppm for the 6-H, a triplet at 7.36 ppm for 3-H, a multiplet at 7.21 ppm for the 4,5-H and a singlet at 2.35 ppm corresponding to the methyl group. The ^{13}C NMR spectrum contains 6 signals, with one signal in the aliphatic region at 23.42 ppm corresponding to the methyl group. The ^{1}H NMR spectrum for 2,4-xylyl$_3$GeX (6) contains a doublet at 7.30 ppm for 6-H, a singlet at 7.07 ppm for 3-H, a doublet at 6.99 for 2-H and two singlets at 2.33 ppm and 2.30 ppm for the two methyl groups. In the ^{13}C NMR spectrum, 8 signals are observed, each carbon atom presented as a singlet with two signals in the aliphatic region. The ^{1}H NMR spectrum for 2,5-xylyl$_3$GeX (7) contains a singlet at 7.28 ppm for 6-H, a doublet at 7.14 ppm for 3,4-H and two sin-

glets in the aliphatic region (2.29 ppm and 2.25 ppm) corresponding to the methyl groups. In the ^{13}C NMR spectrum, 8 signals can be observed, with each carbon atom presented as a singlet and the two methyl groups in the aliphatic region. A triplet at 7.19 ppm for 4-H, a doublet at 7.00 ppm for 3,5-H and a singlet at 2.31 for the methyl groups can be observed in the ^{1}H NMR spectrum of 2,6-xylyl$_3$GeX (8). The ^{13}C NMR spectrum shows 4 signals in the aromatic region and one signal in the aliphatic region as expected. 3,5-xylyl$_3$GeCl (11) shows a singlet at 7.22 ppm for 2,6-H, a singlet at 7.08 ppm for 4-H and a singlet at 2.31 ppm for the methyl group in its ^{1}H NMR spectrum. The ^{13}C NMR spectrum contains 5 peaks, with one singlet in the aliphatic region. The ^{1}H NMR spectrum for 1-naphthyl$_3$GeX (9) shows a doublet at 8.28 ppm for 8-H, a doublet at 7.98 ppm for 2-H, a doublet at 7.90 ppm for 4-H, a doublet at 7.73 ppm for 5-H, a triplet at 7.47 ppm for 7-H and a multiplet at 7.36 ppm for 3,6-H. In the ^{13}C NMR spectrum, the signals corresponding to the respective carbon atoms are present as singlets, containing 10 in total. The ^{1}H NMR spectrum for 2,4,6-mesityl$_3$GeX (10) shows a singlet at 6.78 ppm for 3,5-H, a singlet at 2.24 ppm for the *para* methyl group and another singlet at 2.13 ppm for the *ortho* methyl groups. The ^{13}C NMR spectrum contains 6 signals with two signals in the aliphatic region. The ^{1}H NMR spectrum of 2-naphthyl$_3$GeCl (12) contains a singlet at 8.17 ppm for 1-H, a doublet at 7.92 ppm for 3-H, a doublet at 7.86 ppm for 4-H, a doublet at 7.81 ppm for 5-H, a doublet at 7.75 ppm for 8-H and a multiplet at 7.51 ppm 6,7-H. In the ^{13}C NMR spectrum, the signals corresponding to the respective carbon atoms are present as singlets, containing 10 in total.

Methyl groups can be used as a reference, whether the product is clean or not, since shoulders or another set of methyl signals will appear. In most cases the aryl region is too crowded, to deliver much useful information for characterization.

Table 14. Overview of ^{1}H NMR and IR data of arylgermanium hydrides and arylgermanium hydrochlorides. [a] in CCl_4; [b] in THF-d_8; [c] in C_6D_6/TMS; [d] in C_6D_6

	R	ν Ge—H (cm^{-1})	δ Ge—H (ppm)	δ R—H (ppm)	δ *o*-CH_3 (ppm)	δ *m*-CH_3 (ppm)	δ *p*-CH_3 (ppm)
R_3GeH	**phenyl**	2025 [25] 2046 [242,276]	5.66 [a, 276]				
	2,4-xylyl	2050	5.84 s	7.04 s, 3-H 7.02 d, 5,6-H	2.26 s		2.30 s
	2,5-xylyl	2037	5.82 s	7.09 s, 3,4-H 6.98 s, 6-H	2.20 s	2.24 s	
	2,6-xylyl	2072	5.90 s	7.13 t, 4-H 6.96 d, 3,5-H	2.17 s		
	3,5-xylyl	2035	5.52 s	7.13 s, 2,6-H 7.00 s, 4-H		2.28 s	
	1-naphthyl	2063	6.48 s	7.99 d, 8-H 7.85 d, 2-H 7.83 d, 4-H 7.33 m, 3,5,6,7-H			
	mesityl	2052 [242]	5.80 [b, 277]	6.75 [b, 277]	2.10 [b, 277]		2.20 [b, 277]
R_2GeHCl	**phenyl**	2077 [276] 2080 [25]	6.38 [a, 276]				
	2,5-xylyl	2090	6.61	7.38 s, 6-H 7.13 dd, 3,4-H	2.34 s	2.31 s	
	2,6-xylyl	2103	6.89	7.20 t, 4-H 7.02 d, 3,5-H	2.46 s		
	1-naphthyl	2104	7.22	8.06 d, 8-H 7.97 d, 2-H 7.90 d, 4-H 7.69 d, 5-H 7.49 m, 3,6,7-H			
	mesityl	2085 [276]	6.83 [c, 276]	6.57 [c, 276]	2.36 [c, 276]		2.03 [c, 276]
R_2GeH_2	**phenyl**	2051 [278] 2054 [25]	5.02 [b, 51]	7.10- 7.50 [b, 51]			
	2,5-xylyl	2055	5.03	7.21 s, 6-H 7.08 s, 3,4-H	2.31 s	2.26 s	
	2,6-xylyl	2056	5.13	7.13 t, 4-H 6.99 d, 3,5-H	2.36 s		
	1-naphthyl	2050	5.64	8.00 d, 8-H 7.89 dd, 2,4-H 7.67 d, 5-H 7.43 m, 3,6,7-H			
	mesityl	2074 [242]	5.27 [d, 15]	6.72 [d, 15]	2.33 [d, 15]		2.09 [d, 15]
$RGeH_3$	**phenyl**	2070 [25] 2082 [242]	4.22 [a, 276]				
	2,5-xylyl		4.14 s	7.02 m, 3,4,6- H	2.28 s	2.22 s	
	2,6-xylyl		4.12 s	7.11 t, 4-H 6.98 d, 3,5-H	2.37s		
	mesityl	2077 [242]	4.06 [b, 279]	6.72 [b, 279]	2.29 [b, 279]		2.20 [b, 279]

It becomes more interesting, however, when studying the arylgermanium hydrides, due to ^{1}H NMR becoming an useful tool for distinguishing whether the desired compound was formed or not. In all cases, a single peak further upfield from the aryl region is observed, corresponding to the number of hydridic protons. All the Ge–H shifts (Table 14) lie within the expected region, showing the characteristics couplings for aryl substituents in the aromatic region. A comparison with similar compounds is difficult, due to the fact that different solvents were used or not sufficient data was reported. However, in the case of the triarylgermanium hydrides it can be stated that increase of the steric bulk of the ligands leads to a lowfield shift of δ Ge–H. As expected, a low field shift for δ Ge–H of the germanium hydrochlorides in comparison with the triarylgermanium hydrides can be observed. Compounds bearing the 1-naphthyl moieties seem to be some kind of aberration again, since δ Ge–H indeed differs compared to all other compounds. However, the shift of the Ge–H signal corresponds with the trend: the Ge–H peak shifts upfield when increasing the number of hydridic protons. This can also be noticed for all other residues.

^{19}F NMR was applied to monitor the progress of reactions where trifluoromethanesulfonic acid (HOTf) was applied. HOTf gave a single signal around -79.20 ppm, while 2-naphthyl$_3$GeHOtf, 2,5-xylyl$_2$GeHOTf, 2,6-xylyl$_2$GeHOTf and 1-naphthyl$_2$GeHOTf show single signals at δ -82.10 ppm, δ -76.78 ppm, δ -77.11 ppm and δ -76.86 ppm respectively. The reaction was considered to be complete when no or only a very small signal for HOTf was observed. Addition of LiCl resulted in a downfield shift. This is demonstrated for the 2,6-xylyl moiety in Figure (Figure 77), where in the NMR measured after 18 hours, two peaks at δ -77.11 ppm (2,6-xylyl$_2$GeHOTf) and δ -79.18 ppm (unreacted HOTf) are visible. After 24 hours the reaction is completed resulting in a single signal. LiCl was added and stirred for 24 hours. Again, a single peak at δ -78.68 is observed belonging to the arylgermanium hydrochloride 2,6-xylyl$_2$GeHCl (20).

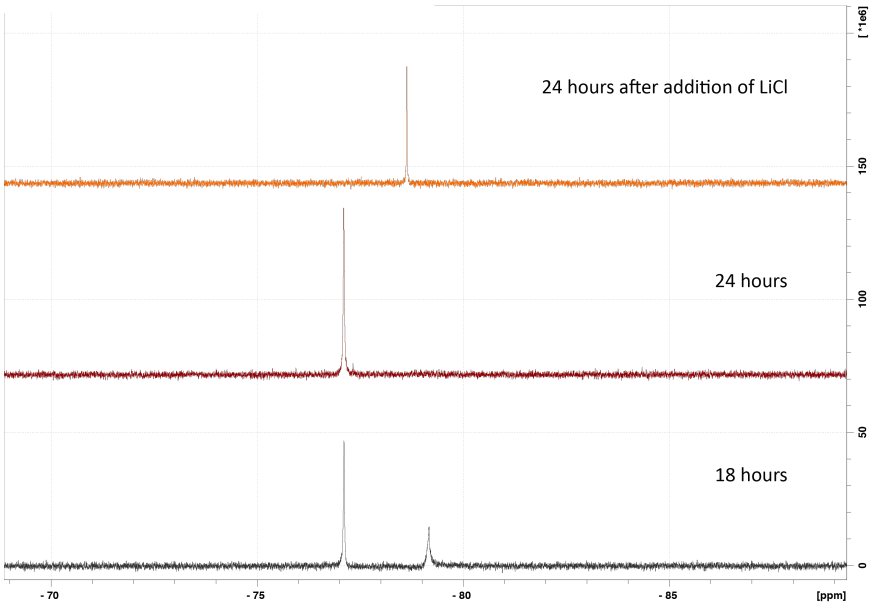

Figure 77. ^{19}F NMR- reaction of 2,6-xylyl$_3$GeH (16) with HOTf and reaction with LiCl.

^{1}H NMR is also a useful tool for monitoring the progress of the reactions, even more so when 1-naphthyl moieties are involved, since naphthalene shows a very specific pattern. The ^{1}H NMR spectrum for naphthalene shows two equal multiplets at δ 7.25 and δ 7.63 ppm in C_6D_6 (δ 7.50 ppm and δ 7.86 ppm in $CDCl_3$) and is thus very characteristic, making it easy to observe, whether the aryl moiety has been cleaved (Figure 78).

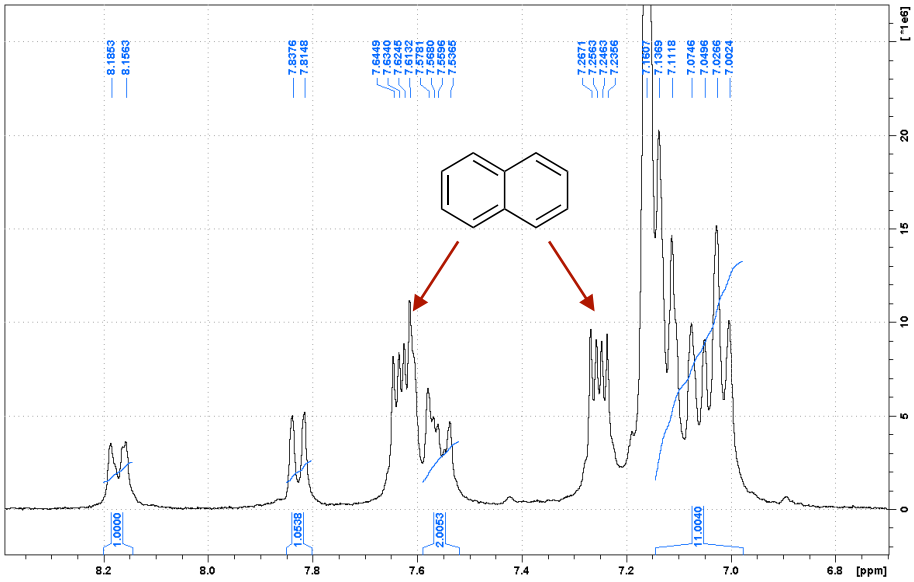

Figure 78. ^{1}H NMR of 1-naphthyl$_2$GeHCl (21), impurities of naphthalene, measured in C_6D_6.

2.1.2.3. Infrared spectroscopy

For a long time, IR shifts, elemental analysis and melting points where very important for the characterization of organogermanium compounds. Even today, these characterization methods have an important role, moreover compared to other group 14 elements. IR shifts for all arylgermanium hydrides (Table 14) were measured and show distinctive peaks for the Ge-H vibration between 2000 cm^{-1} and 2104 cm^{-1}, as shown on the example 2,4-xylyl$_3$GeH (Figure 79). It must be taken into account that although phenyl and mesityl derivatives were included for comparison reasons all referenced spectra were measured in liquid state, while all compounds prepared within this work were measured *via* ATR-IR.

Studies show that the frequency and intensity of ν(Ge–H) depends on electronic effects of the ligands.[242] It was shown that in phenyl$_3$GeH, phenyl$_2$GeH$_2$ and phenylGeH$_3$, $\Delta\nu$ is determined by d_π -p_π interactions, however, this effect decreases from phenyl to xylyl due to of the smaller inductive effect of xylyl in comparison to phenyl.[280,281] IR values, even more so when considering the di- and trihydrides, do not seem to follow a general pattern. However, it was shown in the case of mesitylGeH$_3$, that the surprisingly low frequency is the result of the smaller negative inductive effect of the mesityl group. Furthermore, the steric effect of the mesityl group decreases compared to higher arylated systems, due to the fact that there is only one aromatic ligand.[242] It was already stated before, that *o*-methyls are causing steric effects by interacting with neighboring aromatic ligands.[218] This would also explain why all Ge-H frequencies are elevated when taking a look at the 2,6-xylyl substituent. Generally, ν(Ge–H) increases with increasing steric bulk of the ligand, with the exception of mesityl substituents. Substituting one aryl group with a Cl atom leads to the expected increase of ν(Ge–H) in the case of the arylgermanium hydrochlorides. To conclude, all IR values measured lie within the expected values for ν(Ge–H). In all spectra broad peaks with weak or medium intensity were found around 2800-3100 cm^{-1} and attributed to the C–H stretching vibrations of the aryl ligands as shown on the example 2,4-xylyl$_3$GeH (Figure 79).

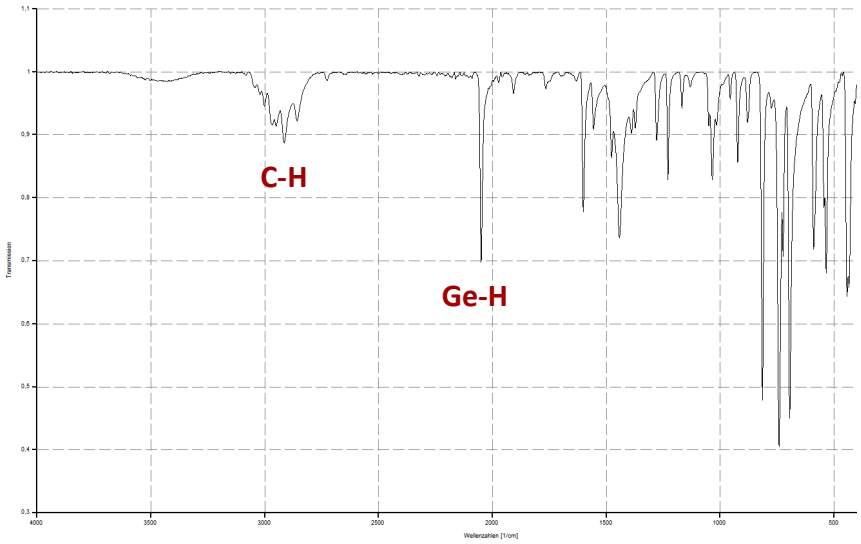

Figure 79. IR of 2,4-xylyl$_3$GeH (14) as an example.

2.1.2.4. GCMS measurements

Mass spectrometry has been of great interest in the case of germanium, since other characterization methods only give sparse information. Also during this work, mass spectrometry methods have been of importance, due to providing a good insight into whether the desired compound was formed or not. Nevertheless, reaction control using MS methods is complicated in various cases, because of side products interfering with measurements or affecting column material in the case of gas chromatography couples systems. For detailed information see Chapter 3.3.

Generally, retention times shortened upon substituting aryl ligands with either chloride or hydride atoms. Comparison of the arylgermanium trihydrides, diarylgermanium dihydrides and triarylgermanium hydrides shows that retention times decrease remarkably. In the case of the triarylgermanium halides, it can be assessed that chloride species elude before their bromide derivatives.

It is expected for the germanium spectra to be similar to the tin analogues due to their same outer shell electronic structure. Lawson *et al.* investigated the

fragmentation pattern of Ph_xGeCl_{4-x} in great detail and found that indeed the electron impact ionization process is comparable.[282]

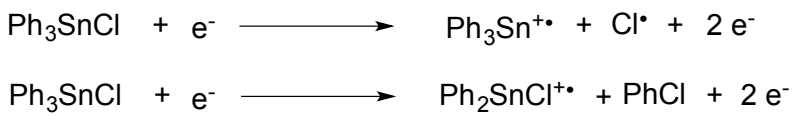

Figure 80. EI ionization processes for Ph_3SnCl.[282]

In all cases involving a germanium atom, broad peaks can be expected due to the germanium isotopes. The highest peak was chosen for assignment of molecular ions.

In the case of tetraarylgermanes, loss of the aryl radicals can be observed. Interestingly, in all cases, formation of biaryl species can be observed, often showing even the highest abundance, which was already reported for a variety of other aryl substituted germanium and tin compound and can be attributed to rearrangement reactions leading to the chloroaryl and the biaryl species.[282,283] The loss of one aryl group after the other has been observed before by Glocking *et al.* and can be confirmed for all tetraarylgermanes within this work.[283] It was not possible to detect 2-naphthyl$_4$Ge (4) with the usual methods, wherefore DI/EI mass spectrometry was performed, showing the same results. In all cases, decomposition of the aryl substituents can be observed.

Halide compounds can be easily detected due to their special peak pattern. Two molecule ion peaks are normally visible, in accordance with their isotope abundance. In general, halide atoms can be cleaved off easily.

Table 15. Isotopes of chlorine and bromine and their abundance.

	Isotope mass	**Isotope abundance**
Cl	35	75.8 %
	37	24.2 %
Br	79	50.7 %
	81	49.3 %

In the case of triarylgermanium halides, two different fragmentation pathways can be identified, which involve loss of aryl and/or halide in the first step.[283] In all cases the abundance of the molecule ion peak is very low. In the case of *o*-tolyl$_3$GeX, it was observed that one aryl group is leaving first, followed by the halide cleavage. Again, the formation of biaryl species takes place, caused by the elimination of RGeX from $R_3GeX^{+\bullet}$. The biaryl fragment shows the highest abundance in all cases, with the exception of *o*-tolyl$_3$GeBr, where the peak at 334.0 assigned to ($M^{+\bullet}$ - *o*-tolyl) shows the highest abundance. Decomposition of the aryl ligands themselves can be observed in all cases.

In the case of triarylgermanium hydrides, molecule ion peaks can be assigned for all xylyl substituted compounds (14-17) at m/z 389.1 and at m/z 456.1 for 1-naphthyl$_3$GeH (18). No formation of biaryl species can be detected in the case of compounds bearing a xylyl moiety, thus ($M^{+\bullet}$ - xylylH) showing the highest abundance. In the case of 2,6-xylyl$_3$GeH (16), a second peak at m/z 178.0 assigned to ($M^{+\bullet}$ - 2,6-xylyl$_2$) of the same abundance can be observed. For compounds (14-17), decomposition of the aryl groups can be observed. It can be noticed that methyl groups are leaving first, followed by the aryl residue. In the case of 1-naphthyl$_3$GeH (18), binaphthalene can be referred to as the peak with the highest abundance.

In the case of the diarylgermanium hydrochlorides, molecule ion peaks can be observed. Loss of aryl and chloride are noticeable, with ($M^{+\bullet}$ - xylyHCl) as the peak with the highest abundance in the case of 2,5-xylyl$_2$GeHCl (19) and 2,6-xylyl$_2$GeHCl (20) and ($M^{+\bullet}$ - 1-naphthylGeHCl) in the case of 1-naphthyl$_2$GeHCl (21). In all cases, decomposition of the aryl ligands can be observed.

For 2,5-xylyl$_2$GeH$_2$ (22) and 2,6-xylyl$_2$GeH$_2$ (23), a molecular ion peak at m/z 286.1 can be observed. The highest peak at m/z 105.1 can be assigned to ($M^{+\bullet}$ - 2,5-xylylGeH$_2$) for 2,5-xylyl$_2$GeH$_2$ (22). 2,6-xylyl$_2$GeH$_2$ (23) shows its highest peak at m/z 180.0 (($M^{+\bullet}$ - 2,6-xylyH$_2$). For 1-naphthyl$_2$GeH$_2$ (24) the molecule ion peak can be detected at m/z 330.1. The peak at m/z 201.0 shows the highest abundance and can be assigned to ($M^{+\bullet}$ - 2-naphthylH$_2$). In contrast to compounds

2,5-xylyl$_2$GeH$_2$ (22) and 2,6-xylyl$_2$GeH$_2$ (23), the formation of binaphthalene in high abundance can be detected. Decomposition of the aryl ligand can be observed again.

2,5-xylylGeH$_3$ (25) and 2,6-xylylGeH$_3$ (26) show their molecule ion peaks at m/z 180.0 with high abundance. The peak at 105.1 assigned to ($M^{+\bullet}$ - GeH$_3$) shows the highest abundance. Decomposition of the aryl ligand can be observed again.

2.2. Antimony compounds

2.2.1. Synthesis

Various organoantimony compounds were synthesized and characterized using techniques such as NMR, single crystal X-ray or GCMS techniques. In all cases, the antimony atom is bonded to at least one aromatic ligand. The ligands were chosen concerning their steric bulk, bearing either one or two methyl groups in different positions towards the germanium atom, or include even larger polyaromatic systems. All ligands used are presented in Figure 81.

While compounds 2,6-xylyl$_3$Sb (40), 1-naphthyl$_3$Sb (41), 2,6-xylyl$_2$SbBr (42), as well as *o*-tolylSbCl$_2$ (45) have been reported and characterized before, to our knowledge their crystal structures have not been determined yet. Compounds 9-anthracenyl$_2$SbBr (43) and [9-anthracenyl$_2$Sb]$_2$ (44) bearing the 9-anthracenyl moieties are, to the best of our knowledge, the first Sb anthracene compounds to be prepared and fully characterized.

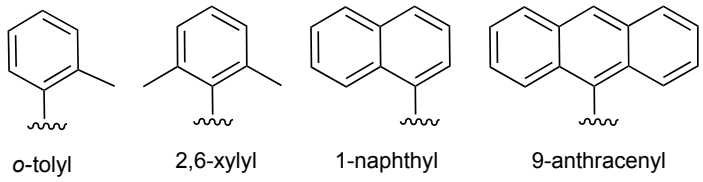

Figure 81. Aromatic ligands employed for the preparation of organoantimony compounds.

Although it was possible to prepare alkylantimony halides directly from $SbCl_3$ and the corresponding Grignard reagent, reactions for the mesityl moiety performed poorly, yielding a mixture of products which were difficult to separate.[150] Redistribution reactions have been employed various times, thus our initial approach was to prepare the triarylantimony species, which in the case of mesityl seems to be the favored product formed, and subsequently react these with $SbCl_3$ to obtain the arylsubstituted antimony mono- and dihalides.[150,284,285] The compounds 2,6-xylyl$_3$Sb (40), 1-naphthyl$_3$Sb (41), 2,6-xylyl$_2$SbBr (42), anthracenyl$_2$SbBr (43) and [9-anthracenyl$_2$Sb]$_2$ (44) were synthesized over the Grignard route (Figure 82).

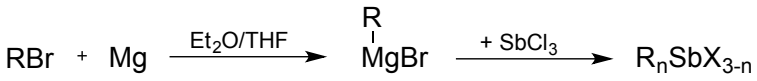

Figure 82. Grignard reaction for the preparation of organoantimony compounds with R = *o*-tolyl, 2,6-xylyl (40), 1-naphthyl (41) and 9-anthracenyl (43,44).

A flask equipped with a dropping funnel and a reflux condenser was charged with Mg in THF. The dropping funnel was charged with arylbromide in THF, about 10% of the solution was added to the reaction vessel and the solution was heated carefully to start the reaction. The arylbromide was subsequently added slowly. After complete addition, the reaction was refluxed overnight. A second flask equipped with a mechanical stirrer and a reflux condenser was charged with $SbCl_3$ in THF and cooled to 0°C with an ice bath. The Grignard solution was added to the $SbCl_3$ solution *via* cannula. In some cases it was necessary, to cannulate whilst hot in order to avoid precipitation of the Grignard reagent. The solution was stirred overnight at room temperature. After removal of THF, toluene was added for salt elimination and the mixture was filtered *via* cannula. All solvents were evaporated under reduced pressure to obtain the desired products. All products were usually purified by recrystallization at low temperatures or *via* evaporation. All compounds were stable at room temperature.

Interaction between the aryl Grignard reagent and $SbCl_3$ was sometimes accompanied by precipitation of finely disseminated antimony. If stoichiometry

was not applied correctly, mixtures of both 2,6-xylyl$_3$Sb (40) and 2,6-xylyl$_2$SbBr (42) were observed, making purification difficult, due to similar physical properties. Once, when exactly three equivalents of RMgBr towards $SbCl_3$ were employed 2,6-xylyl$_2$SbBr (42) was formed directly without any byproducts. As was described for R_3GeX, halide exchange takes place for the antimony derivatives as well, thus yielding the bromine derivatives. In all other cases, 2,6-xylyl$_3$Sb (40) was obtained as the main product.

The sterically less demanding ligands 1-naphthyl and *o*-tolyl lead to the formation of 1-naphthyl$_3$Sb (41) or *o*-tolyl$_3$Sb, respectively. This leads to the conclusion that the structure and physical/chemical properties of aryl substituted antimony compounds depend, to a great extent, on the ligands, or more specifically on the substituents of the phenyl ring, used, which has been described previously.[150,173] Yields were generally better for *o*-tolyl and 1-naphthyl than for the 2,6-xylyl derivatives. The yields of 1-naphthyl$_3$Sb (41) varied due to difficulties in handling. As was already described for the germanium compounds in Chapter 2.1.1.1, 1-naphthylMgBr tends to crystallize upon cooling to room temperature. This can be avoided by either using larger amounts of solvent or by cannulation whilst still hot. If the Grignard reagent precipitated, in some cases it was not even possible to dissolve it again by refluxing, which is why more solvent had to be added. Yields tend to be low in general, possibly due to the fact that organoantimony halides are very sensitive towards acids, causing cleavage of R-Sb and thus loss of the ligands. Even though $SbCl_3$ was sublimed before usage, the starting material might still contain traces of hydrochloric acid, thus affecting the outcome of the reaction. All crystalline materials obtained were air stable and well soluble in organic solvents. They melted above 80°C without any decomposition.

The level of difficulty concerning synthesis increased even more when the preparative method was expanded to the 9-anthracenyl moiety. In these cases, the Grignard reaction was hard to start, which could be enhanced using 2-bromoethane and heat, but yields remained generally low. Additionally, free anthracene was formed during the course of the reaction, not only lowering yields, but also overcomplicating work-up procedures. Similar issues have been

observed for silicon and tin derivatives within our working group. Nevertheless, a small amount of 9-anthracenyl$_2$SbBr (42) was obtained upon reaction of 9-anthracenylMgBr with $SbCl_3$. After removal of THF, extraction with toluene, and drying under reduced pressure, a yellow solid was obtained, giving a small amount of yellow crystals surrounded by yellow powder upon recrystallization. Investigation of the yellow solid showed that it was anthracene. Repeating the same reaction, but substituting $SbCl_3$ with $SbBr_3$, lead to the formation of [9-anthracenyl$_2$Sb]$_2$ (44) and after recrystallization from toluene and addition of small amounts of pentane, orange crystals, surrounded again by yellow solid, were obtained. The formation of [9-anthracenyl$_2$Sb]$_2$ (44) is presumably the result of incomplete filtration of the Grignard reagent and thus residual magnesia left during the reaction with $SbBr_3$. The formation of distibanes upon reaction with metals has been reported.[150] In the case of highly dispersed magnesium residues it is advisable to not use filter cannulas, but a Schlenk-frit charged with Celite® instead.

Grignard reactions were substituted *via* lithiation, however, normally resulted in a mixture of unidentified products, which could not be reproduced in the case of antimony. A Schlenk was charged with 9-bromoanthracene in THF and cooled to -78°C *via* a EtOH/N_2(l) bath. ^{n}BuLi was added dropwise and the pink solution was stirred for one hour at -78°C before allowed to warm to 0°C. It is important to mention that the outcome of the lithiations varied widely, solutions showing colors anywhere from pink to orange (Figure 83).

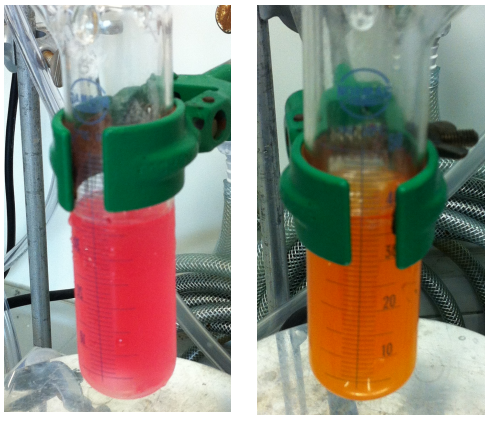

Figure 83. Lithiation of 9-bromoanthracene.

After additional 15 minutes of stirring, a solution of $SbCl_3$ in THF was added dropwise. After stirring at room temperature for 48 hours, the solvent was removed under *vacuo* and toluene was added for extraction of salts.

After filtration *via* cannula, the solvent was removed again yielding an orange solid. Characterization showed a mixture of products from which it was possible to recrystallize a small batch of orange crystals from toluene. X-ray analysis proved [9-anthracenyl$_2$^{n}butylSb][9-anthracenyl^{n}butyl$_2$SbCl$_2$] (46) to be the product at hand.

o-tolylSbCl$_2$ (45) was prepared *via* redistribution reaction between *o*-tolyl$_3$Sb, which was prepared according to literature, and $SbCl_3$ in a 1:2 ratio (Figure 84). Redistribution reactions performed neat, as was published for other aryl substituents, resulted in a mixture of products.[150,166,170] This is the reason why all reaction were performed in Et_2O, as was described in literature for the formation of phenyl derivatives .[164,286]

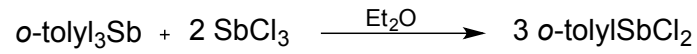

Figure 84. Preparation of *o*-tolylSbCl$_2$ (45) *via* redistribution reactions.

$SbCl_3$ was freshly sublimed, dissolved in dry Et_2O and added dropwise to a solution of *o*-tolyl$_3$Sb in dry Et_2O. The reaction was refluxed for 4 hours and afterwards stirred at room temperature overnight. After removal of solvent under *vacuo* the colorless solid was recrystallized. Recrystallization performed best when the product was dissolved in toluene and layered with a few drops of heptane. [211] 2,6-xylyl$_2$SbBr (42) was prepared not only by employment of a Grignard, but also by reaction between 2,6-xylyl$_3$Sb (40) and $SbBr_3$ in a 2:1 ratio in the same manner as *o*-tolylSbCl$_2$ (45) (Figure 85). In this case, $SbBr_3$ was employed for comparison with the compound prepared over the Grignard route.

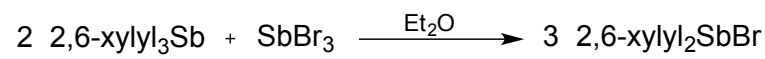

Figure 85. Preparation of 2,6-xylyl$_2$SbBr (42) *via* redistribution reactions.

2.2.2. Characterization

2.2.2.1. X-ray crystallography

As was described in a previous section, a large variety of aromatic germanium compounds display stabilizing forces originating from the substituent on the metal center (Chapter 2.1.2.1). Specifically, secondary non-covalent interactions are electrostatic interactions in the form of π-stacking stemming from the aromatic substituents and van der Waals contacts from the halogenide substituent and adjacent hydrogens, C–H···X (X = Cl, Br). While individually these are weak interactions, combined they offer an overall stabilizing effect to these molecules in the solid state and aid in their crystallization. The role of aromatic non-covalent interactions in the stabilization of compounds in solid state and their importance in chemical and biological processes have been well documented.[252-255] However, their presence and ultimately their effect on arylstibane species has been rarely discussed or simply overlooked. Additionally, the Lewis acidic nature of the antimony metal center varies with the nature of the substituent and consequently, further secondary interactions (Sb···C(π), Sb···X)[260,287,288] can arise in the solid state to afford stabilization.

In an effort to expand the existing library of compounds and study the underlying factors leading to solid state structures, we present a series of novel arylstibane compounds with aryl substituents ranging in steric demand from phenyl to polyaromatic substituents such as 9-anthracenyl. The types of non-covalent interactions present in these systems will be highlighted and compared to previously reported compounds. In addition, the nature of the aromatic substituent and its direct effects on the type of electrostatic interaction that arises in these structures will be discussed.

2.2.2.1.1. Triarylstibanes- R_3Sb

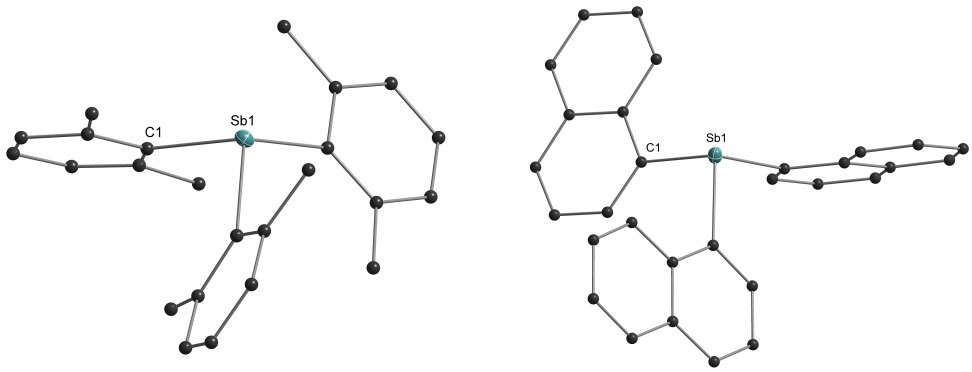

2,6-xylyl$_3$Sb(40) 1-naphthyl$_3$Sb(41)

Figure 86. Crystal structures of presented solid state triarylstibanes. All non-carbon atoms shown as 30% shaded ellipsoids. Hydrogen atoms removed for clarity.

Compounds 2,6-xylyl$_3$Sb (40), 1-naphthyl$_3$Sb · toluene (41a), and 1-naphthyl$_3$Sb · benzene (41b) are comparable to previously reported triarylstibanes (Table 16). Each molecule is in a near trigonal pyramidal geometry with the Sb atom above the plane of the rings. With respect to averaged Sb–C bond lengths, these are affected by the degree of bulkiness afforded by the organic substituent onto the antimony atom. In phenyl$_3$Sb,[289-291] an averaged Sb–C bond length of 2.148(8) Å is observed. As detailed in Chapter 2.1.2.1 with a series of aryl substituted germanium derivatives, steric bulk is not dependent on the addition of methyl substituents to the aryl residue but to its relative position on the aromatic ring. Therefore, addition of a methyl group in *p*-tolyl$_3$Sb[292] results in a similar bond length of 2.141 Å to that of 2.148(8) Å in phenyl$_3$Sb.[289-291] Steric bulk effect on the Sb–C bond length becomes more apparent as the methyl substituent is at the *ortho* position as observed in *o*-tolyl$_3$Sb[293] (2.164(6) Å). The fused aromatic residues in 1-naphthyl$_3$Sb · toluene (41a), 1-naphthyl$_3$Sb · benzene (41b), and 9-phenanthrenyl$_3$Sb[294] seem to offer a similar steric bulk as *o*-tolyl$_3$Sb,[293] with averaged Sb–C bond lengths of 2.162(3) Å, 2.162(2) Å, and 2.157(4) Å respectively. However, the effects of the steric bulk on the Sb–C bond is most pronounced when the aryl residue is substituted at both the 2- and 6- positions as observed for the methyl substituted 2,6-xylyl$_3$Sb (40)[295] (2.190(2) Å), 2,4,6-mesityl$_3$Sb[296] (2.184(8) Å), and the ^{i}propyl substituted 2,4,6-^{i}propylphenyl$_3$Sb[297] (2.184(8) Å).

These display the longest Sb–C bond lengths as compared to phenyl$_3$Sb.[289-291] In conjunction with the increased Sb–C bond length for the 2- and 6 substituted derivatives, averaged C–Sb–C angles for these compounds is also affected by steric bulk. Compounds 2,6-xylyl$_3$Sb (40)[295] (104.71(3)°), 2,4,6-mesityl$_3$Sb[296] (104.12(3)°), and 2,4,6-^{i}propylphenyl$_3$Sb[297] (105.63(3)°) display much wider averaged C–Sb–C angles than for example the non-substituted phenyl$_3$Sb[289-291] (96.61(3)°) or even for *o*-tolyl$_3$Sb[293] (97.22(3)°) and the related derivatives with substitution at the *ortho* position.

Table 16. List of selected bond lengths and angles and non-covalent interactions for selected triarylstibanes.

	Space Group	Sb–C (Å) (avg.)	C–Sb–C (°) (avg.)	Edge to Face (Å)	$CH_3\cdots\pi$ (Å)
phenyl$_3$Sb[289-291]	*P*-1	2.148(8)	96.61(3)	3.37	—
***o*-tolyl$_3$Sb**[293]	*P*-1	2.164(6)	97.22(3)	*	*
***p*-tolyl$_3$Sb**[292]	*R*-3	2.141(1)	97.33(3)	2.89 – 3.31	—
2,6-xylyl$_3$Sb (40)[295]	$P2_1/c$	2.190(2)	104.71(3)	—	2.82 – 3.18
2,4,6-mesityl$_3$Sb[296]	*P*-1	2.184(8)	104.12(3)	—	3.21
2,4,6-^{i}propylphenyl$_3$Sb[297]	*P*-1	2.184(8)	105.63(3)	3.31	3.26 – 3.35
1-naphthyl$_3$Sb · toluene (41a)	*P*-1	2.162(3)	96.87(3)	2.76 – 2.81	—
1-naphthyl$_3$Sb · benzene (41b)	*P*-1	2.162(2)	96.87(9)	2.86 – 3.18	—
9-phenanthrenyl$_3$Sb[294]	*P*-1	2.157(4)	96.77(1)	2.81 – 2.86	—

*No hydrogen atoms reported

All triarylstibanes display close packing motifs in the solid state creating 3D networks through the presence of non-covalent electrostatic interactions. Table 16 summarizes the non-covalent interactions in presented triarylstibanes. With respect to the type of secondary non-covalent interactions in the extended solid state of triarylstibanes, clear trends begin to arise related to the substitution pattern of the aryl residue (Table 16). Unsurprisingly, phenyl$_3$Sb[289-291] only displays edge to face interactions (3.37 Å) due to the obvious lack of a methyl substituent or a polyaromatic residue. In addition to these electrostatic interactions between the aryl residues, phenyl$_3$Sb[289-291] also displays Sb···C(π) interactions between the

metal center and neighboring phenyl ring carbons (η^2 = 3.81, 3.95 Å). Sb···C(π) interactions are within the sum of van der Waals for a Sb–C bond (4.24 Å)[260] and experimental cutoffs as determined by a Cambridge Structural Database search (3.99 Å).[287] No other triaryl antimony displays Sb···C(π) interactions, possibly due to the shielding effects of the more sterically hindered aryl residues. In *p*-tolyl$_3$Sb,[292] only edge to face interactions (2.89–3.31 Å) are observed, despite the presence of a methyl substituent, which as was shown for previously discussed arylgermanium derivatives, should lead to CH_3···π interactions. As expected, the addition of a methyl substituent at the *ortho* position results in the presence of CH_3···π interactions for 2,6-xylyl$_3$Sb (40)[295] (2.82–3.18 Å), 2,4,6-mesityl$_3$Sb[296] (3.21 Å), and 2,4,6-^{i}propylphenyl$_3$Sb[297] (3.26–3.35 Å). In both 1-naphthyl$_3$Sb · toluene (41a) and 1-naphthyl$_3$Sb · benzene (41b) (Figure 88), the bulkiness of all three naphthyl residues around the central antimony atom and the presence of cocrystallized solvent molecules does not allow for any π–π stacking interactions to be observed. However, edge to face interactions are observed between the naphthyl residues and both solvents benzene and toluene, 2.86–3.18 Å and 2.76–2.81 Å respectively. 1-naphthyl$_3$Sb · toluene (41a) also display CH_3···π interactions from the methyl group of toluene and neighboring naphthyl residues (2.77–2.86 Å). 9-phenanthrenyl$_3$Sb[294] also only displays edge to face interactions (2.81–2.86 Å).

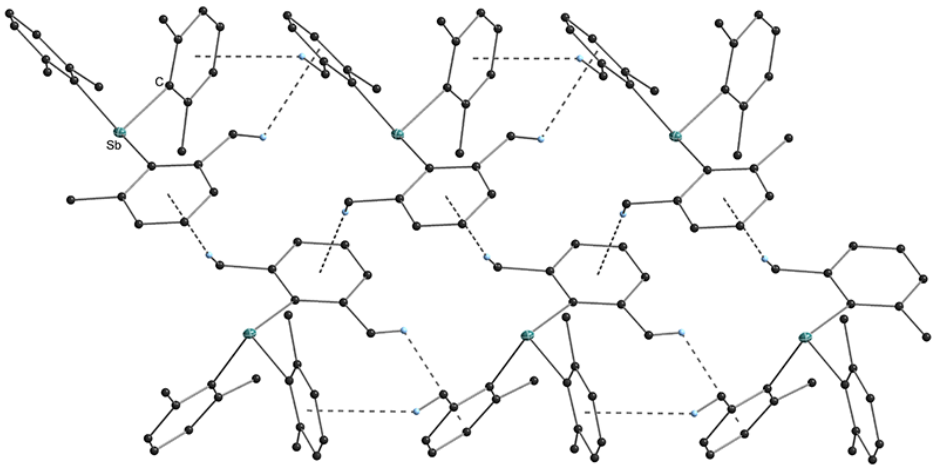

Figure 87. Crystal packing diagram for 2,6-xylyl$_3$Sb (40).[295] CH_3···π interactions highlighted by dashed bonds. All non-carbon atoms shown as 30% shaded ellipsoids. Edge to face interactions and hydrogen atoms not involved in intermolecular interactions removed for clarity.

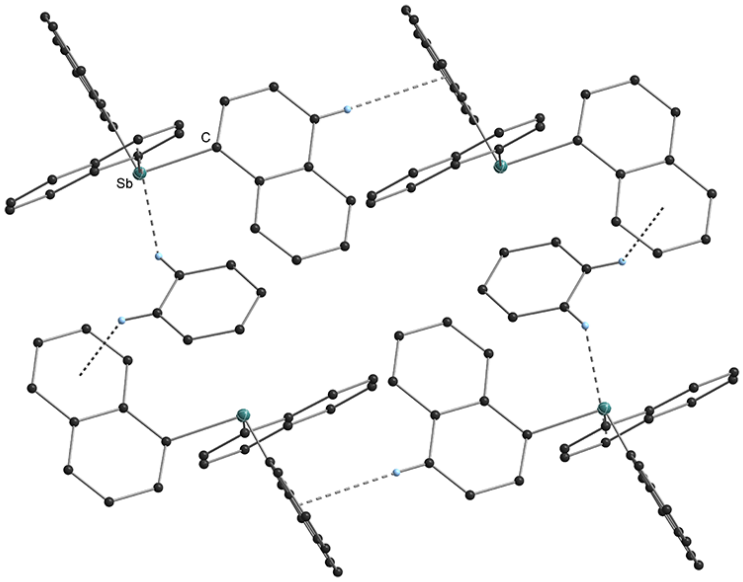

Figure 88. Crystal packing diagram for 1-naphthyl$_3$Sb · benzene (41b). Edge to face interactions highlighted by dashed bonds. All non-carbon atoms shown as 30% shaded ellipsoids. Hydrogen atoms not involved in intermolecular interactions removed for clarity.

2.2.2.1.2. Diarylantimony bromides- R_2SbBr

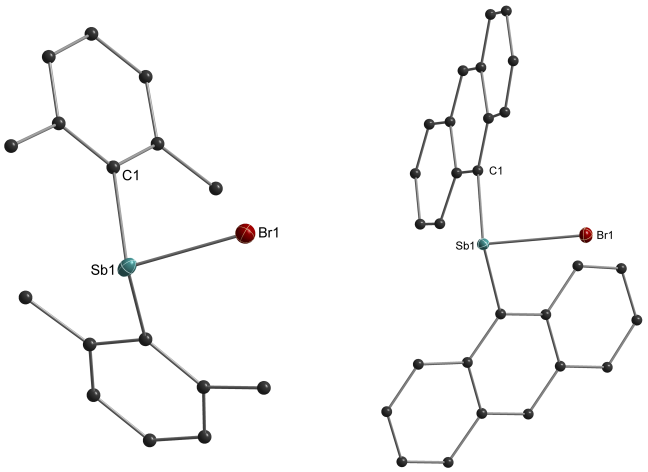

2,6-xylyl$_2$SbBr (42) 9-anthracenyl$_2$SbBr (43)

Figure 89. Crystal structures of presented solid state diarylantimony bromides. All non-carbon atoms shown as 30% shaded ellipsoids. Hydrogen atoms removed for clarity.

As was observed for the triarylstibanes, the substitution pattern on the aryl residue and hence the steric bulk the aryl residue affords the antimony metal

center, has a marked effect on the Sb–C bond (Table 17). Similar to the triarylstibane derivatives, the shortest Sb–C bond lengths are observed for compounds with aryl residues that are not substituted as in phenyl$_2$SbBr[298] (2.146(1) Å), or with substitution on only one *ortho* position as in 1-naphthyl$_2$SbBr[299] (2.151(8) Å). As expected, additional substitution at both *ortho* positions as seen for 2,6-xylyl$_2$SbBr (42) (2.171(7) Å) and 9-anthracenyl$_2$SbBr · toluene (43) (2.183(14) Å) leads to a longer Sb–C bond. In contrast, Sb–Br bond lengths do not seem to follow this trend with phenyl$_2$SbBr[298] (2.552(1) Å), 1-naphthyl$_2$SbBr[299] (2.512(9) Å), and 9-anthracenyl$_2$SbBr · toluene (43) (2.566(2) Å) affording similar bond lengths. Counterintuitively, 2,6-xylyl$_2$SbBr (42) displays the shortest Sb–Br bond length of 2.465(1) Å. However, taking into account the Lewis acidic nature of the antimony metal, which necessitates the presence of secondary interactions to help coordinatively saturate the metal center, this shortened and thus stronger bond length is not surprising in the absence of Sb···C(π) interactions, as is in the case of 2,6-xylyl$_2$SbBr (42).

Table 17. List of selected bond lengths and angles for selected diarylantimony bromides.

	Space Group	Sb–C (Å) (avg.)	Sb–Br (Å)	C–Sb–C (°)	C–Sb–Br (°)(avg.)
phenyl$_2$SbBr[298]	$P2_1/c$	2.146(1)	2.552(1)	98.5(3)	94.4(2)
2,6-xylyl$_2$SbBr (42)	$P2_1/n$	2.171(7)	2.465(1)	101.5(3)	99.22(2)
1-naphthyl$_2$SbBr[299]	$P2_1/c$	2.151(8)	2.512(9)	98.0(2)	94.9(1)
9-anthracenyl$_2$SbBr · toluene (43)	$P2_1/c$	2.183(14)	2.566(2)	105.19(5)	95.74(4)

Table 18. List of non-covalent interactions for selected diarylantimony bromides.

	π–π Stacking (Å)		Edge to Face (Å)	CH_3···π (Å)	C–H···Br (Å) (avg.)	Sb···C(π) (Å) (avg.)
	d	R				
phenyl$_2$SbBr[298]	3.56	2.05	3.22	—	3.08 – 3.56	η^2 = 3.62 – 3.65
2,6-xylyl$_2$SbBr (42)	—	—	3.11	3.44	3.07 – 3.41	—
1-naphthyl$_2$SbBr[299]	3.54	2.11	2.93 – 3.07	—	2.96 – 3.01	η^1 = 3.83
9-anthracenyl$_2$SbBr · toluene (43)	3.47	1.07	2.99 – 3.22	—	3.01 – 3.53	η^3 = 3.68 – 3.78

Despite all diarylantimony bromide derivatives crystallizing in the same monoclinic system, not all crystalize in the same space group, with 2,6-xylyl$_2$SbBr (42) in the $P2_1/n$ space group displaying much different behavior in the solid state (Table 17). This is due to the marked difference between the electrostatic interactions that the 2,6-xylyl residue can afford as compared to the phenyl, naphthyl and anthracenyl residue, which behave as planar aromatic systems. By replacing one of the aryl residues with bromine, phenyl$_2$SbBr (d = 3.56 Å, R = 2.05 Å),[298] 1-naphthyl$_2$SbBr (d = 3.54 Å, R = 2.11 Å),[299] and 9-anthracenyl$_2$SbBr · toluene (d = 3.47 Å, R = 1.07 Å) (43) all show close π–π stacking interactions between neighboring aromatic systems creating extended 3D networks. In contrast, the methyl substituents on the aryl residue of 2,6-xylyl$_2$SbBr (42) (Figure 90) allows molecules to orient themselves in order to maximize $CH_3\cdots\pi$ interactions.

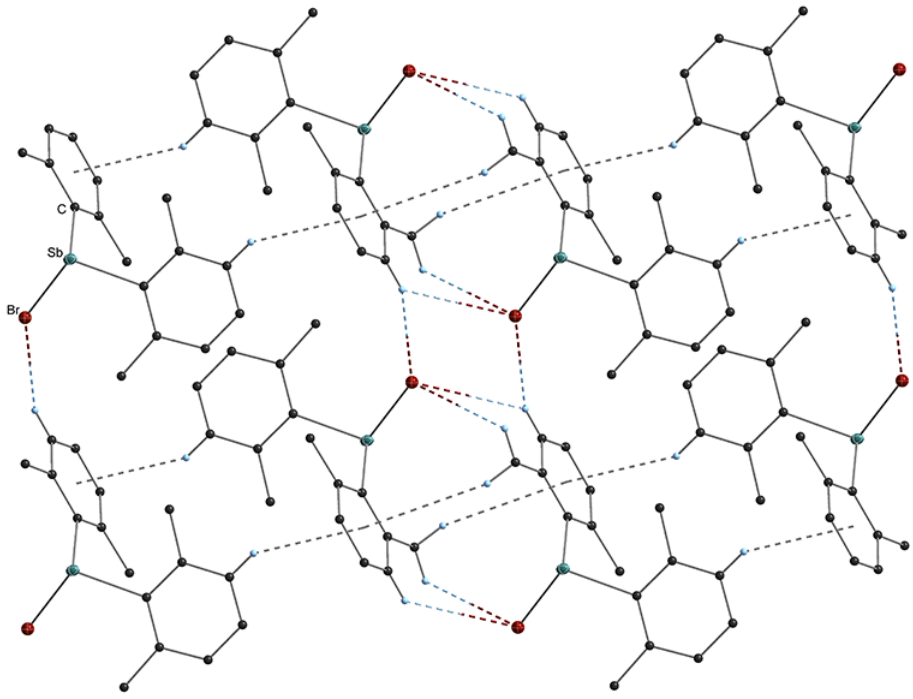

Figure 90. Crystal packing diagram for 2,6-xylyl$_2$SbBr (42). $CH_3\cdots\pi$ interactions and C–H···Br contacts highlighted by dashed bonds. All non-carbon atoms shown as 30% shaded ellipsoids. Edge to face interactions and hydrogen atoms not involved in intermolecular interactions removed for clarity.

In all diarylantimony bromides, edge to face interactions are present and aid in propagating 3D networks. Curiously, 2,6-xylyl$_2$SbBr (42) is the only diaryl antimony bromide to allow a Br···Br contact of 3.45 Å. This Br···Br contact is below the sum of van der Waals for a Br–Br bond (3.72 Å)[260] and below experimental cutoffs as determined by a Cambridge Structural Database search (3.79 Å).[287]

In agreement with the increased Lewis acidity of the diarylantimony bromides as compared to the triarylstibanes, a higher propensity for Sb···C(π) interactions is observed. Phenyl$_2$SbBr[298] displays the closest Sb···C(π) interactions (η^2 = 3.63–3.65 Å) followed by 9-anthracenyl$_2$SbBr · toluene (43) (η^3 = 3.68–3.78 Å) (Figure 91) and 1-naphthyl$_2$SbBr[299] (η^1 = 3.83 Å) with 2,6-xylyl$_2$SbBr (42) preferring the aforementioned Br···Br contact. However, in contrast to the well-known Menshutkin complexes,[288] no appreciable Sb···Br secondary contacts are observed, with all values (4.49–4.56 Å) being above the sum of van der Waals for a Sb–Br bond (4.33 Å)[260] and well above experimental cutoffs as determined by a Cambridge Structural Database search (3.84 Å).[287] In addition to the electrostatic interactions described above, all of the diarylantimony bromide derivatives display van der Waals interactions from the bromide substituent and hydrogens (C–H···Br) from neighboring molecules (Table 18).

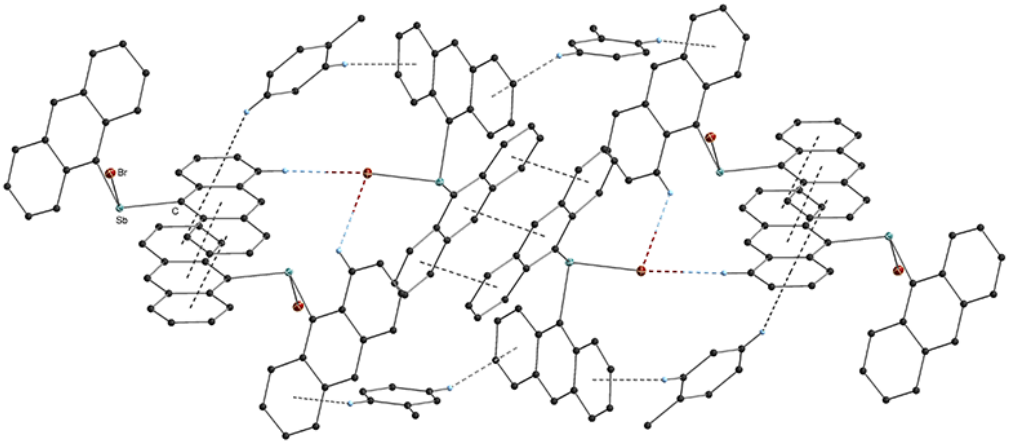

Figure 91. Crystal packing diagram for 9-anthracenyl$_2$SbBr · toluene (43). π–π stacking, edge to face interactions and C–H···Br contacts highlighted by dashed bonds. All non-carbon atoms shown as 30% shaded ellipsoids. Hydrogen atoms not involved in intermolecular interactions removed for clarity.

2.2.2.1.3. Arylantimony dichlorides- $RSbCl_2$

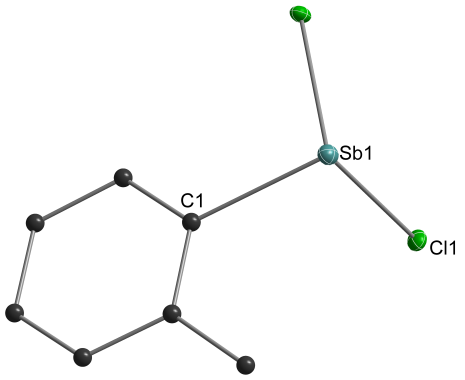

o-tolylSbCl$_2$ (45)

Figure 92. Crystal structures of presented solid state arylantimony dichloride. All non-carbon atoms shown as 30% shaded ellipsoids. Hydrogen atoms removed for clarity.

All arylantimony dichlorides crystallize in the space group *P*-1 and are nearly isostructural (Table 19). Despite the increased steric bulk afforded to the antimony metal by methyl substitution at the *ortho* position of the aryl residue, the Sb–C bonds are quite comparable for *o*-tolylSbCl$_2$ (45) (2.159(17) Å) as compared to phenylSbCl$_2$[286] (2.151(2) Å) and *p*-tolylSbCl$_2$[298] (2.148(6) Å). In addition, no appreciable deviations are observed for the Sb–Cl bond lengths, which fall in a narrow range of 2.384(2)–2.411(2) Å. All C–Sb–Cl and Cl–Sb–Cl angles are comparable and unremarkable.

Table 19. List of selected bond lengths and angles for selected arylantimony dichlorides.

	Space Group	Sb–C (Å)	Sb–Cl (Å) (avg.)	C–Sb–Cl (°)(avg.)	Cl–Sb–Cl (°)(avg.)
phenylSbCl$_2$[286]	*P*-1	2.151(2)	2.411(2)	93.95(2)	94.35(6)
***o*-tolylSbCl$_2$ (45)**	*P*-1	2.159(17)	2.384(2)	93.71(5)	95.070(16)
***p*-tolylSbCl$_2$[298]**	*P*-1	2.148(6)	2.384(2)	93.4(2)	94.05(7)

As compared to the diaryl antimony derivatives, replacement of a second aryl residue by a halide, as is in the case for the monoaryl antimony dichlorides, should cause an increase in the overall Lewis acidity of the antimony metal center. This increase in Lewis acidity forces the presence of additional secondary

interactions to help coordinatively saturate the antimony metal center. And indeed this is the case for the monoaryl antimony dichlorides.

Table 20. List of non-covalent interactions for selected arylantimony dichlorides.

	π–π Stacking (Å)		$CH_3\cdots\pi$ (Å)	C–H···Cl (Å) (avg.)	Sb···Cl (Å)	Sb–C (Å) (avg.) inter-molecular
	d	R				
phenylSbCl$_2$[286]	3.47	1.28	—	2.79 – 3.01	3.44	η^6 = 3.30 – 3.72
***o*-tolylSbCl$_2$ (45)**	—	—	2.89	2.93 – 3.28	3.55, 3.89	η^6 = 3.37 – 3.77
***p*-tolylSbCl$_2$**[298]	—	—	2.69	2.86 – 3.31	3.43, 3.64	η^6 = 3.31 – 3.81

Not only do the monoaryl antimony dichlorides show the presence of a higher number of Sb···C(π) interactions, as compared to the diaryl antimony bromides (Table 18), they display close Sb···Cl secondary contacts, which the bromides did not exhibit.

In each monoaryl antimony dichloride, the metal center is completely saturated through η^6-Sb···C(π) interactions, where the aryl residue is completely tilted towards the metal center in order to maximize these interactions. The closest interactions are observed for phenylSbCl$_2$[286] (η^6 = 3.30–3.72 Å) followed by *o*-tolylSbCl$_2$ (45) (η^6 = 3.37–3.77 Å) (Figure 93), and *p*-tolylSbCl$_2$[298] (η^6 = 3.31–3.81 Å).

In each case, two molecules face each other in order to allow the phenyl ring to saturate the antimony metal center of the neighboring molecule. These two molecules interact with the next two *via* Sb···Cl secondary contacts creating a linear chain, with all values, 3.44 for phenylSbCl$_2$[286] and 3.55 Å for *o*-tolylSbCl$_2$ (45) and 3.43 Å *p*-tolylSbCl$_2$,[298] being well below the sum of van der Waals for a Sb–Cl bond (4.29 Å)[260] and below experimental cutoffs as determined by a Cambridge Structural Database search (3.79 Å).[287]

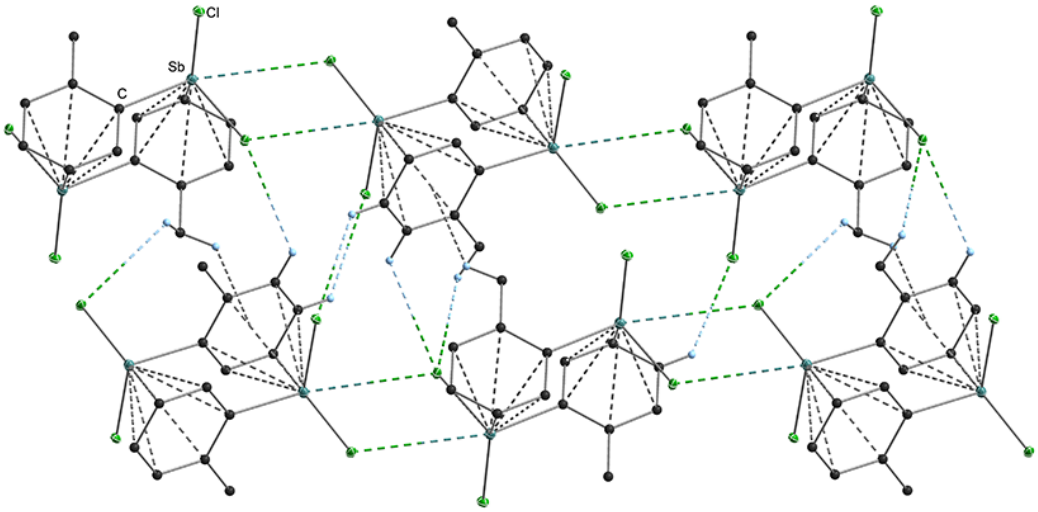

Figure 93. Crystal packing diagram for *o*-tolylSbCl$_2$ (45). Sb···C(π) and CH$_3$···π interactions and C–H···Cl contacts highlighted by dashed bonds. All non-carbon atoms shown as 30% shaded ellipsoids. Edge to face interactions and hydrogen atoms not involved in intermolecular interactions removed for clarity.

Both *o*-tolylSbCl$_2$ (45) and *p*-tolylSbCl$_2$[298] subsequently display a second, slightly longer Sb···Cl secondary contact (3.89 and 3.64 Å respectively) through the exposed chloride substituent from one chain and the antimony metal center of the adjacent chain. An extended 3D network is then achieved with the help of both close CH$_3$···π interactions and C–H···Cl contacts. However, the absence of methyl substituents in phenylSbCl$_2$[286] does not allow for CH$_3$···π interactions and close π–π stacking interactions are present between the chains. This circumvents the presence of an additional Sb···Cl contact, as was observed for *o*-tolylSbCl$_2$ (45) and *p*-tolylSbCl$_2$,[298] but phenylSbCl$_2$,[286] displays the closest C–H···Cl contacts (2.79–3.01 Å) among the three monoaryl antimony dichlorides aiding in propagating an extended 3D network .

Displaying the stabilizing strength and necessity of these Sb···C(π) secondary interactions, none of the monoaryl antimony dichlorides derivatives display edge to face interactions.

2.2.2.1.4. Diaryldistibanes- $[R_2Sb]_2$

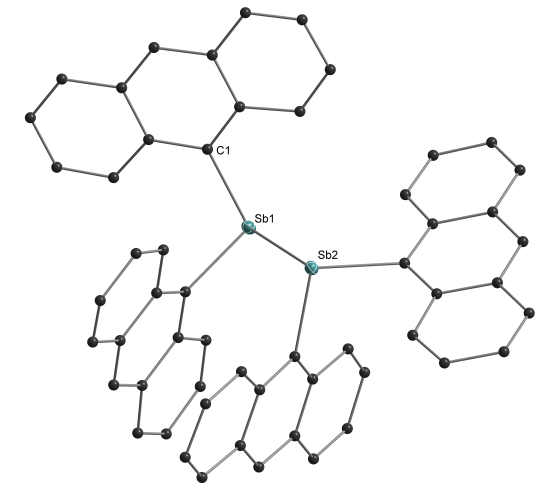

Figure 94. Crystal structures of presented solid state diaryldistibane. All non-carbon atoms shown as 30% shaded ellipsoids. Hydrogen atoms removed for clarity.

Consistent with increased steric demand around the central antimony atom by aryl residues substituted at both the 2- and 6 positions, the longest Sb–C bond length among the presented diaryldistibanes are observed for [2,4,6-mesityl$_2$Sb]$_2$[300,301] with a Sb–C bond length of 2.199(8) Å and [9-anthracenyl$_2$Sb]$_2$ (44) with a Sb–C bond length 2.157(2) Å as compared to 2.157(2) Å in [phenyl$_2$Sb]$_2$ (Table 21).[302,303] A similar trend is observed for Sb—Sb bond lengths, as a slight increase in Sb—Sb bond lengths are observed for [9-anthracenyl$_2$Sb]$_2$ (44) (2.889(4) Å) and [2,4,6-mesityl$_2$Sb]$_2$[300,301] (2.848(1) Å) as compared to 2.836(2) Å in [phenyl$_2$Sb]$_2$.[302,303]

In conjunction with the longer Sb—Sb bond lengths for [9-anthracenyl$_2$Sb]$_2$ (44), the large sterically encumbering anthracenyl residue in this compound also displays the widest C—Sb—C angles with an average value of 100.89(11)° and C—Sb—Sb angles with an average value of 97.62(7)° as compared to [phenyl$_2$Sb]$_2$[302,303] which displays much more narrower C—Sb—C angles of 94.36(1)° and C—Sb—Sb angles with an average value of 95.24(1)°.

Table 21. List of selected bond lengths and angles for selected diaryldistibanes.

	Space Group	Sb–C (Å) (avg.)	Sb—Sb (Å) (avg.)	C—Sb—C (°)	C—Sb—Sb (°)
[phenyl$_2$Sb]$_2$[302,303]	$P2_1/n$	2.157(2)	2.836(2)	94.36(1) 97.5(3)	93.78(1) 96.69(1) 90.0(2) 109.5(2)
[2,4,6-mesityl$_2$Sb]$_2$[300,301]	$P2_1/n$	2.199(8)	2.848(1)	100.8(3)	92.2(2) 108.7(2) 85.67(7) 102.87(8)
[9-anthracenyl$_2$Sb]$_2$ (44)	$P2_1/c$	2.187(3)	2.889(4)	101.03(11) 100.76(11)	90.20(7) 111.73(8)

Table 22. List of non-covalent interactions for selected diaryldistibanes.

	π–π Stacking (Å)		Edge to Face (Å)		$CH_3\cdots\pi$ (Å)	
	d	R	Intra	Inter	Intra	Inter
[phenyl$_2$Sb]$_2$[302,303]	—	—	2.95	3.17 – 3.34	—	—
[2,4,6-mesityl$_2$Sb]$_2$[300,301]	—	—	—	2.92 – 3.34	3.19 – 3.34	2.99
[9-anthracenyl$_2$Sb]$_2$ (44)	3.42	0.86		2.69 – 3.23	—	—

* Intra = intramolecular; Inter = intermolecular

With respect to electrostatic interactions in the extended solid state, the diaryldistibanes exhibit expected interactions directly dependent on the nature of the aryl residue. In [phenyl$_2$Sb]$_2$[302,303] consistent with the smaller planar aromatic residue, the phenyl groups along the Sb—Sb bond do not face each other, but rather orient themselves perpendicularly in order to afford short intramolecular edge to face interactions of 2.95 Å and also allow intermolecular edge to face interactions (3.17–3.34 Å) resulting in a 3D extended network (Table 22). In [2,4,6-mesityl$_2$Sb]$_2$,[300,301] in addition to intramolecular $CH_3\cdots\pi$ interactions of 3.19–3.34 Å, all three methyl substituents on the aryl residue interact intermo-

lecularly through $CH_3\cdots\pi$ interactions (2.92–3.34 Å) with neighboring molecules. Intermolecular edge to face interactions aid in propagating an extended 3D network.

Finally, the 9-anthracenyl residue displays π–π stacking interactions in [9-anthracenyl$_2$Sb]$_2$ (44) (Figure 95), however not with a neighboring molecule, but intramolecularly with a 9-anthracenyl residue across the Sb—Sb bond (d = 3.42 Å, R = 0.86 Å). Subsequently, neighboring molecules interact through edge to face interactions (2.69–3.23 Å) creating an extended 3D network.

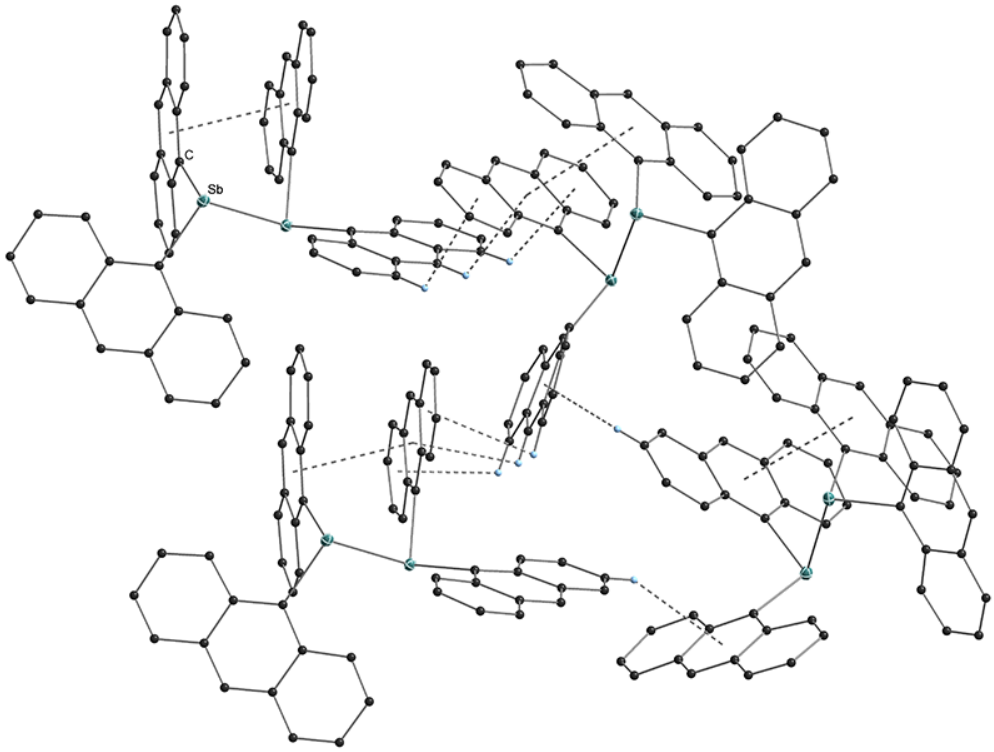

Figure 95. Crystal packing diagram for [9-anthracenyl$_2$Sb]$_2$ (44). π–π stacking and edge to face interactions highlighted by dashed bonds. All non-carbon atoms shown as 30% shaded ellipsoids. Hydrogen atoms not involved in intermolecular interactions removed for clarity.

2.2.2.1.5. Mixed Valence Antimony

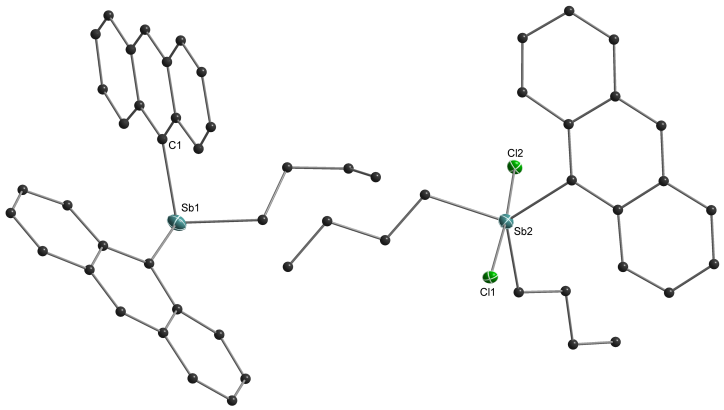

[9-anthracenyl$_2$^{n}butylSb][9-anthracenyl^{n}butyl$_2$SbCl$_2$] (46)

Figure 96. Crystal structures of presented solid state [9-anthracenyl$_2$^{n}butylSb][9-anthracenyl^{n}butyl$_2$SbCl$_2$]. All non-carbon atoms shown as 30% shaded ellipsoids. Hydrogen atoms removed for clarity.

Mixed valence antimony compounds are rare, and the most comparable to [9-anthracenyl$_2$^{n}butylSb][9-anthracenyl^{n}butyl$_2$SbCl$_2$] are [SbCl$_3$][Me$_3$SbCl$_2$][304] and [SbCl$_3$][phenyl$_3$SbCl$_2$][305] (Table 23).

The only deviation worth mentioning among these compounds is the Sb–C(aryl) bond elongation in [9-anthracenyl$_2$^{n}butylSb][9-anthracenyl^{n}butyl$_2$SbCl$_2$] (46) of 2.130(2) Å in the Sb^v cocrystallized molecule as compared to 2.102(3) Å in [SbCl$_3$][phenyl$_3$SbCl$_2$][305] which is a direct result of the more sterically encumbering anthracenyl ligand. All other values are comparable.

Table 23. List of selected bond lengths for selected mixed valency antimony derivatives.

	Space Group	Sb–C(aryl) (Å) (avg.)		Sb–C(alkyl) (Å) (avg.)		Sb–Cl (Å) (avg.)
		Sb^{III}	Sb^V	Sb^{III}	Sb^V	Sb^V
[SbCl$_3$][Me$_3$SbCl$_2$][304]		—	—	—	2.131(3)	2.523(3)
[SbCl$_3$][phenyl$_3$SbCl$_2$][305]		—	2.102(3)	—	—	2.494(3)
[9-anthracenyl$_2$^{n}butylSb] [9-anthracenyl^{n}butyl$_2$SbCl$_2$] (46)	*P-1*	2.184(2)	2.130(2)	2.182 (3)	2.134(3)	2.499(6)

Table 24. List of selected angles for selected mixed valency antimony derivatives.

	C–Sb–C (°)(avg.)		Cl–Sb– Cl (°)(avg.)
	Sb^{III}	Sb^{V}	Sb^{V}
$[SbCl_3][Me_3SbCl_2]$[304]	—	119.89(3)	177.02(2)
$[SbCl_3][phenyl_3SbCl_2]$[305]	—	119.99(3)	177.31(2)
[9-anthracenyl$_2$^{n}butylSb] [9-anthracenyl^{n}butyl$_2$SbCl$_2$] (46)	98.09(7)	119.99(9)	176.03 (2)

As can be seen in Figure 97, [9-anthracenyl$_2$^{n}butylSb][9-anthracenyl^{n}butyl$_2$SbCl$_2$] (46) displays several types of secondary noncovalent interactions aiding in the propagation of a 3D extended network (Table 25). The 9-anthracenyl residue of neighboring Sb^{v} cocrystallized molecules interact through π–π stacking interactions (d = 3.54 Å, R = 1.35 Å). The ^{n}butyl residues of these Sb^{v} cocrystallized molecules then interact through CH_3···π interactions (2.99 – 3.11 Å). Also, close C–H···Cl contacts (2.70–2.96 Å) are present. Finally, the Sb^{III} cocrystallized molecules interact with each other through close Sb···C(π) contacts (η^2 = 3.66–3.69 Å) despite the decreased degree of Lewis acidity of an aryl and alkyl substituted antimony metal center as compared to the chloride substituted Sb^{v} cocrystallized molecule. No close Sb···Cl or Sb···Sb contacts are observed.

Table 25. List of selected non-covalent interactions for [9-anthracenyl$_2$^{n}butylSb][9-anthracenyl^{n}butyl$_2$SbCl$_2$].

	π–π Stacking (Å)		Edge to Face (Å)	CH_3···π (Å)	C–H···Cl (Å)	Sb···C(π) (Å)	
	d	R				Sb^{III}	Sb^{V}
[9-anthracenyl$_2$^{n}butylSb] [9-anthracenyl^{n}butyl$_2$SbCl$_2$] (46)	3.54	1.35	3.16	2.99 – 3.11	2.70 – 2.96		—

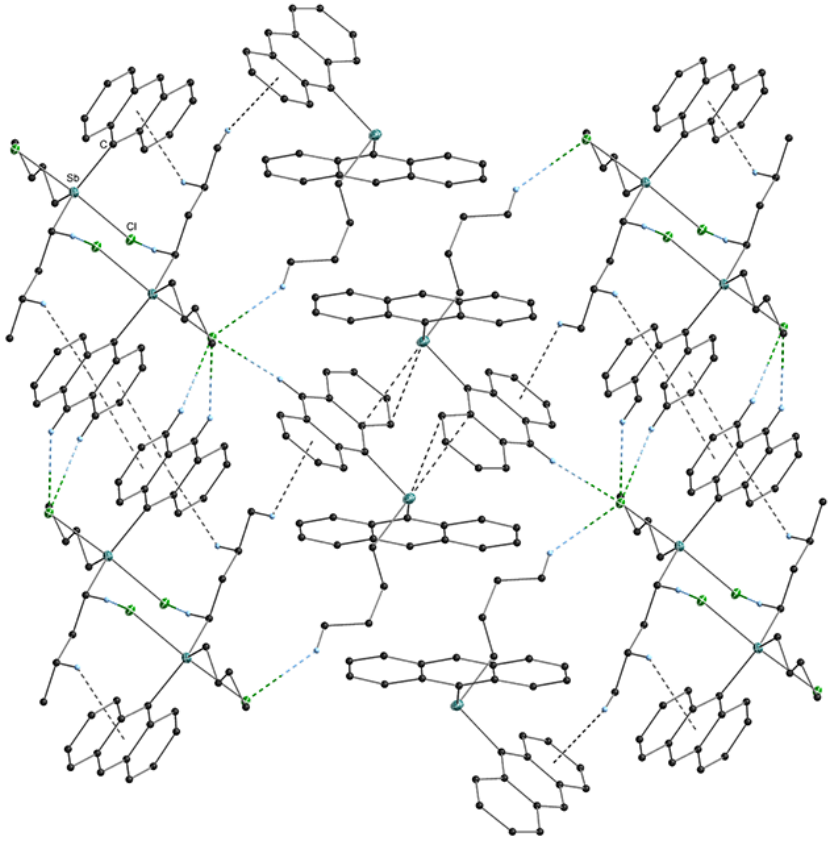

Figure 97. Crystal packing diagram for [9-anthracenyl^{n}butyl$_2$SbCl$_2$] (46). π–π stacking, CH_3···π interactions, Sb···C(π) and C–H···Cl contacts highlighted by dashed bonds. All non-carbon atoms shown as 30% shaded ellipsoids. Hydrogen atoms not involved in intermolecular interactions removed for clarity.

2.2.2.1.6. Conclusions

A series of triarylstibanes, arylantimony halides and diaryldistibanes have been fully characterized with X-ray crystallography. The effects of aryl residue bulk, methyl substitution pattern, and substituent on the antimony metal environment has been discussed for a variety of tri-, di-, and monoaryl species. Consistent with increased in steric demand around the central antimony atom, the longest Sb–C bond lengths are observed for aryl residues substituted at both the 2- and 6 positions.

While not previously mentioned in literature, electrostatic interactions in the form of π-stacking stemming from the aromatic substituents (π–π stacking, edge

to face and $CH_3\cdots\pi$ interactions) and van der Waals contacts from the halogenide substituent and adjacent hydrogens, C–H···X (X = Cl, Br) offer an overall stabilizing effect to these molecules in the solid state and aid in their crystallization. The types of non-covalent interactions present in these systems are directly dependent on the nature of the aryl substituent. The most prominent type of non-covalent interaction is edge to face interactions and was found in most compounds regardless of their bulk or methyl substitution pattern. However, the presence of $CH_3\cdots\pi$ interactions was more dependent on not just the addition of methyl substituents to the aryl residue but to their relative position on the aromatic ring.

Despite the capacity for the planar aromatic residues phenyl, 1-naphthyl and 9-anthracenyl to potentially display π–π stacking interactions, the bulkiness of three of these residues around the central antimony in triarylstibanes (39,) hindered the residues from neighboring molecules from approaching each other in a planar fashion to allow this type of interaction. However, π–π stacking interactions were observed in all phenyl, 1-naphthyl, and 9-anthracenyl diarylantimony bromides and arylantimony dichlorides as well as the distibane, $[9\text{-anthracenyl}_2Sb]_2$.

Consistent with the increase of Lewis acidity of the antimony metal center, through subsequent replacement of aryl residues with halide substituents, a higher number of secondary interactions necessary to help coordinatively saturate the antimony metal center were observed going from the triarylstibanes to the arylantimony dichlorides. While only one triarylstibane, $phenyl_3Sb$,[289-291] displays an η^1-Sb···C(π) interaction, the replacement of two aryl residues by chlorine substituents leads to an increase to η^6-Sb···C(π) interactions in the arylantimony dichlorides. The increase in Lewis acidity observed for the arylantimony dichlorides, as compared to the diaryl antimony bromides, leads to the presence of Sb···Cl secondary contacts helping to further coordinatively saturate the antimony metal center.

2.2.2.2. NMR spectroscopy

Antimony has two NMR active isotopes, namely ^{121}Sb and ^{123}Sb. ^{121}Sb has a spin of $^{5}/_{2}$ and ^{123}Sb has a spin of $^{7}/_{2}$, both are quadrupolar. ^{121}Sb is favored in terms of NMR investigations, because of its higher abundance, smaller nuclear quadrupole moment and larger magnetogyric ratio. However, interpretation of NMR data is normally difficult and is not an option for simple control of reaction progress. Thus, all compounds within the scope of this work were characterized using only standard ^{1}H and ^{13}C NMR techniques. $CDCl_3$ was used for all products. The compounds showed characteristic signals in the aromatic region. For compounds 2,6-xylyl$_3$Sb (40), 2,6-xylyl$_2$SbBr (42) and *o*-tolylSbCl$_2$ (45) additional single peaks for the *o*-methyl groups can be found in the aliphatic region. The compounds 2,6-xylyl$_3$Sb (40) and 2,6-xylyl$_2$SbBr (42) display only one signal for both methyl groups at 2.49 ppm or 2.43 ppm, respectively. The ^{1}H NMR spectrum of 2,6-xylylSb$_2$Br (42) shows a triplet at 7.21 ppm in accordance with the *para* proton (4-H) and a doublet at 7.13 ppm for the *meta* protons (3,5-H). The same pattern can be observed for 2,6-xylyl$_2$SbBr (42) at 7.15 ppm and at 7.02 ppm. The ^{13}C-NMR spectra for both compounds show four signals, each for two *ortho*, *meta* and *para* carbon atoms and one peak for the methyl groups. The ^{1}H NMR spectrum for 1-naphthyl$_3$Sb (41) contains six sets of signals in the aromatic region, a doublet at 8.12 ppm corresponding to 8-H, two doublets at 7.79 ppm and 7.73 for 4,5-H, a multiplet at 7.36 ppm for 6,7-H, a doublet at 7.13 ppm for 2-H and another doublet at 7.10 ppm for 3-H. In the ^{13}C NMR spectra, the signals corresponding to the respective carbon atoms are present as a total of 10 singlets.

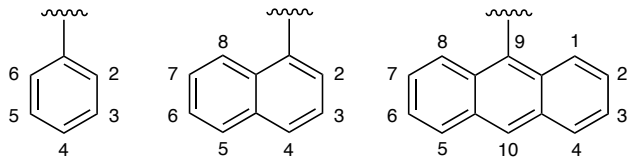

Figure 98. The numbering of carbon positions of 1-phenyl, 1-naphthyl and 9- anthracenyl substituted antimony compounds.

The ^{1}H NMR spectrum for 9-anthracenyl$_2$SbBr (43) contains a singlet 8.53 ppm for 1,8-H, a doublet at 8.40 ppm for 10-H, a doublet at 8.00 ppm for 4,5-H, a triplet at 7.35 ppm for 2,7-H and another triplet at 7.16 ppm for 3,6-H. The ^{13}C NMR spectrum shows, as expected, 14 singlets in the aromatic region corresponding to all carbon atoms. The ^{1}H NMR spectra of [9-anthracenyl$_2$Sb]$_2$ (44) shows a doublet at 8.39 ppm for 1,8-H, a singlet at 7.92 ppm for 10-H, a doublet at 7.66 ppm for 4,5-H, and two triplets at 7.15 ppm and 6.84 ppm for 2,7-H and 3,6-H, respectively. In the ^{13}C NMR spectrum, the signals corresponding to all the carbon atoms are observed as fourteen singlets. The ^{1}H NMR spectrum of *o*-tolylSbCl$_2$ (45) shows a doublet at 8.11 ppm for the *ortho* proton, a multiplet at 7.42 ppm for the *meta* and *para* protons, a doublet at 7.26 ppm for the *meta* proton neighboring the methyl group, and a singlet in the aliphatic region at 2.63 ppm for the methyl group. The ^{13}C spectrum contains, as expected, six signals. The methyl group can be observed at 22.32 ppm.

2.2.2.3. UV-Vis spectroscopy

Since anthracene is a polycyclic aromatic hydrocarbon, $\pi \rightarrow \pi^*$ transition of low energy is possible because of conjugation, making it the perfect system for UV-Vis investigations. It is known that the conjugated double bond system has a great influence on peak wavelength and absorption intensities. Thus, anthracene and its derivatives have been applied for photochemical applications attributed by their photochemical and photophysical properties. Anthracene shows a broad band with four distinctive absorption peaks between 300 and 400 nm in solution.[306] Both colored substances, 9-anthracenyl$_2$SbBr (43) and [9-anthracenyl$_2$Sb]$_2$ (44) were investigated by UV-Vis spectroscopy. All UV-Vis spectra have been measured in DCM and benzene, showing only slight differences, and thus only the spectra in DCM are presented. At 331 nm, 342 nm, 359 nm, 379 nm and 411 nm, the absorption maxima of 9-anthracenyl$_2$SbBr (43) are already overlapping into the region for the visible spectrum, which is attributed

to the larger π-system. The absorption maxima of the distibane [9-anthracenyl$_2$Sb]$_2$ (44) can be found at 345 nm, 364 nm, 382 nm and 402 nm (Figure 99). Therefore both compounds show longer wavelengths than anthracene itself.

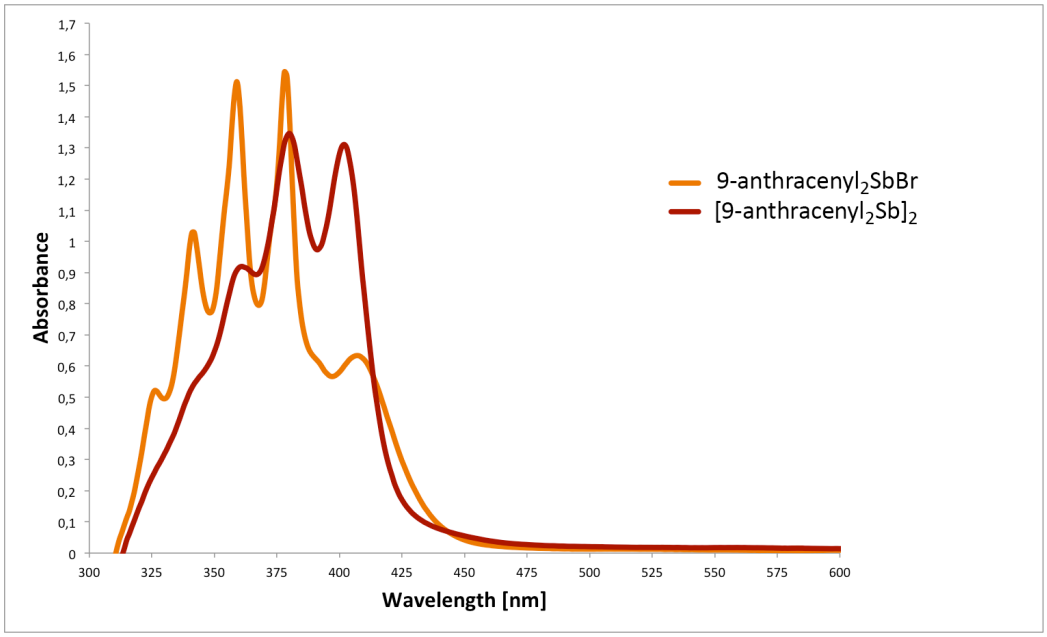

Figure 99. UV-Vis spectra of the p-band of 9-anthracenyl$_2$SbBr (43) and [9-anthracenyl$_2$Sb]$_2$ (44).

Interestingly, many distibanes show lighter color in solution or melts than in their solid state (Figure 100).[206,307] It is assumed that upon melting or solvation of the compound, intermolecular Sb···Sb interactions are disrupted, thus resulting in a bathochromic shift.

Figure 100. [9-anthracenyl$_2$Sb]$_2$ (44) in its solid state and dissolved in DCM, showing lighter color in solution.

The same color change was observed for the novel compound [9-anthracenyl$_2$Sb]$_2$ (44), however, no such interactions were found in the extended solid state (see Chapter 2.2.2.1.4). The same observations were made in the case of [phenyl$_2$Sb]$_2$ and [mesityl$_2$Sb]$_2$, possibly due to the fact that the aryl ligands shield the antimony center, while for alkyldistibanes this is not the case.

2.2.2.4. GCMS measurements

Despite the inherent and represented difficulties with the characterization of organogermanium compounds, X-ray diffraction analysis for solid compounds and GCMS measurements proved to be the most important characterization techniques.

Similar to the germanium derivatives in the case of the triarylstibanes, the loss of aryl groups can be observed. Molecule ion peaks are detected in all cases. For 1-naphthyl$_3$Sb (41), the peak with the highest abundance at m/z 253.1 can be assigned to ($M^{+\bullet}$ - 1-naphthylSb), drawing conclusions, that rearrangement reactions take place as was the case for the germanium derivatives, thus yielding the corresponding biaryl species. Stepwise decomposition of the aryl ligands can be observed. While the biaryl species can be observed in the case of 2,6-xylyl$_3$Sb (40) as well, the peak with the highest abundance is the molecule ion peak at m/z 436.2. Stepwise loss of the aryl groups and decomposition of the very same can be observed in the mass spectrum.

The mass spectrum of 2,6-xylyl$_2$SbBr (42) shows the expected isotope pattern for bromine containing compounds. Two different pathways of fragmentation can be detected, showing either loss of aryl group or loss of halide in the first step. The molecule ion peak can be observed at m/z 412.0. Two peaks with approximately the same abundance can be observed at m/z 305.9 and m/z 105.1 and can be assigned to ($M^{+\bullet}$ - 2,6-xylyl) and ($M^{+\bullet}$ - 2,6-xylylSbBr), respectively. Decomposition of the aryl ligand can be comprehended.

In the case of *o*-tolyl$SbCl_2$ (45), again two possible pathways can be observed, one shows the loss of the aryl group followed by subsequent loss of halides, while in the other case one halide is lost, followed by the loss of the aryl group. In all cases, the expected isotope pattern for chlorine atoms can be observed. The peak at m/z 91.1 shows the highest abundance and is consistent with ($M^{+\bullet}$ - $SbCl_2$).

Although it was attempted several times to measure 9-anthracenyl$_2$SbBr (43) and [9-anthracenyl$_2$Sb]$_2$ (44), it was not possible to obtain a mass spectrum of the two compounds, even when measuring parameters were changed. The reason for this is that 9-anthracenyl$_2$SbBr (43) and [9-anthracenyl$_2$Sb]$_2$ (44) do not separate out of the column at the maximum operating temperature. Measurements were tried on different machines, all yielding the same results.

Chapter 3

Experimental

3.1. Materials and methods

All reactions, unless otherwise stated, were carried out using standard Schlenk line techniques or in a glovebox under nitrogen atmosphere. All dried and deoxygenated solvents were obtained from a solvent drying system (Innovative Technology Inc.). DCM was dried over P_2O_5 and distilled prior to usage. $GeCl_4$, purchased over ABCR, and LiCl were stored under inert gas. $SbCl_3$ was freshly sublimed before usage. $LiAlH_4$ pellets were freshly grounded upon addition. All other chemicals from commercial sources were utilized without further purification. Celite® with a median particle size of 16.4 µm was used (Celite® 512). H_2SO_4 (95%) and HCl (32%) were diluted with degassed, deionized water. The content of Grignard reagent was determined using the Gilman double titration method with phenolphthalein as indicator or by using menthol in dry benzene and 1,10-phenanthroline as an indicator.

General considerations for reactions performed at Oklahoma state university

All reactions were carried out under a nitrogen atmosphere using standard Schlenk, syringe and glovebox techniques. All chemicals from commercial sources were used as received. All solvents were purchased from VWR and dried using a Glass Contour solvent purification system. ^{1}H and ^{13}C NMR spectra were recorded using an INOVA Gemini 2000 spectrometer.

3.2. NMR Spectroscopy

^{1}H (300.22 MHz), ^{13}C (75.5 MHz) and ^{19}F (282.46 MHz) NMR spectra were recorded on a Mercury 300 MHz spectrometer from Varian at 25 °C. Chemical shifts regarding ^{1}H and ^{13}C are given in part per million (ppm) relative to TMS (δ = 0.00 ppm). NMRs were taken in $CDCl_3$ or $C6D_6$.The letters s, d, t, q and m are used to indicate singlet, doublet, triplet, quadruplet and multiplet.

3.3. GCMS measurements

GCMS measurements were carried out on an Agilent Technologies 7890A GC system coupled to an Agilent Technologies 5975C VLMSD mass spectrometer using a HP5 column (30 m×0.250mm×0.025 µm) and a carrier helium gas flow of 0.92726 ml/min. A „hot-needle“, manual injection method at an injector temperature of 280 °C was performed. The MS conditions included positive EI ionization at an ionization energy of 70 eV and a full scan mode (50-500 m/z). All methods can be examined in detail in the Appendix (Table 27 and Table 28).

In some cases, EI-DI measurements up to 500°C were performed on a Waters GCT Premier with EI ionization at an ionization energy of 70 eV and an ion source temperature of 200°C. Samples were prepared in either THF or toluene with a concentration of 1 mg/ml. All data was interpreted using Masslynx software.

3.4. Crystal structure determination

All crystals suitable for single crystal X-ray diffractometry were removed from a vial or a Schlenk under N_2 and immediately covered with a layer of silicone oil. A single crystal was selected, mounted on a glass rod on a copper pin, and placed in the cold N_2 stream provided by an Oxford Cryosystems cryostream. XRD data

collection was performed on a Bruker APEX II diffractometer with use of an Incoatec microfocus sealed tube of Mo Kα radiation (λ= 0.71073 Å) and a CCD area detector.

Empirical absorption corrections were applied using SADABS or TWINABS.[308,309] The structures were solved with use of the intrinsic phasing option in SHELXT and refined by the full-matrix least-squares procedures in SHELXL.[310-312] The space group assignments and structural solutions were evaluated using PLATON.[313,314] The solvent of crystallization of toluene for compound 2,4,6-mesityl$_3$GeBr and 1-naphthyl$_3$GeBr was removed from the refinement by using the "squeeze" option available in the PLATON program suite.[315,316]

Non-hydrogen atoms were refined anisotropically. Hydrogen atoms bonded to germanium atoms were located in a difference map and refined isotropically. All other hydrogen atoms were located in calculated positions corresponding to standard bond lengths and angles and refined using a riding model. For compound 2,4,6-mesityl$_3$GeH, the hydrogen atom bound to germanium was not found on the difference map and residual electron density is attributed to the heavy germanium atom. This is a common problem with locating light atoms (hydrogen) next to heavy atoms because of their poor scattering abilities.

Disorder was handled by modeling the occupancies of the individual orientations using free variables to refine the respective occupancy of the affected fragments (PART).[317] In some cases, the similarity SAME restraint, the similar-ADP restraint SIMU and the rigid-bond restraint DELU, as well as the constraints EXYZ and EADP were used in modelling disorder to make the ADP values of the disordered atoms more reasonable. In some cases, the distances between arbitrary atom pairs were restrained to possess the same value using the SADI instruction and in some cases distance restraints (DFIX) to certain target values were used. In some tough cases of disorder, anisotropic U^{ij}-values of the atoms were restrained (ISOR) to behave more isotropically.

In compound 3,4-xylyl$_4$Ge, disordered positions for one of the 3,4-xylyl residues were refined using 50/50 positions. In compound 1-naphthyl$_3$GeH, one of the naphthyl residues was refined using 75/25 positions. In compound

2,4,6-mesityl$_3$GeH, disordered positions for the germanium metals were refined using 50/50 positions. In compound 2,6-xylyl$_3$GeH, disordered positions for the germanium metals were refined using 90/10 positions. For compound 1-naphthyl$_3$GeBr · CHCl$_3$, several restraints and constraints (FRAG 17, AFIX 66) were used to afford idealized naphthalene geometry for one of the naphthyl residues. Disordered positions for the solvent of crystallization toluene in 1-naphthyl$_3$Sb · toluene were refined using 50/50 split positions with additional restraints to afford optimized geometries (FLAT and AFIX 66).

Compound phenyl$_4$Ge was twinned and was refined using the TWIN option in SHELXL and the matrix (0 1 0 -1 0 0 0 0 1) was applied. The main contributions of the two twin components refined to a BASF of 0.03. Compound 2,6-xylyl$_3$GeBr was twinned and was refined using the matrix (-1 0 0 0 -1 0 0 0 -1). The main contributions of the two twin components refined to a BASF of 0.02. Compound 1-naphthyl$_3$GeBr · naphthyl was twinned and was refined using the matrix (0 1 0 1 0 0 0 0 -1). The main contributions of the two twin components refined to a BASF of 0.03. Compound 2,5-xylyl$_2$GeHCl was twinned and was refined using the matrix (-1 0 0 0 -1 0 0 0 1). The main contributions of the two twin components refined to a BASF of 0.02.

Electrostatic non-covalent intermolecular interactions,[252-255] van der Waals contacts[260,273,274] and Ge–H···Ge contacts[271,272] for presented and published compounds based on a Cambridge Structural Database[318] search were determined by features of the programs Mercury[319] and Diamond[315,318,320] and fall within expected ranges. All crystal structures representations were made with the program Diamond.

Table 29 to Table 33 contain crystallographic data and details of measurements and refinement.

3.5. Complementary techniques

Elemental analysis was performed on a Elementar vario EL or a Elementar vario MICRO cube. In all cases CHN contents were verified by a threefold analysis.

IR spectra were performed on a Bruker APHA FT-IR spectrometer with platinum ATR diamond top. Samples were exposed to air shortly before flushed with constant N_2 gas.

Melting point measurements were carried out by threefold determination with a Stuart Scientific SMP 10 (up to 300 °C).

TGA/DSC measurements were performed on a NETSCH STA 409. Elemental analysis was performed with an Elementar Vario EL III.

Scanning electron microscopy (SEM) analysis was performed on a Vega 3 SBU SEM with a tungsten hair-pin cathode. Samples were sputtered with gold for topographic characterization.

3.6. Synthesis

3.6.1. Germanium compounds

3.6.1.1. Preparation of R_4Ge

General Procedure

A flask equipped with a dropping funnel and a reflux condenser was charged with Mg in THF or Et_2O. The dropping funnel was charged with arylbromide in THF or Et_2O, about 10% of the solution was added to the reaction vessel and the solution was heated carefully or dibromoethane was added to start the reaction. The arylbromide was subsequently added dropwise. After complete addition, the reaction was refluxed for 3-12 hours. Residual Mg was filtered off using a filter cannula or a Schlenk-frit charged with Celite®. Germanium tetrachloride ($GeCl_4$)

in toluene was added slowly to the Grignard solution at 0°C and the solvent exchanged with toluene. The reaction was stirred for 1 hour, heated to reflux for several hours and was subsequently allowed to cool down to room temperature. After quenching with 10% degassed HCl at 0°C, the water layer was washed twice with boiling toluene and the organic layers were dried over Na_2SO_4. After removal of solvent under reduced pressure, the product was washed several times with pentane and purified *via* recrystallization.

***m*-tolyl$_4$Ge (1)**: 10.0 g (411 mmol, 15.4 eq.) Mg in 100 ml Et_2O, 64.3 g (376 mmol, 14.1 eq.) 3-bromotoluene in 50 ml Et_2O, 5.70 g (26.6 mmol, 1.00 eq.) $GeCl_4$ in 60 ml toluene at 0°C, refluxed for 12 hours. The resulting oil was recrystallized from toluene at room temperature to obtain colorless crystals. Yield: 65%. M.p.: 145°C. Elemental analysis (%) for $C_{28}H_{28}Ge$: C, 76.93; H, 6.46. Found: C, 77.68; H, 6.57. ^{1}H NMR ($CDCl_3$, 300 MHz): δ 7.13 (m, 16H, ArH), 2.21 (s, 12H, CH_3) ppm. ^{13}C NMR ($CDCl_3$, 75.5 MHz): δ 137.71, 136.34, 136.04, 132.65, 129.93, 128.14, 21.72 (CH_3) ppm. GCMS: Methode1: t_R = 24.67 min, m/z: 438.2 ($M^{+\cdot}$), 347.1 ($M^{+\cdot}$ - *m*-tolyl), 256.0 ($M^{+\cdot}$ - *m*-tolyl$_2$), 165.0 ($M^{+\cdot}$ - *m*-tolyl$_3$) 91.1 ($M^{+\cdot}$ - *m*-tolyl$_3$Ge).

3,4-xylyl$_4$Ge (2): 4.94 g (204 mmol, 13.8 eq.) Mg in 100 ml THF, 34.3 g (185 mmol, 12.5 eq.) 4-bromo-*o*-xylene in 50 ml THF, 3.17 g (14.8 mmol, 1.00 eq.) $GeCl_4$ in 60 ml toluene at 0°C, refluxed for 3 hours. The resulting solid was washed several times with pentane and recrystallized from toluene at -30°C to obtain colorless crystals. Yield: 76%. M.p.: 172°C. Elemental analysis (%) for $C_{32}H_{36}Ge$: C, 77.92; H, 7.36. Found: C, 77.95; H, 7.16. ^{1}H NMR ($CDCl_3$, 300 MHz): δ 7.25 (d, 8H, 5,6- H, ArH), 7.11 (d, 4H, 2-H, ArH), 2.25 (s, 12H, CH_3), 2.20 (s, 12H, CH_3) ppm. ^{13}C NMR ($CDCl_3$, 75.5 MHz): δ 137.44, 136.63, 133.92, 133.26, 129.59, 19.97 (CH_3), 19.96 (CH_3) ppm. GCMS: Methode2: t_R = 22.90 min, m/z: 494.3 ($M^{+\cdot}$), 389.2 ($M^{+\cdot}$ - 3,4-xylyl), 284.1 ($M^{+\cdot}$ - 3,4-xlyl$_2$), 179.0 ($M^{+\cdot}$ - 3,4-xylyl$_3$), 105.1 ($M^{+\cdot}$ - 3,4-xylyl$_3$Ge), 77.1 ($M^{+\cdot}$ - 3,4-xylylGe$_3$Me$_2$).

3,5-xylyl$_4$Ge (3): 10.0 g (411 mmol, 12.5 eq.) Mg in 100 ml THF, 60.9 g (329 mmol, 9.97 eq.) 4-bromo-*o*-xylene in 50 ml THF, 7.04 g (33.0 mmol, 1.00 eq.) $GeCl_4$ in 60 ml toluene at 0°C, refluxed for 4.5 hours. The resulting solid was washed several times with pentane and recrystallized from toluene at -30°C to obtain colorless crystals. Yield: 70%. M.p.: 195°C. Elemental analysis (%) for $C_{32}H_{36}Ge$: C, 76.60; H, 7.12. Found: C, 77.92; H, 7.36. ^{1}H NMR ($CDCl_3$, 300 MHz): δ 7.12 (s, 8H, 2,6-H, ArH), 7.01 (s, 4H, 4-H, ArH), 2.27 (s, 24H, CH_3) ppm. ^{13}C NMR ($CDCl_3$, 75.5 MHz): δ 137.50, 136.55, 133.28, 130.88, 21.64 (CH_3) ppm. GCMS: Methode1: t_R = 25.49 min, m/z: 494.3 ($M^{+\cdot}$), 389.2 ($M^{+\cdot}$ - 3,5-xylyl), 284.1 ($M^{+\cdot}$ - 3,5-xlyl$_2$), 179.1 ($M^{+\cdot}$ - 3,5-xylyl$_3$), 105.1 ($M^{+\cdot}$ - 3,5-xylyl$_3$Ge), 77.1 ($M^{+\cdot}$ - 3,5-xylylGe$_3$Me$_2$).

2-naphthyl$_4$Ge (4): 3.23 g (133 mmol, 5.50 eq.) Mg in 100 ml THF, 25 g (121 mmol, 5.00 eq.) 2-bromonaphthalene in 50 ml THF, 5.17 g (24.1 mmol, 1.00 eq.) $GeCl_4$ in 60 ml toluene at 0°C, refluxed for 3 hours. The resulting solid was washed several times with pentane and recrystallized from toluene at -30°C to obtain colorless crystals. Yield: 68%. M.p.: 190°C. Elemental analysis (%) for $C_{40}H_{28}Ge$: C, 82.65; H, 4.86. Found: C, 82.11; H, 4.82. ^{1}H NMR ($CDCl_3$, 300 MHz): δ 8.12 (s, 4H, 1-H, ArH), 7.87 (d, 4H, 3-H, ArH), 7.85 (d, 4H, 4-H, ArH), 7.74 (t, 8H, 5,8-H, ArH), 7.48 (m, 8H, 6,7-H, ArH) ppm. ^{13}C NMR ($CDCl_3$, 75.5 MHz): δ 136.47, 134.01, 133.78, 133.47, 131.80, 128.35, 128.02, 127.86, 126.78, 126.26 ppm. DI/MS EI m/z: 582.14 ($M^{+\cdot}$), 455.1 ($M^{+\cdot}$ - 2-naphthyl), 328.1 ($M^{+\cdot}$ -2-naphthyl$_2$), 201.0 ($M^{+\cdot}$ -2-naphthyl$_3$).

3.6.1.2. Preparation of R_3GeX (X = Cl, Br)

Four different routes (A), (B), (C) and (D) were applied for the synthesis of triaryl-germanium halides.

Route A: A flask equipped with a dropping funnel and a reflux condenser was charged with Mg in THF or Et_2O. The dropping funnel was charged with arylbromide in THF, about 10% of the solution was added to the reaction vessel and the solution was heated carefully or dibromoethane was added to start the reaction. The arylbromide was subsequently added dropwise. After complete addition, the reaction was refluxed for 3-12 hours. Residual Mg was filtered off using a filter cannula or a Schlenk-frit charged with Celite®. Germanium tetrachloride ($GeCl_4$) in toluene was added slowly to the Grignard solution at 0°C and the solvent exchanged with toluene. The reaction was stirred for 1 hour, heated to reflux for several hours and was subsequently allowed to cool down to room temperature. After quenching with 10% degassed HCl at 0°C, the water layer was washed twice with boiling toluene and the organic layers were dried over Na_2SO_4. After removal of solvent under reduced pressure, the product was washed several times with pentane and purified *via* recrystallization or condensation.

***o*-tolyl$_3$GeX (5)**: 6.00 g (247 mmol, 12.2 eq.) Mg in 80 ml THF, 38.4 g (224 mmol, 11.1 eq.) 2-bromotoluene in 50 ml THF, 4.32 g (20.2 mmol, 1.00 eq.) $GeCl_4$ in 60 ml toluene at 0°C. The resulting colorless solid (15-22% *o*- tolyl$_3$GeCl, 78-85% *o*-tolyl$_3$GeBr) was recrystallized from toluene at -30°C to obtain colorless crystals of *o*-tolyl$_3$GeBr. Yield: 85%. M.p.: 119°C. Elemental analysis (%) for $C_{21}H_{21}GeX$: Cl: C, 66.12; H, 5.55. Br: C, 59.22; H, 4.92. Found: C, 60.70; H, 4.92. ^{1}H NMR ($CDCl_3$, 300 MHz): δ 7.46 (d, 3H, 6-H, ArH), 7.36 (t, 3H, 3-H, ArH), 7.21 (m, 6H, 4,5-H, ArH), 2.35 (s, 9H, CH_3) ppm. ^{13}C NMR ($CDCl_3$, 75.5 MHz): δ 143.89, 135.15, 130.98, 130.84, 126.00, 23.42 (CH_3) ppm. GCMS: Methode2: Cl: t_R = 18.25 min, m/z: 382.1 ($M^{+\cdot}$), 347.1 ($M^{+\cdot}$ - Cl), 290.1 ($M^{+\cdot}$ - *o*-tolyl), 255.1 ($M^{+\cdot}$ - *o*-tolylCl), 199.0 ($M^{+\cdot}$ - *o*-tolyl$_2$), 181.1 ($M^{+\cdot}$ -*o*-tolylGeCl), 165.1 ($M^{+\cdot}$ - *o*-tolyl$_2$Cl), 91.1 ($M^{+\cdot}$ - *o*-tolyl$_2$GeCl). Br: t_R = 18.87 min, m/z: 426.1 ($M^{+\cdot}$), 347.1 ($M^{+\cdot}$ -Br), 334.0 ($M^{+\cdot}$ - *o*-tolyl), 255.1 ($M^{+\cdot}$ -*o*-tolylCl), 243.9 ($M^{+\cdot}$ -*o*-tolyl$_2$), 181.1 ($M^{+\cdot}$ - *o*-tolylGeCl), 165.1 ($M^{+\cdot}$ - *o*-tolyl$_2$Br), 91.1 ($M^{+\cdot}$ - *o*-tolyl$_2$GeBr).

2,4-xylyl$_3$GeX (6): 10.00 g (411 mmol, 11.0 eq.) Mg in 200 ml THF, 69.2 g (374 mmol, 10.0 eq.) 4-bromo-*m*-xylene in 100 ml THF, 8.00 g (37.4 mmol, 1.00 eq.) $GeCl_4$ in 100 ml toluene at 0°C. A brown slurry was obtained (74-80% 2,4-xylyl$_3$GeCl, 26-20% 2,4-xylyl$_3$GeBr). After several crystallization attempts 2,4-xylyl$_3$GeCl was obtained as a colorless solid. Yield: 72%. Elemental analysis (%) for $C_{24}H_{27}GeCl$: Cl: C, 68.06; H, 6.43. Found: C, 67.97; H, 6.35. ^{1}H NMR ($CDCl_3$, 300 MHz): δ 7.30 (d, 3H, 6-H, ArH), 7.07 (s, 3H, 3-H, ArH), 6.99 (d, 3H, 2-H, ArH), 2.33 (s, 9H, CH_3), 2.30 (s, 9H, CH_3) ppm. ^{13}C NMR ($CDCl_3$, 75.5 MHz): δ 143.83, 140.77, 135.02, 131.78, 131.39, 126.70, 23.17 (CH_3), 21.59 (CH_3) ppm. GCMS: Methode2: Cl: t_R = 20.15 min, m/z: 424.1 ($M^{+\cdot}$), 389.1 ($M^{+\cdot}$ - Cl), 318.1 ($M^{+\cdot}$- 2,4-xylyl), 281.1 ($M^{+\cdot}$ - 2,4-xylylCl), 209.2 ($M^{+\cdot}$ - 2,4-xylylGeCl), 179.1 ($M^{+\cdot}$ - 2,4-xylyl$_2$Cl), 105.0 ($M^{+\cdot}$ - 2,4-xylyl$_2$GeCl), 77.1 ($M^{+\cdot}$ - 2,4-xylyl$_2$GeCl$(CH_3)_2$).

2,5-xylyl$_3$GeX (7): 2.74 g (113 mmol, 5.70 eq.) Mg in 100 ml THF, 19.0 g (102 mmol, 5.20 eq.) 2-bromo-*p*-xylene in 50 ml THF, 4.50 g (19.7 mmol, 1.00 eq.) $GeCl_4$ in 60 ml toluene at 0°C. The resulting colorless solid (16-50% 2,5- Xylyl$_3$GeCl, 50-84% 2,5- Xylyl$_3$GeBr) was recrystallized from toluene at -30°C to obtain colorless crystals of 2,5- Xylyl$_3$GeBr. Yield: 65-70%. M.p.: 149°C. Elemental analysis (%) for $C_{24}H_{27}GeX$: Cl: C, 68.06; H, 6.43. Br: C, 61.59; H, 5.82. Found: C, 62.97; H, 5.89. ^{1}H NMR ($CDCl_3$, 300 MHz): δ 7.28 (s, 3H, 6-H, ArH), 7.14 (d, 6H, 3,4-H, ArH), 2.29 (s, 9H, CH_3), 2.25 (s, 9H, CH_3) ppm. ^{13}C NMR ($CDCl_3$, 75.5 MHz): δ 140.59, 135.66, 135.28, 134.24, 131.52, 130.80, 22.88 (CH_3), 21.27 (CH_3) ppm. GCMS: Methode2: Cl: t_R = 18.80 min, m/z: 424.1 ($M^{+\cdot}$), 389.2 ($M^{+\cdot}$ - Cl), 318.0 ($M^{+\cdot}$- 2,5-xylyl), 283.1 ($M^{+\cdot}$ - 2,5-xylylCl), 209.1 ($M^{+\cdot}$ - 2,5-xylylGeCl), 179.1 ($M^{+\cdot}$ - 2,5-xylyl$_2$Cl), 105.0 ($M^{+\cdot}$ - 2,5-xylyl$_2$GeCl), 77.1 ($M^{+\cdot}$ - 2,5-xylyl$_2$GeCl$(CH_3)_2$) Br: t_R = 19.31 min, m/z: 468.1 ($M^{+\cdot}$), 389.2 ($M^{+\cdot}$ - Br), 362.0 ($M^{+\cdot}$ - 2,5-xylyl), 283.1 ($M^{+\cdot}$ - 2,5-xylylBr), 256.9 ($M^{+\cdot}$ - 2,5-xylyl$_2$), 209.2 ($M^{+\cdot}$ - 2,5-xylylGeBr), 179.1 ($M^{+\cdot}$ - 2,5-xylyl$_2$Br), 105.0 ($M^{+\cdot}$ - 2,5-xylyl$_2$GeBr), 77.1 ($M^{+\cdot}$ - 2,5-xylyl$_2$GeBr$(CH_3)_2$).

2,6-xylyl$_3$GeX (8): 10.00 g (411 mmol, 6.85 eq.) Mg in 100 ml THF, 69.2 g (374 mmol, 6.00 eq.) 2-bromo-*m*-xylene in 150 ml THF, 12.85 g (60.0 mmol, 1.00 eq.) $GeCl_4$ in 60 ml toluene at 0°C. The resulting solid was recrystallized from toluene at -30°C to obtain colorless crystals (17-21% 2,6-xylyl$_3$GeCl, 79-83% 2,6-xylyl$_3$GeBr). Yield: 55-70%. M.p.: 153°C. Elemental analysis (%) for $C_{24}H_{27}GeX$: Cl: C, 68.06; H, 6.43. Br: C, 61.59; H, 5.82. Found: C, 62.17; H, 5.95. ^{1}H NMR ($CDCl_3$, 300 MHz): δ 7.19 (t, 3H, 4-H, ArH), 7.00 (d, 6H, 3,5-H, ArH), 2.31 (s, 18H, CH_3) ppm. ^{13}C NMR ($CDCl_3$, 75.5 MHz): δ 143.60, 140.32, 129.89, 129.10, 25.19 (CH_3) ppm. GCMS: Methode2: Cl: t_R = 19.92 min, m/z: 424.1 ($M^{+\cdot}$), 389.1 ($M^{+\cdot}$ - Cl), 284.1 ($M^{+\cdot}$ - 2,6-xylylCl), 209.1 ($M^{+\cdot}$ - 2,6-xylylGeCl), 179.1 ($M^{+\cdot}$ - 2,6-xylyl$_2$Cl), 105.0 ($M^{+\cdot}$ - 2,6-xylyl$_2$GeCl), 77.1 ($M^{+\cdot}$ - 2,6-xylyl$_2$GeCl$(CH_3)_2$). Br: t_R = 20.57 min, m/z: 468.1 ($M^{+\cdot}$), 389.2 ($M^{+\cdot}$ - Br), 362.0 ($M^{+\cdot}$ - 2,6-xylyl), 283.1 ($M^{+\cdot}$ - 2,6-xylylBr), 256.9 ($M^{+\cdot}$ - 2,6-xylyl$_2$), 209.1 ($M^{+\cdot}$ - 2,6-xylylGeBr), 179.1 ($M^{+\cdot}$ - 2,6-xylyl$_2$Br), 105.0 ($M^{+\cdot}$ -2,6-xylyl$_2$GeBr), 77.1 ($M^{+\cdot}$ - 2,6-xylyl$_2$GeBr$(CH_3)_2$).

1-naphthyl$_3$GeX (9): 8.00 g (329 mmol, 6.85 eq.) Mg in 70 ml THF, 61.9 g (299 mmol, 6.23 eq.) 1-bromonaphthalene in 200 ml THF, filtered hot over Celite® using a Schlenk frit. 10.3 g (48.0 mmol, 1.00 eq.) $GeCl_4$ in 60 ml toluene at rt. The resulting solid (10-35% 1-naphthyl$_3$GeCl, 65-90% 1- naphthyl$_3$GeBr) was washed several times with pentane and toluene and recrystallized from toluene, chloroform and THF at -30°C to obtain colorless crystals of 1- naphthyl$_3$GeCl or 1- naphthyl$_3$GeBr, which were used for further analysis. Yield: 50-65%. M.p.: 239°C. Elemental analysis (%) for $C_{30}H_{21}GeX$: Br: C, 67.47; 3.96 H, 4.32. Found: C, 68.07; H, 3.96. ^{1}H NMR ($CDCl_3$, 300 MHz): δ 8.28 (d, 3H, 8-H, ArH), 7.98 (d, 3H, 2-H, ArH), 7.90 (d, 3H, 4-H, ArH), 7.73 (d, 3H, 5-H, ArH), 7.47 (t, 3H, 7-H, ArH), 7.36 (m, 6H, 3,6-H, ArH) ppm. ^{13}C NMR ($CDCl_3$, 75.5 MHz): δ 136.06, 135.45, 134.19, 133.30, 131.79, 129.10, 128.98, 126.58, 126.32, 125.48 ppm. GCMS: Methode2: Cl: t_R = 29.02 min, m/z: 490.1 ($M^{+\cdot}$), 455.0 ($M^{+\cdot}$ - Cl), 363.0 ($M^{+\cdot}$ - 1-naphthyl), 253.1 ($M^{+\cdot}$ - 1-naphthylGeCl), 127.1 ($M^{+\cdot}$ - 1-naphthyl$_2$GeCl), 77.1 ($M^{+\cdot}$ - 1-naphthyl$_2$GeCl(C_4H_4)). Br: t_R = 30.55 min, m/z: 534.1 ($M^{+\cdot}$), 455.1 ($M^{+\cdot}$ - Br), 407.0 ($M^{+\cdot}$ -1-naphthyl), 327.0 ($M^{+\cdot}$ -1-naphthylBr), 252.1 ($M^{+\cdot}$ - 1-naphthylGeBr), 201.0

($M^{+\cdot}$ -1-naphthyl$_2$Br), 127.1 ($M^{+\cdot}$ -1-naphthyl$_2$GeBr), 77.1 ($M^{+\cdot}$ - 1-naphthyl$_2$GeBr(C_4H_4)).

2,4,6-mesityl$_3$GeX (10): 7.50 g (309 mmol, 8.80 eq.) Mg in 70 ml THF, 55.9 g (281 mmol, 8.00 eq.) 2-bromo-1,3,5-trimethylbenzene in 300 ml THF, 7.52 g (35.1 mmol, 1.00 eq.) $GeCl_4$ in 100 ml toluene at rt. The resulting solid (25-40% 2,4,6-mesityl$_3$GeCl, 60-75% 2,4,6-mesityl$_3$GeBr) recrystallized from toluene at -30°C to obtain colorless crystals of 2,4,6-mesityl$_3$GeBr. Yield: 55-65%. M.p.: 165°C. Elemental analysis (%) for $C_{30}H_{21}GeX$: Cl: C, 69.65; H, 7.14. Br: C, 63.58; H, 6.52. Found: C, 67.56; H, 6.97. ^{1}H NMR ($CDCl_3$, 300 MHz): δ 6.78 (s, 6H, 3,5-H ArH), 2.24 (s, 9H, CH_3), 2.13 (s, 18H, CH_3) ppm. ^{13}C NMR ($CDCl_3$, 75.5 MHz): δ 143.78, 138.32, 135.0, 128.89, 23.72, 21.20 ppm. GCMS: Methode2: Cl: t_R = 29.02 min, m/z: 466.1 ($M^{+\cdot}$), 431.1 ($M^{+\cdot}$ - Cl), 346.10 ($M^{+\cdot}$ - 2,4,6-mesityl), 237.2 ($M^{+\cdot}$ - 2,4,6- mesitylGeCl), 228.0 ($M^{+\cdot}$ - 12,4,6-mesityl$_2$), 119.1 ($M^{+\cdot}$ - 2,4,6-mesityl$_2$GeCl). Br: t_R = 21.84 min, m/z: 510.1 ($M^{+\cdot}$), 431.2 ($M^{+\cdot}$ - Br), 390.1 ($M^{+\cdot}$ - 2,4,6-mesityl), 311.1 ($M^{+\cdot}$ -2,4,6-mesitylBr), 270.9 ($M^{+\cdot}$ - 2,4,6-mesityl$_2$), 237.2 ($M^{+\cdot}$ - 2,4,6-mesitylGeBr), 119.1 ($M^{+\cdot}$ - 2,4,6-mesityl$_2$GeBr).

Route B: A Schlenk was charged with tetraarylgermane and freshly distilled DCM. HOTf was added dropwise at 0°C and the reaction was allowed to warm to room temperature. After stirring for 24-48 hours, after which time the ^{19}F NMR spectrum of the solution exhibited a single resonance indicating complete consumption of HOTf and formation of the desired product, the solvent was removed under *vacuo* and dry DME was added. LiCl was added as a solid in small portions at 0°C and the reaction was stirred for 24 hours. After removal of solvent under *vacuo*, the crude product was suspended in toluene, filtered *via* cannula and dried in *vacuo*.

3,5-xylyl$_3$GeCl (11): 3.00 g (6.08 mmol, 1.00 eq.) 3,5-xylyl$_4$Ge (3) in 100 ml DCM, 1.00 g HOTf (6.69 mmol, 1.10 eq.), stirred overnight at rt, solvent exchange with

50 ml DME, 0.26 g (6.08 mmol, 1.00 eq.) LiCl. After complete workup an off-white solid was obtained. Yield: 43%. M.p.: 159°C. Elemental analysis (%) for $C_{24}H_{27}GeCl$: C, 68.06; H, 6.43. Found: C, 67.77; H, 6.23. ^{1}H NMR ($CDCl_3$, 300 MHz): δ 7.22 (s, 6H, 2,6-H, ArH), 7.08 (s, 3H, 4-H, ArH), 2.31 (s, 18H, CH_3) ppm. ^{13}C NMR ($CDCl_3$, 75.5 MHz): δ 138.19, 134.96, 132.35, 131.79, 21.53 (CH_3) ppm. GCMS: Methode2: t_R = 18.94 min, m/z: 424.2 ($M^{+\cdot}$), 319.1 ($M^{+\cdot}$ - Cl), 210.2 ($M^{+\cdot}$ - 3,5-xylylGeCl), 179.1 ($M^{+\cdot}$ - 3,5-xylyl$_2$Cl), 105.0 ($M^{+\cdot}$ - 3,5-xylyl$_2$GeCl), 77.1 ($M^{+\cdot}$ - 3,5-xylyl$_2$GeCl$(CH_3)_2$).

Route C: A Schlenk was charged with tetraarylgermane and freshly distilled DCM. HOTf was added dropwise at 0°C and the reaction was allowed to warm to room temperature. After stirring for 24-48 hours, after which time the ^{19}F NMR spectrum of the solution exhibited a single resonance indicating complete consumption of HOTf and formation of the desired product, a suspension of LiCl in DME was added at 0°C and the reaction was stirred for an additional 24 hours. Toluene was added and DCM and DME were evaporated under reduced pressure. After filtration *via* cannula and removal of solvent, the resulting product was dried in *vacuo*.

2-naphthyl$_3$GeCl (12): 4.50 g (7.74 mmol, 1.00 eq.) 2-naphthyl$_4$Ge (4) in 100 ml DCM, 1.28 g HOTf (8.52 mmol, 1.10 eq), stirred overnight at rt, solvent exchange with 50 ml DME, 0.39 g (9.29 mmol, 1.20 eq.) LiCl. After complete workup an off-white solid was obtained. Yield: 52%. M.p.: 132°C. Elemental analysis (%) for $C_{30}H_{21}GeCl$: C, 73.60; H, 4.32. Found: C, 72.24; H, 4.32. ^{1}H NMR ($CDCl_3$, 300 MHz): δ 8.17 (s, 3H, 1-H, ArH), 7.92 (d, 3H, 3-H, ArH), 7.86 (d, 3H, 4-H, ArH), 7.81 (d, 3H, 5-H, ArH), 7.75 (d, 3H, 8-H, ArH), 7.51 (m, 6H, 6,7-H, ArH) ppm. ^{13}C NMR ($CDCl_3$, 75.5 MHz): δ 135.59, 134.55, 133.27, 129.86, 128.58, 128.50, 128.13, 127.53, 126.73, 125.96 ppm. GCMS: Methode2: t_R = 35.42 min, m/z: 490.2 ($M^{+\cdot}$), 455.0 ($M^{+\cdot}$ - Cl), 363.0 ($M^{+\cdot}$ - 2-naphthyl), 254.1 ($M^{+\cdot}$ - 2-naphthylGeCl), 201.0 ($M^{+\cdot}$ - 2-naphthyl$_2$Cl), 127.1 ($M^{+\cdot}$ - 2-naphthyl$_2$GeCl), 77.1 ($M^{+\cdot}$ - 2-naphthyl$_2$GeCl(C_4H_4)).

Route D: A Schlenk was charged with R_3GeH and freshly distilled CCl_4. After addition of catalytic amounts of pure Pd powder, the reaction was stirred at room temperature for several hours. After filtration *via* cannula, the solvent was removed under *vacuo*.

2,5-xylyl$_3$GeCl (13): 0.20 g (0.51 mmol, 1.00 eq.) 2,5-xylyl$_3$GeH (15) in 15 ml freshly distilled CCl_4, catalytic amounts of Pd, stirred for 52 hours. The colorless solid was recrystallized in toluene as colorless crystals. Yield: 80%. M.p.: 141°C. Elemental analysis (%) for $C_{24}H_{27}GeCl$: C, 68.06; H, 6.43. Found: C, 67.82; H, 6.38. ^{1}H NMR ($CDCl_3$, 300 MHz): δ 7.27 (s, 3H, 6-H, ArH), 7.14 (d, 6H, 3,4-H, ArH), 2.28 (s, 9H, CH_3), 2.25 (s, 9H, CH_3) ppm. ^{13}C NMR ($CDCl_3$, 75.5 MHz): δ 140.63, 135.42, 135.27, 134.60, 131.51, 130.70, 22.76 (CH_3), 21.27 (CH_3) ppm. GCMS: Methode2: t_R = 18.80 min, m/z: 424.1 ($M^{+\cdot}$), 389.2 ($M^{+\cdot}$ - Cl), 318.1 ($M^{+\cdot}$- 2,5-xylyl), 283.1 ($M^{+\cdot}$ - 2,5-xylylCl), 209.2 ($M^{+\cdot}$ - 2,5-xylylGeCl), 179.1 ($M^{+\cdot}$ - 2,5-xylyl$_2$Cl), 105.0 ($M^{+\cdot}$ - 2,5-xylyl$_2$GeCl), 77.1 ($M^{+\cdot}$ - 2,5-xylyl$_2$GeCl$(CH_3)_2$).

3.6.1.3. Preparation of R_3GeH

General Procedure

A Schlenk was charged with $LiAlH_4$ and dry THF. The R_3GeX (X = Cl, Br) was added as a powder or in solution in small portions at 0°C. The reaction was stirred at 0°C for 1 hour and then allowed to warm to room temperature. After additional stirring for 1-2 hours the reaction was quenched using 3% degassed H_2SO_4. After extraction with a saturated degassed sodium tartrate solution, the solution was filtered *via* cannula and dried over Na_2SO_4. After filtration and washing twice with toluene, all solvents were removed under *vacuo*.

2,4-xylyl$_3$GeH (14): 2.84 g (74.8 mmol, 1.20 eq.) $LiAlH_4$ added as solid to a solution of 27.88 g (62.3 mmol, 1.00 eq.) 2,4-xylyl$_3$GeX (6) in 200 ml THF. Yield: 75%. M.p.: 138°C. Elemental analysis (%) for $C_{24}H_{28}Ge$: C, 74.08; H, 7.25. Found: C, 72.48; H, 6.99. ^{1}H NMR ($CDCl_3$, 300 MHz): δ 7.04 (s, 3H, 3-H, ArH), 7.02 (d, 6H, 5,6-H, ArH), 5.84 (s, 1H, Ge-H), 2.30 (s, 9H, *p*-CH_3), 2.26 (s, 9H, *o*-CH_3) ppm. ^{13}C NMR ($CDCl_3$, 75.5 MHz): δ 143.89, 139.26, 135.83, 131.46, 130.74, 126.40, 23.03 (CH_3), 21.51 (CH_3) ppm. ATR-IR: 2050.4 (Ge-H) cm^{-1}. GCMS: Methode2: t_R = 18.63 min, m/z: 389.2 ($M^{+\cdot}$ -H), 284.1 ($M^{+\cdot}$ - 2,4-xylylH), 269.1 ($M^{+\cdot}$ - 2,4-xylylH(CH_3)), 179.1 ($M^{+\cdot}$ - 2,4-xylyl$_2$), 105.1 ($M^{+\cdot}$ - 2,4-xylyl$_2$GeH), 91.1 ($M^{+\cdot}$ - 2,4-xylyl$_2$GeH(CH_3)), 77.1 ($M^{+\cdot}$ - 2,4-xylyl$_2$GeH(CH_3)$_2$).

2,5-xylyl$_3$GeH (15): 0.88 g (22.3 mmol, 1.00 eq.) $LiAlH_4$ in 250 ml THF, 10.0 g (22.3 mmol, 1.00 eq.) 2,5-xylyl$_3$GeX (7) in 70 ml THF. The resulting colorless solid was recrystallized from toluene. Yield: 82%. M.p.: 177°C. Elemental analysis (%) for $C_{24}H_{28}Ge$: C, 74.08; H, 7.25. Found: C, 74.12; H, 7.20. ^{1}H NMR ($CDCl_3$, 300 MHz): δ 7.09 (s, 6H, 3,4-H, ArH), 6.98 (s, 3H, 6-H ArH), 5.82 (s, 1H, Ge-H), 2.24 (s, 9H, *m*-CH_3), 2.20 (s, 9H, *o*-CH_3) ppm. ^{13}C NMR ($CDCl_3$, 75.5 MHz): δ 140.83, 136.39, 134.89, 134.82, 130.29, 129.66, 22.70 (CH_3), 21.23 (CH_3) ppm. ATR-IR: 2036.9 (Ge-H) cm^{-1}. GCMS: Methode2: t_R = 17.42 min, m/z: 389.2 ($M^{+\cdot}$ -H), 284.1 ($M^{+\cdot}$ - 2,5-xylylH), 269.0 ($M^{+\cdot}$ - 2,5-xylylH(CH_3)), 209.2 ($M^{+\cdot}$ - 2,5-xylylGeH), 179.0 ($M^{+\cdot}$ - 2,5-xylyl$_2$), 105.1 ($M^{+\cdot}$ - 2,5-xylyl$_2$GeH), 91.0 ($M^{+\cdot}$ - 2,5-xylyl$_2$GeH(CH_3)), 77.0 ($M^{+\cdot}$ - 2,5-xylyl$_2$GeH(CH_3)$_2$).

2,6-xylyl$_3$GeH (16): 1.45 g (38.3 mmol, 1.10 eq.) $LiAlH_4$ in 200 ml THF, 16.3 g (34.8 mmol, 1.00 eq.) 2,6-xylyl$_3$GeX (8). The resulting colorless solid was recrystallized from toluene. Yield: 86%. M.p.: 147°C. Elemental analysis (%) for $C_{24}H_{28}Ge$: C, 74.08; H, 7.25. Found: C, 73.93; H, 7.09. ^{1}H NMR ($CDCl_3$, 300 MHz): δ 7.13 (t, 3H, 4-H, ArH), 6.95 (d, 6H, 3,5-H, ArH), 5.90 (s, 1H, Ge-H), 2.17 (s, 18H, CH_3) ppm. ^{13}C NMR ($CDCl_3$, 75.5 MHz): δ 143.90, 128.92, 128.08, 23.93 (CH_3) ppm. ATR-IR: 2072.1 (Ge-H) cm^{-1}. GCMS: Methode2: t_R = 18.33 min, m/z: 389.2 ($M^{+\cdot}$ -H), 284.1

($M^{+\cdot}$ - 2,6-xylylH), 269.1 ($M^{+\cdot}$ - 2,6-xylylH(CH_3)), 209.1 ($M^{+\cdot}$ - 2,6-xylylGeH), 178.0 ($M^{+\cdot}$ - 2,6-xylyl$_2$), 105.1 ($M^{+\cdot}$ - 2,6-xylyl$_2$GeH), 91.1 ($M^{+\cdot}$ - 2,6-xylyl$_2$GeH(CH_3)), 77.1 ($M^{+\cdot}$ - 2,6-xylyl$_2$GeH(CH_3)$_2$).

3,5-xylyl$_3$GeH (17): 0.33 g (8.64 mmol, 1.50 eq.) $LiAlH_4$ in 100 ml THF, 3.53 g (7.20 mmol, 1.00 eq.) 3,5-xylyl$_3$GeCl (11). The resulting colorless solid was recrystallized from toluene. Yield: 82%. M.p.: 124°C. Elemental analysis (%) for $C_{24}H_{28}Ge$: C, 74.08; H, 7.25. Found: C, 73.93; H, 7.09. ^{1}H NMR ($CDCl_3$, 300 MHz): δ 7.13 (s, 6H, 2,6-H, ArH), 7.00 (s, 3H, 4-H, ArH), 5.52 (s, 1H, Ge-H), 2.28 (s, 18H, CH_3) ppm. ^{13}C NMR ($CDCl_3$, 75.5 MHz): δ 137.78, 135.83, 132.98, 131.01, 21.55 (CH_3) ppm. ATR-IR: 2034.6 (Ge-H) cm^{-1}. GCMS: Methode2: t_R = 17.83 min, m/z: 389.2 ($M^{+\cdot}$ - H), 284.1 ($M^{+\cdot}$ - 3,5-xylylH), 269.1 ($M^{+\cdot}$ - 3,5-xylylH(CH_3)), 179.1 ($M^{+\cdot}$ - 3,5-xylyl$_2$), 105.1 ($M^{+\cdot}$ - 3,5-xylyl$_2$GeH), 91.1 ($M^{+\cdot}$ - 3,5-xylyl$_2$GeH(CH_3)), 77.1 ($M^{+\cdot}$ - 3,5-xylyl$_2$GeH(CH_3)$_2$).

1-naphthyl$_3$GeH (18): 1.00 g (26.4 mmol, 1.00 eq.) $LiAlH_4$ in 150 ml THF, 12.7 g (24.0 mmol, 1.00 eq.) 1-naphthyl$_3$GeX (9) in 70 ml THF The resulting colorless solid was washed several times with toluene and pentane and recrystallized from toluene. Yield: 81%. M.p.: 244°C. Elemental analysis (%) for $C_{30}H_{22}Ge$: C, 79.17; H, 4.87. Found: C, 79.50; H, 4.92. ^{1}H NMR ($CDCl_3$, 300 MHz): δ 7.99 (d, 3H, 8-H, ArH), 7.85 (d, 3H, 2-H, ArH), 7.83 (d, 3H, 4-H, ArH), 7.33 (m, 12H, 2,5,6,7-H, ArH), 6.84 (s, 1H, Ge-H) ppm. ^{13}C NMR ($CDCl_3$, 75.5 MHz): δ 137.34, 135.86, 133.79, 133.72, 130.19, 128.93, 128.76, 126.36, 125.89, 125.72 ppm. ATR-IR: 2062.9 (Ge-H) cm^{-1}. GCMS: Methode2: t_R = 26.92 min, m/z: 456.1 ($M^{+\cdot}$), 327.0 ($M^{+\cdot}$ - 1-naphthylH), 252.1 ($M^{+\cdot}$ - 2-naphthylGeH), 201.0 ($M^{+\cdot}$ - 1-naphthyl$_2$H), 128.0 ($M^{+\cdot}$ - 1-naphthyl$_2$GeH), 77.0 ($M^{+\cdot}$ - 1-naphthyl$_2$GeH(C_4H_4)).

3.6.1.4. Preparation of R_2GeHCl

General Procedure

A Schlenk was charged with triarylgermanium hydride and freshly distilled DCM. HOTf was added dropwise at 0°C and the reaction was allowed to warm to room temperature. After stirring for 24 hours, after which time the ^{19}F NMR spectrum of the solution exhibited a single resonance indicating complete consumption of HOTf and formation of the desired product, DCM was exchanged with DME and LiCl was added as a solid at 0°C and the reaction was stirred for an additional 24 hours. After removal of solvent, toluene was added the solution was purified *via* cannula. After removal of solvent, the resulting product was dried in *vacuo*.

2,5-xylyl$_2$GeHCl (19): 3.40 g (8.74 mmol, 1.00 eq.) 2,5-xylyl$_3$GeH (15) in 70 ml DCM, 1.31 g HOTf (8.74 mmol, 1.00 eq), stirred overnight at rt, solvent exchange with 50 ml DME, 0.37 g (8.74 mmol, 1.00 eq.) LiCl. A colorless solid was obtained and recrystallized in toluene. Yield: 85%. Mp: 61°C. Elemental analysis (%) for $C_{16}H_{19}GeCl$: C, 60.17; H, 6.00. Found: C, 58.52; H, 5.58. ^1H NMR ($CDCl_3$, 300 MHz): δ 7.38 (s, 2H, 6-H, ArH), 7.13 (dd, 4H, 3,4-H, ArH), 6.61 (s, 1H, Ge-H), 2.34 (s, 6H, *m*-CH_3), 2.31 (s, 6H, *o*-CH_3) ppm. ^{13}C NMR ($CDCl_3$, 75.5 MHz): δ 139.85, 135.57, 134.97, 131.78, 130.20, 21.95 (CH_3), 21.20 (CH_3) ppm. ATR-IR: 2090.0 (Ge-H) cm^{-1}. GCMS: Methode2: t_R = 14.99 min, m/z: 320.1 ($M^{+\cdot}$), 283.1 ($M^{+\cdot}$ - HCl), 269.0 ($M^{+\cdot}$ - HCl(CH_3)), 214.0 ($M^{+\cdot}$ - 2,5-xylylH), 178.0 ($M^{+\cdot}$ - 2,5-xylylHCl), 165.0 ($M^{+\cdot}$ - 2,5-xylylHCl(CH_3)), 106.0 ($M^{+\cdot}$ - 2,5-xylylGeHCl), 91.1 ($M^{+\cdot}$ - 2,5-xylylGeHCl(CH_3)), 77.1 ($M^{+\cdot}$ -2,5-xylylGeHCl(CH_3)$_2$).

2,6-xylyl$_2$GeHCl (20): 6.00 g (15.4 mmol, 1.00 eq.) 2,6-xylyl$_3$GeH (16) in 70 ml DCM, 2.77 g HOTf (18.5 mmol, 1.20 eq), stirred overnight at rt, solvent exchange with 50 ml DME, 0.98 g (23.1 mmol, 1.50 eq.) LiCl. An orange solid was obtained, washed several times and recrystallized in toluene yielding colorless crystals and an orange insoluble solid. Yield: 75% Mp: 82°C. Elemental analysis (%) for $C_{16}H_{19}GeCl$: C, 60.17; H, 6.00. Found: C, 58.52; H, 5.58. ^1H NMR ($CDCl_3$, 300 MHz):

δ 7.20 (t, 2H, 4-H, ArH), 7.02 (d, 4H, 3,5-H, ArH), 6.89 (s, 1H, Ge-H), 2.46 (s, 12H, CH_3) ppm. ^{13}C NMR ($CDCl_3$, 75.5 MHz): δ 143.35, 135.36, 130.50, 128.74, 23.37 (CH_3) ppm. ATR-IR: 2103.2 (Ge-H) cm^{-1}. GCMS: Methode2: t_R = 15.63 min, m/z: 320.1 ($M^{+\cdot}$), 283.1 ($M^{+\cdot}$ - HCl), 214.0 ($M^{+\cdot}$ - 2,6-xylylH), 178.0 ($M^{+\cdot}$ - 2,6-xylylHCl), 165.1 ($M^{+\cdot}$ - 2,6-xylylHCl(CH_3)), 106.1 ($M^{+\cdot}$ - 2,6-xylylGeHCl), 91.1 ($M^{+\cdot}$ - 2,6-xylylGeHCl(CH_3)), 77.1 ($M^{+\cdot}$ -2,6-xylylGeHCl(CH_3)$_2$).

1-naphthyl$_2$GeHCl (21): 3.05 g (6.70 mmol, 1.00 eq.) 1-naphthyl$_3$GeH (18) in 100 ml DCM, 2.01 g HOTf (13.4 mmol, 2.0 eq), stirred overnight at rt, solvent exchange with 50 ml DME, 0.71 g (16.8 mmol, 2.51 eq.) LiCl. A colorless solid was obtained and recrystallized in toluene. Yield: 82%. T_d: 225°C. Elemental analysis (%) for $C_{20}H_{15}GeCl$: C, 66.10; H, 4.16. Found: C, 64.12; H, 4.05. ^{1}H NMR ($CDCl_3$, 300 MHz): δ 8.06 (d, 2H, 8-H, ArH), 7.97 (d, 2H, 2-H, ArH), 7.90 (d, 2H, 4-H, ArH), 7.69 (d, 2H, 5-H, ArH), 7.49 (m, 6H, 3,6,7-H, ArH), 7.22 (s, 1H, Ge-H) ppm. ^{13}C NMR ($CDCl_3$, 75.5 MHz): δ 136.07, 134.53, 133.88, 132.64, 131.75, 129.26, 127.48, 127.11, 126.45, 125.69 ppm. ATR-IR: 2104.6 (Ge-H) cm^{-1}. GCMS: Methode2: t_R = 20.17 min, m/z: 364.0 ($M^{+\cdot}$), 327.0 ($M^{+\cdot}$ - HCl), 252.1 ($M^{+\cdot}$ - GeHCl), 235.9 ($M^{+\cdot}$ - 1-naphthylH), 201.0 ($M^{+\cdot}$ - 1-naphthylHCl), 128.0 ($M^{+\cdot}$ - 1-naphthylGeHCl), 77.0 ($M^{+\cdot}$ -1-naphthylGeHCl(C_4H_4)).

3.6.1.5. Preparation of R_2GeH_2

Route A: A Schlenk was charged with R_3GeH and freshly distilled DCM. HOTf was added dropwise at 0°C and the reaction was allowed to warm to room temperature. After stirring for 24-48 hours, after which time the ^{19}F NMR spectrum of the solution exhibited a single resonance indicating complete consumption of HOTf and formation of the desired product, a suspension of LiCl in DME was added at 0°C and the reaction was stirred for an additional 24 hours. Toluene was added and DCM and DME were evaporated under reduced pressure. After filtration *via*

cannula, $LiAlH_4$ was added as a solid in small portions at 0°C. After stirring for 3 hours at room temperature, the reaction was quenched with 3% degassed H_2SO_4. After extraction with a saturated degassed sodium tartrate solution, the solution was filtered *via* cannula and dried over Na_2SO_4. After filtration and washing twice with toluene, all solvents were removed under *vacuo*.

2,5-xylyl$_2$GeH$_2$ (22): 5.03 g (12.9 mmol, 1.00 eq.) 2,5-xylyl$_3$GeH (15) in 70 ml DCM, 2.13 g HOTf (14.2 mmol, 1.10 eq), 0.66 g (15.5 mmol, 1.20 eq.) LiCl in 30 ml DME, 0.59 g $LiALH_4$ (15.5 mmol, 1.20 eq.) as a solid. The resulting colorless solid was recrystallized from toluene. Yield: 69%. M.p.: 61°C. Elemental analysis (%) for $C_{16}H_{20}Ge$: C, 67.44; H, 7.07. Found: C, 67.52; H, 6.91. ^{1}H NMR ($CDCl_3$, 300 MHz): δ 7.21 (s, 2H, 6-H, ArH), 7.08 (s, 4H, 3,4-H, ArH), 5.03 (s, 2H, Ge-H), 2.31 (s, 6H, *m*-CH_3), 2.26 (s, 6H, *o*-CH_3) ppm. ^{13}C NMR ($CDCl_3$, 75.5 MHz): δ 140.60, 136.91, 134.96, 133.85, 130.40, 129.53, 22.48 (CH_3), 20.90 (CH_3) ppm. ATR-IR: 2055.2 (Ge-H) cm^{-1}. GCMS: Methode2: t_R = 13.53 min, m/z: 286.1 ($M^{+\cdot}$), 180.0 ($M^{+\cdot}$ - 2,5-xylylH_2), 165.0 ($M^{+\cdot}$ - 2,5-xylyl$H_2(CH_3)$), 151.0 ($M^{+\cdot}$ - 2,5-xylyl$H_2(CH_3)_2$), 105.1 ($M^{+\cdot}$ - 2,5-xylylGeH_2), 91.1 ($M^{+\cdot}$ - 2,5-xylyl$GeH_2(CH_3)$), 77.1 ($M^{+\cdot}$ -2,5-xylyl$GeH_2(CH_3)_2$).

2,6-xylyl$_2$GeH$_2$ (23): 4.00 g (10.3 mmol, 1.00 eq.) 2,6-xylyl$_3$GeH (16) in 100 ml DCM, 2.01 g HOTf (13.4 mmol, 1.20 eq.), 0.71 g (16.8 mmol, 1.50 eq.) LiCl in 30 ml DME, 0.44 g $LiAlH_4$ (11.5 mmol, 1.20 eq.) as a solid. The resulting colorless solid was recrystallized from toluene. Yield: 82%. M.p.: 50.7°C. Elemental analysis (%) for $C_{16}H_{20}Ge$: C, 74.08; H, 7.25. Found: C, 72.48; H, 6.99. ^{1}H NMR ($CDCl_3$, 300 MHz): δ 7.13 (t, 2H, 4-H, ArH), 6.99 (d, 4H, 3,5-H, ArH), 5.13 (s, 2H, Ge-H), 2.36 (s, 12H, CH_3) ppm. ^{13}C NMR ($CDCl_3$, 75.5 MHz): δ 143.85, 134.90, 129.04, 127.62, 24.00 (CH_3) ppm. ATR-IR: 2056.2 (Ge-H) cm^{-1}. GCMS: Methode2: t_R = 14.18 min, m/z: 286.1 ($M^{+\cdot}$), 180.0 ($M^{+\cdot}$ - 2,6-xylylH_2), 165.0 ($M^{+\cdot}$ - 2,6-xylyl$H_2(CH_3)$), 151.0 ($M^{+\cdot}$ - 2,6-xylyl$H_2(CH_3)_2$), 105.1 ($M^{+\cdot}$ - 2,6-xylylGeH_2), 91.1 ($M^{+\cdot}$ - 2,6-xylyl$GeH_2(CH_3)$), 77.1 ($M^{+\cdot}$ -2,6-xylyl$GeH_2(CH_3)_2$).

Route B: A Schlenk was charged with R_3GeH and freshly distilled DCM. HOTf was added dropwise at -30°C. After stirring for 24 hours at -30°C, the ^{19}F NMR spectrum of the solution exhibited a single resonance indicating complete consumption of HOTf and formation of the desired product, a suspension of LiCl in DME was added at -30°C and the reaction was stirred for an additional 24 hours. Toluene was added and DCM and DME were evaporated under reduced pressure. $LiAlH_4$ was added as a solid in small portions at -30°C. After stirring for 3 hours, the reaction was quenched with 3% degassed H_2SO_4. After extraction with a saturated degassed sodium tartrate solution, the solution was filtered *via* cannula and dried over Na_2SO_4. After filtration and washing twice with toluene, all solvents were removed under *vacuo*.

1-naphthyl$_2$GeH$_2$ (24): 2.11 g (4.60 mmol, 1.00 eq.) 1-naphthyl$_3$GeH (18) in 70 ml DCM, 0.83 g HOTf (5.60 mmol, 1.20 eq.), stirred overnight at -30°C, 0.29 g (6.90 mmol, 1.50 eq.) LiCl in 20 ml DME, 0.26 g $LiAlH_4$ (6.90 mmol, 1.50 eq.) as a solid. The resulting colorless solid was recrystallized from toluene. Yield: 24%. M.p.: 94.3°C. Elemental analysis (%) for $C_{20}H_{16}Ge$: C, 73.02; H, 4.90. Found: C, 74.21; H, 4.92. ^1H NMR ($CDCl_3$, 300 MHz): δ 8.00 (m, 2H, 8-H, ArH), 7.89 (dd, 4H, 2,4-H, ArH), 7.67 (d, 2H, 5-H, ArH), 7.43 (m, 6H, 3,6,7-H, ArH), 5.64 (s, 2H, Ge-H) ppm. ^{13}C NMR ($CDCl_3$, 75.5 MHz): δ 137.14, 135.56, 133.47, 132.90, 130.04, 128.84, 128.30, 126.36, 125.85, 125.56 ppm. ATR-IR: 2049.5 (Ge-H) cm^{-1}. GCMS: Methode2: t_R = 18.99 min, m/z: 330.1 ($M^{+\cdot}$), 252.1 ($M^{+\cdot}$ - GeH_2), 201.0 ($M^{+\cdot}$ - 1-naphthylH_2), 128.0 ($M^{+\cdot}$ - 1-naphthylGeH_2).

3.6.1.6. Preparation of $RGeH_3$

General Procedure

A Schlenk was charged with R_2GeH_2 and freshly distilled DCM. HOTf was added dropwise at 0°C and the reaction was allowed to warm to room temperature.

After stirring for 24-48 hours, after which time the ^{19}F NMR spectrum of the solution exhibited a single resonance indicating complete consumption of HOTf and formation of the desired product, a suspension of LiCl in DME was added at 0°C and the reaction was stirred for an additional 24 hours. Toluene was added and DCM and DME were evaporated under reduced pressure. After filtration *via* cannula, $LiIAlH_4$ was added as a solid in small portions at 0°C. After stirring for 3 hours at room temperature, the reaction was quenched with 3% degassed H_2SO_4. The solution was filtered *via* cannula and dried over Na_2SO_4. After filtration, all solvents were removed carefully under *vacuo*. In some cases, the product was further purified *via* condensation.

2,5-xylylGeH$_3$ (25): 1.00 g (3.50 mmol, 1.00 eq.) 2,5-xylyl$_2$GeH$_2$ (22) in 35 ml DCM, 0.53 g HOTf (3.50 mmol, 1.05 eq.), 0.15 g (3.50 mmol, 1.00 eq.) LiCl in 20 ml DME, 0.13 g $LiAlH_4$ (3.50 mmol, 1.10 eq.) as a solid. Yield: 21%. ^1H NMR ($CDCl_3$, 300 MHz): δ 7.02 (m, 3H, ArH), 4.14 (s, 3H, Ge-H), 2.28 (s, 3H, CH_3), 2.22 (s, 3H, CH_3) ppm. ^{13}C NMR ($CDCl_3$, 75.5 MHz): δ 144.07, 131.48, 129.20, 127.28, 24.44 (CH_3) ppm. GCMS: Methode2: t_R = 7.483 min, m/z: 180.0 ($M^{+\cdot}$), 165.0 ($M^{+\cdot}$ - CH_3), 151.0 ($M^{+\cdot}$ - $(CH_3)_2$), 105.1 ($M^{+\cdot}$ -GeH_3), 91.1 ($M^{+\cdot}$ - $GeH_3(CH_3)$), 77.1 ($M^{+\cdot}$ - $(GeH_3(CH_3)_2)$

2,6-xylylGeH$_3$ (26): 2.00 g (7.01 mmol, 1.00 eq.) 2,6-xylyl$_2$GeH$_2$ (23) in 35 ml DCM, 1.11 g HOTf (7.37 mmol, 1.05 eq.), 0.71 g (7.72 mmol, 1.10 eq.) LiCl in 20 ml DME, 0.29 g $LiAlH_4$ (7.72 mmol, 1.10 eq.) as a solid. Yield: 24%. ^1H NMR ($CDCl_3$, 300 MHz): δ 7.11 (t, 1H, 4-H, ArH), 6.98 (d, 2H, 3,5-H, ArH), 4.12 (s, 3H, Ge-H), 2.37 (s, 6H, CH_3) ppm. ^{13}C NMR ($CDCl_3$, 75.5 MHz): δ 144.07, 131.48, 129.20, 127.28, 24.44 (CH_3) ppm. GCMS: Methode2: t_R = 7.483 min, m/z: 180.0 ($M^{+\cdot}$), 164.9 ($M^{+\cdot}$ -CH_3), 150.9 ($M^{+\cdot}$ - $(CH_3)_2$), 105.1 ($M^{+\cdot}$ -GeH_3), 91.0 ($M^{+\cdot}$ - $GeH_3(CH_3)$), 77.0 ($M^{+\cdot}$ - $GeH_3(CH_3)_2$)

3.6.1.7. Various germanium compounds

[2,6-xylyl$_2$Ge]$_2$O (27): A Schlenk was charged with 3.50 g (8.99 mmol, 1.00 eq.) 2,6-xylyl$_3$GeH (16) and freshly distilled DCM. 1.41 g HOTf (9.44 mmol, 1.05 eq.) was added dropwise at -5°C. After stirring for 24 hours at -30°C, the ^{19}F NMR spectrum of the solution exhibited a single resonance indicating complete consumption of HOTf and formation of the desired product, toluene was added and DCM and DME were evaporated under reduced pressure. 0.41 g $LiAlH_4$ (10.8 mmol, 1.20 eq.) was added as a solid in small portions at 0°C. After stirring for 3 hours, the reaction was quenched with 3% degassed H_2SO_4. After extraction with a saturated degassed sodium tartrate solution, the solution was filtered *via* cannula and dried over Na_2SO_4. After filtration and washing twice with toluene, all solvents were removed under *vacuo*. The resulting colorless solid was recrystallized from toluene. Yield: 46%. M.p.: 134 °C. Elemental analysis (%) for $C_{32}H_{38}Ge_2O$: C, 65.82; H, 6.56. Found: C, 64.82; H, 6.30. ^{1}H NMR ($CDCl_3$, 300 MHz): δ 7.10 (t, 4H, ArH), 6.88 (d, 8H, ArH), 6.64 (s, 2H, Ge-H), 2.28 (s, 24H, CH_3) ppm. ^{13}C NMR ($CDCl_3$, 75.5 MHz): δ 143.73, 129.51, 128.03, 22.63 (CH_3) ppm. ATR-IR: 2058.4 (Ge-H) cm^{-1}. GCMS: Methode2: t_R = 24.86 min, m/z: 584.3 ($M^{+\cdot}$), 569.3 ($M^{+\cdot}$ - GeH_2), 478.2 ($M^{+\cdot}$ - 2,6-xylylH_2), 373.1 ($M^{+\cdot}$ - 2,6-xylyl$_2H_2$)), 300.1 ($M^{+\cdot}$ - 2,6-xylyl$_2$GeH_2), 283.1 ($M^{+\cdot}$ - 2,6-xylyl$_2$GeOH_2), 179.0 ($M^{+\cdot}$ - 2,6-xylyl$_3$GeOH_2), 165.0 ($M^{+\cdot}$ - 2,6-xylyl$_3$Ge$OH_2(CH_3)$), 151.0 ($M^{+\cdot}$ - 2,6-xylyl$_3$Ge$OH_2(CH_3)_2$), 105.1 ($M^{+\cdot}$ - 2,6-xylyl$_3$Ge$_2OH_2$), 91.0 ($M^{+\cdot}$ - 2,6-xylyl$_3$Ge$_2OH_2(CH_3)$), 77.1 ($M^{+\cdot}$ - 2,6-xylyl$_3$Ge$_2OH_2(CH_3)_2$).

K$_2$[(C$_4$H$_6$O$_2$)$_3$Ge] (28): 2.09 g (20.0 mmol, 1.00 eq.) GeO_2 were suspended in previously degassed MeOH and added slowly *via* syringe to a solution of 2.80 g MeOK (40.0 mmol, 2.00 eq.) in MeOH. A solution of 5.40 ml 2,3-butanediole (60.0 mmol, 3.00 eq.) in MeOH were added slowly after 15 minutes and the cloudy solution was stirred for 1.5 hours. After removal of solvent and washing with Et_2O, an off-white powder was obtained. Yield: 90%. ^{1}H NMR (CD_3OD, 25°C, 300MHz): δ 3.54 (m, 2H), 1.13 (d, 6H) ppm.

$K_2[(C_6H_4O_2)_3Ge]$ (29): To a solution of 2.44 g (5.96 mmol, 1.00 eq.) $K_2((C_4H_6O_2)_3Ge)$ (28) in previously degassed MeOH, 1.97 g $C_6H_6O_2$ (17.9 mmol, 3.00 eq.) in MeOH was added dropwise. The cloudy, slightly pink solution was heated and kept at reflux for 2 hours. After removal of solvent and washing with Et_2O, the desired product was obtained. Yield: 92%. ^{1}H NMR (CD_3OD, 25°C, 300MHz): δ 6.54-6.32 (m, 4H) ppm.

^{i}propyl$_3$GeCl (30): To a solution of ^{i}propylLi (15.8 g, 17.5 mmol, 2.25 eq.) in hexane, 1.80 g $Ge(OEt)_4$ (8.80 mmol,1.00 eq.) was added dropwise, yielding an orange, polymeric liquid. After stirring at room temperature for 2 hours, 2M ethereal HCl was added dropwise until no white precipitate precipitated anymore. The solution was filtered over Celite®, washed with hexane and the solvent was removed under reduced pressure, yielding an orange, oily liquid. Yield: 64.5%. ^{1}H NMR (C_6D_6, 25°C, 400MHz): δ 1.41 (m, 1H); 1.10 (d, 18H) ppm. ^{13}C NMR (C_6D_6, 25°C, 125.7MHz): δ 19.21 (CH_3), 17.67 (CH) ppm.

^{i}propyl$_3$GeN(CH$_3$)$_2$ (31): 0.16 g (3.25 mmol, 2.50 eq.) $LiN(CH_3)_2$ were added dropwise to a solution of 0.30 g (1.30 mmol, 1.00 eq.) ^{i}propyl$_3$GeCl (30) dissolved in benzene, yielding a cloudy, orange liquid. After stirring at room temperature overnight, the liquid was filtered over Celite®, washed with hexane and the solvent was removed, yielding ^{i}Pr$_3$GeN(CH$_3$)$_2$. Yield: 48%. ^{1}H NMR (C_6D_6, 25°C, 400MHz): δ 2.65 (s, 6H), 1.41 (m, 3H), 1.10 (d, 18H) ppm. ^{13}C NMR (C_6D_6, 25°C, 125.7MHz): δ 42.14 ($N(CH_3)_2$), 19.58, 15.6 ppm.

(^{i}propyl)$_3$GeGe(phenyl)$_3$ (32): 0.10 g (0.41 mmol, 1.00 eq.) ^{i}propyl$_3$GeN(CH$_3$)$_2$ (31) and 0.13 g (0.43 mmol, 1.00 eq.) phenyl$_3$GeH were added to a Schlenk tube and dissolved in acetonitrile. The Schlenk tube was closed and put into an oil bath for 48 hours at 90°C. After removal of solvent, the solid was distillated under vacuum, yielding the desired compound. Yield: 75%. ^{1}H NMR (C_6D_6, 25°C, 400MHz): δ 7.72–7.68 (m, 6H, ArH), 7.20–7.15 (m, 9H, ArH), 1.67 (m, 3H), 1.18 (d, 18H) ppm.

^{13}C NMR (C_6D_6, 25°C, 125.7MHz): δ 139.8, 135.9, 128.6, 128.5, 21.3 (CH_3), 16.8 (CH) ppm.

phenyl$_2$GeH$_2$ (33): 10.0 g (33.6 mmol, 1.00 eq.) phenyl$_2$GeCl$_2$ were dissolved in Et_2O and 3.19 g $LiAlH_4$ (84.0 mmol, 2.50 eq.) was added in small portions as a solid. The mixture was stirred at room temperature for 2 hours, quenched dropwise with H_2O and filtered over Celite®. After drying over $MgSO_4$, filtration and removal of solvent a colorless liquid was obtained. Yield: 73%. ^{1}H NMR (C_6D_6, 25°C, 400MHz): δ 7.48–7.15 (m, 20 H, ArH), 5.20 (s, 2H, Ge-H) ppm. ^{13}C NMR (C_6D_6, 25°C, 125.7MHz): δ 135.49, 134.20, 129.30, 128.66 ppm.

H(phenyl$_2$Ge)$_3$H (34): A solution of 2.50 g (11.0 mmol, 1.00 eq.) of phenyl$_2$GeH$_2$ (33) in 8 ml Et_3N was cooled to -40°C. 7.68 ml (13.0 mmol, 1.20 eq.) ^{t}BuLi (1.7 M in hexane) was added dropwise. After 15 minutes of stirring at -40°C, the yellow solution was allowed to warm to room temperature and stirred for additional 9.5 hours. After quenching with H_2O and drying over $MgSO_4$, the solution was filtered over Celite®, washed with hexane and the solvent was removed under reduced pressure, yielding a colorless oil. Yield: 27%. ^{1}H NMR (C_6D_6, 25°C, 400MHz): δ 7.59 (m, 4H, ArH), 7.44 (m, 8H, ArH), 7.03 (m, 18H, ArH), 5.68 (s, 2H, Ge-H) ppm. ^{13}C NMR (C_6D_6, 25°C, 125.7MHz): δ 136.20, 135.99, 135.77, 135.75, 129.09, 129.05, 128.76, 128.64 ppm.

(phenyl$_2$Ge)$_4$ (35): 9.34 g (31.4 mmol, 1.00 eq.) phenyl$_2$GeCl$_2$ were dissolved in 20 ml toluene and added slowly over 35 minutes to a boiling suspension of 2.35 g (102 mmol, 3.30 eq.) of Na pieces in toluene. The reaction was kept at reflux for 1 hour, and filtered of over Celite®. The product was allowed to crystallize out at room temperature. The yellow liquid was decanted *via* cannula and the colorless crystals were dried under *vacuo* and recrystallized from toluene at 4°C. Yield: 21%. ^{1}H NMR ($CDCl_3$, 25°C, 400MHz): δ 7.28 – 7.10 (m, 40 H, ArH) ppm. ^{13}C NMR

($CDCl_3$, 25°C, 125.7MHz): δ 136.11, 135.57, 132.23, 131.32, 128.54, 127.80, 127.52, 127.31 ppm.

Br-(phenyl$_2$Ge)$_4$-Br (36): Br_2 was dissolved in benzene and slowly added to a solution of (phenyl$_2$Ge)$_4$ (35) (0.62 g, 0.68 mmol, 1.00 eq.) in 20 ml benzene until the orange color was persistent. After removal of solvent, a colorless precipitate was obtained. Yield: 75%. ^{1}H NMR (C_6D_6, 25°C, 400MHz): δ 7.60 (d, 8 H, ArH), 7.41 (d, 8H, ArH), 7.06-6.90 (m, 24H, ArH) ppm.^{13}C NMR (C_6D_6, 25°C, 125.7MHz): δ 136.82, 134.77, 129.98, 129.45, 128.79, 128.67, 128.1, 127.9 ppm.

H-(phenyl$_2$Ge)$_4$-H (37): A solution of 0.54 g (0.51 mmol, 1.00 eq.) Br-(phenyl$_2$Ge)$_4$-Br (36) was treated with 0.04 g (1.10 mmol, 2.20 eq.) $LiAlH_4$ in Et_2O. The mixture was stirred at room temperature overnight. After removal of solvent, the product was obtained as a colorless solid. Yield: 79%. ^{1}H NMR (C_6D_6, 25°C, 400MHz): δ 7.50 (d, 8 H, ArH), 7.37 (d, 8H, ArH), 7.05-6.96 (m, 24H, ArH), 5.62 (s, 2H, Ge-H) ppm. ^{13}C NMR (C_6D_6, 25°C, 125.7MHz): δ 136.5, 136.0, 128.9, 128.8, 128.5, 128.67, 128.1, 127.7 ppm.

phenyl$_3$GeN(CH$_3$)$_2$ (38): 0.36 g (7.00 mmol, 1.20 eq.) $LiN(CH_3)_2$ were added dropwise to a solution of 2.00 g (5.90 mmol, 1.00 eq.) phenyl$_3$GeCl dissolved in benzene, yielding a cloudy, orange liquid. After stirring at room temperature overnight, the liquid was filtered over Celite®, washed with hexane and the solvent was removed, yielding phenyl$_3$GeN(CH$_3$)$_2$. Yield: 49%. ^{1}H NMR (C_6D_6, 25°C, 400MHz): δ 7.65 (t, 18H, ArH), 7.24 (d, 18H, ArH), 6.93 (t, 9H, ArH), 2.71 (s, 6H,-N(CH$_3$)$_2$) ppm. ^{13}C NMR (C_6D_6, 25°C, 125.7MHz): δ 138.3, 135.5, 129.7, 127.7 ppm

HGe(phenyl$_3$Ge)$_3$ (39): 0.04 g (0.49 mmol, 1.00 eq.) of GeH_4 was condensed using an U-shaped device in liquid nitrogen and then added to 0.51 g (1.47 mmol, 3.00 eq.) phenyl$_3$GeN(CH$_3$)$_2$ (38) dissolved in acetonitrile. The Schlenk was sealed, al-

lowed to warm to room temperature, stirred overnight at room temperature and stirred another 72 hours at 90°C. After removal of solvent, the desired product was obtained, which was recrystallized under superheated conditions. Yield: 41%. ^{1}H NMR (C_6D_6, 25°C, 400MHz): δ 7.26 (d, 18H, ArH), 7.15–6.92 (m, 27H, ArH), 5.85 (s, 1H, Ge-H) ppm. ^{13}C NMR (C_6D_6, 25°C, 125.7MHz): δ 136.5, 128.8, 128.6, 127.5 ppm

Dehydrogenative coupling reactions of 2,5-xylyl$_2$GeH$_2$ by employment of TMEDA

0.06 ml freshly distilled TMEDA (0.40 mmol, 1 eq.) in 1 ml Et_2O was added dropwise to a solution of 0.11 g 2,5-xylyl$_2$GeH$_2$ (0.40 mmol, 1 eq.) in 1.5 ml Et_2O at room temperature and was stirred for 52 hours. Dry toluene was added, THF was removed under reduced pressure and the reaction was heated to 90°C using an oil bath. After stirring for 48 hours, all solvents were removed. A colorless solid was obtained and further characterized *via* elemental analysis. Elemental analysis (%): Found: C, 66.75; H, 7.24.

Dehydrogenative coupling reactions of 2,6-xylylGeH$_3$ by employment of TMEDA

Freshly distilled TMEDA (3 drops) in 1 ml Et_2O was added to a solution of 1 drop of 2,6-xylylGeH$_3$ in 2 ml Et_2O at room temperature and was stirred for four days. After removal of liquids under reduced pressure. A colorless solid was obtained and further characterized *via* elemental analysis. Elemental analysis (%): Found: C, 40.55; H, 8.70.

3.6.2. Antimony compounds

General procedure for compounds (40)-(44)

A flask equipped with a dropping funnel and a reflux condenser was charged with Mg in THF or Et_2O. The dropping funnel was charged with arylbromide in THF or Et_2O, about 10% of the solution was added to the reaction vessel and the solu-

tion was heated carefully or dibromoethane was added to start the reaction. The arylbromide was subsequently added dropwise. After complete addition, the reaction was refluxed for 3-12 hours. Residual Mg was filtered off *via* filter cannula and was added to a solution of $SbCl_3$ in THF cooled to 0°C. The solution was stirred overnight at room temperature. After removal of THF, toluene was added and the liquid was filtered *via* cannula. Toluene was removed under reduced pressure and the product was recrystallized.

2,6-xylyl$_3$Sb (40): 4.01 g (165 mmol, 3.30 eq.) Mg in 50 ml THF, 27.8 g (150 mmol, 3.00 eq.) 1-bromo-2,6-dimethylbenzene in ml THF, 10.0 g (50.0 mmol, 1.00 eq.) $SbCl_3$ in 50 ml THF at 0°C. The resulting solid was recrystallized from toluene at -30°C to obtain light yellow crystals. Yield: 45%. M.p.: 121°C. Elemental analysis (%) for $C_{24}H_{27}Sb$: C, 65.93; H, 6.22. Found: C, 64.88; H, 6.18. ^{1}H NMR ($CDCl_3$, 300 MHz): δ 7.21 (t, 3H, ArH), 7.13 (d, 6H, ArH), 2.47 (s, 18H, CH_3) ^{13}C NMR ($CDCl_3$, 75.5 MHz): δ 128.47, 128.20, 127.83, 25.22 (CH_3) ppm. GCMS: Methode1 t_R = 19.49 min, m/z: 436.2 ($M^{+\cdot}$), 331.1 ($M^{+\cdot}$ -2,6-xylyl), 224.9 ($M^{+\cdot}$ - 2,6-xylyl$_2$), 209.1 ($M^{+\cdot}$ - 2,6-xylyl$_2$(CH_3)), 193.1 ($M^{+\cdot}$ -2,6-xylyl$_2$(CH_3)$_2$).

1-naphthyl$_3$Sb (41): 2.00 g (82.3 mmol, 4.20 eq.) Mg in 100 ml THF, 15.5 g (74.9 mmol, 3.80 eq.) 1-bromonaphthalene in 50 ml THF, 4.50 g (19.7 mmol, 1.00 eq.) $SbCl_3$ in 60 ml THF at 0°C. The resulting solid was recrystallized from benzene at - 30°C to obtain colorless crystals. Yield: 65 %. M.p.: 222°C. Elemental analysis (%) for $C_{30}H_{21}Sb$: C, 71.60; H, 4.21. Found: C, 74.06; H, 4.43. ^{1}H NMR ($CDCl_3$, 300 MHz): δ 8.12 (d, 3H, ArH), 7.79 and 7.73 (d, 6H, ArH), 7.36 (m, 6H, ArH), 7.13 (d, 3H, ArH), 7.10 (d, 3H, ArH) ppm. ^{13}C NMR ($CDCl_3$, 75.5 MHz): δ 138.23, 136.75, 136.48, 134.09, 129.63, 129.55, 129.14, 126.68, 126.53, 126.08 ppm. GCMS: Methode1: t_R = 38.36 min, m/z: 502.1 ($M^{+\cdot}$), 374.0 ($M^{+\cdot}$ -1-naphthyl), 253.1 ($M^{+\cdot}$ - 1-naphthylSb), 248.0 ($M^{+\cdot}$ - 1-naphthyl$_2$), 127.0 ($M^{+\cdot}$ - 1-naphthyl$_2$Sb), 77.1 ($M^{+\cdot}$ - 1-naphthyl$_2$Sb(C_4H_4)).

2,6-xylyl$_2$SbBr (42): 1.04 g (42.8 mmol, 1.34 eq.) Mg in 100 ml THF, 7.00 g (37.8 mmol, 1.20 eq.) 1-bromo-2,6-dimethylbenzene in 30 ml THF, 7.18 g (31.5 mmol, 1.00 eq.) $SbCl_3$ in 100 ml THF at 0°C. The resulting solid was recrystallized from toluene at -30°C to obtain light yellow crystals. Yield: 55 %.

Alternative: A solution of 0.37 g $SbCl_3$ (1.60 mmol, 1.00 eq.) in dry Et_2O was added dropwise to a stirred solution of 1.40 g 2,6-xylyl$_3$Sb (40) (3.20 mmol, 1.00 eq.) in Et_2O. The solution was refluxed for 4 hours and stirred at room temperature overnight. After removal of solvent, colorless crystals were obtained upon recrystallization from toluene at -30°C. M.p.: 82°C. Elemental analysis (%) for $C_{16}H_{18}SbBr$: C, 46.65; H, 4.40. Found: C, 49.70; H, 4.52. ^{1}H NMR ($CDCl_3$, 300 MHz): δ 7.15 (t, 2H, ArH), 7.02 (d, 4H, ArH), 2.43 (s, 12H, CH_3) ppm ^{13}C NMR ($CDCl_3$, 75.5 MHz): δ 144.59, 143.98, 143.89, 142.29, 129.93, 128.89, 25.22 (CH_3), 24.60 (CH_3) ppm. GCMS: Methode1 t_R = 14. min, m/z: 412.0 ($M^{+\cdot}$), 330.0 ($M^{+\cdot}$ -Br), 305.9 ($M^{+\cdot}$ -2,6-xylyl), 225.0 ($M^{+\cdot}$ -2,6-xylylBr), 105.1 ($M^{+\cdot}$ -2,6-xylylSbBr), 77.1 ($M^{+\cdot}$ -2,6-xylylSbBr(CH_3)$_2$)

9-anthracenyl$_2$SbBr (43): 0.85 g (35.0 mmol, 4.10 eq.) Mg in 80 ml THF, 8.17 g (31.8 mmol, 3.70 eq.) 9-bromoanthracene in 30 ml THF, 1.94 g (8.50 mmol, 1.00 eq.) $SbCl_3$ in 40 ml THF at 0°C. The resulting solid was recrystallized from toluene and pentane at -30°C to obtain yellow crystals. Yield: 45%. M.p.: 222°C. Elemental analysis (%) for $C_{28}H_{18}SbBr$: C, 60.47; H, 3.26. Found: C, 64.37; H, 3.53. ^{1}H NMR ($CDCl_3$, 300 MHz): δ 8.53 (s, 2H), 8.40 (d, 4H), 8.00 (d, 4H), 7.35 (t, 4H), 7.16 (t, 4H) ppm. ^{13}C NMR ($CDCl_3$, 75.5 MHz): δ 132.25, 131.89, 131.24, 130.67, 129.53, 128.66, 128.22, 127.70, 127.26, 127.17, 125.85, 125.71, 125.36, 125.21 ppm.

[9-anthracenyl$_2$Sb]$_2$ (44): 0.61 g (25.0 mmol, 4.10 eq.) Mg in 60 ml THF, 5.79 g (22.5 mmol, 3.70 eq.) 9-bromoanthracene in 20 ml THF, 2.20 g (6.09 mmol, 1.00 eq.) $SbBr_3$ in 40 ml THF at 0°C. The resulting solid was recrystallized from toluene and pentane at -30°C to obtain orange crystals. Yield: 33%. M.p.: 231 °C. Ele-

mental analysis (%) for $C_{56}H_{36}Sb_2$: C, 70.62; H, 3.81. Found: C 69.45; H, 3.81. ^{1}H NMR ($CDCl_3$, 300 MHz): δ 8.40 (d, 8H, ArH), 7.92 (s, 4H, ArH), 7.65 (d, 8H, ArH), 7.15 (t, 8H, ArH), 6.84 (t, 8H, ArH) ppm. ^{13}C NMR ($CDCl_3$, 75.5 MHz): δ 138.65, 136.65, 131.21, 130.35, 129.49, 129.38, 128.52, 128.11, 126.12, 125.56, 125.32, 125.25, 124.85, 124.53 ppm.

***o*-tolylSbCl$_2$ (45)**: A solution of 9.12 g $SbCl_3$ (40.0 mmol, 2.00 eq.) in dry Et_2O was added dropwise to a stirred solution of 7.90 g *o*-tolyl$_3$Sb (20.0 mmol, 1.00 eq.) in Et_2O. The solution was refluxed for 4 hours and stirred at room temperature overnight. After removal of solvent, colorless crystals were obtained upon re-crystallization from a mixture of toluene and heptane. Yield: 58%. Mp: 105°C. Elemental analysis (%) for $C_7H_7SbCl_2$: C, 29.78; H, 2.43. Found: C, 29.78; H, 2.43. ^{1}H NMR ($CDCl_3$, 300 MHz): δ 8.11 (d, 1H, ArH), 7.42 (m, 2H, ArH), 7.26 (d, 1H, ArH), 2.63 (s, 3H, CH_3) ^{13}C NMR ($CDCl_3$, 75.5 MHz): δ 150.16, 141.88, 133.28, 131.99, 131.05, 127.89 22.32 (CH_3) ppm. GCMS: Methode1: t_R = 14.87 min, m/z: 283.9 ($M^{+\cdot}$), 247.9 ($M^{+\cdot}$ -Cl), 213.0 ($M^{+\cdot}$ -Cl_2), 192.9 ($M^{+\cdot}$ - *o*-tolyl), 157.9 ($M^{+\cdot}$ -*o*-tolylCl), 91.1 ($M^{+\cdot}$ -$SbCl_2$).

[9-anthracenyl$_2$^{n}butylSb][9-anthracenyl^{n}butyl$_2$SbCl$_2$] (46): 1.69 g 9-bromoanthracene (6.57 mmol, 3.70 eq.) were dissolved in 50 mL THF and cooled to -78 °C. Subsequently, 2.82 ml of ^{n}BuLi (7.05 mmol, 4.20 eq., 2.5 M in hexane) was added resulting in a dark orange reaction mixture which was stirred for 1h at -78°C and was then allowed to warm to 0°C. Afterwards, a solution of 0.40 g $SbCl_3$ (1.76 mmol, 1.00 eq.) and 20 mL THF cooled to 0 °C was added dropwise. The reaction mixture was stirred at room temperature for 48 hours to give an orange solution. THF was removed under *vacuo* and the resulting solid was taken up in 20 mL toluene, filtered and the solvent was removed. Recrystallization from toluene at 0°C gave red-orange crystals. Yield: 21%

Chapter 4

Summary and outlook

In this work, a series of organoantimony and organogermanium compounds have been prepared and characterized to gather new information on this challenging topic.

Tetraarylgermanes, triarylgermanium halides, triarylgermanium hydrides, diarylgermanium hydrochlorides, diarylgermanium dihydrides and arylgermanium trihydrides were prepared and fully characterized. Aryl ligands with different steric demand were applied, showing *ortho*, *meta* or *para* substitution on the phenyl ring, as is the case for *o*-tolyl, *m*-tolyl, 2,4-xylyl, 2,5-xylyl, 2,6-xylyl, 3,4-xylyl and 3,5-xylyl or even larger polyaromatic systems such as 1-naphthyl, 2-naphthyl and 2,4,6-mesityl.

The synthesis of tetraarylgermanes and triarylgermanium halides could be achieved by preparation of the corresponding Grignard and subsequent reaction with a germanium tetrahalide. It could be shown, that excess of Grignard reagent towards GeX_4 (X = Cl, Br) leads exclusively to either the tetraarylgermanium compound or the triarylgermanium halide mixture, depending on the ligand and its steric bulk, which was confirmed by DFT compulsory approximations and supports previously made observations by direct means. All solids were analyzed using X-ray crystallography and revealed the presence of electrostatic non-covalent intermolecular interactions motifs, which might be stabilizing factors in solid state. These stacking interactions include $CH_3\cdots\pi$ and edge to face interactions. In the case of halide compounds additional interactions between the aryl substituents and the halides were observed through van der Waals type interactions (C–H···X). The corresponding organogermanium hydrides were obtained in

good yields by reaction of the halide derivatives with $LiAlH_4$ in ethereal solutions. Solid state structures show again the occurrence of secondary interactions, including edge to face and $CH_3\cdots\pi$. Furthermore we show the successful preparation of arylgermanium hydrochlorides, diarylgermanium dihydrides and arylgermanium trihydrides by successively cleaving off aryl groups by the employment of trifluoromethanesulfonic acid (HOTf) starting from tetraarylgermanes, triarylgermanium hydrides or even diarylgermanium dihydrides. The reaction conditions were studied comprehensively and enhanced towards yields, selectivity and complexity. This indeed is of importance, since other pathways are often accompanied with mixture of products or low yields. All compounds were characterized using NMR, IR and MS methods. Additionally, all solids were analyzed *via* X-ray diffraction, showing interesting bonding motifs including $CH_3\cdots\pi$ and edge to face. Compounds 1-naphthyl$_2$GeHCl (21) and 1-napththyl$_2$GeH$_2$ (24) additionally show π-π- stacking.

Furthermore, first attempts towards possible applications were made, including the thermolysis of 1-naphthyl$_3$GeH (16), TGA measurements of 1-naphthyl$_3$GeX (X = Cl, Br) (9) and dehydrogenative coupling reactions with the amine base TMEDA. Formation of aryl-decorated nanoparticles, as was seen in previous work in the case of Sn, could not be observed yet, we can assume, that reaction took place, because of visible changes and decrease of carbon content detected by elemental analysis. Therefore, initial results seem promising, which makes the investigation of the potential of aryl substituted germanium compounds and their possible usage in applications the main focus of attention of future investigations. Overall, gaps regarding aryl substituted germanium compounds were filled and useful insights were made concerning their preparation and characterization, especially their solid state structures. The employment of more detailed studies dealing with alternative routes and scale up procedures can be helpful to gather more information concerning preparation, characterization or even the reaction mechanism of aryl substituted organogermanium compounds. A complete understanding of the chemistry of these compounds is essential for the further applications and should not be neglected.

A range of known and novel aryl substituted antimony compounds have been synthesized and fully characterized, providing an insight and an overview over preparation methods as well as spectroscopic features of these compounds. The preparation was achieved either by a Grignard reagent and reaction with $SbCl_3$ or *via* redistribution reactions between the triarylantimony species and $SbCl_3$. Aryl ligands with one methyl group, namely *o*-tolyl, two methyl groups, namely 2,6-xylyl or even larger polyaromatic systems, namely 1-naphthyl and 9-anthracenyl, were employed. The compounds 9-anthracenyl$_2$SbBr and [9-anthracenyl$_2$Sb]$_2$ are, to the best of our knowledge, the first antimony compounds bearing anthracenyl substituents. Interestingly, [9-anthracenyl$_2$Sb]$_2$ does not only show intermolecular interactions between neighboring molecules, as is observed for all presented aryl substituted antimony compounds, but, moreover, displays intramolecular interactions between anthracenyl substituents through the Sb–Sb bond.

Appendix

Numbering of compounds

Table 26. Numbering of compounds.

#	compound	#	compound
1	*m*-tolyl$_4$Ge	**24**	1-naphthyl$_2$GeH$_2$
2	3,4-xlyl$_4$Ge	**25**	2,5-xylylGeH$_3$
3	3,5-xyly$_{l4}$Ge	**26**	2,6-xylylGeH$_3$
4	2-naphthyl$_4$Ge	**27**	[2,6-xylyl$_2$Ge]$_2$O
5	*o*-tolyl$_3$GeX	**28**	K$_2$[(C$_4$H$_6$O$_2$)$_3$Ge]
6	2,4-xylyl$_3$GeX	**29**	K$_2$[(C$_6$H$_4$O$_2$)$_3$]Ge
7	2,5-xylyl$_3$GeX	**30**	^{i}propyl$_3$GeCl
8	2,6-xylyl$_3$GeX	**31**	^{i}propyl$_3$GeN(CH$_3$)$_2$
9	1-naphthyl$_3$GeX	**32**	(^{i}propyl)$_3$GeGe(phenyl)$_3$
10	2,4,6-mesityl$_3$GeX	**33**	phenyl$_2$GeH$_2$
11	3,5-xylyl$_3$GeCl	**34**	H(phenyl$_2$Ge)$_3$H
12	2-naphthyl$_3$GeCl	**35**	(phenyl$_2$Ge)$_4$
13	2,5-xylyl$_3$GeCl	**36**	Br(phenyl$_2$Ge)$_4$Br
14	2,4-xylyl$_3$GeH	**37**	(phenyl$_2$Ge)$_4$H$_2$
15	2,5-xylyl$_3$GeH	**38**	phenyl$_3$GeN(CH$_3$)$_2$
16	2,6-xylyl$_3$GeH	**39**	Ge(phenyl$_3$Ge)$_3$H
17	3,5-xylyl$_3$GeH	**40**	2,6-xylyl$_3$Sb
18	1-naphthyl$_3$GeH	**41**	1-naphthyl$_3$Sb
19	2,5-xylyl$_2$GeHCl	**42**	2,6-xylyl$_2$SbBr
20	2,6-xylyl$_2$GeHCl	**43**	9-anthracenyl$_2$SbBr
21	1-naphthyl$_2$GeHCl	**44**	[9-anthracenyl$_2$Sb]$_2$
22	2,5-xylyl$_2$GeH$_2$	**45**	*o*-tolylSbCl$_2$
23	2,6-xylyl$_2$GeH$_2$	**46**	[9-anthracenyl$_2$^{n}butylSb][9-anthracenyl^{n}butyl$_2$SbCl$_2$]

GCMS measurements

Table 27. GCMS Method 1.

	Rate (°C/min)	Value (°C)	Hold (min)
Initial		70	2
Ramp1	20	230	0
Ramp2	0	240	0
Ramp3	0	270	0

Table 28. GCMS Method 2.

	Rate (°C/min)	Value (°C)	Hold (min)
Initial		40	2
Ramp1	20	100	0
Ramp2	16	200	0
Ramp3	12	320	20

Table 29. Crystallographic data and details of measurements for compounds (1)- (4); Mo Kα (λ=0.71073Å). R1 = $\Sigma/ |F_o|- |F_c|/|\Sigma|F_d$; wR2 = $[\Sigma_w(F_o^2-F_2^2)^2/\Sigma_w(F_o^2)^2]^{1/2}$

Compound	***m*-tolyl$_4$Ge (1)**	**3,4-xylyl$_4$Ge (2)**	**3,5-xylyl$_4$Ge (3)**	**2-naphthyl$_4$Ge (4)**
Formula	$C_{28}H_{28}Ge$	$C_{32}H_{36}Ge$	$C_{32}H_{36}Ge$	$C_{40}H_{28}Ge$
Fw (g mol^{-1})	437.09	493.20	493.20	581.21
a (Å)	16.770(3)	20.8073(11)	17.7375(14)	9.9575(4)
b (Å)	16.770(3)	10.3891(6)	8.5647(7)	20.4834(8)
c (Å)	8.1538(16)	12.9790(8)	18.2056(13)	14.6722(6)
α (°)	90	90	90	90
β (°)	90	106.676(2)	100.795(3)	105.441(1)
γ (°)	90	90	90	90
V (Å^3)	2293.0(8)	2687.7(3)	2716.8(4)	2884.6(2)
Z	4	4	4	4
Crystal size (mm)	0.20 × 0.16 × 0.13	0.13 × 0.12 × 0.09	0.19 × 0.04 × 0.02	0.10 × 0.09 × 0.05
Crystal habit	Block, colourless	Block, colourless	Needle, colourless	Block, colourless
Crystal system	Tetragonal	Monoclinic	Monoclinic	Monoclinic
Space group	$I4_1/a$	$P2_1/c$	$P2/c$	$P2_1/n$
d_{calc} (mg/m^3)	1.266	1.219	1.206	1.338
μ (mm^{-1})	1.35	1.16	1.14	1.09
T (K)	100(2)	100(2)	100(2)	100(2)
2ϑ range (°)	2.4–21.2	2.6–20.8	2.4–29.6	2.4–30.8
F(000)	912	1040	1040	1200
R_{int}	0.339	0.287	0.222	0.047
independent reflns	994	4715	10410	5022
No. of params	68	372	307	370
R1, wR2 (all data)	R1 = 0.0613 wR2 = 0.0913	R1 = 0.1384 wR2 = 0.1792	R1= 0.1272 wR2 = 0.1447	R1 = 0.0243 wR2 = 0.0676
R1, wR2 (>2σ)	R1 = 0.0386 wR2 = 0.0827	R1 = 0.0607 wR2 = 0.1421	R1 = 0.0529 wR2 = 0.1123	R1 = 0.0225 wR2 = 0.0661

Table 30. Crystallographic data and details of measurements for compounds (5), (7-10), (13); Mo Kα (λ=0.71073Å). R1 = $\Sigma/\ |F_o|-|F_c|/|\Sigma|F_d$; wR2 = $[\Sigma_w(F_o^2-F_2^2)^2/\Sigma_w(F_o^2)^2]^{1/2}$

Compound	**2,5-xylyl$_3$GeCl (13)**	***o*-tolyl$_3$GeBr (5)**	**2,5-xylyl$_3$GeBr (7)**	**2,6-xylyl$_3$GeBr (8)**	**1-naphthyl$_3$GeCl · thf (9a)**	**1-naphthyl$_3$GeBr · toluene (9b)**	**1-naphthyl$_3$GeBr · CHCl$_3$ (9c)**	**1-naphthyl$_3$GeBr · naphthyl (9d)**	**2,4,6-mesityl$_3$GeBr (10)**
Formula	$C_{24}H_{27}ClGe$	$C_{21}H_{21}BrGe$	$C_{24}H_{27}BrGe$	$C_{24}H_{27}BrGe$	$C_{30}H_{21}ClGe{\cdot}C_4H_8O$	$C_{30}H_{21}BrGe$	$C_{30}H_{21}BrGe{\cdot}CHCl_3$	$2(C_{30}H_{21}BrGe){\cdot}3(C_{10}H_8)$	$C_{27}H_{33}BrGe$
Fw (g mol^{-1})	423.49	425.88	467.95	467.95	561.61	533.97	653.33	1452.42	510.03
a (Å)	16.7398(6)	16.1689(7)	16.8093(12)	16.3101(7)	9.7298(7)	31.6461(8)	9.7878(10)	32.0498(10)	8.2641(4)
b (Å)	9.3434(3)	13.5904(6)	9.3970(7)	8.2302(3)	12.0548(8)	31.6461(8)	12.0877(12)	32.0498(10)	16.7777(9)
c (Å)	14.5663(6)	16.6914(7)	14.4768(10)	15.5484(6)	13.2203(9)	21.9935(14)	13.1558(14)	22.3336(16)	19.6137(8)
α (°)	90	90	90	90	64.154(3)	90	65.306(4)	90	78.053(2)
β (°)	110.669(1)	97.553(2)	110.529(2)	90	73.876(4)	90	74.542(4)	90	84.368(2)
γ (°)	90	90	90	90	77.513(4)	90	78.053(4)	90	89.444(2)
V (Å^3)	2131.63(14)	3636.0(3)	2141.5(3)	2087.15(14)	1332.47(17)	19075.0(16)	1354.8(2)	19867.3(19)	2647.6(2)
Z	4	8	4	4	2	24	2	12	4
Crystal size (mm)	0.20 × 0.15 × 0.12	0.09 × 0.08 × 0.08	0.20 × 0.19 × 0.10	0.16 × 0.13 × 0.09	0.08 × 0.07 × 0.06	0.12 × 0.10 × 0.09	0.20 × 0.16 × 0.09	0.22 × 0.21 × 0.10	0.15 × 0.10 × 0.09
Crystal habit	Block, colourless	Block, colourless	Block, colourless	Block, colourless	Block, colourless	Block, colourless	Block, colourless	Block, colourless	Block, colourless
Crystal system	Monoclinic	Monoclinic	Monoclinic	Orthorhombic	Triclinic	Trigonal	Triclinic	Trigonal	Triclinic
Space group	$P2_1/c$	$P2_1/c$	$P2_1/c$	$Pca2_1$	*P*-1	*R*-3	*P*-1	*R*-3	*P*-1
d_{calc} (mg/m^3)	1.320	1.556	1.451	1.489	1.400	1.116	1.602	1.457	1.280
μ (mm^{-1})	1.57	3.88	3.30	3.39	1.28	2.23	2.92	2.17	2.68
T (K)	100(2)	100(2)	100(2)	100(2)	100(2)	100(2)	100(2)	100(2)	100(2)
2ϑ range (°)	2.5–30.7	2.5–32.4	2.5–26.6	2.5–33.1	2.5–24.7	2.6–28.8	2.7–30.6	2.5–28.5	2.5–28.7
F(000)	880	1712	952	952	580	6432	652	8880	9250
R_{int}	0.458	0.082	0.135	0.055	0.138	0.150	0.145	0.118	0.091
independent reflns	3740	13819	8261	3628	4482	16168	4747	7696	9250
No. of params	200	421	241	242	334	385	313	566	541
R1, wR2 (all data)	R1 = 0.0598 wR2 = 0.1429	R1 = 0.0479 wR2 = 0.0926	R1 =0.0945 wR2 = 0.0987	R1 = 0.0218 wR2 = 0.0608	R1 = 0.1032 wR2 = 0.1924	R1 = 0.0957 wR2 = 0.1339	R1 = 0.0653 wR2 = 0.1376	R1 = 0.0587 wR2 = 0.1226	R1 = 0.0847 wR2 = 0.2234
R1, wR2 (>2σ)	R1 = 0.0522 wR2 = 0.1350	R1 = 0.0344 wR2 = 0.0864	R1 = 0.0442 wR2 = 0.0815	R1 = 0.0214 wR2 = 0.0605	R1 = 0.0640 wR2 = 0.1612	R1 = 0.0645 wR2 = 0.1210	R1 = 0.0562 wR2 = 0.1327	R1 = 0.0368 wR2 = 0.1021	R1 = 0.0731 wR2 = 0.2148

Table 31 . Crystallographic data and details of measurements for compounds (14-21); Mo Kα (λ=0.71073Å). R1 = $\Sigma/ |F_o|- |F_c|/|\Sigma|F_d$; wR2 = $[\Sigma_w(F_o^2-F_2^2)^2/\Sigma_w(F_o^2)^2]^{1/2}$

Compound	**3,5-xylyl$_3$GeH (17)**	**2,4-xylyl$_3$GeH (14)**	**2,5-xylyl$_3$GeH (15)**	**2,6-xylyl$_3$GeH (16)**	**1-naphthyl$_3$GeH · C$_7$H$_8$ (18)**	**2,5-xylyl$_2$GeHCl (19)**	**2,6-xylyl$_2$GeHCl (20)**	**1-naphthyl$_2$GeHCl (21)**
Formula	$C_{24}H_{28}Ge$	$C_{24}H_{28}Ge$	$C_{24}H_{28}Ge$	$C_{24}H_{28}Ge$	$C_{30}H_{22}Ge{\cdot}C_7H_8$	$C_{16}H_{19}ClGe$	$C_{16}H_{19}ClGe$	$C_{20}H_{15}ClGe$
Fw (g mol^{-1})	389.05	389.05	389.05	389.05	545.18	319.35	319.35	363.36
a (Å)	8.4915(10)	5.2022(3)	5.1720(4)	16.4090(7)	13.2403(7)	4.9407(2)	13.7216(9)	12.6919(5)
b (Å)	12.6203(15)	26.2268(15)	34.175(3)	8.1398(4)	13.2403(7)	12.9428(7)	8.4806(5)	10.6746(4)
c (Å)	19.104(2)	14.6535(8)	11.2128(10)	30.3372(14)	27.2732(13)	11.2952(6)	13.9861(9)	11.7011(5)
α (°)	90	90	90	90	90	90	90	90
β (°)	90.918(5)	92.262(2)	95.676(3)	101.356(2)	90	94.170(2)	115.295(2)	115.295(2)
γ (°)	90	90	90	90	90	90	90	90
V (Å^3)	2047.0(4)	1997.7(2)	1972.2(3)	3972.7(3)	4140.6(5)	720.38(6)	1471.48(16)	1584.35(11)
Z	4	4	4	8	6	2	4	4
Crystal size (mm)	0.20 × 0.14 × 0.12	0.16 × 0.14 × 0.12	0.09 × 0.08 × 0.06	0.10 × 0.09 × 0.08	0.16 × 0.14 × 0.12	0.10 × 0.09 × 0.07	0.12 × 0.10 × 0.09	0.34 × 0.33 × 0.30
Crystal habit	Block, colourless	Block, colourless	Block, colourless	Block, colourless	Block, colourless	Block, colourless	Block, colourless	Block, colourless
Crystal system	Monoclinic	Monoclinic	Monoclinic	Monoclinic	Trigonal	Monoclinic	Monoclinic	Monoclinic
Space group	$P2_1/c$	$P2_1/n$	$P2_1/c$	$P2_1/n$	*R*-3	$P2_1$	$P2_1/n$	$P2_1/c$
d_{calc} (mg/m^3)	1.262	1.294	1.310	1.301	1.312	1.472	1.442	1.523
μ (mm^{-1})	1.50	1.54	1.56	1.55	1.13	2.29	2.24	2.10
T (K)	100(2)	100(2)	100(2)	100(2)	100(2)	100(2)	100(2)	100(2)
2*ϑ* range (°)	2.9–33.1	2.7–33.0	2.4–33.3	2.5–32.7	3.1–27.8	2.4–29.2	2.8–33.2	2.5–29.7
F(000)	816	816	816	1632	1692	328	656	736
R_{int}	0.047	0.079	0.176	0.093	0.074	0.041	0.048	0.079
independent reflns	3582	3458	7512	15183	2190	2368	5440	4600
No. of params	236	236	236	491	217	1	171	203
R1, wR2 (all data)	R1 = 0.0250 wR2 = 0.0664	R1 = 0.0297 wR2 = 0.0731	R1 = 0.1079 wR2 = 0.0906	R1 = 0.0528 wR2 = 0.0378	R1 = 0.0913 wR2 = 0.2186	R1 = 0.0208 wR2 = 0.0433	R1 = 0.0469 wR2 = 0.1043	R1 = 0.0518 wR2 = 0.0758
R1, wR2 (>2σ)	R1 = 0.0235 wR2 = 0.0652	R1 = 0.0273 wR2 = 0.0721	R1 = 0.0543 wR2 = 0.0816	R1 = 0.0913 wR2 = 0.0843	R1 = 0.0721 wR2 = 0.1951	R1 = 0.0196 wR2 = 0.0429	R1 = 0.0381 wR2 = 0.0992	R1 = 0.0356 wR2 = 0.0727

Table 32. Crystallographic data and details of measurements for compounds (22- 24); Mo Kα (λ=0.71073Å). R1 = $\Sigma/ |F_o|- |F_c|/|\Sigma|F_d$; wR2 = $[\Sigma_w(F_o^2-F_2^2)^2/\Sigma_w(F_o^2)^2]^{1/2}$

Compound	**2,5-xylyl$_2$GeH$_2$ (22)**	**2,6-xylyl$_2$GeH$_2$ (23)**	**1-naphthyl$_2$GeH$_2$ (24)**
Formula	$C_{16}H_{20}Ge$	$C_{16}H_{20}Ge$	$C_{20}H_{16}Ge$
Fw (g mol^{-1})	284.91	284.91	328.92
a (Å)	4.9192(4)	12.2198(13)	14.0069(6)
b (Å)	11.5404(9)	8.4805(9)	8.8593(4)
c (Å)	12.5043(10)	14.5531(15)	24.653(1)
α (°)	96.558(2)	90	90
β (°)	96.523(2)	110.279(4)	90
γ (°)	94.900(2)	90	90
V (Å^3)	697.16(10)	1414.7(3)	3059.2(2)
Z	2	4	8
Crystal size (mm)	0.10 × 0.09 × 0.08	0.10 × 0.08 × 0.06	0.15 × 0.12 × 0.09
Crystal habit	Block, colourless	Block, colourless	Block, colourless
Crystal system	Triclinic	Monoclinic	Orthorhombic
Space group	*P*-1	$P2_1/c$	*Pbca*
d_{calc} (mg/m^3)	1.357	1.338	1.428
μ (mm^{-1})	2.17	2.14	1.99
T (K)	100(2)	100(2)	100(2)
2*ϑ* range (°)	2.6–33.2	2.8–33.2	2.8–30.8
F(000)	296	592	1344
R_{int}	0.031	0.053	0.054
independent reflns	5349	5435	264
No. of params	166	166	198
R1, wR2 (all data)	R1 = 0.0228 wR2 = 0.0684	R1 = 0.0314 wR2 = 0.0781	R1 = 0.0367 wR2 = 0.0766
R1, wR2 (>2σ)	R1 = 0.0198 wR2 = 0.0558	R1 = 0.0262 wR2 = 0.0696	R1 = 0.0282 wR2 = 0.0719

Table 33. Crystallographic data and details of measurements for compounds (40-46); Mo Kα (λ=0.71073Å). R1 = $\Sigma/ |F_o| - |F_c|/|\Sigma|F_d$; wR2 = $[\Sigma_w(F_o^2-F_2^2)^2/\Sigma_w(F_o^2)^2]^{1/2}$

Compound	**2,6-xylyl$_3$Sb (40)**	**1-naphthyl$_3$Sb (toluene) (41a)**	**1-naphthyl$_3$Sb (benzene) (41b)**	**2,6-xylyl$_2$SbBr (42)**	**9-anthracenyl$_2$SbBr (43)**	***o*-tolylSbCl$_2$ (45)**	**[9-anthracenyl$_2$Sb]$_2$ (44)**	**[Sbanthra-cenyl$_2$butyl][Sbanthracenylbutyl$_2$Cl$_2$] (46)**
Formula	$C_{24}H_{27}Sb$	$C_{30}H_{21}Sb{\cdot}C_7H_8$	$C_{30}H_{21}Sb{\cdot}C_6H_6$	$C_{16}H_{18}BrSb$	$C_{28}H_{18}BrSb{\cdot}C_7H_8$	$C_7H_7Cl_2Sb$	$C_{56}H_{36}Sb_2$	$C_{32}H_{27}Sb{\cdot}C_{22}H_{27}Cl_2Sb$
Fw (g mol^{-1})	437.20	595.35	581.32	411.96	648.22	283.78	952.35	1017.37
a (Å)	15.6862(4)	9.6308(8)	9.4275(7)	13.5584(4)	13.9460(6)	8.3865(4)	21.2483(18)	9.5679(4)
b (Å)	8.1310(2)	12.4357(9)	12.3440(9)	8.6359(3)	10.2466(5)	9.1365(5)	12.9941(11)	12.4806(5)
c (Å)	16.0632(4)	12.8834(10)	12.9127(9)	14.0553(5)	19.1860(8)	12.0877(6)	28.908(2)	19.4346(8)
α (°)	90	62.830(2)	62.177(3)	90	90	70.8510(15)	90	95.424(2)
β (°)	103.2149(12)	88.743(3)	88.402(4)	114.2180(13)	104.6570(14)	81.6470(16)	93.896(4)	90.245(2)
γ (°)	90	85.203(3)	85.282(4)	90	90	78.3500(16)	90	102.504(2)
V (Å^3)	1994.52(9)	1367.69(19)	1324.37(17)	1500.88(9)	2652.4(2)	853.79(8)	7963.2(12)	2254.82(16)
Z	4	2	2	4	4	4	8	2
Crystal size (mm)	0.08 × 0.07 × 0.06	0.23 × 0.21 × 0.19	0.10 × 0.09 × 0.08	0.15 × 0.13 × 0.12	0.20 × 0.20 × 0.19	0.33 × 0.25 × 0.15	0.18 × 0.16 × 0.10	0.10 × 0.08 × 0.08
Crystal habit	Block, colourless	Block, colourless	Block, colourless	Block, yellow	Block, yellow	Block, colourless	Block, yellow	Block, colourless
Crystal system	Monoclinic	Triclinic	Triclinic	Monoclinic	Monoclinic	Triclinic	Monoclinic	Triclinic
Space group	*P*2$_1$/*c*	*P*-1	*P*-1	*P*2$_1$/*n*	*P*2$_1$/*c*	*P*-1	*P*2$_1$/*c*	*P*-1
d_{calc} (mg/m^3)	1.456	1.446	1.458	1.823	1.623	2.208	1.589	1.498
μ (mm^{-1})	1.39	1.03	1.07	4.48	2.57	3.78	1.589	1.35
T (K)	100(2)	100(2)	100(2)	100(2)	100(2)	100(2)	100(2)	100(2)
2*ϑ* range (°)	2.6–30.0	2.7–27.1	2.8–27.1	2.7–27.1	2.3–27.1	2.4–27.1	2.5–27.1	2.5–29.3
F(000)	888	604	588	800	1288	536	3792	1028
R_{int}	0.033	0.024	0.042	0.041	0.019	0.016	0.049	0.088
independent reflns	5280	5581	5385	3049	5417	3456	16263	12395
No. of params	232	385	334	167	335	183	1045	526
R1, wR2 (all data)	R1 = 0.0197 wR2 = 0.0371	R1 = 0.0167 wR2 = 0.0406	R1 = 0.0399 wR2 = 0.0615	R1 = 0.0612 wR2 = 0.1867	R1 = 0.0150 wR2 = 0.0362	R1 = 0.0129 wR2 = 0.0302	R1 = 0.0423 wR2 = 0.0610	R1 = 0.0514 wR2 = 0.0705
R1, wR2 (>2*σ*)	R1 = 0.0164 wR2 = 0.0357	R1 = 0.0158 wR2 = 0.0401	R1 = 0.0306 wR2 = 0.0583	R1 = 0.0604 wR2 = 0.1861	R1 = 0.0146 wR2 = 0.0360	R1 = 0.0125 wR2 = 0.0299	R1 = 0.0294 wR2 = 0.0568	R1 = 0.0329 wR2 = 0.0642

List of Figures

Bibliography

(1) Holleman, A. F.; Wiberg, E.; Wiberg, N. *Lehrbuch der anorganischen Chemie*; Walter de Gruyter, 2007.

(2) Winkler, C. A. *Chemische Berichte* **1887**, 677.

(3) Lukevics, E.; Gar, T. K.; Ignatovich, L. M.; Mironov, V. F. *Biological Activity of Germanium Compounds*; Zinatne, 1990.

(4) Glockling, F. *The Chemistry of Germanium*; Academic, 1969.

(5) Ward, S. G.; Taylor, R. C.; Freund: 1988, p 1.

(6) Razuvaev, G. A.; Gribov, B. G.; Domrachev, G. A.; Salamatin, B. A. *Organometallic Compounds in Electronics*; Nauka, 1972.

(7) Gribov, B. G.; Domrachev, G. A.; Zhuk, B. V.; et, a. *Deposition of Films and Coatings by Decomposition of Organometallic Compounds*; Nauka, 1981.

(8) Oshima, K. *Sci. Synth.* **2003**, *5*, 9.

(9) Simons, J. K.; Wagner, E. C.; Muller, J. H. *J. Am. Chem. Soc.* **1933**, *55*, 3705.

(10) Morgan, G. T.; Drew, H. D. K. *J. Chem. Soc., Trans.* **1925**, *127*, 1760.

(11) Kraus, C. A.; Foster, L. S. *J. Am. Chem. Soc.* **1927**, *49*, 457.

(12) Harris, D. M.; Nebergall, W. H.; Johnson, O. H. *Inorg. Synth.* **1957**, *5*, 70.

(13) Cerveau, G.; Chuit, C.; Corriu, R. J. P.; Reye, C. *Organometallics* **1988**, *7*, 786.

(14) Cerveau, G.; Chuit, C.; Corriu, R. J. P.; Reye, C. *Organometallics* **1991**, *10*, 1510.

(15) Cooke, J. A.; Dixon, C. E.; Netherton, M. R.; Kollegger, G. M.; Baines, K. M. *Synthesis and Reactivity in Inorganic and Metal-Organic Chemistry* **1996**, *26*, 1205.

(16) Chaubon, M. A.; Dittrich, B.; Escudie, J.; Ramdane, H.; Ranaivonjatovo, H.; Satge, J. *Synth. React. Inorg. Met.-Org. Chem.* **1997**, *27*, 519.

(17) Samanamu, C. R.; Anderson, C. R.; Golen, J. A.; Moore, C. E.; Rheingold, A. L.; Weinert, C. S. *J. Organomet. Chem.* **2011**, *696*, 2993.

(18) Amadoruge, M. L.; Short, E. K.; Moore, C.; Rheingold, A. L.; Weinert, C. S. *J. Organomet. Chem.* **2010**, *695*, 1813.

(19) Komanduri, S. P.; Shumaker, F. A.; Roewe, K. D.; Wolf, M.; Uhlig, F.; Moore, C. E.; Rheingold, A. L.; Weinert, C. S. *Organometallics* **2016**, *35*, 3240.

(20) Thornton, P. *Sci. Synth.* **2003**, *5*, 55.

(21) Kozeschkow, K. A. *Ber. Dtsch. Chem. Ges.* **1933**, *66*, 1661.

(22) Neumann, W. P.; Burkhardt, G. *Justus Liebigs Ann. Chem.* **1963**, *663*, 11.

(23) Luijten, J. G. A.; Rijkens, F. *Recl. Trav. Chim. Pays-Bas* **1964**, *83*, 857.

(24) Rijkens, F.; van der Kerk, G. J. M. *Recl. Trav. Chim. Pays-Bas* **1964**, *83*, 723.

(25) Kuehlein, K.; Neumann, W. P. *Justus Liebigs Ann. Chem.* **1967**, *702*, 17.

(26) Laurent, R.; Laporterie, A.; Dubac, J.; Berlan, J. *Organometallics* **1994**, *13*, 2493.

(27) Orndorff, W. R.; Tabern, D. L.; Dennis, L. M. *J. Am. Chem. Soc.* **1927**, *49*, 2512.

(28) Seyferth, D.; Hetflejs, J. *J. Organomet. Chem.* **1968**, *11*, 253.

(29) Bardin, V. V.; Aparina, L. N.; Furin, G. G. *Zh. Obshch. Khim.* **1991**, *61*, 1414.

(30) Zhun, V. I.; Sbitneva, I. V.; Chernyshev, E. A. *Russ. J. Gen. Chem.* **2005**, *75*, 867.

(31) Zhun, V. I.; Sbitneva, I. V.; Polivanov, A. N.; Chernyshev, E. A. *Russ. J. Gen. Chem.* **2006**, *76*, 1564.

(32) Kultyshev, R. G.; Prakash, G. K. S.; Olah, G. A.; Faller, J. W.; Parr, J. *Organometallics* **2004**, *23*, 3184.

(33) Faller, J. W.; Kultyshev, R. G.; Parr, J. *J. Organomet. Chem.* **2004**, *689*, 2565.

(34) Bhattacharya, S. N.; Raj, P.; Srivastava, R. C. *J. Organomet. Chem.* **1976**, *105*, 45.

(35) Satge, J.; Riviere, P. *Bull. Soc. Chim. Fr.* **1966**, 1773.

(36) Park, J.; Batcheller, S. A.; Masamune, S. *J. Organomet. Chem.* **1989**, *367*, 39.

(37) Ohshita, J.; Toyoshima, Y.; Iwata, A.; Tang, H.; Kunai, A. *Chem. Lett.* **2001**, 886.

(38) Riviere, P.; Castel, A.; Guyot, D.; Satge, J. *J. Organomet. Chem.* **1985**, *290*, C15.

(39) Haeberle, K.; Draeger, M. *J. Organomet. Chem.* **1986**, *312*, 155.

(40) Riedmiller, F.; Wegner, G. L.; Jockisch, A.; Schmidbaur, H. *Organometallics* **1999**, *18*, 4317.

(41) Janiak, C.; Schwichtenberg, M.; Hahn, F. E. *J. Organomet. Chem.* **1989**, *365*, 37.

(42) Neumann, W. P. *Chem. Rev.* **1991**, *91*, 311.

(43) Kolesnikov, S. P.; Nefedov, O. M. *Angew. Chem.* **1965**, *77*, 345.

(44) Okamoto, M.; Asano, T.; Suzuki, E. *Organometallics* **2001**, *20*, 5583.

(45) Meyer, R. J. In *Germanium*; Meyer, R. J., Ed.; Springer Berlin Heidelberg: Berlin, Heidelberg, 1961, p 1.

(46) Voegelen, E. *Z Anorg Chem* **1902**, *30*, 325.

(47) Gilman, H.; Gerow, C. W. *J. Am. Chem. Soc.* **1955**, *77*, 4675.

(48) Gilman, H.; Gerow, C. W. *J. Am. Chem. Soc.* **1955**, *77*, 5509.

(49) Tamborski, C.; Ford, F. E.; Lehn, W. L.; Moore, G. J.; Soloski, E. J. *J. Org. Chem.* **1962**, *27*, 619.

(50) Johnson, O. H.; Harris, D. M. *J. Am. Chem. Soc.* **1950**, *72*, 5566.

(51) Castel, A.; Riviere, P.; Satge, J.; Ko, H. Y. *Organometallics* **1990**, *9*, 205.

(52) Gerion, D.; Zaitseva, N.; Saw, C.; Casula, M. F.; Fakra, S.; Van Buuren, T.; Galli, G. *Nano Lett.* **2004**, *4*, 597.

(53) Trummer, M.; Choffat, F.; Smith, P.; Caseri, W. *Macromol. Rapid Commun.* **2012**, *33*, 448.

(54) Lechner, M.-L.; Trummer, M.; Braeunlich, I.; Smith, P.; Caseri, W.; Uhlig, F. *Appl. Organomet. Chem.* **2011**, *25*, 769.

(55) Lu, V. Y.; Tilley, T. D. *Macromolecules* **2000**, *33*, 2403.

(56) Adams, S.; Draeger, M. *Main Group Met. Chem.* **1988**, *11*, 151.

(57) Choffat, F.; Smith, P.; Caseri, W. *Adv. Mater.* **2008**, *20*, 2225.

(58) Sacarescu, L.; Mangalagiu, I.; Simionescu, M.; Sacarescu, G.; Ardeleanu, R. *Macromol. Symp.* **2008**, *267*, 123.

(59) Seki, S.; Matsui, Y.; Yoshida, Y.; Tagawa, S.; Koe, J. R.; Fujiki, M. *J. Phys. Chem. B* **2002**, *106*, 6849.

(60) West, R. In *The Chemistry of Organic Silicon Compounds*; John Wiley & Sons, Ltd: 2003, p 541.

(61) Zaitsev, K. V.; Kapranov, A. A.; Churakov, A. V.; Poleshchuk, O. K.; Oprunenko, Y. F.; Tarasevich, B. N.; Zaitseva, G. S.; Karlov, S. S. *Organometallics* **2013**, *32*, 6500.

(62) Hlina, J.; Zitz, R.; Wagner, H.; Stella, F.; Baumgartner, J.; Marschner, C. *Inorg. Chim. Acta* **2014**, *422*, 120.

(63) Fukazawa, A.; Tsuji, H.; Tamao, K. *J. Am. Chem. Soc.* **2006**, *128*, 6800.

(64) Tamao, K.; Tsuji, H.; Terada, M.; Asahara, M.; Yamaguchi, S.; Toshimitsu, A. *Angew. Chem., Int. Ed.* **2000**, *39*, 3287.

(65) Tsuji, H.; Terada, M.; Toshimitsu, A.; Tamao, K. *J. Am. Chem. Soc.* **2003**, *125*, 7486.

(66) Balaji, V.; Michl, J. *Polyhedron* **1991**, *10*, 1265.

(67) Weinert, C. S. *Dalton Trans.* **2009**, 1691.

(68) Mironov, V. F.; Dzhurinskaya, N. G. *B. Acad. Sci. USSR Ch.* **1963**, *12*, 66.

(69) Schrick, E. K.; Forget, T. J.; Roewe, K. D.; Schrick, A. C.; Moore, C. E.; Golen, J. A.; Rheingold, A. L.; Materer, N. F.; Weinert, C. S. *Organometallics* **2013**, *32*, 2245.

(70) Mochida, K.; Hata, R.; Shimoda, M.; Matsumoto, F.; Kurosu, H.; Kojima, A.; Yoshikawa, M.; Masuda, S.; Harada, Y. *Polyhedron* **1996**, *15*, 3027.

(71) Amadoruge, M. L.; Gardinier, J. R.; Weinert, C. S. *Organometallics* **2008**, *27*, 3753.

(72) Mochida, K.; Chiba, H. *J. Organomet. Chem.* **1994**, *473*, 45.

(73) Metlesics, W.; Zeiss, H. *J. Am. Chem. Soc.* **1960**, *82*, 3321.

(74) Brown, M. P.; Fowles, G. W. A. *J. Chem. Soc.* **1958**, 2811.

(75) Johnson, O. H. *Chem. Rev.* **1951**, *48*, 259.

(76) Schwarz, R.; Lewinsohn, M. *Ber. Dtsch. Chem. Ges. B* **1931**, *64B*, 2352.

(77) Neumann, W. P.; Kuehlein, K. *Justus Liebigs Ann. Chem.* **1965**, *683*, 1.

(78) Roller, S.; Simon, D.; Draeger, M. *J. Organomet. Chem.* **1986**, *301*, 27.

(79) Roller, S.; Draeger, M. *J. Organomet. Chem.* **1986**, *316*, 57.

(80) Castel, A.; Riviere, P.; Saint-Roch, B.; Satge, J.; Malrieu, J. P. *J. Organomet. Chem.* **1983**, *247*, 149.

(81) Azemi, T.; Yokoyama, Y.; Mochida, K. *J. Organomet. Chem.* **2005**, *690*, 1588.

(82) Yokoyama, Y.; Hayakawa, M.; Azemi, T.; Mochida, K. *J. Chem. Soc., Chem. Commun.* **1995**, 2275.

(83) Draeger, M.; Simon, D. *J. Organomet. Chem.* **1986**, *306*, 183.

(84) Glockling, F.; Hooton, K. A. *J. Chem. Soc.* **1962**, 3509.

(85) Harris, D. M.; Nebergall, W. H.; Johnson, O. H. *Inorg. Synth.* **1957**, *5*, 72.

(86) Glockling, G.; Hooton, K. A. *J. Chem. Soc.* **1963**, 1849.

(87) Curtis, M. D.; Wolber, P. *Inorg. Chem.* **1972**, *11*, 431.

(88) Zaitsev, K. V.; Lermontova, E. K.; Churakov, A. V.; Tafeenko, V. A.; Tarasevich, B. N.; Poleshchuk, O. K.; Kharcheva, A. V.; Magdesieva, T. V.; Nikitin, O. M.; Zaitseva, G. S.; Karlov, S. S. *Organometallics* **2015**, *34*, 2765.

(89) Roewe, K. D.; Rheingold, A. L.; Weinert, C. S. *Chem. Commun.* **2013**, *49*, 8380.

(90) Subashi, E.; Rheingold, A. L.; Weinert, C. S. *Organometallics* **2006**, *25*, 3211.

(91) Bochkarev, M. N.; Vyazankin, N. S.; Bochkarev, L. N.; Razuvaev, G. A. *J. Organomet. Chem.* **1976**, *110*, 149.

(92) Samanamu, C. R.; Rheingold, A. L.; Weinert, C. S. *J. Organomet. Chem.* **2011**, *696*, 3721.

(93) Trefonas, P.; West, R. *J. Polym. Sci., Polym. Chem. Ed.* **1985**, *23*, 2099.

(94) Kobayashi, S.; Cao, S. *Chem. Lett.* **1993**, 1385.

(95) Kashimura, S.; Ishifune, M.; Yamashita, N.; Bu, H.-B.; Takebayashi, M.; Kitajima, S.; Yoshiwara, D.; Kataoka, Y.; Nishida, R.; Kawasaki, S.-i.; Murase, H.; Shono, T. *J. Org. Chem.* **1999**, *64*, 6615.

(96) Okano, M.; Takeda, K.-i.; Toriumi, T.; Hamano, H. *Electrochim. Acta* **1998**, *44*, 659.

(97) Mochida, K.; Nagano, S.-s.; Kawata, H.; Wakasa, M.; Hayashi, H. *J. Organomet. Chem.* **1997**, *542*, 75.

(98) Huo, Y.; Berry, D. H. *Chem. Mater.* **2005**, *17*, 157.

(99) Fa, W.; Zeng, X. C. *Chem. Commun.* **2014**, *50*, 9126.

(100) Hlina, J.; Baumgartner, J.; Marschner, C. *Organometallics* **2010**, *29*, 5289.

(101) Fischer, J.; Baumgartner, J.; Marschner, C. *Organometallics* **2005**, *24*, 1263.

(102) Brook, A. G.; Abdesaken, F.; Soellradl, H. *J. Organomet. Chem.* **1986**, *299*, 9.

(103) Wang, D.; Chang, Y.-L.; Wang, Q.; Cao, J.; Farmer, D. B.; Gordon, R. G.; Dai, H. *J. Am. Chem. Soc.* **2004**, *126*, 11602.

(104) Hanrath, T.; Korgel, B. A. *J. Am. Chem. Soc.* **2002**, *124*, 1424.

(105) Fang, C.; Foell, H.; Carstensen, J. *Nano Lett.* **2006**, *6*, 1578.

(106) Rossetti, R.; Hull, R.; Gibson, J. M.; Brus, L. E. *J. Chem. Phys.* **1985**, *83*, 1406.

(107) Talapin, D. V.; Lee, J.-S.; Kovalenko, M. V.; Shevchenko, E. V. *Chem. Rev. (Washington, DC, U. S.)* **2010**, *110*, 389.

(108) Henderson, E. J.; Hessel, C. M.; Veinot, J. G. C. *J. Am. Chem. Soc.* **2008**, *130*, 3624.

(109) Chiu, H. W.; Kauzlarich, S. M. *Chem. Mater.* **2006**, *18*, 1023.

(110) Chiu, H. W.; Chervin, C. N.; Kauzlarich, S. M. *Chem. Mater.* **2005**, *17*, 4858.

(111) Fok, E.; Shih, M.; Meldrum, A.; Veinot, J. G. C. *Chem. Commun.* **2004**, 386.

(112) Wu, H. P.; Liu, J. F.; Wang, Y. W.; Zeng, Y. W.; Jiang, J. Z. *Mater. Lett.* **2006**, *60*, 986.

(113) Lu, X.; Ziegler, K. J.; Ghezelbash, A.; Johnston, K. P.; Korgel, B. A. *Nano Lett.* **2004**, *4*, 969.

(114) Chou, N. H.; Oyler, K. D.; Motl, N. E.; Schaak, R. E. *Chem. Mater.* **2009**, *21*, 4105.

(115) Guha, S.; Wall, M.; Chase, L. L. *Nucl. Instrum. Methods Phys. Res., Sect. B* **1999**, *147*, 367.

(116) Kornowski, A.; Giersig, M.; Vogel, R.; Chemseddine, A.; Weller, H. *Adv. Mater.* **1993**, *5*, 634.

(117) Ma, X.; Wu, F.; Kauzlarich, S. M. *J. Solid State Chem.* **2008**, *181*, 1628.

(118) Taylor, B. R.; Kauzlarich, S. M.; Delgado, G. R.; Lee, H. W. H. *Chem. Mater.* **1999**, *11*, 2493.

(119) Vaughn, D. D., II; Schaak, R. E. *Chem. Soc. Rev.* **2013**, *42*, 2861.

(120) Xue, D.-J.; Wang, J.-J.; Wang, Y.-Q.; Xin, S.; Guo, Y.-G.; Wan, L.-J. *Adv. Mater.* **2011**, *23*, 3704.

(121) Matioszek, D.; Ojo, W. S.; Cornejo, A.; Katir, N.; El Ezzi, M.; Le Troedec, M.; Martinez, H.; Gornitzka, H.; Castel, A.; Nayral, C.; Delpech, F. *Dalton Trans.* **2015**, *44*, 7242.

(122) Schrick, A. C.; Weinert, C. S. *Mater. Res. Bull.* **2013**, *48*, 4390.

(123) Prabakar, S.; Shiohara, A.; Hanada, S.; Fujioka, K.; Yamamoto, K.; Tilley, R. D. *Chem. Mater.* **2010**, *22*, 482.

(124) Heath, J. R.; Shiang, J. J.; Alivisatos, A. P. *J. Chem. Phys.* **1994**, *101*, 1607.

(125) Bruchez, M., Jr.; Moronne, M.; Gin, P.; Weiss, S.; Alivisatos, A. P. *Science* **1998**, *281*, 2013.

(126) Derfus, A. M.; Chan, W. C. W.; Bhatia, S. N. *Nano Lett.* **2004**, *4*, 11.

(127) Bruce, P. G.; Scrosati, B.; Tarascon, J.-M. *Angew. Chem., Int. Ed.* **2008**, *47*, 2930.

(128) Li, X.; Liang, J.; Hou, Z.; Zhang, W.; Wang, Y.; Zhu, Y.; Qian, Y. *J. Power Sources* **2015**, *293*, 868.

(129) Lim, L. Y.; Fan, S.; Hng, H. H.; Toney, M. F. *Adv. Energy Mater.* **2015**, *5*.

(130) Li, W.; Li, M.; Yang, Z.; Xu, J.; Zhong, X.; Wang, J.; Zeng, L.; Liu, X.; Jiang, Y.; Wei, X.; Gu, L.; Yu, Y. *Small* **2015**, *11*, 2762.

(131) Liu, Y.; Zhang, S.; Zhu, T. *ChemElectroChem* **2014**, *1*, 706.

(132) Xu, Y.; Zhu, X.; Zhou, X.; Liu, X.; Liu, Y.; Dai, Z.; Bao, J. *J. Phys. Chem. C* **2014**, *118*, 28502.

(133) Kim, H.; Son, Y.; Park, C.; Cho, J.; Choi, H. C. *Angew. Chem., Int. Ed.* **2013**, *52*, 5997.

(134) Jo, G.; Choi, I.; Ahn, H.; Park, M. J. *Chem. Commun.* **2012**, *48*, 3987.

(135) Park, C.-M.; Kim, J.-H.; Kim, H.; Sohn, H.-J. *Chem. Soc. Rev.* **2010**, *39*, 3115.

(136) Yoon, S.; Park, C.-M.; Sohn, H.-J. *Electrochem. Solid-State Lett.* **2008**, *11*, A42.

(137) Park, M.-H.; Cho, Y. H.; Kim, K.; Kim, J.; Liu, M.; Cho, J. *Angew. Chem., Int. Ed.* **2011**, *50*, 9647.

(138) Jin, S.; Li, N.; Cui, H.; Wang, C. *ACS Appl. Mater. Interfaces* **2014**, *6*, 19397.

(139) Loewig; Schweitzer *J. pr. Chem.*, *XLIX*, 385.

(140) Cho, C. S.; Motofusa, S.-i.; Ohe, K.; Uemura, S. *Bull. Chem. Soc. Jpn.* **1996**, *69*, 2341.

(141) Kawamura, T.; Kikukawa, K.; Takagi, M.; Matsuda, T. *Bull. Chem. Soc. Jpn.* **1977**, *50*, 2021.

(142) Asano, R.; Moritani, I.; Fujiwara, Y.; Teranishi, S. *Bull. Chem. Soc. Jap.* **1973**, *46*, 2910.

(143) Breunig, H. J.; Ghesner, I. *Adv. Organomet. Chem.* **2003**, *49*, 95.

(144) Huang, Y. *Acc. Chem. Res.* **1992**, *25*, 182.

(145) Freedman, L. D.; Doak, G. O.; Wiley: 1989; Vol. 5, p 397.

(146) Cullen, W. R.; Wu, A. W. *J. Fluorine Chem.* **1976**, *8*, 183.

(147) Ashe, A. J., III; Kampf, J. W.; Al-Taweel, S. M. *Organometallics* **1992**, *11*, 1491.

(148) Naumann, D.; Tyrra, W.; Leifeld, F. *J. Organomet. Chem.* **1987**, *333*, 193.

(149) Ganja, E. A.; Ontiveros, C. D.; Morrison, J. A. *Inorg. Chem.* **1988**, *27*, 4535.

(150) Ates, M.; Breunig, H. J.; Soltani-Neshan, A.; Tegeler, M. *Z. Naturforsch., B: Anorg. Chem., Org. Chem.* **1986**, *41B*, 321.

(151) Doak, G. O.; Freedman, L. D. *Synthesis* **1974**, 328.

(152) Meinema, H. A.; Romao, C. J. R. C.; Noltes, J. G. *J. Organometal. Chem.* **1973**, *55*, 139.

(153) Wada, M.; Natsume, S.; Suzuki, S.; Uo, A.; Nakamura, M.; Hayase, S.; Erabi, T. *J. Organomet. Chem.* **1997**, *548*, 223.

(154) Lee, E. J.; Hong, J. S.; Kim, T.-J.; Kang, Y.; Han, E. M.; Lee, J. J.; Song, K.; Kim, D.-U. *Bull. Korean Chem. Soc.* **2005**, *26*, 1946.

(155) Breunig, H. J.; Lork, E.; Moldovan, O.; Rat, C. I. *J. Organomet. Chem.* **2008**, *693*, 2527.

(156) Yasuike, S.; Kishi, Y.; Kawara, S.-i.; Kurita, J. *Chem. Pharm. Bull.* **2005**, *53*, 425.

(157) Moiseev, D. V.; Morugova, V. A.; Gushchin, A. V.; Dodonov, V. A. *Tetrahedron Lett.* **2003**, *44*, 3155.

(158) Sharutin, V. V.; Sharutina, O. K.; Artem'eva, E. V.; Makerova, M. S. *Russ. J. Inorg. Chem.* **2015**, *60*, 170.

(159) Sharutin, V. V.; Molokova, O. V.; Sharutina, O. K.; Smirnova, S. A. *Russ. J. Inorg. Chem.* **2012**, *57*, 1252.

(160) Sharutin, V. V.; Sharutina, O. K.; Kazakov, M. V. *Russ. J. Inorg. Chem.* **2014**, *59*, 1115.

(161) Sharutin, V. V.; Senchurin, V. S.; Sharutina, O. K.; Kazakov, M. V. *Russ. J. Gen. Chem.* **2012**, *82*, 95.

(162) Garje, S. S.; Jain, V. K. *Main Group Met. Chem.* **1999**, *22*, 45.

(163) Opris, L. M.; Silvestru, A.; Silvestru, C.; Breunig, H. J.; Lork, E. *Dalton Trans.* **2003**, 4367.

(164) Wieber, M.; Wirth, D.; Fetzer, I. *Z. Anorg. Allg. Chem.* **1983**, *505*, 134.

(165) Kakusawa, N.; Ikeda, T.; Osada, A.; Kurita, J.; Tsuchiya, T. *Synlett* **2000**, 1503.

(166) Nunn, M.; Sowerby, D. B.; Wesolek, D. M. *J. Organomet. Chem.* **1983**, *251*, C45.

(167) Matoba, K.; Motofusa, S.-I.; Cho, C. S.; Ohe, K.; Uemura, S. *J. Organomet. Chem.* **1999**, *574*, 3.

(168) Doak, G. O.; Freedman, L. D. *Organometallic Compounds of Arsenic, Antimony, and Bismuth*; Interscience, 1970.

(169) Freedman, L. D.; Doak, G. O. *Organometal. Chem. Rev., Sect. B* **1970**, *6*, 615.

(170) Millington, P. L.; Sowerby, D. B. *J. Organomet. Chem.* **1994**, *480*, 227.

(171) Issleib, K.; Hamann, B.; Schmidt, L. *Z. Anorg. Allg. Chem.* **1965**, *339*, 298.

(172) Gedridge, R. W., Jr. *Organometallics* **1992**, *11*, 967.

(173) Breunig, H. J.; Kanig, W.; Soltani-Neshan, A. *Polyhedron* **1983**, *2*, 291.

(174) Ates, M.; Breunig, H. J.; Gulec, S. *J. Organomet. Chem.* **1989**, *364*, 67.

(175) Copolovici, D.; Bojan, V. R.; Rat, C. I.; Silvestru, A.; Breunig, H. J.; Silvestru, C. *Dalton Trans.* **2010**, *39*, 6410.

(176) Becker, G.; Mundt, O.; Sachs, M.; Breunig, H. J.; Lork, E.; Probst, J.; Silvestru, A. *Z. Anorg. Allg. Chem.* **2001**, *627*, 699.

(177) Balazs, G.; Breunig, H. J.; Lork, E.; Offermann, W. *Organometallics* **2001**, *20*, 2666.

(178) Berry, A. *Polyhedron* **1999**, *18*, 2609.

(179) Cowley, A. H.; Jones, R. A.; Nunn, C. M.; Westmoreland, D. L. *Angew. Chem.* **1989**, *101*, 1089.

(180) Twamley, B.; Hwang, C.-S.; Hardman, N. J.; Power, P. P. *J. Organomet. Chem.* **2000**, *609*, 152.

(181) Wiberg, E.; Modritzer, K. *Z. Naturforsch.* **1957**, *12b*, 128.

(182) Breunig, H. J.; Probst, J. *J. Organomet. Chem.* **1998**, *571*, 297.

(183) Hendershot, D. G.; Pazik, J. C.; Berry, A. D. *Chem. Mater.* **1992**, *4*, 833.

(184) Balazs, G.; Breunig, H. J.; Lork, E. *Organometallics* **2002**, *21*, 2584.

(185) Huang, Y.; Shen, Y.; Chen, C. *Tetrahedron Lett.* **1985**, *26*, 5171.

(186) Nesmeyanov, A. N.; Borisov, A. E.; Novikova, N. V. *Izv. Akad. Nauk SSSR, Ser. Khim.* **1967**, 815.

(187) Issleib, K.; Balszuweit, A. *Z. Anorg. Allg. Chem.* **1976**, *419*, 87.

(188) Cho, C. S.; Tanabe, K.; Itoh, O.; Uemura, S. *J. Org. Chem.* **1995**, *60*, 274.

(189) Cho, C. S.; Tanabe, K.; Uemura, S. *Tetrahedron Lett.* **1994**, *35*, 1275.

(190) Freedman, L. D.; Doak, G. O. *J. Organomet. Chem.* **1995**, *496*, 137.

(191) Kakusawa, N.; Tsuchiya, T.; Kurita, J. *Tetrahedron Lett.* **1998**, *39*, 9743.

(192) Kakusawa, N.; Yamaguchi, K.; Kurita, J.; Tsuchiya, T. *Tetrahedron Lett.* **2000**, *41*, 4143.

(193) Yasuike, S.; Okajima, S.; Kurita, J. *Chem. Pharm. Bull.* **2002**, *50*, 1404.

(194) Yasuike, S.; Okajima, S.; Yamaguchi, K.; Seki, H.; Kurita, J. *Tetrahedron: Asymmetry* **2000**, *11*, 4043.

(195) Yasuike, S.; Okajima, S.; Yamaguchi, K.; Seki, H.; Kurita, J. *Tetrahedron* **2003**, *59*, 4959.

(196) Kang, Y.; Song, D.; Schmider, H.; Wang, S. *Organometallics* **2002**, *21*, 2413.

(197) Schulz, S. *Coord. Chem. Rev.* **2015**, *297-298*, 49.

(198) Levason, W.; Matthews, M. L.; Reid, G.; Webster, M. *Dalton Trans.* **2004**, 51.

(199) Breunig, H. J.; Roesler, R. *Coord. Chem. Rev.* **1997**, *163*, 33.

(200) Balazs, L.; Breunig, H. J. *Coord. Chem. Rev.* **2004**, *248*, 603.

(201) Paneth, F. A. *Trans. Faraday Soc.* **1934**, *30*, 179.

(202) Becker, G.; Freudenblum, H.; Witthauer, C. *Z. Anorg. Allg. Chem.* **1982**, *492*, 37.

(203) Kuczkowski, A.; Heimann, S.; Weber, A.; Schulz, S.; Blaser, D.; Wolper, C. *Organometallics* **2011**, *30*, 4730.

(204) Spence, R. E. v. H.; Hsu, D. P.; Buchwald, S. L. *Organometallics* **1992**, *11*, 3492.

(205) Roller, S.; Draeger, M.; Breunig, H. J.; Ates, M.; Guelec, S. *J. Organomet. Chem.* **1989**, *378*, 327.

(206) Ashe, A. J., III; Ludwig, E. G., Jr.; Oleksyszyn, J.; Huffman, J. C. *Organometallics* **1984**, *3*, 337.

(207) Ashe, A. J., III; Ludwig, E. G., Jr. *Organometallics* **1982**, *1*, 1408.

(208) Ates, M.; Breunig, H. J.; Guelec, S. *Polyhedron* **1988**, *7*, 2601.

(209) Barrett, A. G. M.; Melcher, L. M. *J. Am. Chem. Soc.* **1991**, *113*, 8177.

(210) Ohshita, J.; Tsuchida, T.; Murakami, K.; Ooyama, Y.; Nakanishi, T.; Hasegawa, Y.; Kobayashi, N.; Higashimura, H. *Z. Naturforsch., B: J. Chem. Sci.* **2014**, *69*, 1181.

(211) Breunig, H. J.; Ebert, K. H.; Guelec, S.; Probst, J. *Chem. Ber.* **1995**, *128*, 599.

(212) Ates, M.; Breunig, H. J.; Guelec, S.; Offermann, W.; Haeberle, K.; Draeger, M. *Chem. Ber.* **1989**, *122*, 473.

(213) Breunig, H. J.; Soltani-Neshan, A.; Haeberle, K.; Draeger, M. *Z. Naturforsch., B: Anorg. Chem., Org. Chem.* **1986**, *41B*, 327.

(214) Breunig, H. J.; Haeberle, K.; Draeger, M.; Severengiz, T. *Angew. Chem.* **1985**, *97*, 62.

(215) Johnson, O. H.; Harris, D. M. *J. Am. Chem. Soc.* **1950**, *72*, 5564.

(216) Hevesi, L.; Elsevier: 1995; Vol. 2, p 899.

(217) West, R. *J. Am. Chem. Soc.* **1952**, *74*, 4863.

(218) Dumler, V. A.; Kolbasina, V. D.; Evstafeeva, N. E.; Proshutinskii, V. I.; Lapkin, I. I. *Izv. Vyssh. Uchebn. Zaved., Khim. Khim. Tekhnol.* **1977**, *20*, 1797.

(219) Takeuchi, Y.; Yamamoto, H.; Tanaka, K.; Ogawa, K.; Harada, J.; Iwamoto, T.; Yuge, H. *Tetrahedron* **1998**, *54*, 9811.

(220) Frisch, M. J.; Trucks, G. W.; Schlegel, H. B.; Scuseria, G. E.; Robb, M. A.; Cheeseman, J. R.; Scalmani, G.; Barone, V.; Mennucci, B.; Petersson, G. A.; Nakatsuji, H.; Caricato, M.; Li, X.; Hratchian, H. P.; Izmaylov, A. F.; Bloino, J.; Zheng, G.; Sonnenberg, J. L.; Hada, M.; Ehara, M.; Toyota, K.; Fukuda, R.; Hasegawa, J.; Ishida, M.; Nakajima, T.; Honda, Y.; Kitao, O.; Nakai, H.; Vreven, T.; Montgomery Jr, J. A.; Peralta, J. E.; Ogliaro, F.; Bearpark, M. J.; Heyd, J.; Brothers, E. N.; Kudin, K. N.; Staroverov, V. N.; Kobayashi, R.; Normand, J.; Raghavachari, K.; Rendell, A. P.; Burant, J. C.; Iyengar, S. S.; Tomasi, J.; Cossi, M.; Rega, N.; Millam, N. J.; Klene, M.; Knox, J. E.; Cross, J. B.; Bakken, V.; Adamo, C.; Jaramillo, J.; Gomperts, R.; Stratmann, R. E.; Yazyev, O.; Austin, A. J.; Cammi, R.; Pomelli, C.; Ochterski, J. W.; Martin, R. L.; Morokuma, K.; Zakrzewski, V. G.; Voth, G. A.; Salvador, P.; Dannenberg, J. J.; Dapprich, S.; Daniels, A. D.; Farkas, Ö.; Foresman, J. B.; Ortiz, J. V.; Cioslowski, J.; Fox, D. J.; Gaussian, Inc.: Wallingford, CT, USA, 2009.

(221) Adamo, C.; Barone, V. *J. Chem. Phys.* **1998**, *108*, 664.

(222) Brown, P.; Mahon, M. F.; Molloy, K. C. *J. Organomet. Chem.* **1992**, *435*, 265.

(223) Krueerke, U.; Wittouck, E. *Chem. Ber.* **1962**, *95*, 174.

(224) Zaitsev, K. V.; Kapranov, A. A.; Oprunenko, Y. F.; Churakov, A. V.; Howard, J. A. K.; Tarasevich, B. N.; Karlov, S. S.; Zaitseva, G. S. *J. Organomet. Chem.* **2012**, *700*, 207.

(225) Johnson, O. H.; Harris, D. M. *Inorg. Synth.* **1957**, *5*, 74.

(226) Dallaire, C.; Brook, M. A. *Organometallics* **1993**, *12*, 2332.

(227) Dallaire, C.; Brook, M. A. *Organometallics* **1990**, *9*, 2873.

(228) Bott, R. W.; Earborn, C.; Greasly, P. M. *J. Chem. Soc.* **1964**, 4804.

(229) Eaborn, C.; Pande, K. C. *J. Chem. Soc.* **1960**, 1566.

(230) Simons, J. K. *J. Am. Chem. Soc.* **1935**, *57*, 1299.

(231) Uhlig, W. *Trends Organomet. Chem.* **1997**, *2*, 1.

(232) Uhlig, W. *Polym. Adv. Technol.* **1997**, *8*, 731.

(233) Uhlig, W. *J. Organomet. Chem.* **1991**, *421*, 189.

(234) Uhlig, W. *J. Organomet. Chem.* **1991**, *409*, 377.

(235) Uhlig, W. *J. Organomet. Chem.* **1991**, *402*, C45.

(236) Uhlig, W.; Heinicke, J.; Tzschach, A. *Z. Chem.* **1990**, *30*, 217.

(237) Uhlig, W.; Tzschach, A. *J. Organomet. Chem.* **1989**, *378*, C1.

(238) Fronda, A.; Maas, G. *J. Organomet. Chem.* **1990**, *391*, 289.

(239) Bassindale, A. R.; Stout, T. *J. Organomet. Chem.* **1984**, *271*, C1.

(240) Zaitsev, K. V.; Oprunenko, Y. F.; Churakov, A. V.; Zaitseva, G. S.; Karlov, S. S. *Main Group Met. Chem.* **2014**, *37*, 67.

(241) Spikes, G. H.; Fettinger, J. C.; Power, P. P. *J. Am. Chem. Soc.* **2005**, *127*, 12232.

(242) Skobeleva, S. E.; Egorochkin, A. N.; Khorshev, S. Y.; Ratushnaya, S. K.; Rivière, P.; Satgé, J.; Richelme, S.; Cazes, A. *J. Organomet. Chem.* **1979**, *182*, 1.

(243) Chatgilialoglu, C.; Ballestri, M.; Escudié, J.; Pailhous, I. *Organometallics* **1999**, *18*, 2395.

(244) Unno, M.; Kawai, Y.; Matsumoto, H. *Heteroat. Chem.* **2001**, *12*, 238.

(245) Muller, E.; Martin, H. P. *J. Prakt. Chem./Chem.- Ztg.* **1997**, *339*, 401.

(246) Colombo, P.; Mera, G.; Riedel, R.; Soraru, G. D. *J. Am. Ceram. Soc.* **2010**, *93*, 1805.

(247) Fuchsbichler, B.; Stangl, C.; Kren, H.; Uhlig, F.; Koller, S. *J. Power Sources* **2011**, *196*, 2889.

(248) Neumann, W. P.; Koenig, K. *Angew. Chem.* **1962**, *74*, 215.

(249) Draeger, M.; Mathiasch, B.; Ross, L.; Ross, M. *Z. Anorg. Allg. Chem.* **1983**, *506*, 99.

(250) Aitken, C.; Harrod, J. F.; Malek, A.; Samuel, E. *J. Organomet. Chem.* **1988**, *349*, 285.

(251) Zeppek, C. *Doctoral Thesis, Universtiy of Technology Graz* **2016**.

(252) Meyer, E. A.; Castellano, R. K.; Diederich, F. *Angew. Chem., Int. Ed.* **2003**, *42*, 1210.

(253) Nayak, S. K.; Sathishkumar, R.; Row, T. N. G. *CrystEngComm* **2010**, *12*, 3112.

(254) Janiak, C. *J. Chem. Soc., Dalton Trans.* **2000**, 3885.

(255) Hunter, C. A.; Sanders, J. K. M. *J. Am. Chem. Soc.* **1990**, *112*, 5525.

(256) Binder, J.; Fischer, R. C.; Flock, M.; Stammler, H.-G.; Torvisco, A.; Uhlig, F. *Phosphorus, Sulfur Silicon Relat. Elem.* **2016**, *191*, 478.

(257) Binder, J.; Fischer, R. C.; Flock, M.; Torvisco, A.; Uhlig, F. *Phosphorus, Sulfur Silicon Relat. Elem.* **2015**, *190*, 1980.

(258) Zeppek, C.; Fischer, R. C.; Torvisco, A.; Uhlig, F. *Can. J. Chem.* **2014**, *92*, 556.

(259) Zeppek, C.; Pichler, J.; Torvisco, A.; Flock, M.; Uhlig, F. *J. Organomet. Chem.* **2013**, *740*, 41.

(260) Alvarez, S. *Dalton Transactions* **2013**, *42*, 8617.

(261) Chieh, P. C. *J. Chem. Soc. A.* **1971**, 3243.

(262) Karipides, A.; Haller, D. A. *Acta Crystallogr., Sect. B: Struct. Sci.* **1972**, *28*, 2889.

(263) Claborn, K.; Kahr, B.; Kaminsky, W. *CrystEngComm* **2002**, *4*, 252.

(264) Belsky, V. K.; Simonenko, A. A.; Reikhsfeld, V. O. *J. Organomet. Chem.* **1984**, *265*, 141.

(265) Charissé, M.; Roller, S.; Dräger, M. *J. Organomet. Chem.* **1992**, *427*, 23.

(266) Simons, R. S.; Haubrich, S. T.; Mork, B. V.; Niemeyer, M.; Power, P. P. *Main Group Chem.* **1998**, *2*, 275.

(267) Preut, H.; Huber, F. *Acta Crystallogr., Sect. B: Struct. Sci.* **1979**, *35*, 83.

(268) McGrady, G. S.; Odlyha, M.; Prince, P. D.; Steed, J. W. *CrystEngComm* **2002**, *4*, 271.

(269) Cameron, T. S.; Mannan, K. M.; Stobart, S. R. *Cryst. Struct. Commun.* **1975**, *4*, 601.

(270) Lambert, J. B.; Stern, C. L.; Zhao, Y.; Tse, W. C.; Shawl, C. E.; Lentz, K. T.; Kania, L. *J. Organomet. Chem.* **1998**, *568*, 21.

(271) Barrow, M. J.; Ebsworth, E. A. V.; Harding, M. M.; Rankin, D. W. H. *J. Chem. Soc., Dalton Trans.* **1980**, 603.

(272) Mitzel, N. W.; Losehand, U.; Hinchley, S. L.; Rankin, D. W. H. *Inorg. Chem.* **2001**, *40*, 661.

(273) Nelyubina, Y. V.; Antipin, M. Y.; Lyssenko, K. A. *J. Phys. Chem. A* **2007**, *111*, 1091.

(274) Willett, R. D.; Twamley, B.; Montfrooij, W.; Granroth, G. E.; Nagler, S. E.; Hall, D. W.; Park, J.-H.; Watson, B. C.; Meisel, M. W.; Talham, D. R. *Inorg. Chem.* **2006**, *45*, 7689.

(275) Weinert, C. S. *ISRN Spectroscopy* **2012**, *2012*, 18.

(276) Riviere, P.; Riviere-Baudet, M.; Castel, A.; Satge, J.; Lavabre, A. *Synth. React. Inorg. Met.-Org. Chem.* **1987**, *17*, 539.

(277) Castel, A.; Riviere, P.; Satge, J.; Ko, Y. H.; Desor, D. *J. Organomet. Chem.* **1990**, *397*, 7.

(278) Cross, R. J.; Glockling, F. *J. Organomet. Chem.* **1965**, *3*, 146.

(279) Castel, A.; Riviere, P.; Satge, J.; Desor, D. *J. Organomet. Chem.* **1992**, *433*, 49.

(280) Egorochkin, A. N.; Khorshev, S. Y.; Satge, J.; Riviere, P.; Barrau, J. *J. Organomet. Chem.* **1975**, *99*, 239.

(281) Egorochkin, A. N.; Khorshev, S. Y.; Ostasheva, N. S.; Satge, J.; Riviere, P.; Barrau, J.; Massol, M. *J. Organomet. Chem.* **1974**, *76*, 29.

(282) Ostah, N.; Lawson, G. *Appl. Organomet. Chem.* **1995**, *9*, 609.

(283) Glockling, F.; Light, J. R. C. *J. Chem. Soc. A* **1968**, 717.

(284) Bone, S. P.; Sowerby, D. B. *J. Chem. Soc., Dalton Trans.* **1979**, 1430.

(285) Alonzo, G.; Bruening, H. J.; Denker, M.; Ebert, K. H.; Offerman, W. *J. Organomet. Chem.* **1996**, *522*, 237.

(286) Mundt, O.; Becker, G.; Stadelmann, H.; Thurn, H. *Z. Anorg. Allg. Chem.* **1992**, *617*, 59.

(287) Allen, F. *Acta Crystallogr., Sect. B: Struct. Sci.* **2002**, *58*, 380.

(288) Becker, G.; Mundt, O.; Sachs, M.; Breunig, H. J.; Lork, E.; Probst, J.; Silvestru, A. *Z. Anorg. Allg. Chem.* **2001**, *627*, 699.

(289) Effendy; Grigsby, W. J.; Hart, R. D.; Raston, C. L.; Skelton, B. W.; White, A. H. *Aust. J. Chem.* **1997**, *50*, 675.

(290) Wetzel, J. *Z. Kristallogr., Kristallgeom., Kristallphys., Kristallchem.* **1942**, *104*, 305.

(291) Adams, E. A.; Kolis, J. W.; Pennington, W. T. *Acta Crystallogr., Sect. C: Cryst. Struct. Commun.* **1990**, *46*, 917.

(292) Sobolev, A. N.; Romm, I. P.; Belsky, V. K.; Guryanova, E. N. *J. Organomet. Chem.* **1979**, *179*, 153.

(293) Sharma, P.; Cabrera, A.; Rosas, N.; Le Lagadec, R.; Hernandez, S.; Valdes, J.; Arias, J. L.; Ambrouse, C. V. *Main Group Met. Chem.* **1998**, *21*, 303.

(294) Eun Ji Lee, J. S. H., Tae-Jeong Kim, Youngjin Kang, Eun Me Han, Jae Jung Lee, Kihyung Song, Dong-Uk Kim *Bull. Korean Chem. Soc.* **2005**, *26*, 1946.

(295) Sobolev, A. N.; Romm, I. P.; Belsky, V. K.; Syutkina, O. P.; Guryanova, E. N. *J. Organomet. Chem.* **1981**, *209*, 49.

(296) Ates, M.; Breunig, H. J.; Ebert, K. H.; Kaller, R.; Draeger, M.; Behrens, U. *Z. Naturforsch., B: Chem. Sci.* **1992**, *47*, 503.

(297) Sasaki, S.; Sutoh, K.; Murakami, F.; Yoshifuji, M. *J. Am. Chem. Soc.* **2002**, *124*, 14830.

(298) Millington, P. L.; Sowerby, D. B. *J. Organomet. Chem.* **1994**, *480*, 227.

(299) Shawkataly, O. b.; Hussien Abdelnasir, H. M.; Rosli, M. M. *Acta Crystallogr., Sect. E: Struct. Rep. Online* **2014**, *70*, m351.

(300) Cowley, A. H.; Nunn, C. M.; Westmoreland, D. L. *Acta Crystallogr., Sect. C: Cryst. Struct. Commun.* **1990**, *46*, 774.

(301) Ates, M.; Breunig, H. J.; Ebert, K. H.; Kaller, R.; Draeger, M.; Behrens, U. *Z. Naturforsch., B: Chem. Sci.* **1992**, *47*, 503.

(302) Deuten, K. v.; Rehder, D. *Cryst. Struct. Commun.* **1980**, 167.

(303) Becker, G.; Freudenblum, H.; Witthauer, C. *Z. Anorg. Allg. Chem.* **1982**, *492*, 37.

(304) Werner, J.; Schwarz, W.; Schmidt, A. *Z. Naturforsch., B: Anorg. Chem., Org. Chem.* **1981**, *36B*, 556.

(305) Hall, M.; Sowerby, D. B. *J. Chem. Soc., Dalton Trans.* **1983**, 1095.

(306) Fan, B.; Qu, L.; Shi, G. *J. Electroanal. Chem.* **2005**, *575*, 287.

(307) Schulz, S.; Heimann, S.; Kuczkowski, A.; Blaeser, D.; Woelper, C. *Organometallics* **2013**, *32*, 3391.

(308) Bruker; Bruker AXS Inc.: Madison, Wisconsin, USA, 2012.

(309) Blessing, R. *Acta Crystallogr., Sect. A: Found. Adv.* **1995**, *51*, 33.

(310) Sheldrick, G. *Acta Crystallogr., Sect. A: Found. Adv.* **1990**, *46*, 467.

(311) Sheldrick, G. *Acta Crystallogr., Sect. A: Found. Adv.* **2008**, *64*, 112.

(312) Sheldrick, G. M. *Acta Crystallogr., Sect. A: Found. Adv.* **2015**, *71*, 3.

(313) Spek, A. L. *J. Appl. Crystallogr.* **2003**, *36*, 7.

(314) Spek, A. L. *Acta Crystallogr., Sect. D: Biol. Crystallogr.* **2009**, *65*, 148.

(315) van der Sluis, P.; Spek, A. L. *Acta Crystallogr., Sect. A: Found. Adv.* **1990**, *46*, 194.

(316) Spek, A. L. *Acta Crystallogr., Sect. C: Cryst. Struct. Commun.* **2015**, *71*, 9.

(317) Müller, P.; Herbst-Irmer, R.; Spek, A. L.; Schneider, T. R.; Sawaya, M. R. *Crystal Structure Refinement: A Crystallographer's Guide to SHELXL* Oxford University Press, 2006.

(318) Allen, F. H. *Acta Crystallogr., Sect. B: Struct. Sci.* **2002**, *B58*, 380.

(319) Macrae, C. F.; Bruno, I. J.; Chisholm, J. A.; Edgington, P. R.; McCabe, P.; Pidcock, E.; Rodriguez-Monge, L.; Taylor, R.; van de Streek, J.; Wood, P. A. *J. Appl. Crystallogr.* **2008**, *41*, 466.

(320) Putz, H.; Brandenburg, K.; 3.2i ed.; Crystal Impact: Bonn, Germany.